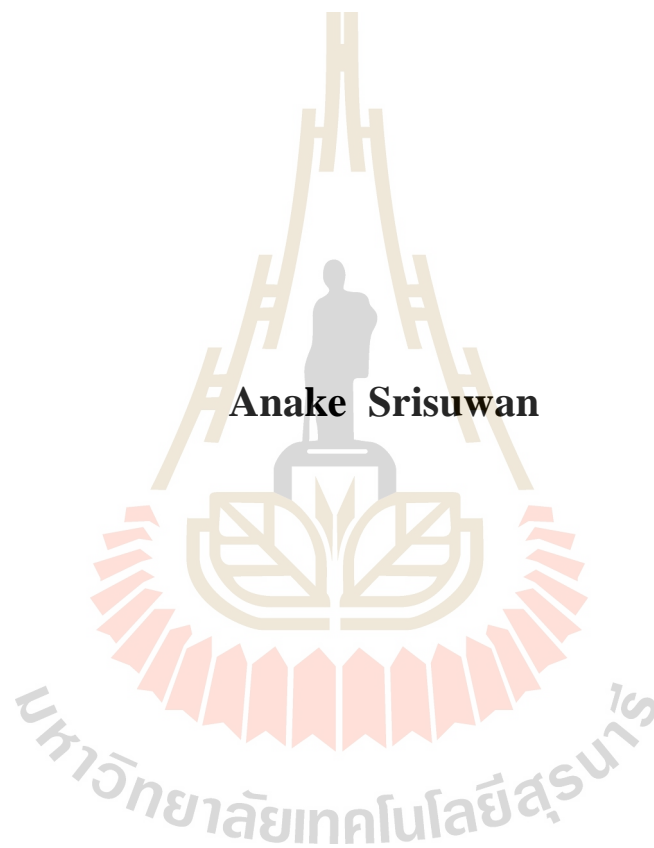# URBAN GROWTH IMPACT ASSESSMENT ON

LANDSCAPE ECOLOGY AND

ECOSYSTEM SERVICE VALUE

Anake Srisuwan

A Thesis Submitted in Partial Fulfillment of the Requirements for the

Degree of Doctor of Philosophy in Geoinformatics

Suranaree University of Technology

Academic Year 2018

การประเมินผลกระทบของการเติบโตของเมืองต่อนิเวศภูมิทัศน์และการบริการของระบบนิเวศ

นายเอนก ศรีสุวรรณ

วิทยานิพนธ์นี้เป็นส่วนหนึ่งของการศึกษาตามหลักสูตรปริญญาวิทยาศาสตรดุษฎีบัณฑิต
สาขาวิชาภูมิสารสนเทศ
มหาวิทยาลัยเทคโนโลยีสุรนารี
ปีการศึกษา 2561

URBAN GROWTH IMPACT ASSESSMENT ON LANDSCAPE ECOLOGY AND ECOSYSTEM SERVICE VALUE

Suranaree University of Technology has approved this thesis submitted in partial fulfillment of the requirements for the Degree of Doctor of Philosophy.

Thesis Examining Committee

_____
(Assoc. Prof. Dr. Songkot Dasananda)

Chairperson

_____
(Assoc. Prof. Dr. Suwit Ongsomwang)

Member (Thesis Advisor)

_____
(Asst. Prof. Dr. Sunya Sarapirome)

Member

_____
(Assoc. Prof. Dr. Sura Pattanakiat)

Member

_____
(Assoc. Prof. Dr. Supet Jirakajohnkool)

Member

_____
(Prof. Dr. Santi Maensiri)

Vice Rector for Academic Affairs and

Internationalization

_____
(Asst. Prof. Dr. Worawat Meevasana)

Dean of Institute of Science

เอนก ศรีสุวรรณ : การประเมินผลกระทบของการเติบโตของเมืองต่อนิเวศภูมิทัศน์และ
การบริการของระบบนิเวศ (URBAN GROWTH IMPACT ASSESSMENT ON
LANDSCAPE ECOLOGY AND ECOSYSTEM SERVICE VALUE) อาจารย์ที่ปรึกษา :
รองศาสตราจารย์ ดร.สุวิทย์ อ๋องสมหวัง, 323 หน้า.

การเปลี่ยนแปลงการใช้ประโยชน์ที่ดินและสิ่งปกคลุมดินจากการขยายตัวของเมืองเนื่องจาก
ไม่มีการวางแผนและการควบคุมการขยายตัวของเมืองส่งผลกระทบต่อนิเวศภูมิทัศน์ของเมืองและ
การให้บริการของระบบนิเวศอย่างมีนัยสำคัญ วัตถุประสงค์หลักของการศึกษาคือ (1) เพื่อจำแนก
สถานภาพการใช้ประโยชน์ที่ดินและสิ่งปกคลุมดินและการเปลี่ยนแปลงในระหว่างปี พ.ศ. 2549 ถึง
พ.ศ. 2559 และจำลองภาพเหตุการณ์ 2 รูปแบบที่แตกต่างกันในปี พ.ศ. 2569 (2) เพื่อประเมินผล
กระทบจากการเติบโตของเมืองต่อนิเวศภูมิทัศน์ของเมืองและการให้บริการของระบบนิเวศใน
ระหว่างปี พ.ศ. 2549 ถึง พ.ศ. 2569 (3) เพื่อระบุความสัมพันธ์ระหว่างฟังก์ชันการให้บริการของ
ระบบนิเวศและตัวชี้วัดรูปแบบภูมิทัศน์และ (4) เพื่อประเมินและคาดการณ์ผลกระทบของการเติบโต
ของเมืองต่ออุณหภูมิพื้นผิวบริเวณอำเภอเมืองขอนแก่น จังหวัดขอนแก่น ในการศึกษาครั้งนี้ เริ่มต้น
จากการนำภาพถ่ายจากดาวเทียม Landsat ที่บันทึกข้อมูลในปี พ.ศ. 2549 2554 และ 2559 มาใช้
จำแนกประเภทการใช้ประโยชน์ที่ดินและสิ่งปกคลุมดินด้วยการวิเคราะห์ข้อมูลภาพเชิงวัตถุ และนำ
ผลลัพธ์ที่ได้รับไปใช้คาดการณ์การเปลี่ยนแปลงการใช้ประโยชน์ที่ดินและสิ่งปกคลุมดินในปี พ.ศ.
2569 ของภาพเหตุการณ์สองรูปแบบที่แตกต่างกันด้วยแบบจำลอง CLUE-S และประเมินสถานภาพ
และการเปลี่ยนแปลงของการใช้ประโยชน์ที่ดินและสิ่งปกคลุมดินจากการเติบโตของเมืองและ
ผลกระทบต่อดัชนีภูมิทัศน์ มูลค่าฟังก์ชันการให้บริการของระบบนิเวศ และอุณหภูมิพื้นผิว

ผลการศึกษา พบว่า พื้นที่ของการใช้ประโยชน์ที่ดินและสิ่งปกคลุมดินหลักที่ลดลงใน
ระหว่างปี พ.ศ. 2549 ถึง 2569 ของสองภาพเหตุการณ์ได้แก่ นาข้าวและพืชไร่ ในขณะเดียวกัน พื้นที่
เมืองและสิ่งปลูกสร้าง ทุ่งหญ้า และที่ดินที่ไม่ได้มีการใช้ประโยชน์เพิ่มขึ้นอย่างต่อเนื่อง ผลลัพธ์
ได้รับจากการคาดการณ์การใช้ประโยชน์ที่ดินและสิ่งปกคลุมดินของภาพเหตุการณ์แบบที่ I และ II
ในปี พ.ศ. 2569 สามารถให้ผลลัพธ์ที่สมเหตุสมผลตามที่คาดหวัง คุณลักษณะของการเติบโตของ
เมืองจากดัชนี 3 รูปแบบ (AEII PU SI) บ่งชี้ให้เห็นว่าพื้นที่เขตเมืองจะเพิ่มขึ้นด้วยอัตราความเป็น
เมืองสูงมากและการพัฒนาพื้นที่เขตเมืองสูงในอนาคต นอกจากนี้ ภูมิทัศน์เมืองจะมีการขยายตัวและ
มีความซับซ้อนมากขึ้นในลักษณะที่ไม่สม่ำเสมอ และภูมิทัศน์ของพื้นที่เมืองและสิ่งปลูกสร้างของ
ภาพเหตุการณ์แบบที่ I มีการเปลี่ยนแปลงมากกว่าภาพเหตุการณ์แบบที่ II และรูปแบบพื้นที่เมือง
และสิ่งปลูกสร้างมีความสัมพันธ์ในเชิงบวกกับดัชนีมิติทางสาทิสรูปเฉลี่ยแบบถ่วงน้ำหนักของพื้นที่

(area-weighted mean fractal dimension metric) อย่างสูง ในขณะเดียวกัน มูลค่าฟังก์ชันในการ
ให้บริการของระบบนิเวศสามลำดับแรกจากข้อมูลของการใช้ประโยชน์ที่ดินและสิ่งปกคลุมดินแบบ
พลวัตในคาบเวลาเดียวกันได้แก่ การบำบัดของเสีย การให้บริการน้ำและการควบคุมสภาพภูมิอากาศ
ในขณะที่ ประเภทการใช้ประโยชน์ที่ดินและสิ่งปกคลุมดินสามลำดับแรกที่ให้มูลค่าฟังก์ชันในการ
ให้บริการของระบบนิเวศสูงสุดสามลำดับแรกได้แก่ นาข้าว แหล่งน้ำและพื้นที่ลุ่มและน้ำท่วมถึง
นอกจากนี้ พบว่า ร้อยละของภูมิทัศน์ (percent of landscape) ของการใช้ประโยชน์ที่ดินและสิ่ง
ปกคลุมดินแต่ละประเภทเป็นตัวแปรอิสระที่สำคัญสำหรับใช้ในการอธิบายมูลค่าฟังก์ชันในการ
ให้บริการของระบบนิเวศยกเว้นฟังก์ชันการผลิตอาหาร สำหรับผลการศึกษาลำดับสุดท้าย พบว่า
อุณหภูมิพื้นผิวในปี พ.ศ. 2559 มีค่าระหว่าง 18.799 ถึง 34.468 องศาเซลเซียส โดยมีค่าเฉลี่ยเท่ากับ
27.070 องศาเซลเซียส และบริเวณที่มีอุณหภูมิสูงสุดพบในเขตพื้นที่เมืองและสิ่งปลูกสร้าง เช่น
สนามบินหรือย่านศูนย์กลางธุรกิจ นอกจากนี้ พบว่า แนวทางที่เหมาะสมสำหรับใช้ในการคาดการณ์
ค่าอุณหภูมิพื้นผิวในอนาคตได้แก่ ความสัมพันธ์ระหว่างอุณหภูมิพื้นผิวและดัชนีภูมิทัศน์แบบหลาย
ดัชนี เนื่องจากให้ค่าพิสัย ค่าสัมประสิทธิ์สหสัมพันธ์และค่าสัมประสิทธิ์แสดงการตัดสินใจสูงสุด

จากผลการศึกษาสามารถสรุปได้ว่า การบูรณาการระหว่างเทคโนโลยีการรับรู้จากระยะไกล
แบบจำลองเชิงพื้นที่ นิเวศวิทยาภูมิทัศน์และการประเมินมูลค่าการให้บริการของระบบนิเวศ
สามารถนำมาใช้เป็นเครื่องมือเพื่อแสดงข้อมูลเชิงปริมาณของสถานภาพและการเปลี่ยนแปลงการใช้
ประโยชน์ที่ดินและสิ่งปกคลุมดิน และประเมินผลกระทบจากการเติบโตของเมืองต่อนิเวศภูมิทัศน์
ของเมือง การบริการของระบบนิเวศและอุณหภูมิพื้นผิวได้อย่างมีประสิทธิภาพ

สาขาวิชาภูมิสารสนเทศ   ลายมือชื่อนักศึกษา_____
ปีการศึกษา 2561   ลายมือชื่ออาจารย์ที่ปรึกษา_____

ANAKE SRISUWAN : URBAN GROWTH IMPACT ASSESSMENT ON LANDSCAPE ECOLOGY AND ECOSYSTEM SERVICE VALUE. THESIS ADVISOR : ASSOC. PROF. SUWIT ONGSOMWANG, Dr. rer. Nat. 323 PP.

URBAN GROWTH/ OBJECT-BASED IMAGE ANALYSIS /URBAN LANDSCAPE/ LANDSCAPE ECOLOGY/ ECOSYSTEM SERVICE VALUE

Land use and land cover (LULC) change occurs due to urbanization caused by unplanned and uncontrolled urban expansion has significant effects on urban landscape ecology and ecosystem services functions. Main objectives of the study were (1) to extract LULC status and its change during 2006 to 2016 and to simulate two different scenarios in 2026, (2) to assess urban growth impact on urban landscape ecology and ecosystem services during 2006 to 2026, (3) to identify relationship between ecosystem service function value and landscape pattern metrics, and (4) to evaluate and predict impact of urban growth on land surface temperature in Mueang Khon Kaen district, Khon Kaen province. Herein, Landsat imageries in 2006, 2011 and 2016 were firstly used to classify LULC types by OBIA and the derived results were applied to simulate LULC change in 2026 of two different scenarios by CLUE-S model and then to assess status and its change due to urban growth and its impact on landscape metrics, ecosystem service value and land surface temperature.

As results, main decreasing LULC area during 2006 to 2026 of two scenarios were paddy field and field crop while urban and built-up area, range land and unused land had been continuously increased in these periods. The derived LULC prediction of

IV

Scenario I and II in 2026 could provide realistic results as expectation. Urban growth characteristics by three indices (AEII, PU, and SI) indicated that urban area will be increased with very high urbanization rate and high development of urban area in the future. Additionally, urban landscape will be more expansion and complexity in irregularity and urban and built-up area landscape of Scenario I is more modification than Scenario II and pattern of urban and built-up area was strongly positive correlation with the area-weighted mean fractal dimension metric. Meanwhile, top three dominant ecosystem service functions from dynamic LULC data in the same periods were waste treatment, water supply and climate regulation while top three dominant LULC types that provide the highest total ecosystem service functions values (ESFV) were paddy field, water body and marsh and swamp. In addition, percent of landscape of LULC types was the most dominant independent variable to describe most of the ESFV, except food production. Finally, the extracted land surface temperature (LST) in 2016 varied from 18.799 to 34.468°C with mean temperature of 27.07°C and the highest temperature was mostly found at urban and built-up area such as airport or CBD. Additionally, the LST and multiple landscape metrics relationship was here chosen an optimum approach to predict LST since it can provide the highest range, the correlation coefficient and coefficient of determination values.

In conclusion, it can be here concluded that the integration of remote sensing technology, geospatial models, landscape ecology and ecosystem service evaluation can be used as capable tools to quantify LULC status and its change and to assess urban growth impact on urban landscape ecology, ecosystem services and LST.

School of Geoinformatics Student's Signature _____

Academic Year 2018 Advisor's Signature _____

ACKNOWLEDGEMENTS

CONTENTS

CHAPTER

CONTENTS (Continued)

CONTENTS (Continued)

CONTENTS (Continued)

CONTENTS (Continued)

CONTENTS (Continued)

CONTENTS (Continued)

LIST OF TABLES

LIST OF TABLES (Continued)

LIST OF TABLES (Continued)

LIST OF TABLES (Continued)

LIST OF TABLES (Continued)

LIST OF TABLES (Continued)

LIST OF TABLES (Continued)

LIST OF TABLES (Continued)

LIST OF TABLES (Continued)

LIST OF FIGURES

LIST OF FIGURES (Continued)

LIST OF FIGURES (Continued)

LIST OF FIGURES (Continued)

LIST OF FIGURES (Continued)

LIST OF FIGURES (Continued)

LIST OF FIGURES (Continued)

XXIX

LIST OF FIGURES (Continued)

LIST OF ABBREVIATIONS

AEII   = Annual Expansion Intensity index

CA   = Class area

CAP   = Average income per capita at sub-district level

CBD   = Central Business District

CDD   = Community Development Department

CLUE-S   = Conversion of Land Use and its Effects modeling

CONTAG   = Contagion index

DEM   = Digital Elevation Model

DOPA   = Department Of Provincial Administration

DPT   = Department of Public Work and Town & Country Planning:

D2Ur   = Distance to existing urban area

D2R   = Distance to road network

D2STR   = Distance to stream

ED   = Edge density

ELE   = Elevation

ESV   = Etimated ecosystem service value

ESFV   = Ecosystem service function values

ETM+   = Enhanced Thematic Mapper Plus

Fc   = Field Crop

FRAC_AM= Area-weighted mean patch fractal dimension

LIST OF ABBREVIATIONS (Continued)

Fo   = Forest Land

GISTDA   = Geo-Informatics and Space Technology Development Agency

                  (public organization)

IJI   = Interspersion Juxtaposition Index

Km2   = Square kilometer

KKMUNI = Khon Kaen Municipality

LDD   = Land Development Department

LD   = Land Department

LP   = Land value in each land value zone

LSI   = Landscape Shape Index

LST   = Land surface temperature

LULC   = Land Use and and Land Cover

LWM   = Land and Water Mask

Max. diff. = Max intensity difference

Ms   = Marsh and swamp

NDVI   = Normalized Difference Vegetation Index

NDWI   = Normalized Difference Water Index

NHA   = National Housing Authority

NP   = Number of Patch

OBIA   = Object-based image analysis

OLI   = Operational Land Imager

LIST OF ABBREVIATIONS (Continued)

Pd	=	Paddy Field
PD	=	Patch Density
PLAND	=	Percent of landscape
POP	=	Population density at sub-district level
PU	=	Urban land percentage
Ra	=	Range land
RTSD	=	Royal Thai Survey Department
SI	=	Urban land expansion index
SLO	=	Slope
SHAPE_AM	=	Area-weighted mean shape index
SHDI	=	Shannon's Diversity Index
SHEI	=	Shannon's Evenness Index
TCEB	=	Thailand Convention and Exhibition Bureau
TE	=	Total edge
Ul	=	Unused land
Ur	=	Urban and built-up area
Wa	=	Water body

CHAPTER I

INTRODUCTION

1.1 Background problem and significance of the study

Nowadays, the ecology of the planet as a whole increasingly influences by human activities, with cities and source center of demand for ecosystem services and sources of environmental impacts. Elmqvist et al. (2015). One of the most important environmental pressures, which impacts on natural landscape and ecosystem services is land use and land cover (LULC) change due to urbanization (Estoque and Murayama, 2013). The changes of LULC occur due to urbanization caused by unplanned and uncontrolled urban sprawl, which leads to change nature, destroy green cover and pollute the water resources (Al-shalabi, Pradhan, Billa, Mansora and Al-Sharif, 2013). Accelerating urban growth and LULC change increasingly pressure on the natural environment and human welfare and have become a global concern (Turner and Meyer, 1994) since these are believed to be responsible for the ecological degradation such as habitat fragmentation and biodiversity loss (Bihamta, Soffianian, Fakheran and Gholamalifard, 2014). Urban growth is a complex dynamical process associated with landscape change driving forces such as the environment, politics, geography and others that affect the city at multiple spatial and temporal scales (Akın, Aliffi and Sunar, 2014). Rapid urban development usually happens at the expense of prime agricultural land, with the destruction of natural landscape and public open space, which has an

increasing impact on the global environment change. The spatial-temporal process of urban development and the social-environmental consequences of such development deserve serious study by urban geographers, planers, and policy makers because of the direct and profound impacts on human beings (Liu, 2009).

Landscape pattern analysis provides an indirect approach for characterizing the ecological consequences of urbanization (Aguilera, Valenzuela and Botequilha-Leitão, 2011). Landscape ecology focuses on the analysis of landscape structure, the spatial implications of ecological processes in these landscapes and the changes that occur in them (Forman and Godron, 1986; Forman, 1995; Botequilha-Leitão et al., 2006; DiBari 2007). Because of their evident spatial dimension, landscape ecology and spatial planning converge in a common workspace (Antrop, 2001). Consequently, landscape ecology has been increasingly employed in spatial planning (Hummon, White, and Hulse, 1996; Gianoni, Di Noto, Stevanin and Zannin, 2001; Botequilha-Leitão and Ahern, 2002; Steinitz et al., 2003; Corry and Nassauer, 2005; Botequilha-Leitão et al., 2006; Kim and Ellis, 2009). In fact, in the last 10 years, it has been increasingly used to study the spatial characteristics of urban processes (Herold et al., 2003, 2005; Berling-Wolf and Wu, 2004), inter alia, the spatial characteristics of urban patches, including their size, shape, and spatial distribution. Many spatial landscape properties can be quantified by using a set of metrics (McGarigal, Cushman, Neel and Ene, 2002; Li and Wu, 2004; Uuemaa et al., 2009). Herold et al. (2003, 2005) and Seto and Fragkias (2005) use the term spatial metrics to more clearly differentiate these metrics from landscape metrics. Spatial metrics characterize urban form (Herold et al., 2003), whereas in ecological landscape studies, landscape metrics are explicitly linked to ecological functions (Gustafson, 1998; Luck and Wu, 2002; DiBari, 2007). In this

context, spatial metrics can be a very valuable tool for planners who need to better understand and more accurately characterize urban processes and their consequences (Herold et al., 2005; DiBari, 2007; Kim and Ellis, 2009).

The concept of ecosystem services is here defined as "the conditions and processes through which natural ecosystems, and the species that make them up, sustain and fulfil human life" (Luederitz et al., 2015). Daily (1997) provides a framework for conceptualizing and managing human–environmental interactions within the broader context of sustainability. Daily et al. (2009) applied ecosystem services on urban planning. Basically, the ecosystem services concept reveals urban populations' dependence on the goods and services appropriate from ecosystems (Elmqvist et al., 2013; Gómez-Baggethun and Barton, 2013). Li, Fang and Wang (2016) stated that ecosystems provide a multitude of services that are of fundamental significance to humans' well-being, livelihood, health and survival. The importance of these services has stimulated considerable interest in their conservation. After the seminar work of Costanza et al. (1997), the body of research on methods of estimating, mapping, and quantifying ecosystem services has grown exponentially (Fisher et al., 2009), particularly since the release of the Millennium Ecosystem Assessment (MA) with an international study involving over 1,300 scientists (de Groot et al., 2010, 2012). The MA provided an important evidence of the ongoing degradation of approximately 60% of the worlds ecosystems over the past five decades (Millennium Ecosystem Assessment, 2005). The Economics of Ecosystems and Biodiversity (TEEB), an international initiative, further confirmed this global trend of ecosystem deterioration and provided a scientific foundation to help decision makers recognize, demonstrate and capture the values of ecosystems (TEEB, 2010). Currently, hundreds of projects

and groups around the world are generating additional data on ecosystem services and on improving modeling, mapping, valuation, and management techniques stimulated by the aforementioned programs.

Khon Kaen province, one of the most intense urbanization cities in Thailand, situates in the central Northeast region, which is the poorest region of the country with 28.1% of population living in poverty. The acceleration of Khon Kaen's growth has been driven by internal and external urban driving force. As results of the first phase of the National Economic and Social Development Plan in 1962, it positioned Khon Kaen as the developing core of the Northeast region, particularly in the area of the economy, official administration, and education. At present, there are three universities, four colleges of higher education, and regional government center, the trade center of this region locate in the city. A Thai Government policy that is focusing the growth distribution on regional cities is driving these changes. It is applying the "Growth Poles" theory to develop Khon Kaen as a regional core of economic growth through increasing industrial activities. Meanwhile, the globalization driving force via economic cooperation, Greater Mekong Subregion (GMS), ASEAN, and Ayeyawady Chao Phraya Mekong Economic Cooperation Strategy (ACMECS), earmarkes Khon Kaen as a logistic hub of the Greater Mekong Region and East-West Economic Corridor linking the western and eastern regions of Myanmar to Viet Nam.

In addition, the Thailand Convention and Exhibition Bureau (TCEB) signed a Memorandum of Understanding with Khon Kaen in 2013 to promote the province as Thailand's fifth MICE (Meetings, Incentives, Conferencing, and Exhibitions) City. It is also expected to become a new transport hub in the Northeast region of Thailand. An industrial estate has been approved for Khon Kaen province. Previous economic growth

plans as well as new opportunities will have positive impacts on local economy including increased property values, new job opportunities, a rising of income levels, and will improve access to variety of goods and services (Afridi, 2015). Figure 1.1 shows unemployment rate by sex of Khon Kaen province during 2005 - 2013 while and Table 1.1 displays share of house current income by decile groups between 2011 and 2014.

On contrary, they will also create new problems related to social and environmental sustainability from motorization, congestion, air pollution, water pollution, municipal waste, suburban sprawl, increased flooding in the city and a longer duration of the floods in adjacent districts. A recent study by Kikuchi et al. (2013), who examined greenhouse gas emissions caused by transportation in Khon Kaen, observed that even though the city's population is increasing, the population at the city's center is decreasing due to suburban sprawl. Private investors are purchasing cheap land on the outskirts for housing estates and commercial development projects. This land is sometime vulnerable due to its location in risky areas such as flood pathways. As a result of land use change, the flow of water during rainy seasons and high intensity flooding is increasing.
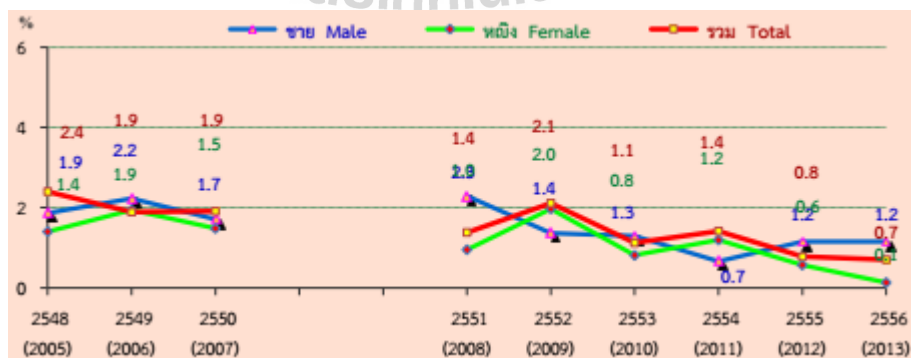
Source: Khon Kaen Provincial Statistical Office (2015).

Figure 1.1 Unemployment rates by sex of Khon Kaen Province during 2005 to 2013.

Table 1.1 Share of household current income by decile groups between 2011 and 2014.

Decile Group by Current Income	Percentage of Population		Percentage Share of Current Income		Current Income Per Capita (Bath)	
	2011	2014	2011	2014	2011	2014
1 (Lowest Income)	13.8	13.9	4.4	5.1	1,676	2,329
2	11.7	11.7	5.8	5.8	2,595	3,133
3	12.8	13.7	7.7	8.1	3,120	3,750
4	11.4	9.8	7.8	6.4	3,583	4,190
5	10.3	10.3	8.2	8	4,153	4,922
6	10.4	10.6	9.5	9.6	4,794	5,773
7	8.3	8.2	8.9	8.7	5,621	6,710
8	8	8.3	10.4	10.8	6,816	8,292
9	7.6	6.1	13.1	10.8	9,041	11,225
10 (Highest Income)	5.8	7.4	24.3	26.7	21,812	23,038

Source: Khon Kaen Provincial Statistical Office (2015).

Hence, this study aims to apply geoinformatics and geospatial models to assess urban growth impact on urban landscape ecology and ecosystem service values (ESV) of ecosystem service function of Mueang Khon Kaen district, Khon Kaen province. In addition, two future LULC scenarios in 2026 are simulated to identify landscape pattern and ecosystem service function value changes. Furthermore, the relationship between ecosystem service function value and landscape pattern metrics is identified to describe the role of landscape metrics of LULC type on ecosystem service function. Additionally, impact of urban growth on land surface temperature is examined by using multiple linear regression analysis for predicting LST of 2 different scenarios. The expected results will be useful for city planning, environment impact study, policy decision making for sustainable use of urban landscape in the near future.

1.2   Research objectives

The aims of the research are to assess urban growth impact due to land use and land cover change on urban landscape ecology and ecosystem service values of ecosystem service functions. The specific objectives of the study are as follows:

(1) To extract land use and land cover status and its change during 2006 to 2016 and to simulate two different scenarios (historical land use development, planning and policy) in 2026;

(2) To assess urban growth impact on urban landscape ecology and ecosystem services during 2006 to 2026;

(3) To identify relationship between ecosystem service function value and landscape pattern metrics; and

(4) To evaluate and predict impact of urban growth on land surface temperature.

1.3   Scope and limitations of the study

1.3.1   Scope of the study

(1) LULC types include (1) urban and built-up area, (2) paddy field, (3) field crop, (4) forest land, (5) water body, (6) marsh and swamp, (7) range land and (8) unused land are extracted from Landsat data in 2006, 2011 and 2016 using nearest neighbor classifier with feature space optimization of eCognition software. The derived results are used to describe urban growth during 2006 to 2016.

(2) The derived LULC data in 2011 with transitional change matrix between 2006 and 2011 and driving factors for LULC location are firstly used to simulate LULC in 2016 and its result is then compared with the classified LULC in 2016 and assessed accuracy for CLUE-S model validation. If overall accuracy and

Kappa hat coefficient of agreement between the simulated LULC in 2016 and classified LULC in 2016 are equal or more than 80%, the derived configuration of CLUE-S model is further applied to simulate two LULC scenarios (historical land use development and planning and policy) in 2026. The derived results are used to describe urban growth of two scenarios in 2026.

(3) Urban growth impact on urban landscape ecology during 2006 to 2026 (Scenario I and II) is assessed by landscape pattern analysis with FRAGSTAT software (McGarigal and Marks, 1995). In this study, 10 landscape metrics at class level (class area, percent of landscape, total edge, edge density, area weighted mean shape index, area weighted mean patch fractal dimension, interspersion and juxtaposition index, landscape shape index, patch density and number of patch) and 3 landscape metrics at landscape level (contagion, Shannon's diversity index and Shannon's evenness index) are applied to characterize impact of urban growth landscape. In addition, the relationship between urban growth pattern in 2016 and landscape metrics at class level is examined to identify optimum landscape metric to characterize urban growth pattern.

(4) Urban growth impact on ecosystem service during 2006 to 2026 (Scenario I and II) is evaluated using simple benefit transfer method of Costanza (1997). Herein, status and change of ESV of ecosystem service function which includes (1) gas regulation, (2) climate regulation, (3) waste treatment, (4) soil formation, (5) biodiversity protection, (6) water supply, (7) food production, (8) raw materials, and (9) recreation and culture are applied to characterize urban growth impact on ecosystem service function during 2006 and 2026.

(5) The relationship between ecosystem service function value and landscape pattern metrics are identified using multiple linear regression analysis with stepwise approach of SPSS statistics software. The derived results can be applied to describe the significant of landscape metrics of LULC type on ecosystem service function value.

(6) Impacts of urban growth on LST are evaluated based on LST in 2016 and landscape metrics using multiple linear regression analysis. The derived result is applied to predict LST of two different scenarios in 2026.

1.3.2 Limitation of the study

(1) Availability of Landsat data in 2006, 2011, and 2016 depends on downloadable data of USGS's service via website.

(2) Due to the limitation of ground reference points on LULC type in 2006 and 2011, Google imageries acquired in 2006 and 2011 are applied as reference ground information for accuracy assessment

1.4   Study area

Muang Khon Kaen district, Khon Kaen province, which consists of 18 sub-districts including (1) Nai Mueang, (2) Samran, (3) Khok Si, (4) Tha Phra, (5) Ban Thum, (6) Mueang Kao, (7) Phra Lap, (8) Sawathi, (9) Ban Wa, (10) Ban Kho, (11) Daeng Yai, (12) Don Chang, (13) Don Han, (14) Sila, (15) Ban Pet, (16) Nong Tum, (17) Bueng Niam and (18) Non Thon is chosen as study area. It situates in the central part of Khon Kaen province and has neighboring districts, namely Sam Sung, Nam Phong, Ubolratana, Ban Fang, Phra Yuen and Ban Haet. The study area covers area of 953.4 km^2 (Figure 1.2).
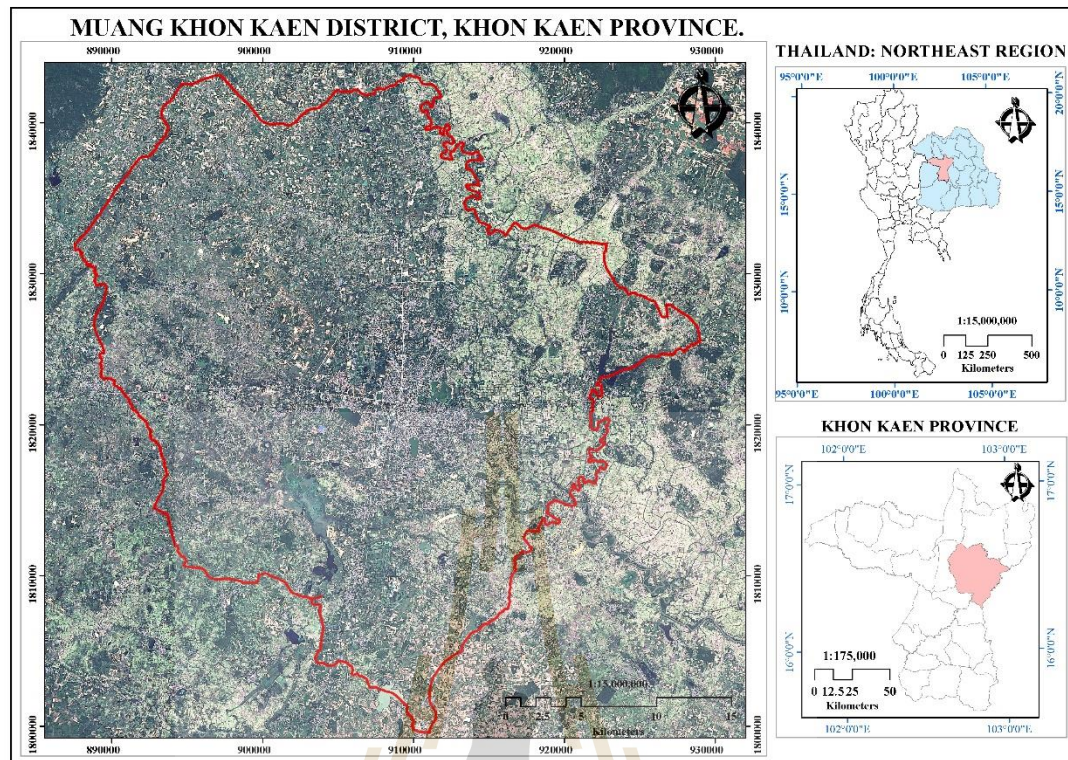
Figure 1.2 Map of the study area.

1.5 Benefit of the results

(1) To understand the situations and changes of LULC development in the study areas in 2006, 2011, 2016 and 2026 (2 scenario);

(2) To understand urban growth impact due to LULC change on urban landscape ecology, ecosystem service function value and land surface temperature;

(3) To understand of how landscape structure contributes to the provision of ecosystem service based on the relationship between urban landscape pattern metrics and ecosystem service function value;

(4) The results of the study, particularly LULC change on ecosystem service function value, can be as a guideline for city planning, environment impact study, policy decision making for sustainable use of urban landscape in the future.

CHAPTER II

BASIC CONCEPTS AND LITERATURE REVIEWS

Basic concepts including (1) Urban growth perspective, (2) Landscape pattern analysis and its metrics, (3) CLUE-S Model, (4) Ecosystem services evaluation, (5) Land surface temperature (LST) and (6) literature reviews are summarized in this chapter.

2.1 Urban growth perspective

2.1.1 Definition of urban growth

Yu (2013) defined that urban growth is spatial and demographic processes, as those of (a) expansion, (b) metabolism and (c) mobility. As a general rule, the typical tendency of urban growth is the extending radically from its central business and commercial district by a serious of concentric circles. It is believed by some scholars that urban growth is the products of the organization's processes and disorganization's processes (Burgess, 2009). The distributions of population into the natural areas of the city, the differentiations into social and cultural groupings and the divisions of labor are all the factors that influence the growth of a city. The spatial configurations and the dynamic tendency of urban growth are essential topics of analysis in the modern urban studies. The pattern of urban land-use can be seen as a static phenomenon while the process can be seen as a dynamic phenomenon (Bhatta, 2010).

2.1.2 Studying spatial and temporal urban growth

Herold, Hemphill and Clarke (2007) had proposed conceptual approaches for studying spatial and temporal urban dynamics that mostly relies on two general perspectives: top-down (from process to structure) and bottom-up (from structure to process) as shown in Figure 2.1. The traditional perspective follows a top down perspective: isolating urban structure as the outcome of pre-specified processes of urban change (from process to structure). This point of view is common in the field of planning, geography, and economics. The main criticism of reductionist perspective is that it is only marginally representative of the spatial and temporal complexities of urban change. Early demographic and socioeconomics research was limited by the ability to conduct detail spatiotemporal pattern analysis at anything other than aggregate levels. These logistical constraints led to conclusions from most early investigation base on a top–down chain of causality. This era generated significant contributions and raise compelling questions regarding urban theory, but one unanswered questions persists: how do cities from over time.

Recently, urban studies from the various agencies have been started to address more dynamics (White, Luo and Hatna, 2001; Batty, 2002) and has become more focusing on isolating the driver of growth rather than solely the emerging geographic patterns. Although new urban model have provided insight in to some aspects of urban dynamics, a deeper understanding to the spatial pattern and processes associated with urbanization is still limited by availability of suitable data and lack of compatible theory (Longley and Mesev, 2000). It is well understood that good models and good theory necessitate reliable measurements that capture spatiotemporal dynamics. This need it emphasized in the deductive, bottom-up perspective. Consistent

empirical observation of actual spatial structure in spatial and temporal detail is need to link change over time to specific hypotheses about the processes involved (from structure to process). A key sources of such information is remotely sensed observations (Herold et al., 2003; Lo, 2004).
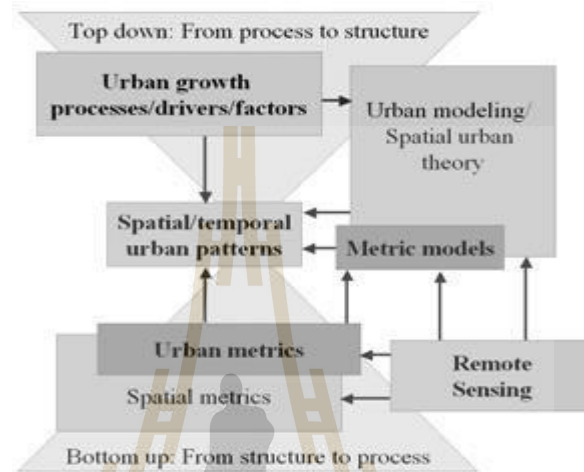
Source: Herold, Hemphill and Clarke (2007).

Figure 2.1 Conceptual approaches for studying spatial and temporal urban dynamics.

2.1.3 Causes of urban growth

Battha (2010) stated that causes of urban growth are quite similar with those of sprawl. In most of instances cannot be discriminated since urban growth and sprawl are highly interlinked. However, it is important to realize that urban growth may be observed without the occurrence of sprawl, but sprawl must induce growth in urban area. Some of the causes, for example population growth, may result in coordinated compact growth or uncoordinated sprawled growth. Whether the growth is good or bad depends on its pattern, process, and consequences. There are also some of the causes that are especially responsible for sprawl, they cannot result in a compact neighborhood. For example, country-living desire some people prefer to live in the rural

countryside; this tendency always results in sprawl. Table 2.1 lists the causes of urban growth results in compact growth and sprawled growth by several researchers (Burchfield, Overman, Puga and Turner, 2006; Squires, 2002; Harvey and Clark, 1965).

2.1.4 Consequences of urban growth

Consequences of urban growth may have both positive and negative impacts; however, negative impacts are generally more highlighted because this growth is often uncontrolled or uncoordinated and therefore the negative impacts override the positive sides. Positive implications of urban growth include higher economic production, opportunities for the underemployed and unemployed, better life because of better opportunities and better services, and better lifestyles. Urban growth can extend better basic services (such as transportation, sewer, and water) as well as other specialist services (such as better educational facilities, health care facilities) to more peoples. However, in many instances, urban growth is uncontrolled and uncoordinated resulting in sprawl. As a result, the upside impacts vanish inviting the downsides.

Table 2.1 Causes of urban growth which may result in compact and/or sprawled growth.

Causes of urban growth	Compact growth	Sprawled growth
Population growth	•	•
Independence of decision		•
Economic growth	•	•
Industrialization	•	•
Speculation		•
Expectations of land appreciation		•
Land hunger attitude		•
Legal disputes		•
Physical geography		•
Road width		•
Development and property tax		•
Living and property cost		•
Lack of affordable housing		•
Demand of more living space		•
Public regulation		•
Transportation		•
Single-family home		•
Nucleus family		•
Credit and capital market		•
Government developmental policies		•
Lack of proper planning policies		•
Failure to enforce planning Policies		•
Country-living desire		•
Housing investment		•
Large lot size		•

Source: Battha (2010).

In the developed countries, during the nineteenth and early twentieth centuries, urbanization resulted from and contributed to industrialization. New job opportunities in the cities motivated the mass movement of surplus population away from the villages. At the same time, migrants provided cheap, plentiful labor for the emerging factories. Currently, due to movements such as globalization, the circumstances are similar in developing countries. The concentration of investments in cities attracts large number of migrants looking for employment, thereby creating a large

16

surplus labor force, which keeps wages low. This situation is attractive to foreign investment companies from developed countries who can produce goods for far less than if the goods were produced where wages are higher. Thus, one might wonder if urban poverty serves a distinct function for the benefit of global capital (Bhatta, 2010).

One of the major effects of rapid urban growth is sprawl that increases traffic, saps local resources, and destroys open space. Urban sprawl is responsible for changes in the physical environment, and in the form and spatial structure of cities. In many countries including the developed countries like United States, poorly planned urban development is threatening the environment, health, and quality of life. In communities across the world, sprawl is taking a serious toll (Bhatta, 2010).

Evidence of the environmental impacts of sprawl continues to mount. Kirtland et al. (1994) report that the impact of urban land on environmental quality is much larger than its spatial extent would imply. The consequences and significance of sprawl, good or ill, are evaluated based on its socioeconomic and environmental impacts. Often these are overlapping or one may have several indirect impacts. Major consequences of urban sprawl can be summarized based on Bhatta (2010) as follows.

(a) Inflated infrastructure and public service costs

Sprawl is usually accepted as being inordinately costly to its occupants and to society (Harvey and Clark, 1965). Sprawl is blamed due to its environmental cost and economic cost (Buiton, 1994). Cities have experienced an increase in demand for public services and for the maintenance and improvement of urban infrastructures (Barnes et al., 2001) such as fire-service stations, police stations, schools, hospitals, roads, water mains, and sewers in the countryside. Sprawl requires more infrastructures, since it takes more roads, pipes, cables and wires to service these low-density areas

compared to more compact developments with the same number of households. Other services such as waste and recyclables collection, mail delivery and street cleaning are more costly in low-density developments, while public transit is impractical because the rider density needed to support a transit service is not there.

(b) Energy inefficiency

Higher densities mean shorter trips but more congestion. Newman and Kenworthy (1988) found that the former effect overwhelms the latter. Even though vehicles are not as fuel efficient in dense areas owing to traffic congestion, fuel consumption per capita is still substantially less in dense areas because people drive so much less.

With electricity, there is a cost associated with extending and maintaining the service delivery system, as with water, but there also is a loss in the commodity being delivered. The farther from the generator, the more power is lost in distribution.

(c) Disparity in wealth

There is marked spatial disparity in wealth between cities and suburbs; and sprawled land development patterns make establishing and using mass transit systems difficult (Benfield et al., 1999; Kunstler, 1993; Mitchell, 2001; Stoel, 1999). Sprawl is also implicated in a host of economic and social issues related to the deterioration of urban communities and the quality of life in suburbia (Wilson et al., 2003). Urban sprawl often occurs in peripheral areas without the discipline of proper planning and zoning; as a result, it blocks the ways of future possible quality services.

(d) Impacts on wildlife and ecosystem

In areas where sprawl is not controlled, the concentration of human presence in residential and industrial settings may lead to an alteration of ecosystems patterns and processes (Grimm et al., 2000). Development associated with sprawl not only decreases the amount of forest area (Macie and Moll, 1989; MacDonald and Rudel, 2005), farmland (Harvey and Clark, 1965), woodland (Hedblom and Soderstrom, 2008), and open space but also breaks up what is left into small chunks that disrupt ecosystems and fragment habitats (Lassila, 1999; McArthur and Wilson, 1967; O'Connor et al., 1990). The reach of urban sprawl into rural natural areas such as woodlands and wetlands ranks as one of the primary forms of wildlife habitat loss. Roads, power lines, subdivisions and pipelines often cut through natural areas, thereby fragmenting wildlife habitat and altering wildlife movement patterns

(e) Loss of farmland

Urbanization generally, and sprawl in particular, contribute to loss of farmlands and open spaces (Berry and Plaut, 1978; Fischel, 1982; Nelson, 1990; Zhang et al., 2007). Urban growth, only in the United States, is predicted to consume 7 million acres of farmland, 7 million acres of environmentally sensitive land, and 5 million acres of other lands during the period 2000–2025 (Burchell et al., 2005). This case is enough to visualize the world scenario.

The loss of agricultural land to urban sprawl means not only the loss of fresh local food sources but also the loss of habitat and species diversity, since farms include plant and animal habitat in woodlots and hedgerows. The presence of farms on the rural landscape provides benefits such as green space, rural economic stability, and preservation of the traditional rural lifestyle.

(f) Increase in temperature

Positive correlation between land surface temperature and impervious surface clearly indicates temperature increase in the sprawled area (Weng et al., 2007, 2003). On warm days, urban areas can be 6–8°F (3.5–4.5°C) warmer than surrounding areas, an effect known as an urban heat island (Frumkin, 2002) (Figure 2.2). The heat island effect is caused by two factors. First, dark surfaces such as roadways and rooftops efficiently absorb heat from sunlight and reradiate it as thermal infrared radiation; these surfaces can reach temperatures of 50–70°F (28–39°C) higher than surrounding air. Second, urban areas are relatively devoid of vegetation, especially trees; that would provide shade and cool the air through evapotranspiration. As cities sprawl outward, the heat island effect expands, both in geographic extent and in intensity. This is especially true if the pattern of development features extensive tree cutting and road construction.

Furthermore, dispersed metropolitan expansion involves a positive feedback loop that may aggravate the heat island effect. Sprawling metropolitan areas, with greater travel distances, generate a large amount of automobile travel. This, in turn, results in more fuel combustion, with more production of carbon dioxide, and consequent contributions to global climate change.

The number of habitants is a decisive factor conditioning the occurrence of urban heat island. Figure 2.3 shows increased city size (represented by circles) with increasing number of habitants is responsible for increasing urban temperature.
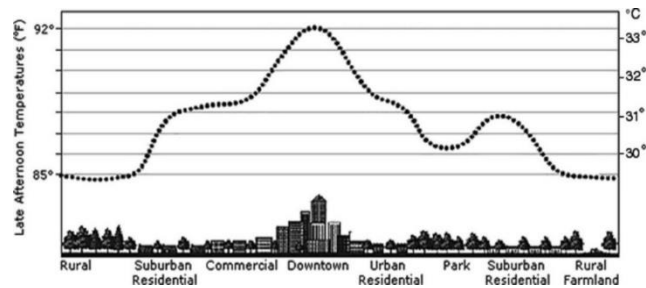
Source: Klinenberg (2002).

Figure 2.2 An urban heat island profile.
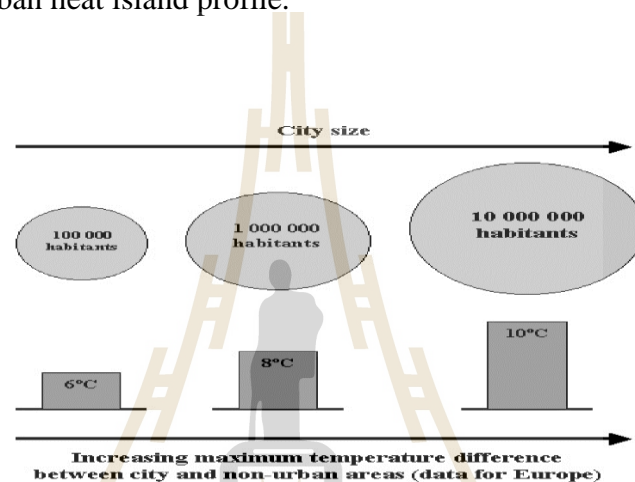
Source: http://www.atmosphere.mpg.de.

Figure 2.3 Increased city size and number of habitants cause increase in temperature.

(g) Poor air quality

Sprawl is cited as a factor of air pollution (Stone, 2008), since the car-dependent lifestyle imposed by sprawl leads to increases in fossil fuel consumption and emissions of greenhouse gases (Stoel, 1999). Urban sprawl contributes to poorer air quality by encouraging more automobile use, thereby adding more air pollutants such as carbon monoxide, carbon dioxide, ground-level ozone, sulphur dioxide, nitrogen oxides, volatile organic carbons, and microscopic particles (Frumkin, 2002).

(h) Impacts on water quality and quantity

Sprawl also has serious impacts on water quality and quantity. With miles of roads, parking lots and houses having paved over the countryside, rainwater and snowmelt are unable to soak into the ground and replenish the groundwater aquifers.

Urban growth and sprawl lead to an increasing imperviousness, which in turn induces more total runoff volume. So urban areas located in flood prone areas are exposed to increased flood hazard, including inundation and erosion (Jacquin et al., 2008).

(i) Impacts on public and social health

One of the original motivations for migration to the suburbs was access to nature. People generally prefer to live with trees, birds, and flowers; and these are more accessible in the suburbs than in denser urban areas. Moreover, contact with nature may offer benefits beyond the purely aesthetic; it may benefit both mental and physical health. In addition, the sense of escaping from the turmoil of urban life to the suburbs, the feeling of peaceful refuge, may be soothing and restorative to some people. In these respects, there may be health benefits to suburban lifestyles (Frumkin, 2002). However, sprawl is generally blamed for its negative impacts on public health (Frumkin, 2002; Savitch, 2003; Yanos, 2007; Sturm and Cohen, 2004).

One of the cardinal features of sprawl is driving, reflecting a well-established, close relationship between lower density development and more automobile travel. Automobile use offers extraordinary personal mobility and independence. However, it is also associated with health hazards, including air pollution, motor vehicle crashes, and pedestrian injuries and fatalities (Frumkin, 2002).

Air pollution causes severe breathing problems, skin diseases, and other health problems. The effects of air pollution on the health of human and other living species are perhaps known to everyone.

From the perspective of social health, low-density development is blamed for reducing social interaction and threatening the ways that people live together (Ewing, 1997; Putnam, 2000). Residents may also lose their sense of community as their town's population swells dramatically.

(j) Other impacts

Exurban development can place additional burdens on rural economic/land-use activities such as forestry, mining, and farming, since the values of exurbanites may clash with those of traditional users regarding the most suitable uses of rural lands.

Urban sprawl, a potential manifestation of development, has its negative impacts in coastal regions also, where beach-oriented tourism and amenity-driven population growth and land development are prominent (Crawford, 2007).

Sprawl also includes aesthetic impacts such as more ugly and monotonous sub- urban landscapes. For other several indirect impacts of sprawl please refer Barnes et al. (2001) and Squires (2002).

2.2   Landscape pattern analysis and its metrics

A disruption in landscape patterns may therefore compromise this structure's functional integrity by interfering with critical ecological processes necessary for population persistence and the maintenance of biodiversity and ecosystem health (With, 1999). For these and other reasons, much emphasis has been placed on developing

methods to quantify landscape patterns, which is considered a prerequisite to the study of pattern–process relationships (e.g. Baker and Cai, 1992; McGarigal and McComb, 1995; O'Neill, Krumel, Gardner, Sukihara, Jackson, De Angelis, Milne, Turner, Zygmunt, Christensen, Dale and Graham, 1988; and Turner and Gardner, 1991). This has resulted in the development of literally hundreds of indices of landscape patterns (McGarigal, 2013).

The common usage of the term landscape metrics refers exclusively to indices developed for categorical maps. In addition, although a large part of landscape pattern analysis deals with the identification of scale and intensity of pattern, landscape metrics are focused on the characterization of the geometric and spatial properties of categorical map patterns represented at a single scale (grain and extent). Thus, while it is important to recognize the variety of types of landscape patterns and goals of landscape pattern analysis, the focus herein is on landscape metrics as they are commonly applied in landscape ecology (McGarigal, 2013).

Recently, urban change detection focus has been shifted from detection to quantification of change, measurement of pattern and analysis of pattern and process of urban growth and sprawl (Bhatta, 2010).

Various methods for measurement and analysis of urban growth, such as transition matrices, spatial metrics, and spatial statistics, among which spatial metrics for quantifying the structure and pattern of thematic map (including those of urban area) are commonly used in landscape ecology, where there are refer to as landscape metrics (O'Neill et al., 1988; Gustafson, 1998).

Bhatta (2010) mentioned that landscape metrics are used to numerically explain spatial structure of landscape or landscape structure. These metrics are useful to

understand how structures affect system interaction in a heterogeneous landscape, and the recognition and monitoring of landscape change (Turner, 1989; O'Neill et al., 1999; Turner et al., 2001).

Metrics and method used in landscape ecology and often influenced by other such as computational complexity theory, fractal geometry, and spatial statistics. Commonly used metrics can be subdivided into two broad categories (Hardin et al., 2007).

- Measurement of individual patch characteristics (e.g., size, shape, perimeter, perimeter-area ratio, fractal dimension).

- Measurement of whole landscape characteristics (e.g., richness, evenness, dispersion, contagion). Metrics of landscape characteristics are typically more computationally and analytically complex than individual patch metrics (Farina, 1998)

Landscape metrics have found important application in quantifying urban growth, sprawl, and fragmentation (Hardin et al., 2007). Herold et al. (2002) shown an early landmark in this shift by establishing that low-density residential, high density residential, and commercial zone can be discriminated by spatial metrics such as fractal dimension, landscape percentage, patch density, edge density, patch size standard deviation, contagion index, and area weighted average patch fractal dimension. These metrics were also capable of quantifying the land conversion. When applied to multi-scale or multi-temporal datasets, spatial metrics can be used to analyze and describe change in the degree of spatial heterogeneity (Dunn et al., 1991; Wu et al., 2000).

Based on the work of O' Neill et al. (1988), set of different spatial metrics have been developed, modified and test (Hergis et al., 1998; McGarigal et al., 2002; Riitters

et al., 1995). Spatial metrics can be grouped into three broad classes: patch, class, and landscape metrics (Bhatta, 2010).

(1) patch-level metrics are computed for every patch in the landscape,

(2) class-level metrics are computed for every class in the landscape,

(3) landscape-level metrics are computed for entire patch mosaic.

Landscape metrics highly concentrate landscape information and reflect the structural composition and spatial configuration of landscape features. They are widely used in the analysis of urban environment (Grimm et al., 2000). In recent years, landscape pattern metrics have been used to quantify the spatiotemporal dynamics of urban landscape pattern of an urban area (Wu et al., 2000) and to describe the regularity of urbanization process (Grimm et al., 2000).

Frequently landscape metrics which are used in urban growth analysis based on journal papers published in 1996–2015 using FRAGSATAT software can be grouped and summarized based on McGarigal (2015) as follows:

(1) Area and edge metrics,

(2) Shape metrics,

(3) Aggregation metrics,

(4) Diversity metrics.

2.2.1 Area and edge metrics

Area metrics quantify landscape composition, not landscape configuration. The area of each patch comprising a landscape mosaic is perhaps the single most important and useful piece of information contained in the landscape. Not only is this information the basis for many of the patch, class, and landscape indices, but patch area has a great deal of ecological utility in its own right.

(1) Class area (CA). CA is a measure of landscape composition; specifically, how much of the landscape is comprised of a particular patch type. This is an important measure in a number of ecological applications. For example, an important by-product of habitat fragmentation is quantitative habitat loss. In the study of forest fragmentation, therefore, it is important to know how much of the target patch type (habitat) exists within the landscape.

$$\text{CA} = \sum_{j=1}^{n} a_{ij} \left(\frac{1}{10,000}\right) \tag{2.1}$$

Where a_{ij} is area (m^2) of patch ij.

(2) Percent of landscape (PLAND). PLAND is fundamental measures of landscape composition; specifically, how much of the landscape is comprised of a particular patch type. This is an important characteristic in a number of ecological applications.

$$\text{PLAND} = P_i = \frac{\sum_{j=1}^{n} a_{ij}}{A} \times (100) \tag{2.2}$$

Where P_i is proportion of the landscape occupied by patch type (class) i,

a_{ij} is area (m^2) of patch ij,

A is total landscape area (m^2).

(3) Total edge (TE). TE is an absolute measure of total edge length of a particular patch type (class level) or of all patch types (landscape level). In applications that involve comparing landscapes of varying size, this index may not be useful.

$$\text{TE} = \sum_{k=1}^{m} e_{ik} \tag{2.3}$$

Where e_{ik} is total length (m) of edge in landscape involving patch type (class)

i; includes landscape boundary and background segments involving

patch type i.

(4) Edge density (ED). ED standardizes edge to a per unit area basis that facilitates comparisons among landscapes of varying size. However, when comparing landscapes of identical size, total edge and edge density are completely redundant. Alternatively, the amount of edge present in a landscape can be compared to that expected for a landscape of the same size but with a simple geometric shape (square) and no internal edge.

$$ED = \frac{\sum_{k=1}^{m} e_{ik}}{A} \ (10,000) \tag{2.4}$$

Where e_{ik} is total length (m) of edge in landscape involving patch type (class)

i; includes landscape boundary and background segments involving

patch type i and A is total landscape area (m^2).

2.2.2 Shape metrics

(1) Area-weighted mean shape index (SHAPE_AM). SHAPE_AM of patches at the class and landscape levels by weighting patches according to their size. This index may be more appropriate than the unweighted mean shape index in cases where larger patches play a dominant role in the landscape function relative to the phenomenon under consideration. The difference between the unweighted and weighted mean shape indices can be particularly noticeable when sample sizes are small

$$\text{SHAPE\_AM} = \sum_{j=1}^{n} \left[\left(\frac{.25 P_{ij}}{\sqrt{a_{ij}}} \right) \left(\frac{a_{ij}}{\sum_{j=1}^{n} a_{ij}} \right) \right] \tag{2.5}$$

Where P_{ij} is perimeter (m) of patch ij, a_{ij} is area (m^2) of patch ij.

(2) Area-weighted mean patch fractal dimension (FRAC_AM). The FRAC_AM at the class and landscape levels by weighting patches according to their size, although these metrics do not have the same interpretation. These indices may be particularly meaningful if the focus of the analysis is on patch characteristics; that is, when patch-level phenomena are deemed most important and patch shape is particularly meaningful.

$$\text{FRAC\_AM} = \sum_{j=1}^{n} \left[\left(\frac{2 \ln(.25P_{ij})}{\ln a_{ij}} \right) \left(\frac{a_{ij}}{\sum_{j=1}^{n} a_{ij}} \right) \right] \qquad (2.6)$$

Where P_{ij} is perimeter (*m*) of patch ij and a_{ij} is area *(m^2)* of patch ij.

2.2.3 Aggregation Metrics

Aggregation refers to the tendency of patch types to be spatially aggregated; that is, to occur in large, aggregated or "contagious" distributions. This property is also often referred to as landscape texture, as follows.

(1) Contagion index (CONTAG). One popular index that subsumes both dispersion and interspersion based on the probability of finding a cell of type i next to a cell of type j. This contagion index consists of the sum over patch types of the product of 2 probabilities: (1) the probability that a randomly chosen cell belongs to patch type i (estimated by the proportional abundance of patch type i), and (2) the conditional probability that given a cell is of patch type i, one of its neighboring cells belongs to patch type j (estimated by the proportional abundance of patch type i adjacencies involving patch type j).

$$\text{CONTAG} = \left[1 + \frac{\sum_{i=1}^{m} \sum_{k=1}^{m} \left[P_i \times \frac{g_{ik}}{\sum_{k=1}^{m} g_{ik}} \right] \times \left[\ln \left(P_i \times \frac{g_{ik}}{\sum_{k=1}^{m} g_{ik}} \right) \right]}{2\ln(m)} \right] (100) \qquad (2.7)$$

Where P_i is proportion of the landscape occupied by patch type (class) i,

g_{ik} is number of adjacencies (joins) between pixels of patch types

(classes) i and k based on the double-count method, and

m is number of patch types (classes) present in the landscape, including

the landscape border if present.

(2) Interspersion and Juxtaposition Index (IJI). The interspersion index measures the extent to which patch types are interspersed (not necessarily dispersed); higher values result from landscapes in which the patch types are well interspersed (i.e., equally adjacent to each other), whereas lower values characterize landscapes in which the patch types are poorly interspersed (i.e., disproportionate distribution of patch type adjacencies). The interspersion index is not directly affected by the number, size, contiguity, or dispersion of patches per se, as is the contagion index.

$$IJI= \frac{-\sum_{i=1}^{m}\sum_{k=i+1}^{m}\left[\left(\frac{e_{ik}}{E}\right)\ln\left(\frac{e_{ik}}{E}\right)\right]}{\ln(0.5[m(m-1)])} (100) \qquad (2.8)$$

Where e_{ik} is total length *(m)* of edge in landscape between patch types *(*classes*)*

i and k,

E is total length *(m)* of edge in landscape, excluding background, and

m is number of patch types *(*classes*)* present in the landscape, including

the landscape border, if present.

(3) Landscape Shape Index (LSI). This index measures the perimeter-to-area ratio for the landscape as a whole. This index is identical to the habitat diversity index proposed by Patton (1975), except it apply this index at the class level. This index quantifies the amount of edge present in a landscape relative to what would be present in a landscape of the same size but with a simple geometric shape (circle in vector,

square in raster) and no internal edge (i.e., landscape comprised of a single circular or square patch).

$$\text{LSI} = \frac{.25 \sum_{k=1}^{m} e_{ik}}{\sqrt{A}} \tag{2.9}$$

Where e_{ik} is total length (m) of edge in landscape between patch types (classes)

i and k; includes the entire landscape boundary and some or all

background edge segments involving class i and

A is total landscape area (m^2).

(4) Patch Density (PD). Patch density has the same basic utility as number of patches as an index, except that it expresses number of patches on a per unit area basis that facilitates comparisons among landscapes of varying size.

$$\text{PD}= \frac{n_i}{A}(10,000)(100) \tag{2.10}$$

Where n_i is number of patches in the landscape of patch type (class) i and

A is total landscape area (m^2).

(5) Number of Patch (NP). Number of Patch of a particular habitat type may affect a variety of ecological processes, depending on the landscape context. A landscape with a greater number of patches has a finer grain; that is, the spatial heterogeneity occurs at a finer resolution. Although the number of patches in a class or in the landscape may be fundamentally important to a number of ecological processes, often it does not have any interpretive value by itself because it conveys no information about area, distribution, or density of patches.

$$\text{NP}= n_i \tag{2.11}$$

Where n_i is number of patches in the landscape of patch type (class) i.

2.2.4 Diversity Metrics

Diversity measures have been used extensively in a variety of ecological applications. They originally gained popularity as measures of plant and animal species diversity. Diversity measures are influenced by 2 components--richness and evenness. Richness refers to the number of patch types present; evenness refers to the distribution of area among different types. Richness and evenness are generally referred to as the compositional and structural components of diversity, respectively.

(1) Shannon's diversity index (SHDI). SHDI is the most popular diversity index based on information theory (Shannon and Weaver 1949). The value of this index represents the amount of "information" per individual (or patch, in this case).

$$SHDI = -\sum_{i=1}^{m}(P_i * \ln P_i) \tag{2.12}$$

Where P_i is proportion of the landscape occupied by patch type (class) i.

(2) Shannon's Evenness Index (SHEI). Evenness measures the other aspect of landscape composition--the distribution of area among patch types. There are numerous ways to quantify evenness and most diversity indices have a corresponding evenness index derived from them. In addition, evenness can be expressed as its compliment--dominance (i.e., evenness = 1 - dominance). Indeed, dominance has often been the chosen form in landscape ecological investigations (e.g., O'Neill et al., 1988; Turner et al., 1989; Turner 1990a), although many researchers prefer evenness because larger values imply greater landscape diversity.

$$SHEI = -\frac{\sum_{i=1}^{m}(P_i \ln P_i)}{\ln m} \tag{2.13}$$

Where P_i is proportion of the landscape occupied by patch type (class) i, and

m is number of patch types (classes) present in the landscape, excluding the landscape border if present.

2.3   CLUE-S Model

CLUE model or the Conversion of Land Use and its Effects modeling framework was developed to simulate land use change using empirically quantified relations between land use and its driving factors in combination with dynamic modeling of competition between land use types (Veldkamp and Fresco, 1996a; Verburg, De Koning, Kok, Veldkamp and Bouma, 1999). The model was developed for the national and continental level. Verburg et al. (2002) stated that the study areas with such a large extent the spatial resolution for analysis was coarse or pixel size varying between 7x7 and 32x32 sq. km such as Central America (Farrow and Winograd, 2001), Costa Rica (Veldkamp and Fresco, 1996b), China (Verburg and Veldkamp, 2001) and Indonesia (Verburg et al., 1999) are available. Each land use is represented by assigning the relative cover of each land use type to the pixels. The CLUE model cannot directly be applied at the regional scale. Therefore, the modeling approach has been modified and is now called CLUE-S (Conversion of Land Use and its Effects at Small regional extent). Verburg (2010) stated that CLUE-S is specifically developed for the spatially explicit simulation of land use change based on an empirical analysis of location suitability combined with the dynamic simulation of competition and interactions between the spatial and temporal dynamics of land use systems. Major characteristics of CLUE-S including (1) CLUE-S module structure, (2) Spatial policies and restrictive, (3) Land use type specific conversion setting, (4) Land use requirement and (5) Location characteristics and (6) allocation procedure are here summarized based on handbook of CLUE model by Verburg (2010).

2.3.1 CULE-S module structure

The model is made up into two distinct modules, a non-spatial module and a spatially module. The non-spatial module calculates the aggregate area, by simple trend extrapolations, the change annual area (demand) for all land use types. In the second part of the model, demands of part one are translated into land use changes at various locations within the study region using a raster-based system. The allocation is based upon a combination of empirical, spatial analysis and dynamic modeling (Verburg et al., 2002). Empirical analysis is applied to determine the relationships between spatial distribution of land use and a number of proximate factors that are driving or constraining land-use change. Based on the competitive advantage of each land use at a location, the competition among land uses for a particular location is simulated.

2.3.2 Spatial policies and restrictions

Spatial policies and restrictions can pressure areas where land use changes are restricted through policies or tenure status (Verburg, Steeg, Van de and Schulp, 2005). The implement of policy to land use types must be supplied such as a forest reserve policy from a logging ban, species-specific habitat of wildlife sanctuary, residential construction in designated agricultural areas or permanent agriculture in the buffer zone of a nature reserve and so on. These policies and restrictions are specific land use conversions condition. It should be mentioned that the conversions that are restricted by a certain spatial policy can be indicated in a land use conversion matrix for all possible land use conversions it is indicated if the spatial policy applies.

2.3.3 Land use type specific conversion settings

The temporal dynamics of the simulations upon the setting of land use type specific conversion determines. Two sets of parameters setting are therefore needed to characterize the individual land use types: conversion elasticity and land use transition sequences.

The first parameter set, the conversion elasticity, is related to land use change between types. Because a high cost to change will not easily be converted in other uses as long as there is sufficient demand. Examples are residential locations but also plantations with permanent crops (e.g., fruit trees). Land use type must be specific the relative elasticity to change from ranging between 0 (easy conversion) to 1 (not allow). The user should decide on this factor based on expert knowledge or observed behavior from history. The second set of land use transition sequences, likewise the first parameter, needs to be specified are the land use type specific conversion settings and their annual temporal characteristics. These settings are specified in a conversion matrix. Verburg (2010) suggested that the conversion matrix definition (Figure 2.4) should be answered the following questions.

1) Can be convert other land use types (present)?

2) The area or region is allowed or not (spatial policy or restriction)?

3) How many years (or time steps) the land use type at a location should remain the same before it can change into another land use type can be possible?

For example, in case of cropland, it cannot change directly into forest. Nevertheless, after a number of years it is achievable that a cropland will change into forest because of regrowth by natural or man-made.

In addition, Verburg (2010) emphasize the range of conversion or the minimum and maximum number of years before a conversion can or should be happen is indicated in the conversion table. It depends on the land use pressure and location specific conditions (Figure 2.5).
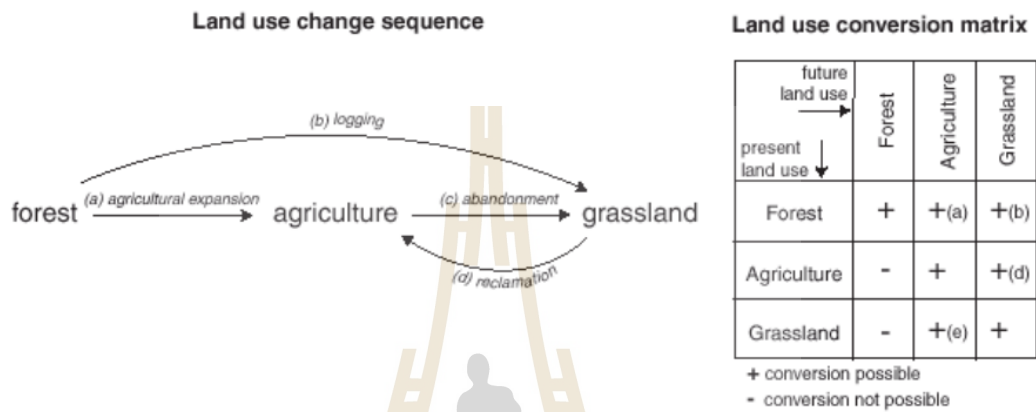
Source: Verburg, 2010.

Figure 2.4 Illustration of the translation of a hypothetical land use change sequence into a land use conversion matrix.
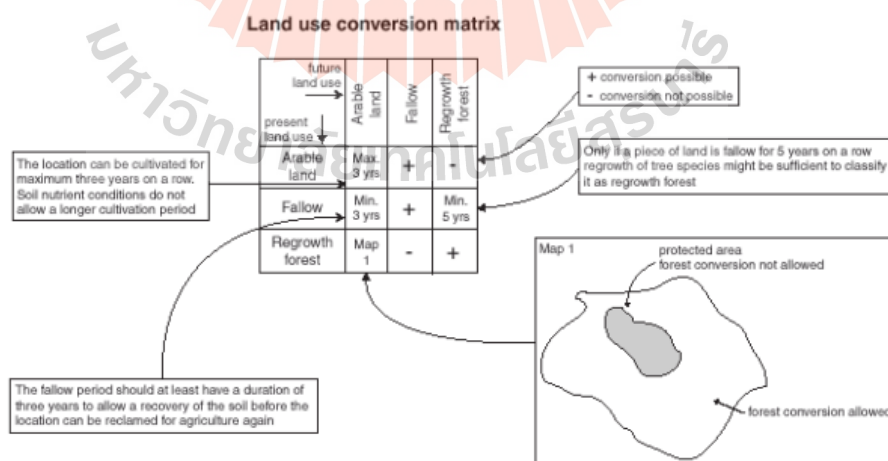
Source: Verburg, 2010.

Figure 2.5 Example of a land use conversion matrix with the different options implemented in the model.

2.3.4 Land use requirements (demand)

The main part of non-spatial are calculated at sum of total area from land use types as part of a specific scenarios. Land use requirements or demand side was determined for CLUE-S model by each area of land use types in processing. The extrapolation of trends in land use change in recent part into the near future is a common technique to calculate land use requirements (Verburg and Overmars 2009; Verburg, 2010). The demand depends on perspective of policy and/or population change or advance model to communicate with CLUE-S model such as SD model (Zheng et al., 2012), SAMBA (Castella, Kamb, Quangc, Verburg and Hoanh, 2007) and LEITAP (Perez-Soba et al., 2010).

2.3.5 Location characteristics

Location of land use conversions are expected to take place at the highest "preference" for the specific type of land use (Verburg, 2010) based on the relation between the occurrence of a land-use type and the physical and socioeconomic conditions of a specific location factors (Trisurat, Alkemade and Verburg, 2010). Those are based on the different, disciplinary, understandings of the determinants of land use change. The preference is calculated following:

$$R_{ki} = a_k X_{1i} + b_k X_{2i} + \dots + n_k X_{ni} , \qquad (2.14)$$

Where R_{ki} is the preference to devote location i to land use type k,

X_{ni} are biophysical or socio-economical characteristics of location i, and a_k,

$b_k \dots n_k$ are the relative impact of these characteristics on the preference for land use type k.

Although, the preference Rki cannot be observed or measured directly and has therefore to be calculated has a probability (Verburg, 2010). The function, that relates these probabilities with the biophysical and socio-economic location characteristics, is defined in a statistical model can be developed as a binomial logit model of two choices: convert location i into land use type k or not. The preference Rki is assumed to be the underlying response of this choice following:

$$Log\left(\frac{P_i}{1-P_i}\right) = \beta_0 + \beta_0 X_{1,i} + \beta_2 X_{2,i} \dots \dots + \beta_n X_{n,i} , \qquad (2.15)$$

Where P_i is the probability of a grid cell for the occurrence of the considered land use type on location I,

$X_{n,i}$ are the location factors, and the coefficients,

β_0 (are estimated through logistic regression using the actual land use pattern as dependent variable.

2.3.6 Allocation procedure

The spatial allocation module allocates the regional level demands to individual grid cells until the demand has been satisfied by iteratively comparing the allocated area of the individual land use types with the area demanded. Figure 2.6 provides a flowchart of the allocation procedure used. The allocation procedure of the Dyna-CLUE (latest version in 2006) at time (t) for each location (i) the land use/cover type (lu) with the highest total probability ($Ptot_{i,t,lu}$). The total probability is defined as the sum of the location suitability ($Ploc_{i,t,lu}$), neighborhood suitability ($Pnbh_{i,t,lu}$), conversion elasticity ($elas_{lu}$) and competitive advantage ($comp_{t,lu}$) (Verburg et al., 2002) as following:

$$Ptot_{i,t,lu} = Ploc_{i,t,lu} + Pnbh_{i,t,lu} + elas_{lu} + comp_{t,lu} , \qquad (2.16)$$

Location suitability and neighborhood suitability can be determined by either empirical methods (Verburg et al., 2004c), process and expert knowledge and the (dynamic) analysis of neighborhood interactions similar to constrained cellular automata models (Verburg, De Nijs, Van Eck, Visser and de Jong, 2004b).

The conversion elasticity is a measure of the cost of conversion of one land use type to another land use type and applied only to those locations where the land use type is found at time t. High values indicate high conversion cost (either monetary or institutional) and thus a higher total probability for the location to remain under the current land use type. Low values for elasticity may apply to annual crops, grassland and similar land use types while high values apply to forest, urban areas and permanent crops for which high costs of establishment have been made.

The competitive advantage is iteratively determined for all land use types during an iterative procedure. Values are increased during the iteration when allocated area is smaller than area demanded while values are decreased when allocated area exceeds the demand. In the case of increasing demand, the value of the competitive advantage is likely to increase while lower values are obtained when the demand for a certain land use type decrease. Finally, the maximization of the total probability at each individual location is checked against a set of conversion rules as specified in a conversion matrix
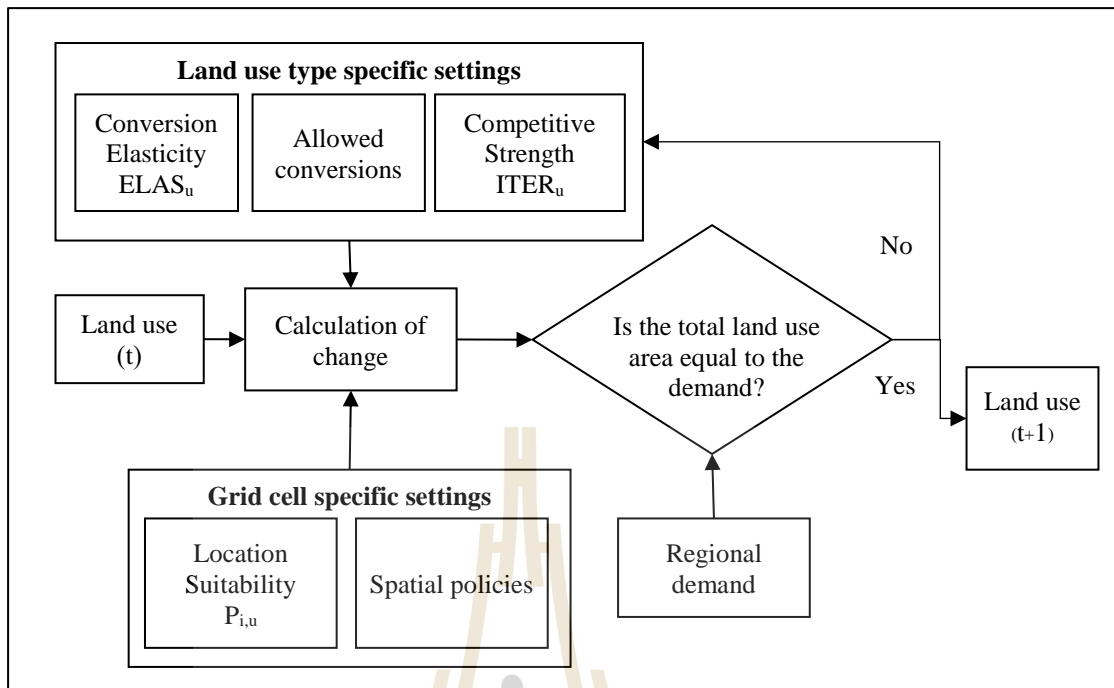
Source: Verburg, 2010.

Figure 2.6 Flowchart of the allocation module of the CLUE-S model.

2.4   Ecosystem services evaluation

The concept of ecosystem services was brought into widespread use by the Millennium Ecosystem Assessment (MA), a global initiative set up in 1999 to assess how ecosystem change would affect human well-being (Millennium Ecosystem Assessment, 2005). The MA defines ecosystem services simply as "the benefits that people obtain from ecosystems". This encompasses both goods, such as timber, and services such as air purification. The MA divided these services into four categories (Figure 2.7) include:

(1) Supporting services. These are services, such as nutrient cycling and soil formation, which are needed for the production of all other services.

(2) Provisioning services. Products obtained from ecosystems, such as food or

timber.

(3) Regulating services. The benefits obtained from the regulation of ecosystems, including services such as purification of water, flood control, or regulation of the climate via carbon sequestration.

(4) Cultural services. The benefits people obtain from ecosystems through spiritual enrichment, cognitive development, reflection, recreation, and aesthetic experiences.
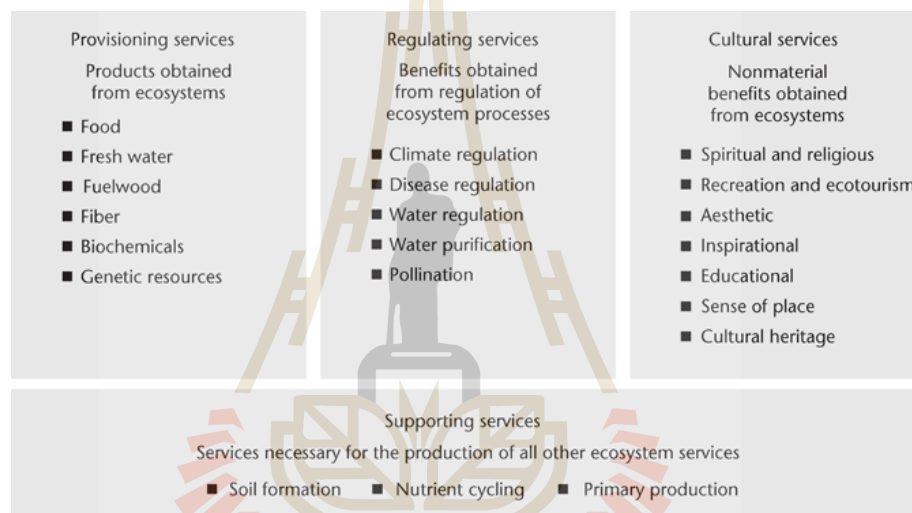
Source: Millennium Ecosystem Assessment (2005).

Figure 2.7 Typologies of ecosystem services.

Costanza et al. (1997) estimated the value per unit area of each ecosystem service for each ecosystem type. To estimate this "unit value", they used (in order of preference) either: (1) the sum of consumer and producer surplus; or (2) the net rent (or producer surplus); or (3) price times quantity as a proxy for the economic value of the service, assuming that the demand curve for ecosystem services looks more like Figure 2.8b than Figure 2.8a, and that therefore the area "pbqc" is a conservative underestimate of the area "abc". They then multiplied the unit values times the surface area of each ecosystem to arrive at global totals.
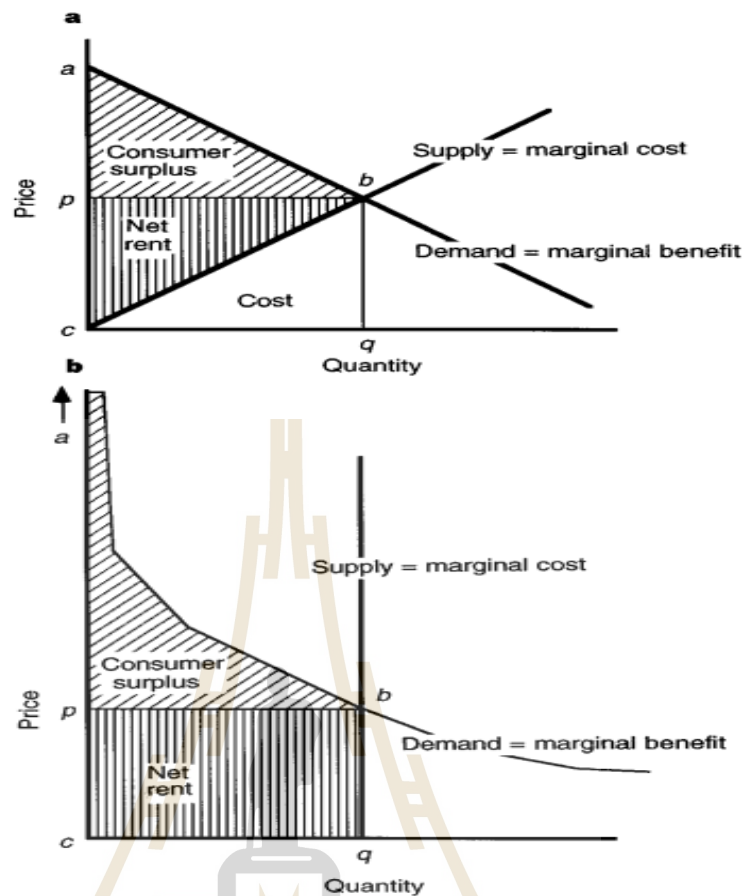
Source: Costanza et al., 1997.

Figure 2.8 Supply and demand curves, showing the definitions of cost, net rent and consumer surplus for normal goods (a) and some essential ecosystem services (b).

Su, Xiao, Jiang and Zhang (2012) suggested that regional ecological service value calculated by the following formula:

$$\text{ESV} = \sum(A_k \times VC_k) \tag{2.17}$$

Where   ESV = estimated ecosystem service value;

A_k = area in hectare of land use category k;

VC_k = value coefficient for land use category k

For the purposes of the analysis of ESV, Costanza et al. (1997) grouped ecosystem services into 17 major categories (Table 2.2).

In practice, the LULC datasets of each reference year to be used as a proxy for the measurement of ESVs are prepared and the corresponding area in hectare is summarized in the GIS environment**.** In the ecosystem service estimation process, the value coefficients are assigned to each LULC type according to the value used by Costanza et al. (1997) (Table 2.3). Then, the area of each LULC type in hectare is multiplied by its corresponding value coefficients to calculate the total ecosystem service value for a particular LULC type. (Kindu et al., 2016).

43

Table 2.2 Ecosystem services and functions.

No.	Ecosystem service*	Ecosystem functions	Examples
1.	Gas regulation	Regulation of atmospheric chemical composition	CO_2/O_2 balance, O_3 for UVB protection, and SO_x levels.
2.	Climate regulation	Regulation of global temperature, precipitation, and other biologically mediated climatic processes at global or local levels	Greenhouse gas regulation, DMS production affecting cloud formation.
3.	Disturbance regulation	Capacitance, damping and integrity of ecosystem response to environmental fluctuations.	Storm protection, flood control, drought recovery and other aspects of habitat response to environmental variability mainly controlled by vegetation structure
4.	Water regulation	Regulation of hydrological flow	Provisioning of water for agricultural (such as irrigation) or industrial (such as milling) processes or transportation.
5.	Water supply	Storage and retention of water.	Provisioning of water by watersheds, reservoirs and aquifers.
6.	Erosion control and sediment retention	Retention of soil within an ecosystem	Prevention of loss of soil by wind, runoff, or other removal processes, storage of stilt in lakes and wetlands
7.	Soil formation	Soil formation processes	Weathering of rock and the accumulation of organic material
8.	Nutrient cycling	Storage, internal cycling, processing and acquisition of nutrients	Nitrogen fixation, N, P and other elemental or nutrient cycles
9.	Waste treatment	Recovery of mobile nutrients and removal or breakdown of excess or xenic nutrients and compounds	Waste treatment, pollution control, detoxification.
10.	Pollination	Movement of floral gametes	Provisioning of pollinators for the reproduction of plant populations.

Table 2.2 (Continued).

No.	Ecosystem service*	Ecosystem functions	Examples
11.	Biological control	Trophic-dynamic regulations of populations.	Keystone predator control of prey species, reduction of herbivory by top predators.
12.	Refugee	Habitat for resident and transient populations.	Nurseries, habitat for migratory species, regional habitats for locally harvested species, or over wintering grounds.
13.	Food production	That portion of gross primary production extractable as food.	Production of fish, game, crops, nuts, fruits by hunting, gathering, subsistence farming or fishing
14.	Raw materials	That portion of gross primary production extractable as raw materials.	The production of lumber, fuel or fodder.
15.	Genetic resources	Sources of unique biological materials and products.	Medicine, products for materials science, genes for resistance to plant pathogens and crop pests, ornamental species (pets and horticultural varieties of plants).
16.	Recreation	Providing opportunities for recreational activities	Eco-tourism, sport fishing, and other outdoor recreational activities.
17.	Cultural	Providing opportunities for non-commercial uses	Aesthetic, artistic, educational, spiritual, and/or scientific values of ecosystems

Source: Costanza et al. (1997).

Table 2.3 Summary of average global value of annual ecosystem services ha^{-1}.

Biome	Area	1	2	3	4	5	6	7	8	9	10	11	12	13	14	15	16	17	Total Value per ha	Total global flow value
	(ha×10⁶)	Gas regulation	Climate regulation	Disturbance regulation	Water regulation	Water supply	Erosion control	Soil formation	Nutrient cycling	Waste treatment	Pollination	Biological control	Habitat/Refugia	Food produc	Raw materials	Genetic resources	Recreation	Cultural	($ha⁻¹)	($yr⁻¹×10⁹)
1. Marine	36302																		577	20949
1.1 Open ocean	33200	38							118			5		15	0			76	252	8381
1.2 Coastal	3102			88					3677			38	8	93	4		82	62	4052	12568
Estuaries	180			567					21100			78	131	521	25		381	29	22832	4110
Seagrass/algae beds	200								19002										19004	3801
Coral reefs	62			2750						58		5	7	220	27		3008	1	6075	375
Shelf	2660								1431			39		68	2			70	1610	4283
2. Terrestrial	15323																		804	12319
2.1 Forest	4855		141	2	2	3	96	10	361	87		2		43	138	16	66	2	969	4706
Tropical	1900		223	5	6	8	245	10	922	87				32	315	41	112	2	2007	3813
Temperate/boreal	2955		88		0			10		87		4		50	25		36	2	302	894
2.2 Grass/rangelands	3898	7	0		3		29	1		87	25	23		67		0	2		232	906
2.3 Wetland	330	133		4539	15	3800				4177			304	256	106		574	881	14785	4879
Tidal marsh/mangroves	165			1839						6696			169	466	162		658		9990	1648
Swamps/floodplains	165	265		7240	30	7600				1659			439	47	49		491	1761	19580	3231
2.4 Lakes/rivers	200				5445	2117				665				41			230		8498	1700
2.5 Desert	1925																			
2.6 Tundra	743																			
2.7 Ice/rock	1640																			
2.8 Cropland	1400										14	24		54					92	128

Table 2.3 (Continued).

Biome	Area (ha×10⁶)	Ecosystem services (1994 USD ha⁻¹yr⁻¹)																	Total Value per ha ($ha⁻¹)	Total global flow value ($yr⁻¹×10⁹)
		1 Gas regulation	2 Climate regulation	3 Disturbance regulation	4 Water regulation	5 Water supply	6 Erosion control	7 Soil formation	8 Nutrient cycling	9 Waste treatment	10 Pollination	11 Biological control	12 Habitat/Refugia	13 Food production	14 Raw materials	15 Genetic resources	16 Recreation	17 Cultural		
2.9 Urban	332																			
Total		51625	1341	684	1779	1115	1692	576	53	17075	2277	117	417	124	1386	721	79	815	3015	33268

Note: Numbers in the body of the table are in USD ha⁻¹ yr⁻¹. Row and column totals are in $yr⁻¹ x 10⁹, column totals are the sum of the products of the per ha services in the table and the area of each biome, not the sum of the per ha services themselves. Shaded cells indicate services that do not occur or are known to be negligible. Open cells indicate lack of available information.
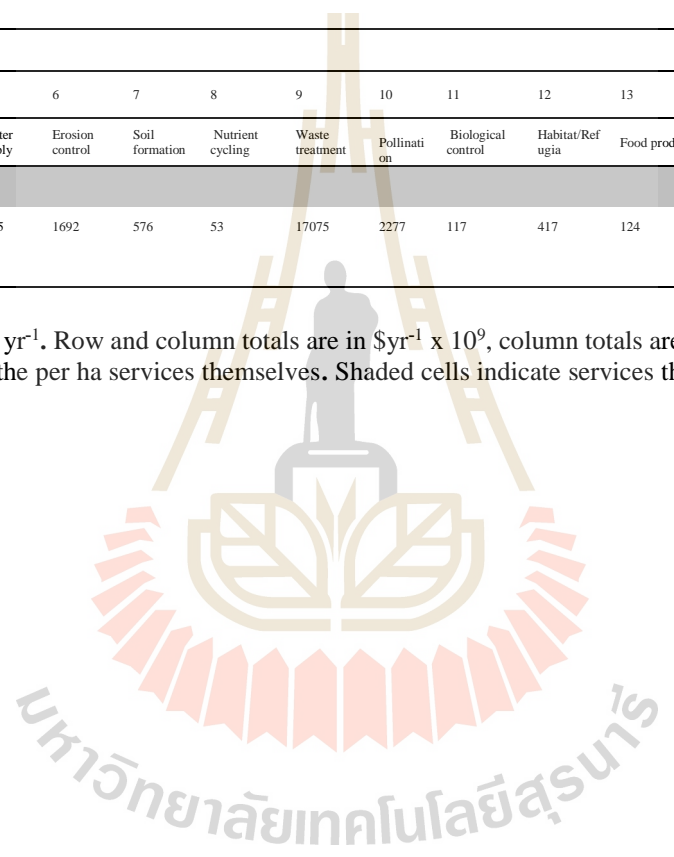
2.5   Land surface temperature (LST)

Land surface temperature (LST) is the main factor determining surface radiation and energy exchange (Weng, 2009), controlling the distribution of heat between the surface and atmosphere (Tan et al., 2009). Guillevic et al. (2012) mentioned that LST is a key variable that helps govern radiative, latent and sensible heat fluxes at the interface." In summary, it governs the urban thermal environment (Sun et al., 2011). Thereby, analysis and comprehension of LST dynamics and its relation to changes of anthropogenic origin is necessary for the modeling and forecasting of environmental changes (Kerr et al., 2004; Moran et al., 2009).

LST serves as an important indicator of chemical, physical and biological processes of the ecosystem. LST is influenced by such properties of urban surfaces as color, surface roughness, humidity, chemical composition, etc (Tan et al., 2009).

All objects with temperatures greater than absolute zero emit radiation and the amount of radiation from a black body in thermal equilibrium at wavelength λ and temperature T is described by Planck's law as:

$$B_\lambda(T) = \frac{C_1}{\lambda^5 \left[\exp\left(\frac{C_2}{\lambda T}\right) - 1\right]}$$

(2.18)

Where $B_\lambda(T)$ is the spectral radiance (W m^{-2} μm^{-1} sr^{-1}) of a black body at temperature T (K) and wavelength λ (μm);

C_1 and C_2 are physical constants (C_1 =1.191×10^8 Wμm^{4}sr^{-1} m^{-2}, C_2=1.439×10^4 μm·K).

Because most natural objects are non-black bodies, the emissivity ε, which is defined as the ratio between the radiance of an object and that of a black body at the same temperature, must be taken into account. The spectral radiance of a non-black

body is given by the spectral emissivity multiplied by Planck's law as shown in Eq. (2.18). Obviously, if the atmosphere exerts no influence on the measured radiance, LST (i.e. T) can be retrieved by making temperature as the subject of Eq. (2.19) once the emitted radiance and emissivity are known. The wavelength λ_{max} of the peak monochromatic radiance at a given temperature (T) is given by Wien's displacement law as

$$T_{\lambda_{max}} = 2897.9 \ K\mu m \tag{2.19}$$

According to this equation, the wavelength λ_{max} at which maximum emission occurs varies roughly from 11.6 μm to 8.8 μm if the LST ranges from 250 K to 330 K with the average temperature of the Earth being approximately 288 K. The wavelength region between 8 and 13 μm coincides within a clear window in the atmosphere, which is most transparent to TIR radiation. In cases where the temperature of the surface exceeds 330 K, the wavelength peak moves to shorter and shorter wavelengths, for example for a wildfire (about 800 K), the maximum emission is around 3.6 μm in the mid-infrared (MIR) region (3–5 μm) which also coincides with a clear window in the atmosphere.

The derivation of LST from satellite thermal data requires several procedures: sensor radiometric calibrations, atmospheric and surface emissivity corrections, characterization of spatial variability in land-cover, etc. As the near-surface atmospheric water vapors content varies over time due to seasonality and inter-annual variability of the atmospheric conditions, it is inappropriate to directly compare temperature values represented by the LST between multiple periods (Zhang et al., 2009; Zhang et al., 2009; Yuan and Bauer, 2007).

The first step is to convert the digital numbers of the bands to top-of-atmosphere (TOA) radiance (Schroeder et al., 2006), and then to further convert TOA radiance of visible and near infrared bands to surface reflectance by applying an atmospheric correction.

Yuan and Bauer (2007) proposed a method of deriving LST in three steps: Firstly, the digital numbers (DNs) of band 6 of Landsat-TM are converted to radiation luminance or top-of-atmospheric (TOA) radiance (Lλ, mW/cm2 sr) using:

$$TOA = \frac{b_6}{255}(L_{max} - L_{min}) + L_{\min} \tag{2.20}$$

Where   b6 is the pixel digital number for band 6, L_{max} = 1.896 (mW/ cm^2 sr), and $L_{\min}$ = 0.1534 (mW/cm^2 sr).

In the case of Landsat 7 ETM+ image, TOA is derived by:

$$TOA = \frac{(L_{max} - L_{min})}{QCAL_{max} - QCAL_{min}}((b_6 - QCAL_{min}) + L_{min)} \tag{2.21}$$

Where $QCAL_{min}$ = 1, $QCAL_{max}$ = 255, and L_{max} = 17.04 W/(m^2 sr μm) and L_{min} = 0.

Secondly, the TOA radiance is converted to surface-leaving radiance by removing the effects of the atmosphere in the thermal region. An atmospheric correction tool – MODTRAN 4.0 for the thermal band of Landsat sensors was applied. This tool uses the MODTRAN radiative transfer code and a suite of integration algorithms to estimate three parameters – atmospheric transmission, and upwelling and downwelling radiance – which enable the calculation of the surface-leaving radiance – L$_T$ or the radiance of a blackbody target of kinetic temperature T, in the form of the following equation:

$$L_T = \frac{L_d(TOA - L_\mu - \tau)(1 - \varepsilon)}{\tau\varepsilon} \tag{2.22}$$

Where TOA is the radiance derived for the instrument, L_μ is the upwelling or atmospheric path radiance, L_d is the downwelling or sky radiance, τ is the atmospheric transmission, and ε is the emissivity of the surface specific to the target type. Radiance values are in units of W/ (m^2 sr µm) and the transmission and emissivity is unitless. The emissivity could be based on the land-cover classification (Yuan et al., 2005) or the emissivity values as derived by Snyder et al. (1998).

Lastly, the radiance (LT) is converted to surface temperature (LST) using the Landsat specific estimate of the Planck curve (Chander and Markham, 2003) as:

$$\text{LST} = \frac{K_2}{\ln\left[\left(\frac{K_1}{LT}\right)+1\right]} \tag{2.23}$$

Where LST is the temperature in Kelvin (K), K_1 is the pre-launch calibration constant in W/ (m^2 sr µm) and K_2 is another pre-launch calibration constant in Kelvin. For Landsat 5 TM, K_1 = 607.76 W/ (m^2 sr µm) and K_2 = 1260.56 K_1; for Landsat 7 ETM+, K_1 = 666.09 W/ (m^2 sr µm) and K_2 = 1282.71 K.

The LST image from the thermal band of ETM+ image (band 6) with original spatial resolution of 60 m was resampled to 120 m using the nearest neighbor algorithm to match the pixel size of the LST image from TM image.

The following equation was used to convert the digital number (DN) of Landsat 8 TIR band 10 into spectral radiance (L_λ) (USGS, 2015):

$$L_\lambda = \left(M_\rho \times Q_{cal}\right) + A_\rho \tag{2.24}$$

Where M_ρ is the reflectance multiplicative scaling factor and A_ρ is the reflectance additive scaling factors. Values of M$_L$, A$_L$, M_ρ and A_ρ for each band of OLI and TIRS can be obtained from metadata file of Landsat 8 data. (Nikam, Ibragimov, Chouksey, Garg and Aggarwal, 2016)

The spectral radiance is then converted to brightness temperature, which is the at-satellite temperature (TB) under an assumption of unity emissivity using the following equation

$$TB = \frac{K2}{ln\left(\frac{K1}{L_\lambda}\right)+1} \tag{2.25}$$

Where   TB= at-satellite brightness temperature in Kelvin (K), $K1$ and $K2$is band specific thermal conversion constants from the metadata

Next, NDVI is computed using the NIR and Red band of the Landsat 8 image since it will be used in determining land surface emissivity (LSE). NDVI is calculated using the following equation (Tucker, 1979):

$$NDVI = \frac{NIR-RED}{NIR+RED} \tag{2.26}$$

$$Pv = \left[\frac{NDVI-NDVI_{min}}{NDVI_{max}-NDVI_{min}}\right]^2 \tag{2.27}$$

Where

Pv is vegetation proportion

$NDVI$ is normalised difference vegetation index

$NDVI_{min}$ is minimum $NDVI$ value

$NDVI_{max}$ is maximum $NDVI$ value

LSE is then computed using the following equation (Sobrino et al., 2004):

$$LSE = 0.004 * Pv + 0.986 \tag{2.28}$$

LST can now be computed (in degrees Celsius) using the at- satellite brightness temperature and the land surface emissivity in this equation (Artis and Carnahan, 1982):

$$\text{LST} = [\frac{T_B}{1} + \left(\lambda * \frac{T_B}{\rho}\right) * \ln(LSE) - 273.15 \qquad (2.29)$$

Where   LST is land surface temperature, T_B is the at-satellite brightness temperature is the wavelength of emitted   radiance (l=11.5µm) (Markham and Barker, 1985), ρ is h * c/σ (1.438 * 10^{-2} m K), σ is Boltzmann constant (1.38 * 10^{-23} J/K), h is Planck''s constant (6.626 * 10^{-34}Js, c is velocity of light (2.998 * 10^{8} m/s)

In addition, the LST that was derived from band 10 gives higher accuracy than band 11 (Yu et al., 2014).

2.6 Literature reviews

The main literature reviews relate to this study include landscape pattern analysis, ecosystem service evaluation and LST are here summarized.

2.6.1 Application of landscape pattern analysis

Parker et al. (2001) summarized the usefulness of spatial metrics with respect to a variety of urban models and argued for the contribution of spatial metrics in helping link economic processes and patterns of land use. They concluded that urban landscape composition and pattern as quantified with spatial metrics are critical independent measures of the economic landscape function and can be used for the interpretation evaluation of modeling.

Herold et al. (2005) argued that the combined application of remote sensing and spatial metrics can provide more spatially consistent and detailed information on urban structure and change than either of these approaches used independently. Likewise, Schneider et al. (2005) also discussed the recent shift in focus from urban change detection to change quantification. Their statistics highlighted the

53

effect of economic, social, and government policy forcing mechanisms on urban structure.

Seto and Fragkias (2005) used spatial metrics to quantify change in four cities over an 11 years period (1988-1999). The selected metrics that were intended to describe urban from complexity and size included total urban area, edge density, urban patch count, mean patch fractal dimension, average patch size, and patch size coefficient of variation. Key aspects of urban development in the two cities were illuminated by the metrics. Envelopment and multiple nuclei growth were revealed as the primary urban expansion processes. Changing administrative practices to control (or not) land use development were likewise reflected in the metrics.

Yu and Ng (2007) had employed landscape metrics in addition to gradient analysis on remote sensing data to analyze and compare both the spatial and temporal dynamics of urban sprawl in Guangzhou, China. Landscape metrics were applied to calculate quantitative values for each block at the class and landscape level. As results, they found that the combination of gradient analysis and landscape metrics with the selected eight metrics including number of patches, mean patch size, largest patch index, area weighted mean shape index, area weighted mean patch fractal dimension, Shannon's diversity index, contagion index, and patch cohesion index can characterize the complex spatial pattern of urban growth.

Huang et al. (2007) had considered seven spatial metrics (compactness, centrality, complexity, porosity, and density) to analyze the urban form of 77 metropolitan area in Asia, US, Europe, Latin America and Australia. Comparison of the spatial metrics was made between developed and developing countries, and then among world regions. The result clearly demonstrated that urban agglomerations of

developing world are less sprawling and dense than their counterparts in either Europe or North America.

Bhatta (2010) stated that recently there has been an increasing interest in applying spatial metrics technique in urban environments because these helps to bring out the spatial component in urban structures and in dynamics of change and growth process (Alberti and Weddell, 2000; Barnsley and Barr, 1997; Herold et al., 2002).

Pham, Yamaguchi and Bui (2011) studied on the relation between city planning and urban growth using remote sensing and spatial metrics to monitor urbanization, and to investigate the relationship between urbanization and urban land use plans consisting of the cities of Hanoi, Hartford, Nagoya and Shanghai. In this study, Landsat and ASTER data from 1975 to 2003 were used to classify LULC and FRAGSTATS software was applied to evaluate the characteristics of urban composition. The results showed that the urban core of Nagoya changed moderately over time. Shanghai had a high population density, and satellite towns absorbed potential suburban development. Hartford exhibited a spread out pattern of urban development with a high concentration of settlement in the suburb. Conversely, the new urban areas of Hanoi developed rapidly along major transportation routes, resulting in urban development in Hanoi assuming an unusual pattern. They found that the combined approach of remote sensing and spatial metrics can provide local city planners with valuable information that can be used to better understand the impacts of urban planning policies in urban areas, particularly in Hanoi.

Aguilera, Valenzuela and Botequilha-Leitao (2011) studied landscape metrics in the analysis of urban land use patterns: a case study in a Spanish metropolitan

area. The studies focused on a medium-sized metropolitan areas (Granada, Spain), and explored the use of spatial metrics to quantify changes in the urban growth patterns reflected in three future scenarios (2020). The scenarios were simulated with a model based on cellular automata, which reproduced three urban growth processes (aggregation, compaction, and dispersion) and four urban growth patterns (aggregated, linear, leapfrogging, and nodal). The scenarios were evaluated with metrics that quantified changes in the spatial characteristics of urban processes. Thus, for example, the NP and AREA MN allowed to characterize the decreased aggregation of high-density residential land uses in one scenario (S1) and the linear growth patterns in industrial land uses in another scenario (S2). They concluded that spatial metrics are useful for the evaluation of urban planning.

Ramachandra, Aithal and Sanna (2012) had applied the temporal remote sensing data with landscape metrics to quantify the urban dynamics in Bangalore, India. The results clearly indicated that whole landscape earlier was aggregating to a large patch in 2010 as compared to earlier years which was dominated by several small patches. The large scale conversion of small patches to large single patch can be seen from 2006 to 2010. In the year 2010 patches were maximally aggregated indicating that the city is becoming more compact and more urbanized in recent years. Bangalore the most sought after destination for its climatic condition, and the availability of various facilities (land economy, political factors) compared to other cities. The growth into a single urban patch can be attribute to rapid urbanization coupled with the industrialization. Monitoring of growth through landscape metrics can help to maintain and manage the natural resources. They found that landscape metrics can provide in

depth knowledge the sprawl and principal component analysis helps in prioritizing the metrics for detailed analyses.

Liu and Yang (2015) studied monitoring land changes in an urban area using satellite imagery, GIS and landscape metrics in the Atlanta metropolitan area, Georgia, USA. This research also examined the size, pattern, and nature of land changes using landscape metrics. This study had demonstrated the usefulness of integrating remote sensing with GIS and landscape metrics in land change analysis that allows the characterization of spatial patterns and helps reveal the underlying processes of urban land changes. Additionally, results indicate a transition of urbanization patterns in the study site with a limited outward expansion despite the dominant suburbanization process.

Padmanaban, Bhowmik, Cabral, Zamyatin, Almegdadi and Wang (2017) applied modelling urban sprawl using remotely sensed data: a case study of Chennai city, Tamilnadu. The research employed the Random Forest (RF) classification on Landsat imageries from 1991, 2003 and 2016, and computed six landscape metrics to delineate the extent of urban areas within a 10 km suburban buffer of Chennai. The result found that spatial metrics values indicate that the existing urban areas became denser and the suburban agricultural, forests and particularly barren lands were transformed into fragmented urban settlements. The forecasted land cover for 2027 indicates a conversion of 13,670.33 ha (16.57% of the total landscape) of existing forests and agricultural lands into urban areas with an associated increase in the entropy value to 1.7, indicating a tremendous level of US. Lastly, they concluded that the study can provide useful metrics for urban planning authorities to address the social-ecological consequences of US and to protect ecosystem services.

Xiao, Liu, Li, Yu and Zhang (2018) studied on spatial variability of local rural landscape change under rapid urbanization in eastern China. This research aimed to investigate local rural landscape compositions and patterns and to identify the spatial variability of local rural landscape change under rapid urbanization in three rural areas, namely, Daxing (DX) in Beijing, Quzhou (QZ) in Hebei Province and Changshu (CS) in Jiangsu Province. The results showed that the three rural areas varied in landscape pattern and land use composition change, even in the short term. Local farmland decreased slightly, demonstrating the effectiveness of the national farmland protection policy. Land use switched among farmland, orchards, nurseries, and other production lands were the major driving force for local change. Considering differential characteristics of landscape change among rural areas, they suggested that the efficient landscape management requires the development of strategies that account for the spatial variability of urbanization effects. Subsidies for the management of semi-natural land with high natural value are meaningful for local natural conservation.

In summary, landscape pattern analysis has been applied by many researchers to urban growth, sprawl and urbanization analysis. The characteristics of urban growth, sprawl and urbanization can be explained by composition and configuration of landscape metrics there related to LULC transition.

2.6.2 Application of CLUE-S model

Xu, Li, Song and Yin (2013) studied land-use planning for urban sprawl based on the CLUE-S model: a case study of Guangzhou, China. This research introduced the novel ideas of a planning regulation coefficient for sustainable land use planning in order to decrease entropy, combined with the CLUE-S model to predict land-use change. Three scenarios were designed as the basis for land use projections

for Guangzhou, China, in 2015, and the changes in the land ecological service function for each scenario were predicted. The results showed that although the current land use plan is quite reasonable, it will be necessary to further strengthen the protection of farmland and important ecological service function areas.

Zhang, Liu, Pan and Yu (2013) had studied land use pattern optimization based on CLUE-S and SWAT models for agricultural non-point source pollution control. This research, the CLUE-S and SWAT (Soil and Water Assessment Tool) models were coupled to simulate pollution loads under different land use scenarios in the upstream watershed of Miyun Reservoir in Beijing, China. The results indicated that changes in land use structure and pattern under different land use scenarios have significantly affected the non-point source pollution load. The increase of orchards and loss of forest cover had led to an increase in the potential pollution loads of nitrogen by 5.27% and phosphorus by 4.03%. However, in the agricultural non-point source pollution control scenario, pollution loads of nitrogen decreased by 13.94% and phosphorus by 9.86%, resulting from the establishment of riparian vegetation buffers and restoring forest on unutilized land and slope arable land. Coupling the hydrological model SWAT and the land use model CLUE-S succeeded in evaluating the land use pattern for agricultural non-point source pollution control. The coupling of two models can provide a new approach for land use optimization towards non-point source pollution control.

Zhou, Xu, Chen, Xu, Gao and Du (2013) studied hydrological response to urbanization at different spatio-temporal scales simulated by coupling of CLUE-S and the SWAT model in the Yangtze river delta region. The objective of the study is to understand and quantify the hydrological responses of land use and land cover changes.

The CLUE-S model was coupled with the SWAT model to simulate the effects of future urbanization scenario based on historical land use change tendency. The simulated land cover map of 2008 was compared to the actual land use map in 2008; the resultant kappa coefficient was 0.82, which means that the calibrated CLUE-S model can be used to simulate future land cover in the study area.

Debolini, Schoorl, Temme, Galli and Bonari (2015) studied changes in agricultural land use affecting future soil redistribution patterns: a case study in southern Tuscany, Italy. This research work was focused: (i) to characterize LULC in the last 11 years in a typical Mediterranean area, the Trasubbie river basin (southern Tuscany, Italy); (ii) to extrapolate LULC changes and create spatially explicit LULC scenarios for the near future; and (iii) to simulate how and where the predicted LULC may affect soil redistribution. They spatially allocated land use by CLUE-S model and used a landscape process model (landscape process modelling at multi-dimensions and scales) to assess soil redistribution patterns. Land use in the study area changed almost linearly between 1996 and 2007, with cereals and annual fodder crops decreasing, and vineyards, perennial pastures and land abandonment increasing. Their scenarios can extrapolate LULC dynamics to make predictions for 2013. A comparison of LAPSUS results between LULC and baseline scenarios for 2013 showed an increase in terms of net soil loss and total erosion, and a decrease in terms of sediment delivery ratio.

Zhang, Zhang, Zhou, Hou, Huang and Cao (2016) studied spatial distribution prediction and benefits assessment of green manure in the Pinggu District, Beijing, by using the CLUE-S model. In this study, two scenarios were used to predict the spatial distribution of green manure based on data from 2011: The promotion of green manure planting in orchards (Scenario 1) and the promotion of simultaneous

green manure planting in orchards and croplands (Scenario2). This research presented spatial distribution of green manure in cropland and orchards in 2020 in Pinggu District located in Beijing, China. The predictions were generally accurate based on the receiver operating characteristic (ROC) and Kappa indices, which validated the effectiveness of the CLUE-S model in the prediction. The spatially explicit results allowed for the assessment of the benefits of these changes based on different economic and ecological indicators. The economic and ecological gains of Scenario 1 and 2 were 175,691,900 and 143,000,300 CNY, respectively, which indicated that the first scenario was more beneficial for promoting the same area of green manure. These results can facilitate policies of promoting green manure and guide the extensive use of green manure in local agricultural production in suitable ways.

Zhou, Zhang, Ye, Wang and Su (2016) studied the delimitation of urban growth boundaries using the CLUE-S land-use change model at Xinzhuang town, Changshu city, China. This research choose the fast-growing Xinzhuang town of Changshu city, eastern China as an example, a new method towards establishing UGBs is proposed based on land-use change model (CLUE-S). The results of their study showed that the land-use change and urban growth simulation accuracy of CLUE-S model is high. The expansion of construction land and the decrease of paddy field would be the main changing trends of local land use, and a good deal of cultivated land and ecological land would be transformed into construction land in 2009–2027. There was remarkable discordance in the spatial distribution between the simulated UGBs based on the CLUE-S model and the planned UGBs based on the conventional method, where the simulated results may more closely reflect the reality of urban growth laws. As

results, they concluded that their study could be a useful planning tool for the delimitation of UGBs in Chinese cities.

In summary, the CLUE-S model (the Conversion of Land Use and its Effect at Small regional extent) has been widely applied by international researches and many scholars to simulate LULC change by controlling different scenario settings and the total demand for the corresponding land patterns.

2.6.3 Application of ecosystem service evaluation

Su, Xiao, Jiang and Zhang (2012) examined urbanization impacts at an eco-regional scale by analyzing landscape pattern and ecosystem services values in four eco - regions in China. Their results showed that the four eco-regions exhibited a similar urbanization process of rapid population growth, economic development and urban expansion. The considerable urban expansion led to a loss of 8.5 billion RMB Yuan ecosystem service values per year on average between 1994 and 2003. Multivariate regression further qualitatively explored the dynamics of landscape changes in response to urbanization as well as interaction between landscape pattern and ecosystem services value. It was found that landscape fragmentation, configuration and diversity, which were induced by urbanization, could significantly impair the provision of ecosystem services.

Long et al. (2014) examined the dynamic patterns of land use in Tianjin Binhai New Area using Landsat TM data in 1985, 1995, 2005 and 2010 and socioeconomic data from both research institutes and government departments. Then they assessed the changes of ecosystem services value (ESV) by drawing a connection between the observed land use dynamics and the evaluation of ESV based on the latest research of Costanza et al. (2014) and some revisions adapted to the situation of China.

The outcomes indicated that, during the period 1985e2010, ESV of the study area decreased by 25.9%, from 12,194 to 9037 billion RMB, due to the losses of large quantities of ecological land (e.g., farmland and water body) to construction land. Then, some of the major implications for improving the urban planning of Tianjin Binhai New Area were discussed.

Li et al. (2014) used remote sensing, GIS technology and economic evaluation method for ecosystem services. The evolution of landscape spatial structure in 1991, 1996, 2001 and 2006 of Changzhou City, People's Republic of China was obtained and the change of ecosystem services resulted from land use change was evaluated. The results showed a continuing expansion of urbanized areas and reduction in ecosystem services. Conversion of farmland to other uses was responsible for the largest reduction in the value of ecosystem services, equal to 239.8 million RMB (equivalent to USD 37.8 million).

Haas et al. (2015) investigated urbanization and its potential environmental consequences in Shanghai and Stockholm metropolitan areas over two decades. From the landscape metrics results, it appears that fragmentation in both study regions occurred mainly due to the growth of high density built-up areas in previously more natural/agricultural environments, while the expansion of low density built-up areas was for the most part in conjunction with pre-existing patches. Urban growth resulted in ecosystem service value losses of approximately 445 million US dollars in Shanghai, mostly due to the decrease in natural coastal wetlands while in Stockholm the value of ecosystem services changed very little. Total urban growth in Shanghai was 1,768 km^2 and 100 km^2 in Stockholm.

Han, Yang and Song (2015) studied scenario simulation and prediction of LULC change in Beijing, China. This research explored the characteristics of LULC change and simulate future land use demand by combining a CLUE-S model with a Markov model to deal with some shortcomings of existing LULC models. Using Beijing as a case study, they described the related driving factors from land-adaptive variables, regional spatial variables and socio-economic variables and then simulate future land use scenarios from 2010 to 2020, which include a development scenario (natural development and rapid development) and protection scenarios (ecological and cultivated land protection). The results indicated good consistency between predicted results and actual land use situations according to a Kappa statistic. The conversion of cultivated land to urban built-up land will form the primary features of LULC change in the future. The prediction for land use demand showed the differences under different scenarios. At higher elevations, the geographical environment limited the expansion of urban built-up land, but the conversion of cultivated land to built-up land in mountainous areas will be more prevalent by 2020; Beijing, however, still faces the most pressure in terms of ecological and cultivated land protection.

Kindu, Schneider, Teketay and Knoke (2016) studied on change of ecosystem services values in response to land use land cover dynamics in Munessa – Shashemene landscape of the Ethiopain highlands. Estimation and change analyses ecosystem services values were conducted using LULC dataset with their corresponding global value coefficients developed earlier and own modified conservative values coefficient for the studied landscape. The result shown that change in ecosystem services values in response to LULC dynamics over the past of decades (1973-2012) from 130.5 million USD in 1973, to 118.5,114.8 and 111.1 million USD

in 1986, 2000 and 2012, respectively. Changes have also occurrence in values of individual ecosystem services functions, such as erosion control, nutrient cycling, climate regulation and water treatment, which were among the highest contribution of total ecosystem services values.

Mamat, Halik and Rouzi (2017) studied on variations of ecosystem service value in response to land-use change in the Kashgar region, northwest China. Results demonstrated that the total value of the ecosystem services in the Kashgar region were approximately $10,845.3, $11,218.6, $10,291.7 and $10,127.3 million in 1986, 1996, 2005 and 2015, respectively. The water supply, waste treatment, biodiversity protection, and recreation and cultural services were the four ecosystem services with the highest service value, contributing 77.05% of the total ecosystem services. The combined contribution rate of food production and raw material value was only about 4.02%, relatively small. The sensitivity analysis indicated that the estimated total ecosystem service value (ESV) for this study area was relatively inelastic with respect to the value coefficients. The findings of this study will be crucial for maintaining the stability and sustainable development of the oasis region, where socio-economic development and the integrity of the natural ecosystem complement each other. Furthermore, the results provide a scientific basis for decision makers in land use management and provide a reference for researchers in the Northwest China.

In summary, ecosystem service values have been applied to evaluation the ecosystem services contribution of ecosystems to human wellbeing and survival, to raise awareness, contribute to developing knowledge on management of natural capital. The ecosystem services values correlated to the situation of ecosystem, e.g. LULC type and coefficients values of ecosystem services function.

2.6.4 Application of land surface temperature

Xie, Wang, Chang, Fu and Ye (2013) studied assessment of landscape patterns affecting land surface temperature in different biophysical gradients in Shenzhen, China. This research focused on the different effects of landscape patterns on LST within different land covers. The land cover was measured by surface biophysical components, including vegetation fraction (VF) and impervious surface area (ISA), acquired by a linear spectral mixture model (LSMM). LST was derived from Landsat-5 TM thermal infrared (TIR) data using the generalized single-channel method. Landscape patterns were measured by landscape metrics, including the Shannon diversity index (SHDI), the aggregation index (AI), patch density (PD), and fractal dimension area-weighted mean index (FRAC_AM). Results showed that VF and ISA are more important than spatial patterns in determining LST. However, these effects change in densely covered areas. VF and LST are negatively correlated, with the inflection of the regression curves being 45%. In areas with VF lower than 45 %, the correlation between LST and VF is monotonically linear. In areas with VF higher than 45%, landscape patterns can act to decrease LST. The aggregation index (AI) and the largest patch index (LPI) can contribute to decreasing LST significantly. Impervious surfaces contribute to high temperature, and the inflection point of the regression curves is 70%. In areas with ISA higher than 70%, a fragmented pattern of impervious surfaces can

Wu, Ye, Shi, Keith and Clarke (2014) studied assessing the effects of land use spatial islands structure on urban heat using HJ-1b remote sensing imagery in Wuhan, China In this research, the radius fractal dimension was used to quantify the spatial variation of different land use types around the hot centers. By integrating

remote sensing Images from the newly launched HJ-1B satellite system, vegetation indexes, landscape metrics and fractal dimension, the effects of land use patterns on the urban thermal environment in Wuhan were comprehensively metrics explored. The results had showed that land surface temperature (LST) is negatively related to only positive normalized difference vegetation index (NDVI) but to Fv across the entire range of values which indicates that fractional vegetation (Fv) is an appropriate predictor of LST more than NDVI in forest areas. Furthermore, the mean LST is highly correlated with four class-based metrics and three metrics landscape-based, which suggests that the landscape composition and the spatial configuration both influence UHIs.

Zhang et al. (2015) used impervious surface area (ISA) as an indicator of urban spatial structure and level of development and quantified characterizing the spatial patterns of landscapes and LST. The characteristics of LST and percent ISA were quantified by landscape metrics such as indices of patch density, aggregation, connectedness, shape and shape complexity. The urban thermal intensity was also analyzed based on percent ISA. The results indicated that landscape metrics are sensitive to the variation of pixel values of fractional ISA, and the integration of LST, LSMA. Landscape metrics provide a quantitative method for describing the spatial distribution and seasonal variation in urban thermal patterns in response to associated urban land cover patterns.

Bernales, Antolihao, Samonte, Campomanes, Rojas, Serna and Silapan (2016) studied modelling the relationship between LST and landscape patterns of LULC classification using multiple linear regression models. This research examined the relationship between LST and LULC as well as to create a model that can predict

LST using class-level spatial metrics from LULC. LST was derived from a Landsat 8 image and LULC classification was derived from LiDAR and Orthophoto datasets. Class-level spatial metrics were created in FRAGSTATS with the LULC and LST as inputs and these metrics were analyses using a statistical framework. Multiple linear regression was done to create models that would predict LST for each class and it was found that the spatial metric "Effective mesh size" was a top predictor for LST in 6 out of 7 classes. The model created can still be refined by adding a temporal aspect by analyzing the LST of another farming period (for rural areas) and looking for common predictors between LSTs of these two different farming periods.

Du et al. (2016) incorporated multilevel models to estimate the hierarchical effects of landscape composition and configuration on LST. Comparisons of the single-level ordinary least squares (OLS) regression model and the multilevel models show four findings. The findings of this study provide new insights into the landscape influences on LST, and suggest that for mitigating urban heat island effects, optimizing the configurations of land cover types in urban areas should be considered because of the larger cooling effect of landscape configurations than compositions on LST.

Zhao, Ren and Tan (2018) studied the spatial patterns of LST and its impact factors: spatial non-stationarity and scale effects based on a geographically-weighted regression model The main purposes of this study are (1) to estimate the spatial distributions of urban heat island (UHI) intensity by using hot spots analysis and (2) to explore the spatial non-stationarity and scale effects of the relationships between LST and related impact factors at multiple resolutions (30–1200 m) and to find appropriate scales for illuminating the relationships in a plain city. Based on the LST

retrieved from Landsat 8 OLI/TIRS images, the Geographically-Weighted Regression (GWR) model was used to explore the scale effects of the relationships in Zhengzhou City between LST and six driving indicators. Spatial scale is coarser than 720 m, both OLS and GWR models were suitable for illustrating the correct relationships between UHI effect and its influence factors in the plain city due to their undifferentiated performance. These findings can provide valuable information for urban planners and researchers to select appropriate models and spatial scales seeking to mitigate urban thermal environment effect.

In summary, LST data has been applied to quantify the observed geographical and ecological patterns and processes tend to be spatial variable and the relationships between LST and its impact factors are often characterized by local changes. Commonly, this feature is referred to as spatial non-stationary. However, most of the existing researches are based on multiple linear regression analysis to model the relationship hiding the important details in the spatial variation and resulting in a failure to capture the spatial dependence of the data This may generate misleading parameter estimates and uncertain significance test results .Hence, the impacts of related influence factors on LST considering the effects of spatial non-stationary need to be further investigated.

CHAPTER III

DATA AND METHODOLOGY

Data collection and preparation and details on research methodology including (1) land use and land cover extraction and simulation, (2) urban growth impact on urban landscape ecology, (3) urban growth impact on ecosystem service value, (4) ecosystem services function value and urban landscape metrics relationship, and (5) impact of urban growth on land surface temperature evaluation and prediction are here explained in this chapter.

3.1 Data

Data collection and preparation included remotely sensed data and GIS data of each research component is summarized in (Table 3.1).

Table 3.1 List of data collection and preparation for analysis and modeling in the study.

Data	Data collection	Data Preparation	Source	Objective
Remote sensing	Landsat 7 ETM+ 1280549 -11 April 2006 -11 December 2011	- Download from website - Layer Stacking - Geometrics collection - Subset image	Earth Science Data Interface (ESDI) at the Global Land Cover Facility **http://glcfapp.glcf.umd.edu:8080/esdi/index.jsp**	1,4
	Landsat 8OLI 1280549 -15 November 2016		United States Geological Survey: USGS (EarthExplorer) **http://earthexplorer.usgs.gov/**	1,4
	Land use map 2006 and 2010	Reference data	Land Development Department: LDD	1
GIS	Digital elevation model	- Elevation extraction - Slope extraction	Royal Thai Survey Department: RTSD	1

Table 3.1 (Continued).

Data	Data collection	Data Preparation	Source	Objective
GIS	Road network	Euclidean distance	Royal Thai Survey Department: RTSD	1
	Stream network	- Euclidean distance	Royal Thai Survey Department: RTSD	1
	Village	Euclidean distance	Department Of Provincial Administration: DOPA	
	Land value	Land value in each land value zone	Land Department: LD	1
	Demography data	Population density	Community Development Department: CDD	1
	Demography data	Capital income	Community Development Department: CDD	1
	Administrative boundary	Data extraction (Sub district)	Royal Thai Survey Department: RTSD	1
	Topographic map L7018	Reference data	Royal Thai Survey Department: RTSD	1
	Urban planning of Khon Kaen (older)	Extraction from existing urban plan	Department of Public Work and Town & Country Planning: DPT	1
	Urban planning of Khon Kaen (new)	LULC 2026 simulation's Scenario II	Department of Public Work and Town & Country Planning: DPT	1
	Urban policy of Khon Kaen	LULC 2026 simulation's Scenario III	National Housing Authority: NHA Khon Kaen Municipality: KKMUNI	1
GPS	Reference data from in 2006 and 2011	- Accuracy assessment	Google earth image	1
	LULC Reference data in 2017	- Training area - Accuracy assessment	In situ data	1, 4

3.2 Methodology

Research methodology is here designed to serve the four main objectives of the study include (1) to extract land use and land cover status and its change during 2006 to 2016 and to simulate two different scenarios (historical land use development, planning and policy) in 2026; (2) to assess urban growth impact on urban landscape ecology and ecosystem services during 2006 to 2026; (3) to identify relationship between ecosystem service function value and landscape pattern metrics; and (4) to evaluate and predict impact of urban growth on land surface temperature. The overview of research methodology according to objectives is presented in Figure 3.1. It consists

of 5 components: (1) land use and land cover extraction and simulation, (2) urban growth impact on urban landscape ecology, (3) urban growth impact on ecosystem service value, (4) ecosystem services function value and urban landscape metrics relationship, and (5) impact of urban growth on land surface temperature evaluation and prediction. Details of each research component are separately described in the following sections.

3.2.1 Component 1: Land use and land cover extraction and simulation

This component consisted of two sub-components: (1) LULC status and its change assessment and (2) LULC scenarios simulation. Under LULC status and its change assessment sub-component, the historical and recent LULC in 2006, 2011 and 2016 were extracted from Landsat imageries acquired in corresponding years using the standard nearest neighbor classifier with feature space optimization of eCognition software. LULC classification system that is modified from standard land use classification system of LDD consisted of (1) urban and built-up area, (2) paddy field (3) field crop (4) forest land, (5) water body, (6) marsh and swamp, (7) range land and (8) unused land (bare land, pit and landfill). Description of LULC type is summarized in Table 3.2.

In addition, accuracy assessment (overall accuracy and Kappa hat coefficient) of LULC data in 2006 and 2011 was performed based on visual interpretation of very high spatial resolution of Google earth image in 2006 and 2011, respectively. Meanwhile accuracy assessment of LULC data in 2016 was performed based on field survey in 2017. In this study, number sample sizes was estimated based on the multinomial distribution theory and sampling method was stratified random sampling as suggested by Congalton and Green (1999).
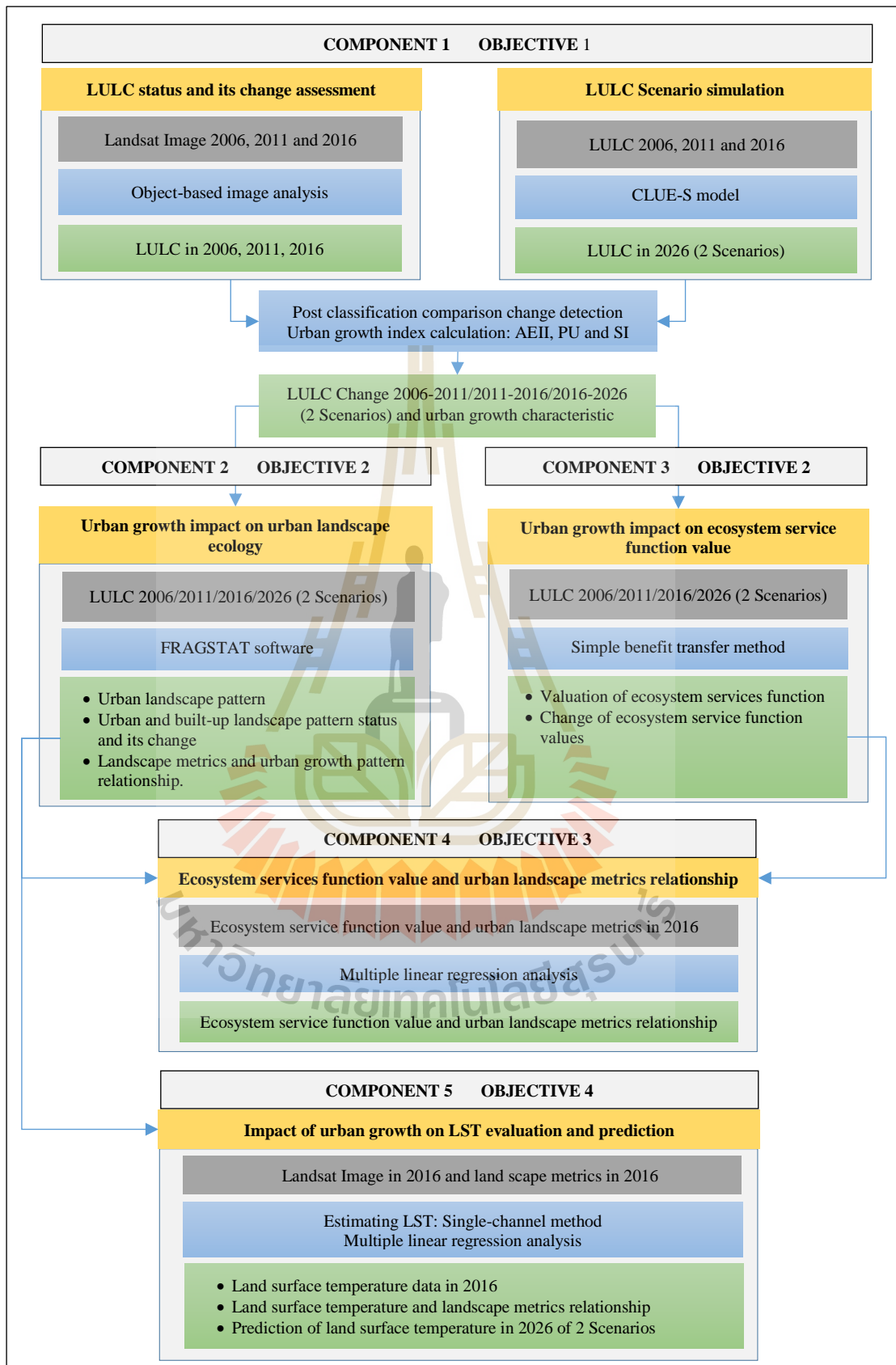
Figure 3.1 Overview of research methodology.

73

Table 3.2 Description of LULC classification system.

LULC type	Description
Urban and built-up area: UR	All land uses to construct human structures, including residential, commercial, and industrial buildings as well as transportation facilities, highways, rail ways, and family houses.
Paddy field: PD	Rice agriculture cultivation area determines by inundating of fields.
Field crop: FC	Land covers with temporary crops followed by harvest and a bare soil period (e.g., single and multiple cropping systems).
Forest land: FO	Areas cover by trees both natural and planted, dense forest, opened forest, orchards, and nurseries.
Water body: WA	Area covers by lake, river and drainages and artificial water areas.
Marsh and swamp: MS	Marsh exists along river banks, characterizes by poor drainage moisture, and surface-grown long-term hygrophytes. Swamp situates on the shallow margins of bays, lakes, ponds, streams, and manmade impoundments such as reservoirs.
Range land: RA	Area covers by grass, shrubs, uncultivated land, lands with herbaceous types of cover. Tree and shrub cover is less than 10%.
Unused land: UL	Uncultivated areas with sparse plant cover, including abandoned sandy land in slopes, bare land, pit and landfill

After that, post classification comparison change detection algorithm was applied to detect LULC change between 2006 and 2011, and between 2011 and 2016. Schematic diagram for input, processing, and output of the sub-component 1: LULC status and its change assessment is illustrated in Figure 3.2.
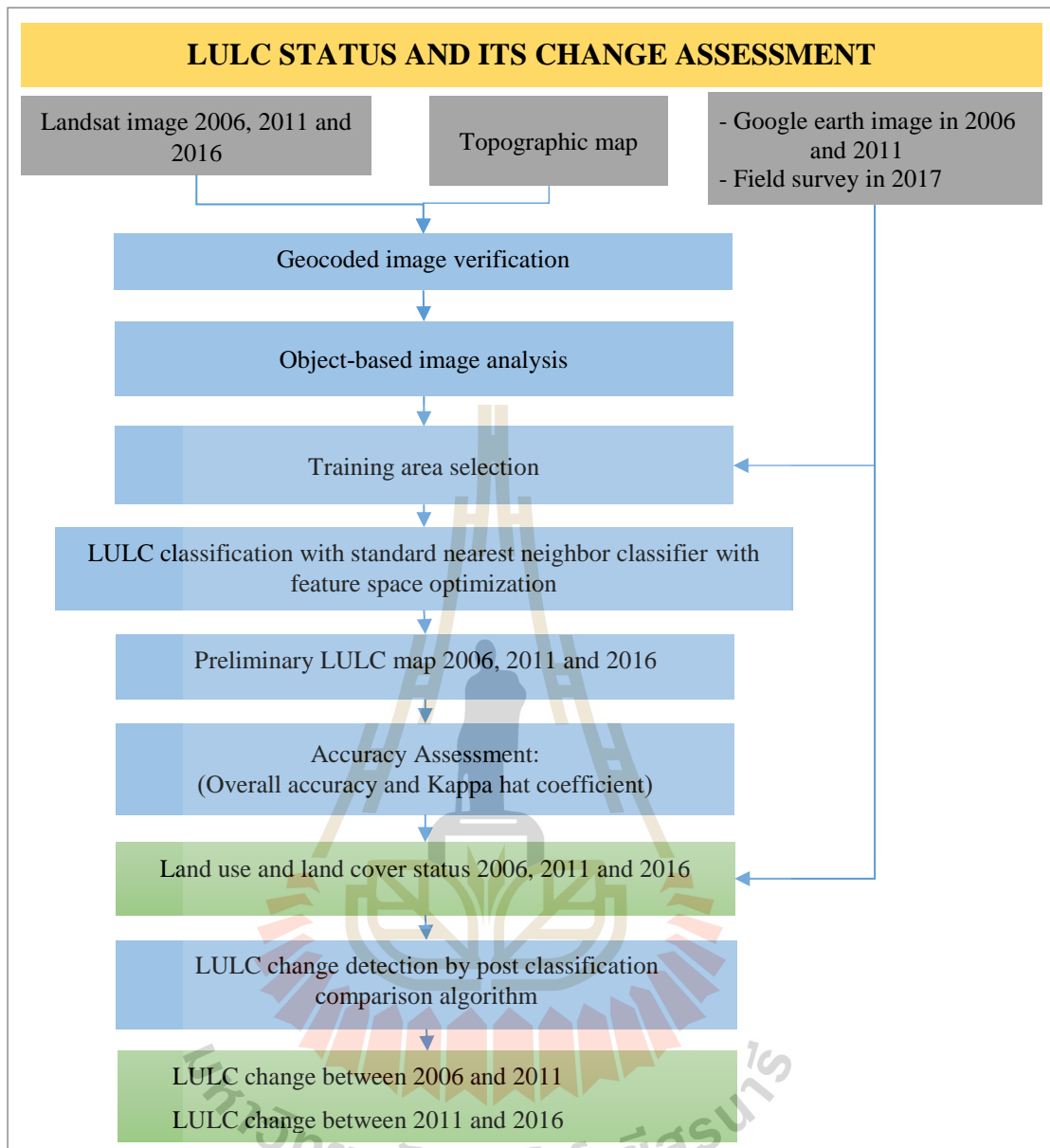
Figure 3.2 Workflow of sub-component 1: LULC status and its change assessment.

Meanwhile, under LULC scenarios simulation sub-component, two different LULC scenarios in 2026 include (1) historical land use development, and (2) planning and policy were simulated using CLUE-S model. Description of input parameter files of CLUE-S mode is summarized as shown in Table 3.3

Table 3.3 Description of application characteristics parameters of CLUE-S model.

Application characteristics	Description
Suitability layer	This is a list of all **driving factor** that are available in the model and the datasets providing the values for these driving factors.
Land system services	This table presents the values that indicate the types and amount of services that each land systems produces, as specified in the **land use matrix**.
Exclusion layers	This part allows to indicate map that present areas where **specific changes are restricted.**
Regression analysis	Multicollinearity – allows to check whether or not driving factor are correlate, in order to build a proper statistical model.
- Sampling	Provides a tool to make a sample of pixels that will be used for the **logistic regression analysis.**
- Parameter selection	Allows to select those parameters that will be included in the model
- Model parameters	Present the **regression parameters**
Conversion order	Indicates how land uses will change in response to land use demands, according to the **land use conversion** order
Elasticity parameters	Shows the resistance for conversion of specific to land use demands, according to the **main parameters file**
Conversion matrix	Indicates what conversion are allowed in this model application, according to the **conversion matrix**
Neighborhoods	Presents the **neighborhood settings**
Scenario parameters	Shows the **demand scenarios** for specific land uses or ecosystem services for a specifics year.

Source: Adapted from Verberg (2012).

In this study, LULC data in 2011 with transitional LULC change matrix during 2006 to 2011 and driving factors on LULC change were firstly applied to predict LULC data in 2016 and its result was compared with the classified LULC in 2016 and assess accuracy for CLUE-S model validation. If overall accuracy and Kappa hat coefficient of agreement between the predicted LULC and the classified LULC in 2016

are equal or more than 80%, the derived configuration of CLUE-S model is acceptance then it will be used to simulate two LULC scenarios (historical land development, and planning and policy) in 2026.

To predict LULC using CLUE-S model. it requires two main parameters, namely LULC conversion matrix and elasticity values and two input data: existing LULC data and future land requirement. Meanwhile, driving factors on LULC change as shown in Table 3.4 were used to identify LULC type location preference by binary logistic regression analysis for allocating LULC type in the future. In this study, land requirement of each LULC type in each scenario in 2026 was predefined for LULC allocation with following criteria.

Scenario I: Historical land use development. The land requirement (land demand) for each LULC type in 2026 simulation was based on annual change rate of each LULC type between 2006 and 2011.

Scenario II: Planning and policy scenario. Under this scenario, urban planning of Mueang Khon Kaen District from Department of Public Work and Town & Country Planning, urban policy from National Housing Authority and mass transport service policy of Khon Kaen Municipality were investigated and transformed into land demand with restriction areas for LULC in 2026 simulation.

Table 3.4 Driving factor on LULC change for LULC type location preference.

Biophysical factor		Githui, Mutua and Bauwens (2009), Oh, Yoo, Lee and Choi
	Elevation	(2011), Zheng et al. (2012), Anputhas, Johannus, Janmaat, Craig, Nichol and Wei (2016)
	Slope	De Souza Soler, Verburg and Veldkamp (2007), Zheng et al. (2012), Githui et al. (2009), Oh et al. (2011), Anputhas et al. (2016)
	Distance from existing urban area	Xu, Li, Song and Yin (2013), Shoyama and Yamagata. (2014), Anputhas, et al. (2016)
	Distance to road network	Erdoğan, Nurlu, and Erdem. (2011), Zheng et al. (2012)
	Distance to stream	Anputhas, et al. (2016), Xu et al. (2013)
Socio-economic factor	Average income per capita at sub-district	De Souza Soler et al. (2007), Xu et al. (2013)
	Land value in each land value zone	Thapa and Murayama. (2010)
	Population density at sub-district	De Souza Soler et al. (2007), Zheng et al. (2012), Githui et al. (2009), Verburg et al. (2002), Trisurat, Alkemade and Verburg (2010), Lin, Lin, Wang, and Hong (2008)

After that, LULC status and its change was further assessed under GIS environment. Herein, post classification comparison change detection algorithm was applied to describe LULC change between 2016 and 2026 of 2 scenarios.

Moreover, urban growth characteristics during 2006 to 2026 of 2 scenarios were characterized using (1) annual expansion intensity index (AEII), (2) urban land percentage (PU) and (3) urban land expansion index (SI). Brief information of three urban growth indices are as follows:

(1) Annual Expansion Intensity index (AEII). AEII describes the degree of differentiation of urban expansion in different directions and denotes the growth of the urban areas of a spatial unit as a percentage of the total area of the land unit is calculated as:

$$\text{AEII} = \frac{UA_{n+i} - UA_i}{nTA_{n+i}} \times 100 \text{ \%} \tag{3.1}$$

Where   AEII is annual expansion intensity index, TA_{n+i} is the total land area of the target unit at the time point of i+n; UA_{n+i} and UA_i is the urban and built-up area in the target unit at time i+n and i, respectively and n is the interval of the calculating period (in years) (Zhao-ling, Pei-Jun and Da-zhi, 2007).

          (2) Urban land percentage (PU). It describes the percentage of urban areas of the total areas is calculated as:

$$\text{PU} = \frac{UL}{TL} \times 100 \text{ \%} \tag{3.2}$$

Where   PU is urban land percentage (%), UL is urban land area (sq.km) and TL is total land area (sq. km) (Tian et al., 2005).

          (3) Urban land expansion index (SI). It represents index for urban development is calculated as:

$$\text{SI} = \frac{UL_j - UL_i}{TL} \times 100 \text{ \%} \tag{3.3}$$

Where   SI is urban expansion index from period i to j, UL_i is urban land area in period i (sq. km) UL_j is urban land area in period j (sq. km) and TL is total land area (sq. km) (Tian et al., 2005).

          Schematic diagram for input, processing, and output of this LULC scenarios simulation sub-component is illustrated in Figure 3.3.
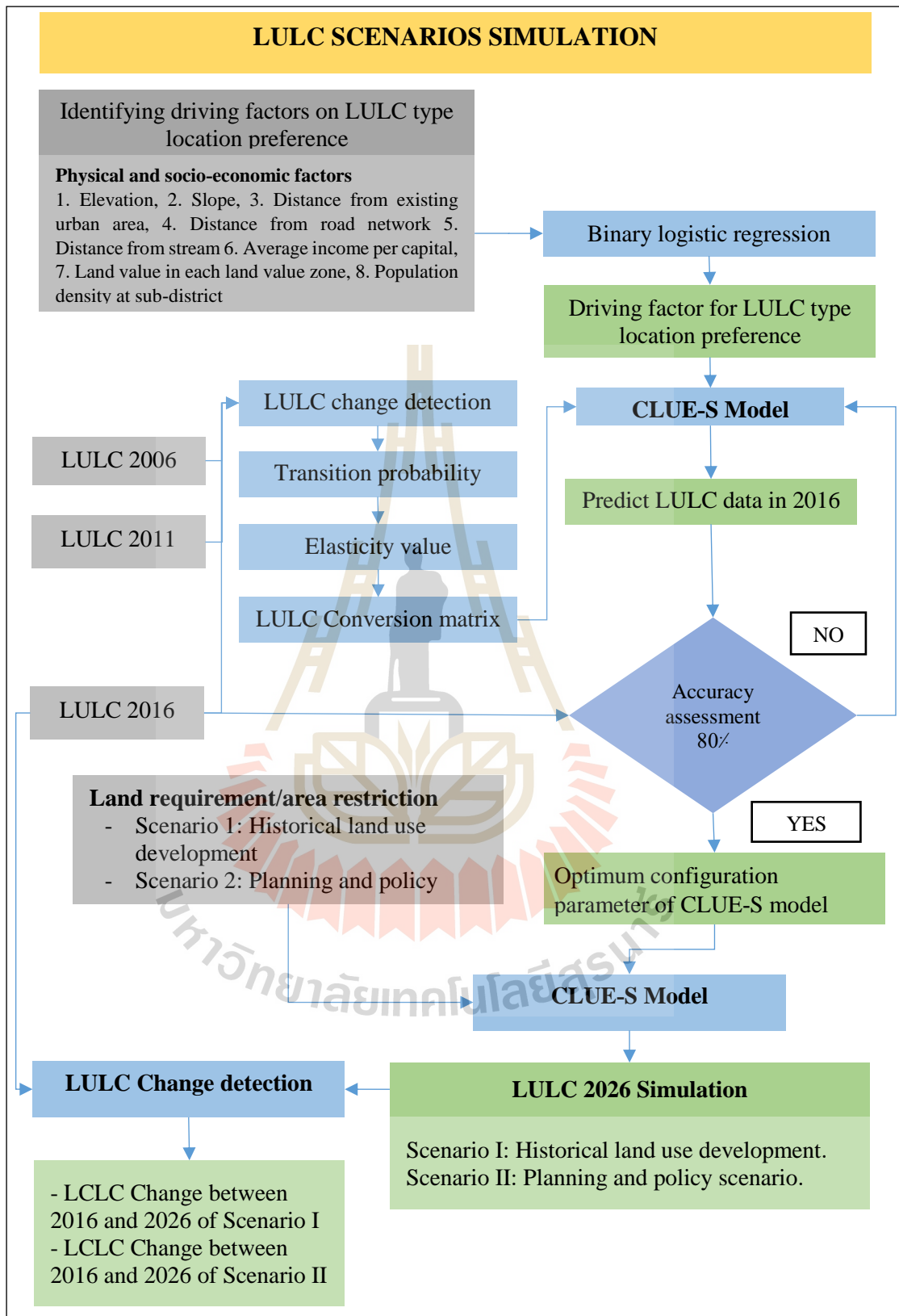
Figure 3.3 Workflow of sub-component 1: LULC scenarios simulation.

3.2.2   Component 2: Urban growth impact on urban landscape ecology

Under this component, the derived LULC data from the previous component were used as input data to calculate urban landscape metric values at class and landscape levels using FRAGSTATS software. In this study, the selected four groups of landscape metrics included (1) area and edge, (2) shape (3) aggregation and (4) diversity metrics (Table 3.5) were here applied to measure urban landscape status and its change during 2006 and 2026 of two scenarios. Likewise, the extracted urban and built-up area from LULC data in 2006, 2011, 2016 and 2026 of two scenarios were also used as input data to quantify urban and built-up area status and change using landscape metric at class level. The derived results will be used to characterize impact of urban growth in the future of two scenarios on urban landscape and urban and built-up area, particularly change of ecological landscape pattern. In practice, urban landscape pattern analysis under FRAGSTATS software was conducted using a moving window method to calculate landscape metric values at class and landscape levels based on the selected landscape metrics.

In addition, the relationship between selected landscape metrics at class level including edge density (ED), total edge (TE), area weighted fractal dimension (FRAG_AM), area weighted mean shape index (SHAPE_AM), landscape shape index (LSI), number of patch (NP) and patch density (PD) and urban growth pattern in 2016 which was represented by percent of urban and built–up area (PLAND) as suggestion by Yeh et al. (2009) and Lal et al. (2017) was examined in this study. In practice, urban landscape pattern analysis under FRAGSTAT software was firstly conducted using a moving window method to quantify landscape metrics at class and then analyze the spatial linear relationship between landscape metrics and urban growth pattern in 2016

using SPSS statistics software. In addition, bivariate correlation analysis was examined to calculate correlation coefficient (r) and coefficient of determination (r^2) using Pearson's product-moment correlation coefficient method.

Schematic diagram for input, processing, and output of the component 3 is illustrated in Figure 3.4.

Table 3.5 List of selected landscape metrics for urban landscape pattern analysis.

Group of metrics	Landscape metrics (Abbreviation)	Eq.	Measurement level
Area and edge metric	Class Area (CA)	2.1	Class
	Percent of Landscape (PLAND)	2.2	Class
	Total Edge (TE)	2.3	Class
	Edge Density (ED)	2.4	Class
Shape metric	Area-weighted mean shape index (SHAPE_AM)	2.5	Class
	Area-weighted mean patch fractal dimension (FRAC_AM)	2.6	Class
Aggregation Metris	Contagion Index (CONTAG)	2.7	Landscape
	Interspersion and Juxtaposition Index (IJI)	2.8	Class
	Landscape Shape Index (LSI)	2.9	Class
	Patch Density (PD)	2.10	Class
	Number of Patch (NP)	2.11	Class
Diversity Metrics	Shannon's Diversity Index (SHDI)	2.12	Landscape
	Shannon's Evenness Index (SHEI)	2.13	Landscape
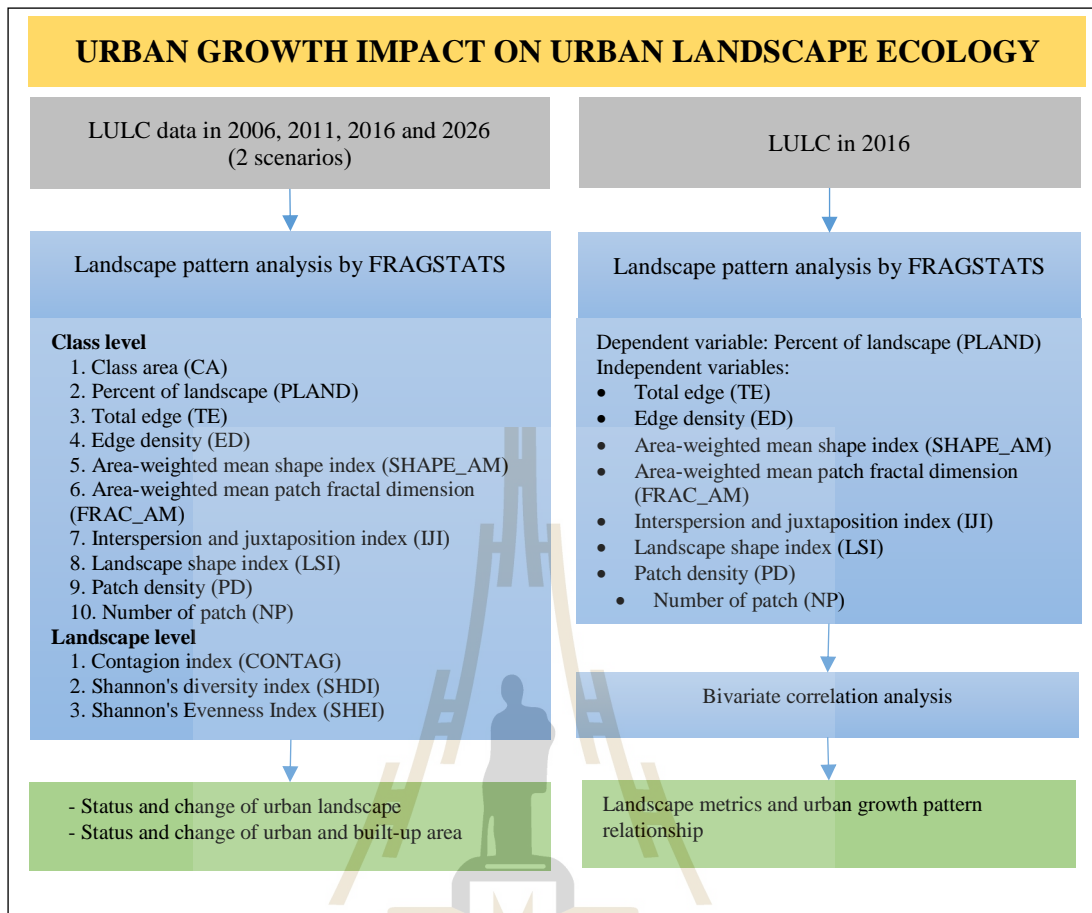
Figure 3.4 Workflow of component 2: Urban growth impact on urban landscape ecology.

3.2.3 Component 3: Impact of urban growth on ecosystem service function value

Under this component, the derived LULC data from Component 1 were firstly used as input data to calculate ecosystem service value status during 2006 and 2026 of two scenarios based on simple benefit transfer method of Costanza (1997) as:

$$ESV = \sum (A_k \times VC_k) \tag{3.4}$$

Where   ESV denotes the total value of ecosystem service while A_k and VC_k represent the area and value coefficient for proxy biome type "k", respectively (Table 3.6). The derived result presents degree of future ESV change in each scenario.

After that, ecosystem services function values change statistics were calculated from comparing values of one dataset with the corresponding value of the second dataset in each period. The contribution ESV changes are calculated using the following equation as suggested by Kindu, Schneider, Teketay and Knoke (2016):

$$ESV\ change = \left[\frac{ESV\ final\ year - ESV\ initial\ year}{ESV\ initial\ year}\right] \tag{3.5}$$

Where,   *ESV* is total estimated ecosystem service value. Positive values suggest an increase whereas negative values imply a decrease in amount and the ES values are presented with USD and percentages. Schematic diagram for input, processing, and output of the component 3 is illustrated in Figure 3.5.

Table 3.6 Coefficient of ecosystem service value for each LULC type (USD/ha/year).

Ecosystem Services Category	Ecosystem services function	Land use land cover type							
		Urban and built-up area	Paddy field	Field crop	Forest land	Water body	Marsh and swamp	Range land	Unused land
1.Regulating services	1.1 Gas regulation	0	74.7	74.7	299.4	0	268.9	104	4.2
	1.2 Climate regulation	0	133	133	282.1	68.7	2,554.70	108	9
	1.3 Waste treatment	0	245	245	119.2	2,719.00	2,716.00	91.5	18
2.Supporting services	2.1 Soil formation	0	218.1	218.1	278.6	1.5	255.5	155	11.8
	2.2 Biodiversity protection	0	106.1	106.1	312.6	372	373.5	130	27.7
3.Provision services	3.1 Water supply	0	89.6	89.6	283.5	3,047.70	2,315.60	105	4.8
	3.2 Food production	0	149.4	149.4	22.9	14.9	44.8	29.8	1.4
	3.3 Raw materials	0	14.9	14.9	206.5	1.5	10.5	25	2.8
4.Cultural services	4.1 Recreation and culture	12.7	1.5	1.5	144.2	648.4	829.2	60.3	16.6
Total		12.7	1,032.3	1,032.3	1,949.0	6,873.7	9,368.7	808.6	96.3

Source: Modified from Mamat, Halik and Rouzi (2017)

URBAN GROWTH IMPACT ON ECOSYSTEM SERVICE FUNCTION VALUE

LULC 2006, 2011, 2016 and 2026 (2 Scenarios)

1. Urban and built-up area (Ur)
2. Paddy field (Pd)
3. Field crop (Fc)
4. Forest land (Fo)
5. Water body (Wa)
6. Marsh and swamp (Ms)
7. Range land (Ra)
8. Unused land (Ul)

Ecosystem service coefficients

1 Gas regulation
2 Climate regulation
3 Waste treatment
4. Soil formation
5. Biodiversity protection
6. Water supply
7. Food production
8. Raw materials
9. Recreation and culture

Ecosystem service functions value calculation

$$ESV = \sum (A_k \times VC_k)$$

Ecosystem services function values change calculation

$$ESV\ change = \left[\frac{ESV\ final\ year - ESV\ initial\ year}{ESV\ initial\ year}\right]$$

- Ecosystem services function value in 2006, 2011, 2016 and 2026 (2 Scenario)
- Change of ecosystem service function values between 2006 and 2011, 2011 and 2016, 2016 and 2026 (2 Scenario) 2006-2026 (Unit: USD/ha/year)

1 Gas regulation service function
2 Climate regulation service function
3 Waste treatment service function
4. Soil formation service function
5. Biodiversity protection service function
6. Water supply service function
7. Food production service function
8. Raw materials service function
9. Recreation and culture service function

Figure 3.5 Workflow of component 3: Urban growth impact on ecosystem service function value.

3.2.4 Component 4: Ecosystem services value and urban landscape metrics relationship

The derived ecosystem service function values of urban landscape that include (1) gas regulation, (2) climate regulation, (3) waste treatment, (4) soil formation, (5) biodiversity protection, (6) water supply, (7) food production, (8) raw materials and (9) recreation and culture were used to identify spatially relationship with the derived landscape metrics using multiple linear regression analysis. The derived result will show the influence of landscape metric on ecosystem service function. Schematic diagram for input, processing, and output of the component 4 is played in Figure 3.6.

ECOSYSTEM SERVICE FUNCTION VALUE AND URBAN LANDSCAPE METRICS RELATIONSHIP

Dependent variable	Independent variable
Ecosystem service function value 2016	**Landscape metrics 2016**
1 Gas regulation	**Class level**
2 Climate regulation	1. Class area
3 Waste treatment	2. Percent of landscape
4. Soil formation	3. Total edge
5. Biodiversity protection	4. Edge density
6. Water supply	5. Area-weighted mean shape index
7. Food production	6. Area-weighted mean patch fractal dimension
8. Raw materials	7. Interspersion and Juxtaposition Index
9. Recreation and culture	8. Landscape Shape Index
	9. Patch Density
	10. Number of Patch
	Landscape level
	1. Shannon's diversity index
	2. Shannon's Evenness Index

Basic information of ecosystem service function values in 2016

Stepwise multiple linear regression analysis ← Basic information of urban landscape metrics in 2016

Ecosystem service function value and urban landscape metrics relationship

Figure 3.6 Workflow of Component 4: Ecosystem services function value and urban landscape metrics relationship.

3.2.5 Component 5: Impact of urban growth on land surface temperature evaluation and prediction

Land surface temperature (LST) in 2016 was firstly derived based on standard conversion method as suggestion by USGS (2015) including 5 steps: (1) convert the digital number (DN) of Landsat 8 TIR band 10 into spectral radiance using Eq. 2.24, (2) the spectral radiance is then converted to brightness temperature, which is the at-satellite temperature (TB) using Eq. 2.25, (3) in order to get the LSE, the

vegetation proportion is using Eq. 2.27 (4) LSE is then computed using Eq.2.28 and (5) LST can be computed (in degrees Celsius) using the at- satellite brightness temperature and the land surface emissivity in Eq. 2.28 as mentioned in details in Section 2.5 of Chapter II and then identified the relationship with the selected single (Class area, CA) and multiple (Percent of landscape, PLAND), Area weighted fractal dimension, FRAG_AM, and Patch density, PD) landscape metrics using stepwise multiple linear regression analysis. The derived results were used to predict effect of urban growth on LST in each scenario. Schematic diagram for input, processing, and output of the component 5 is displayed in Figure 3.7.
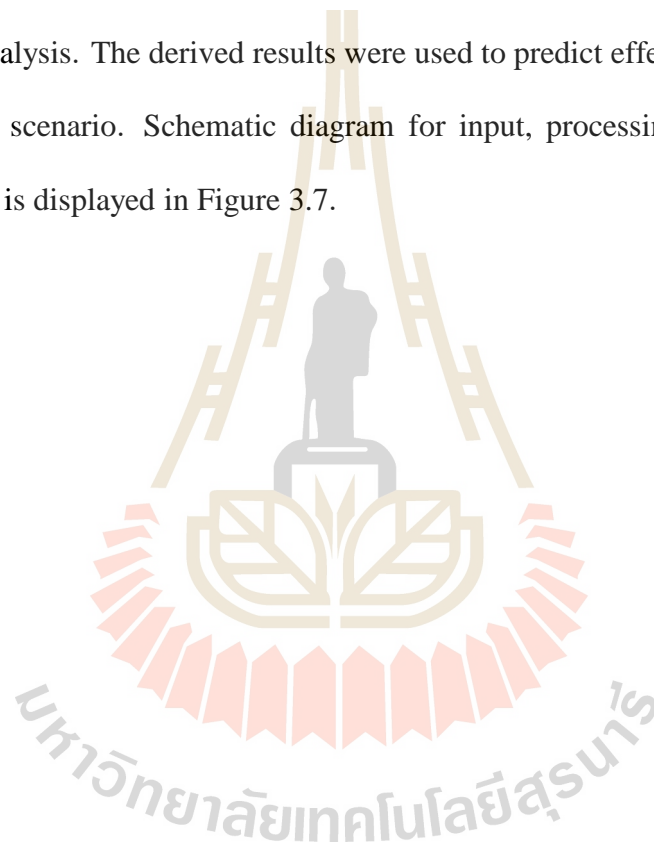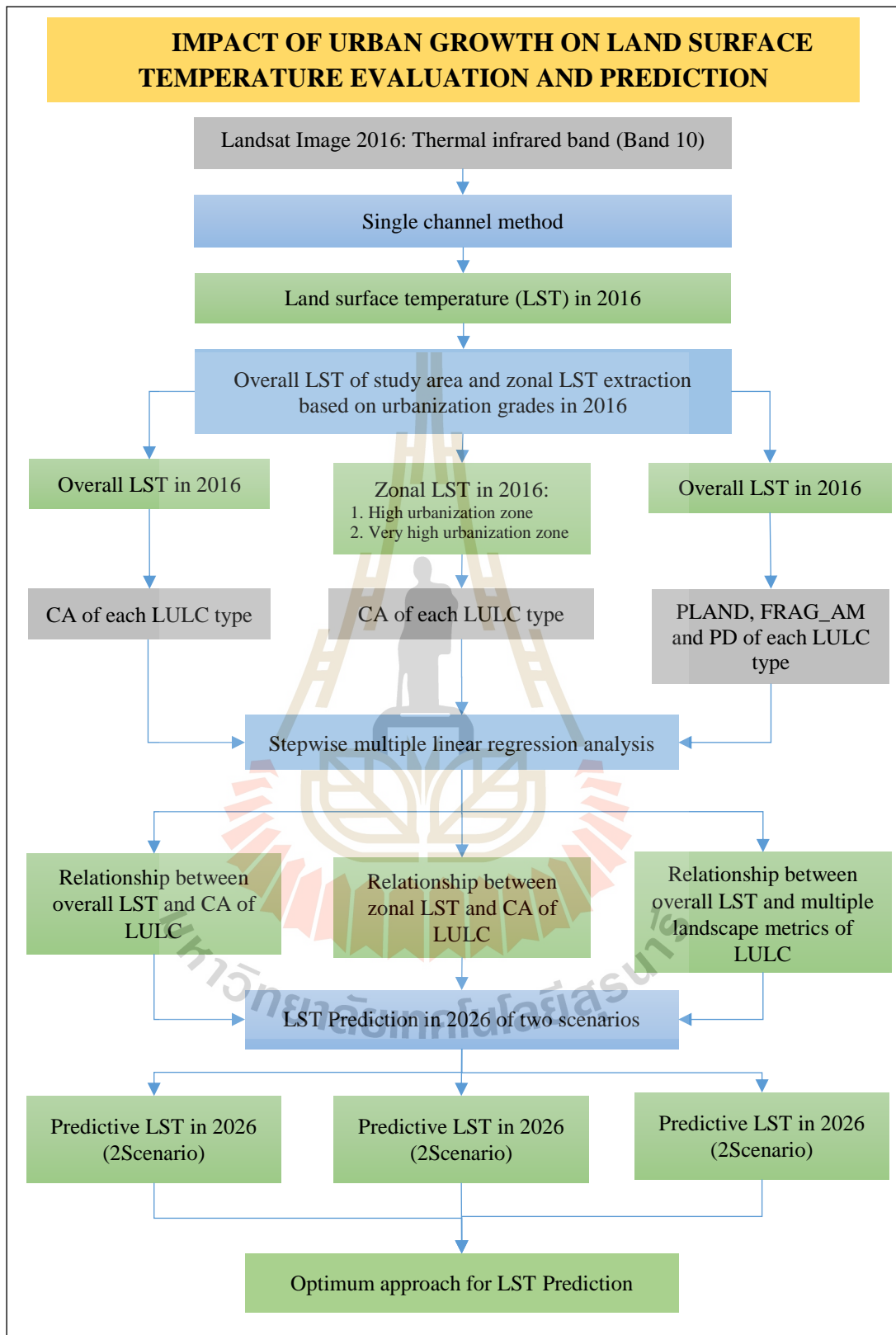
Figure 3.7 Workflow of component 5: Impact of urban landscape change on land surface temperature.

CHAPTER IV

LAND USE AND LAND COVER EXTRACTION AND

SIMULATION

This chapter presents results of the first objective focusing on extraction of LULC during 2006 and 2016 and simulation of LULC in 2026 of two scenarios. The major results consist of (1) LULC extraction in 2006, 2011 and 2016 and its status, (2) LULC simulation in 2026 and its status, (3) change of LULC during 2006 to 2026 (Scenario I and II), and (4) characteristic of urban growth during 2006 and 2026.

4.1   LULC extraction in 2006, 2011 and 2016 and its status

LULC types of Mueang Khon Kaen district, Khon Kaen province in 2006, 2011 and 2016 were here derived from Landsat 7 ETM+ and Landsat 8 OLI data (Figures 4.1 to 4.3) using object-based image analysis (OBIA) with standard nearest neighbor classifier and feature space optimization of eCognition software. LULC classification system that is modified from standard land use classification system of LDD consists of (1) urban and built-up area, (2) paddy field (3) field crop (4) forest land, (5) water body, (6) marsh and swamp, (7) range land and (8) unused land (bare land, pit and marsh). After that, LULC status in 2006, 2011, 2016 were further assessed under GIS environment.
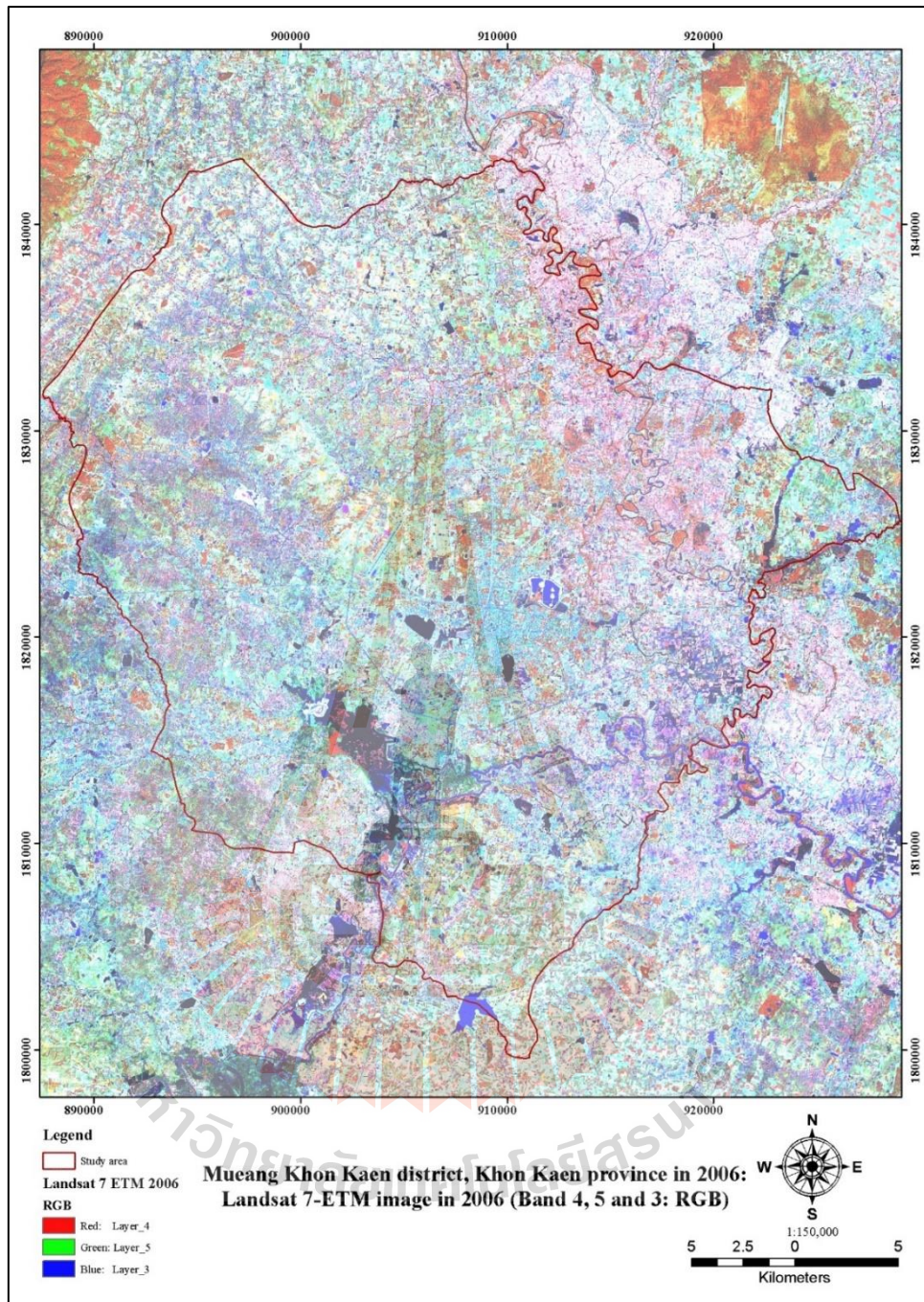
Figure 4.1 Landsat 7-ETM+ image in 2006 (Band 4, 5 and 3: RGB).
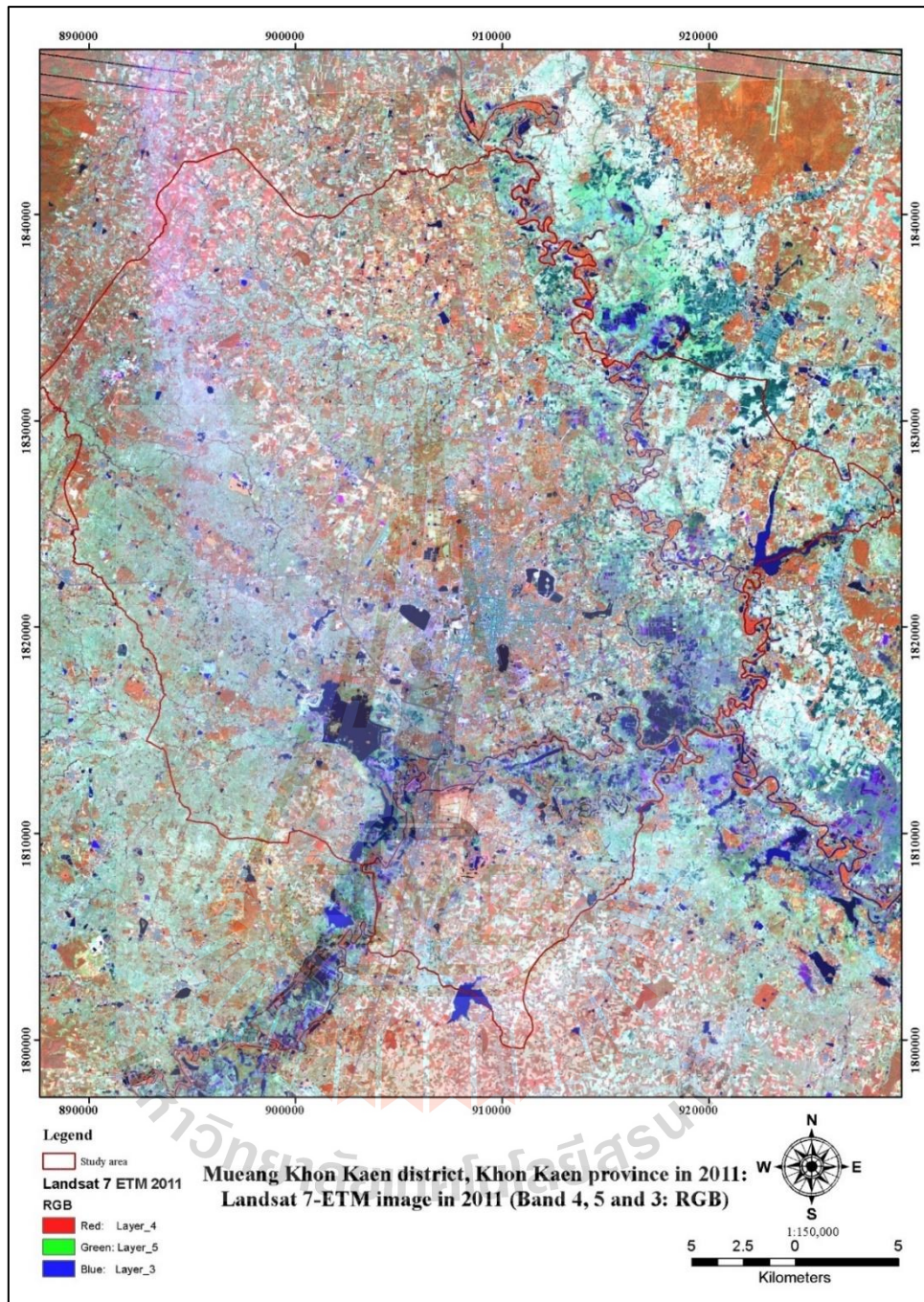
Figure 4.2 Landsat 7-ETM+ image in 2011 (Band 4, 5 and 3: RGB).
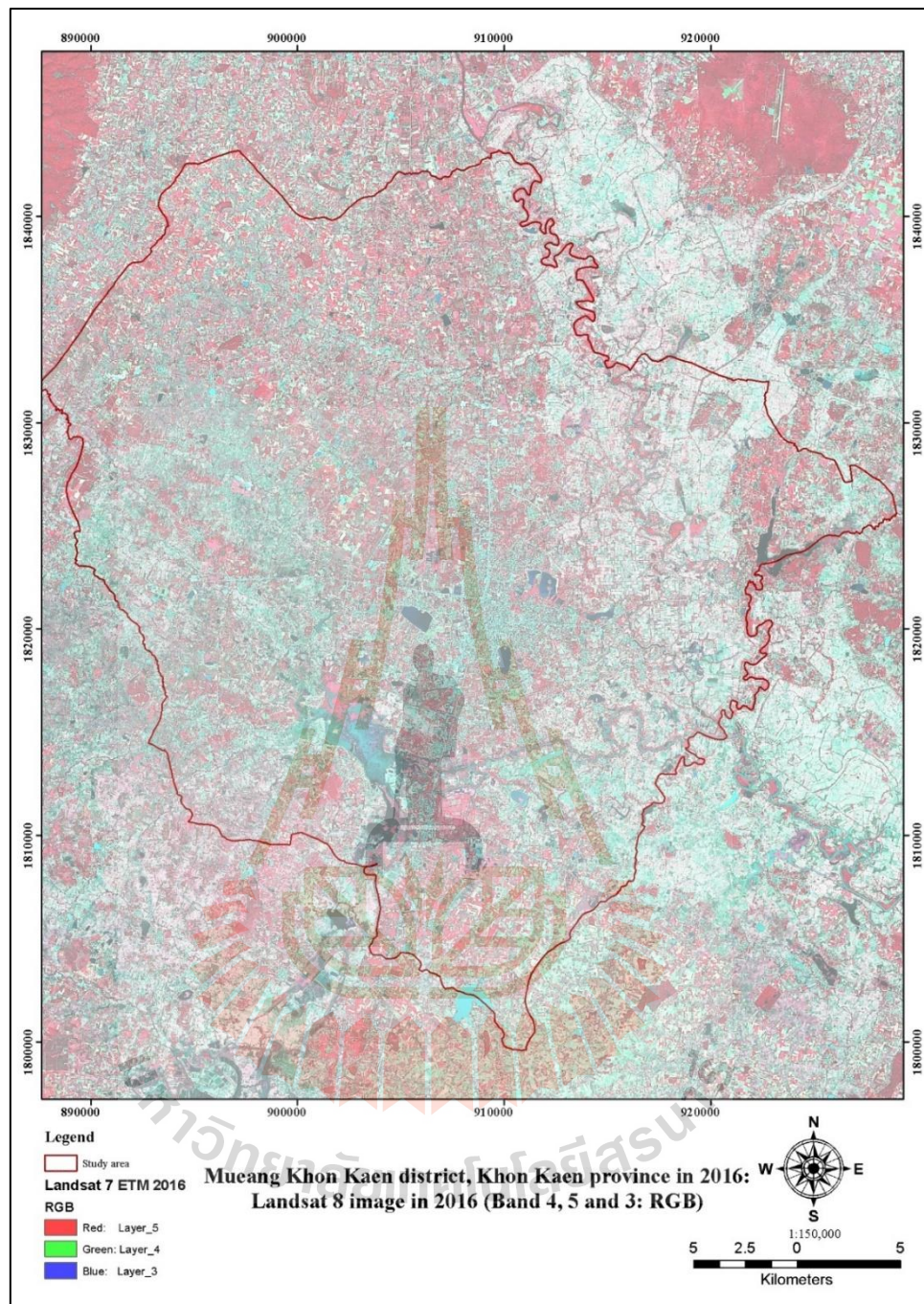
Figure 4.3 Landsat 8 image in 2016 (Band 4, 5 and 3: RGB).

Under OBIA, the multiresolution segmentation algorithm has been applied to segment image and consecutively merge pixels into image object based on the criteria of relative homogeneity for LULC classification. Herein, scale, shape and compactness

parameters were firstly applied to generate segmented image with value of 30, 0.1 and 0.5 respectively (see example in Figures 4.4 to 4.6). The selection of spectral and spatial feature of the training sample were selected for LULC classification with standard nearest neighbor with feature space optimization. In this study, the selected standard features included (1) mean value, (2) standard deviation, (3) brightness, (4) Max. diff. (max intensity difference), (5) NDVI (Normalized Difference Vegetation Index), (6) NDWI (Normalized Difference Water Index), (7) LWM (Land and Water Mask) (Table 4.1) as suggested by Qian et al. (2015) were here applied to classify LULC categories in 2006, 2011 and 2016.

Results of LULC status assessment and its accuracy assessment in 2006, 2011, and 2016 were separately described in detail in the following sections.
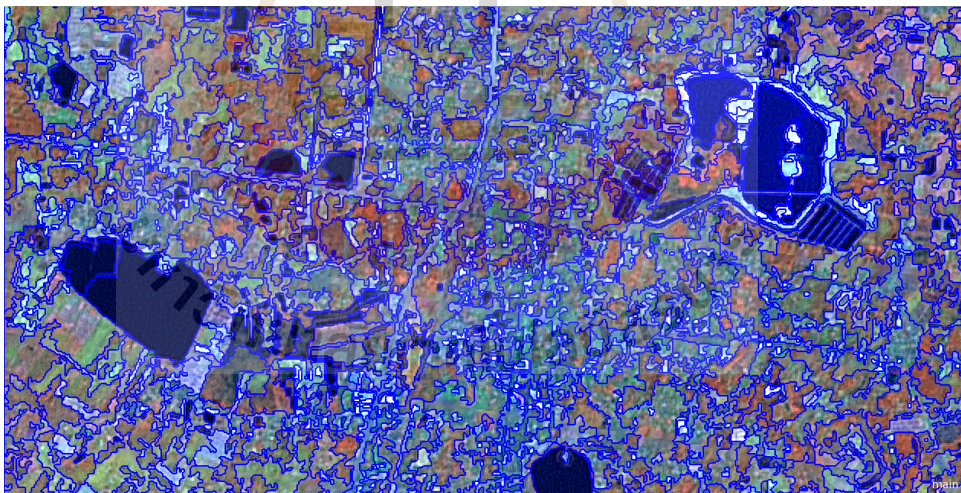
Figure 4.4 Image segmentation of Landsat 7-ETM+ image in 2006.
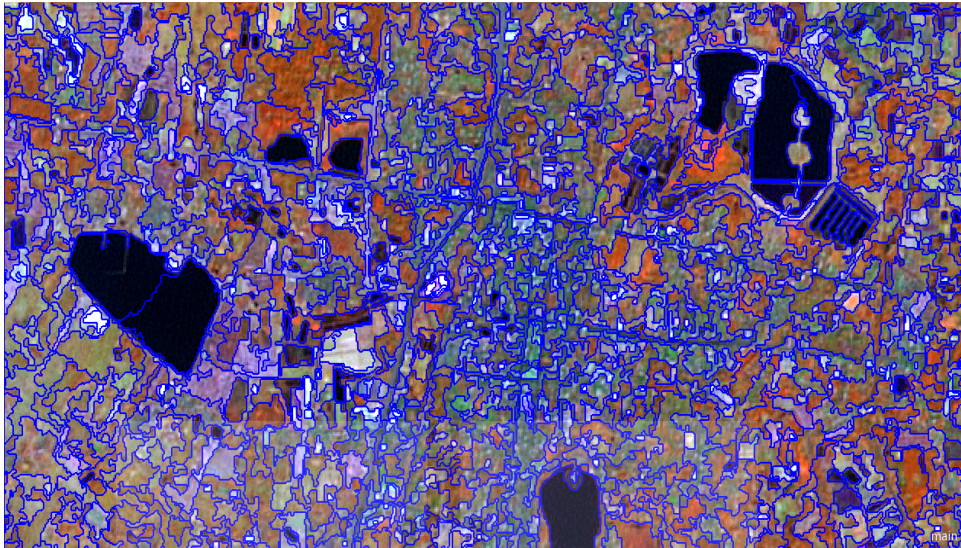
Figure 4.5 Image segmentation of Landsat 7-ETM+ image in 2011.

Figure 4.6 Image segmentation of Landsat 8-OLI image in 2016.

Table 4.1 Object feature used for LULC classification.

Object Feature	Description
Mean value	Mean value of a specific band of an image object
Standard deviation	Standard deviation of an image object
Brightness	Mean value of the multispectral bands
Max. diff.	Max intensity difference of the multispectral bands
NDVI	Normalized Difference Vegetation Index: (NIR-Red)/(NIR+Red)
NDWI	Normalized Difference Water Index: (Green-NIR)/(Green+NIR)
LWM	Land and Water Mask: (MIR/Green) *100

Source: Adapted from Qian et al. (2015).

4.1.1 LULC status in 2006 and accuracy assessment

The most significant LULC type of Mueang Khon Kaen district, Khon Kaen province in 2006 is paddy field covering an area of 556.20 km^2 or 56.63% of the study area. The second dominant LULC type is field crop accounting for 207.40 km^2 or 21.12% of the area. These areas are found in the north and north-west of the study area. The third important LULC category is urban and built-up area covering area of 58.03 km^2 or 5.91% of the area. This area situates in the central of the study area. Other LULC types include forest land, water body, marsh and swamp, range land, and unused land and they distribute around the Mueang Khon Kaen district. These categories cover area of 160.58 km^2 or 16.37% of the study area (Table 4.2 and Figure 4.7).

Table 4.2 Area and percentage of land use and land cover in 2006.

Land use and land cover type	Area in km^2	Percent
1. Urban and built-up area (Ur)	58.03	5.91
2. Paddy field (Pd)	556.20	56.63
3. Field crop (Fc)	207.40	21.12
4. Forest land (Fo)	40.42	4.12
5. Water body (Wa)	52.81	5.38
6. Marsh and swamp (Ms)	33.64	3.43
7. Range land (Ra)	28.82	2.94
8. Unused land (Ul)	4.89	0.50
Total	982.21	100.00

In addition, the classified LULC in 2006 was compared with ground information in 2006 from Google earth image for accuracy assessment using overall accuracy and kappa hat coefficient of agreement. In practice, error matrix between LULC type in 2006 and the reference LULC types from Google earth image in 2006 is firstly constructed and then is evaluated accuracy. In this study, 757 randomly stratified sampling points based on multinomial distribution theory with desired level of confident 95 percent and a precision of 5 percent were used for accuracy assessment (Figure 4.8). The error matrix between the classified LULC in 2006 and the reference LULC from Google earth image in 2006 is shown in Table 4.3.

Legend
- Urban and built-up area (Ur)
- Paddy field (Pd)
- Field crop (Fc)
- Forest land (Fo)
- Water body (Wa)
- Marsh and swamp (Ms)
- Range land (Ra)
- Unused land (Ul)

Spatial distribution of land use and land cover in 2006
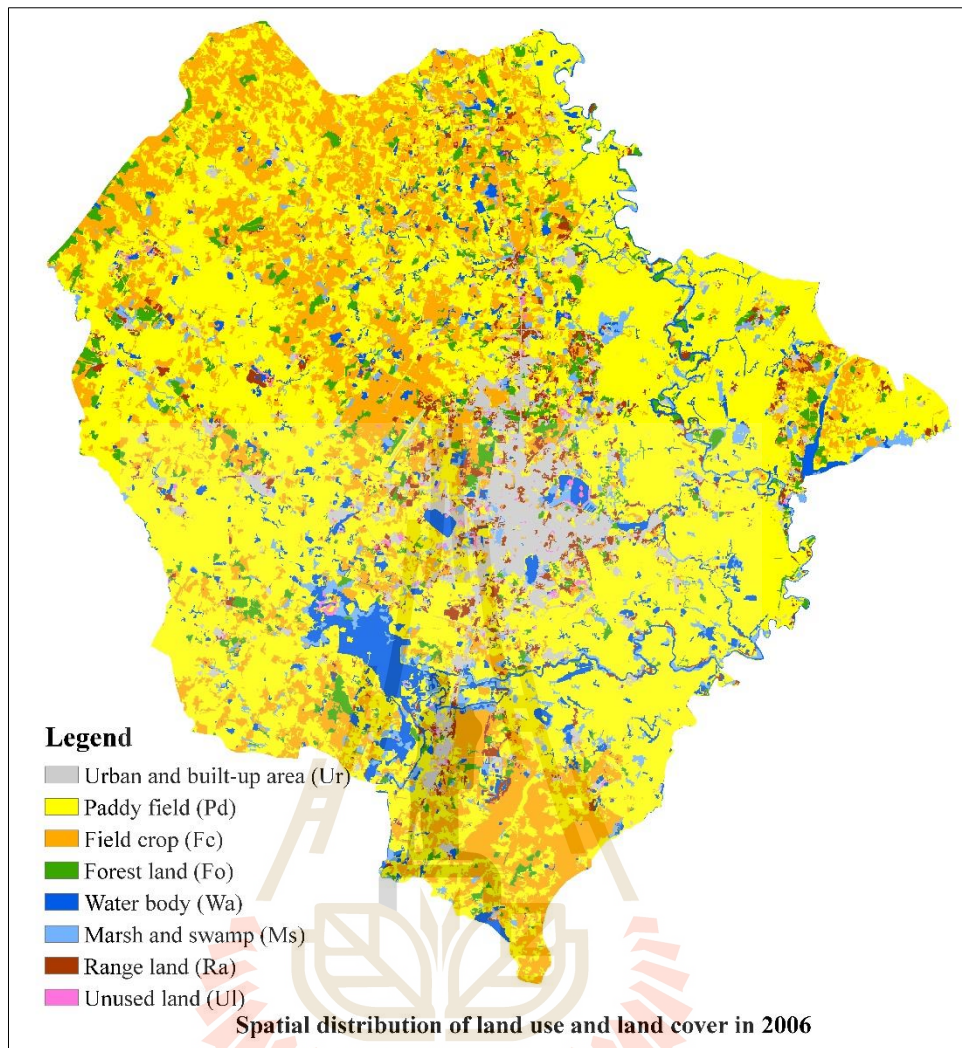
Figure 4.7 Spatial distribution of land use and land cover in 2006.
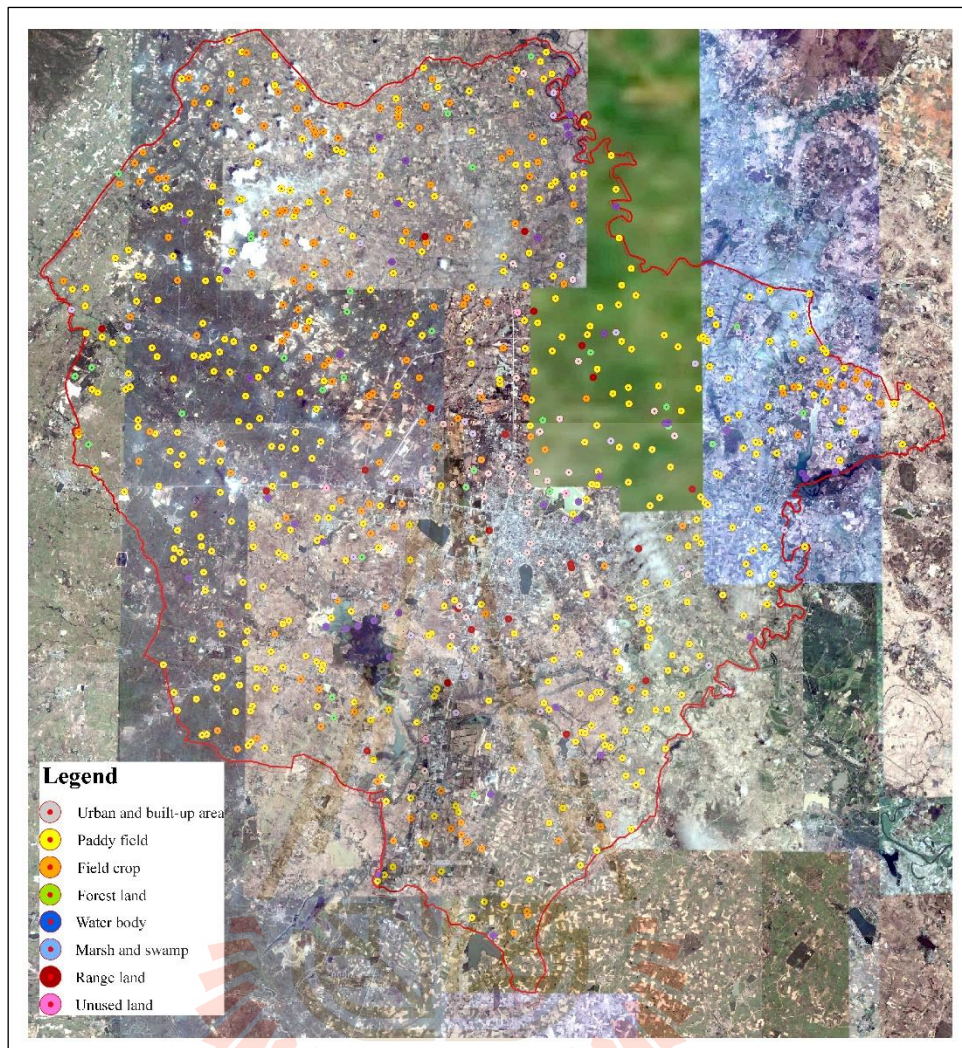
Figure 4.8 Spatial distribution of LULC sampling points in 2006.

Table 4.3 Error matrix between land use and land cover in 2006 and ground reference data from Google earth in 2006.

LULC in 2006	Ground reference data in 2006								
LULC type	Ur	Pd	Fc	Fo	Wa	Ms	Ra	Ul	Total
Urban and Built-Up area (Ur)	44			0			1		45
Paddy field (Pd)	0	364	46	6	3		8		427
Field crop (Fc)	0	32	124	1			3		160
Forest land (Fo)	0	4	1	26					31
Water body (Wa)		2	2		36	1			41
Marsh and swamp (Ma)	0	2	3	1	1	19			26
Range land (Ra)	2				2		19		23
Unused land (Ul)					1			3	4
Total	46	404	176	34	43	20	31	3	757
Producer's accuracy (%)	95.65	90.10	70.45	76.47	83.72	95.00	61.29	100.00	
User's accuracy (%)	97.78	85.25	77.50	83.87	87.80	73.08	82.61	75.00	
Overall accuracy (%)	83.88								
Kappa hat coefficient (%)	74.78								

As result, it was found that the overall accuracy is 83.88% and Kappa hat coefficient of agreement is 74.78%. Meanwhile producer's accuracy (PA), which represents omission error, varies between 61.29% for range land and 95.65% for urban and built-up area while user's accuracy (UA), which represents commission error, varies between 73.08% for range land and 97.78% for urban and built-up area. Based on Fitzpatrick-Lins (1981), Kappa hat coefficient between 40 and 80 percent represents moderate agreement or accuracy between the classified map and the reference map.

4.1.2 LULC status in 2011 and accuracy assessment

The most significant LULC type of Mueang Khon Kaen district, Khon Kaen province in 2011 is still paddy field covering an area of 517.84 km^2 or 52.72% and it distributes throughout the study area. The second dominant LULC type is field crop accounting for 189.81 km^2 or 19.32% of the study area. The third important LULC

category is urban and built-up area covering area of 87.14 km^2 or 8.87% of the study area. Other LULC types include forest land, water body, marsh and swamp, range land, and unused land (bare land, pit and marsh) distribute around the Mueang Khon Kaen district. These categories cover area of 187.42 km^2 or 19.09% of the study area (Table 4.4 and Figure 4.9).

Table 4.4 Area and percentage of land use and land cover in 2011.

Land use and land cover type	Area in km^2	Percent
1. Urban and built-up area (Ur)	87.14	8.87
2. Paddy field (Pd)	517.84	52.72
3. Field crop (Fc)	189.81	19.32
4. Forest land (Fo)	40.41	4.12
5. Water body (Wa)	52.52	5.35
6. Marsh and swamp (Ms)	32.81	3.34
7. Range land (Ra)	54.47	5.55
8. Unused land (Ul)	7.21	0.73
Total	982.21	100.00
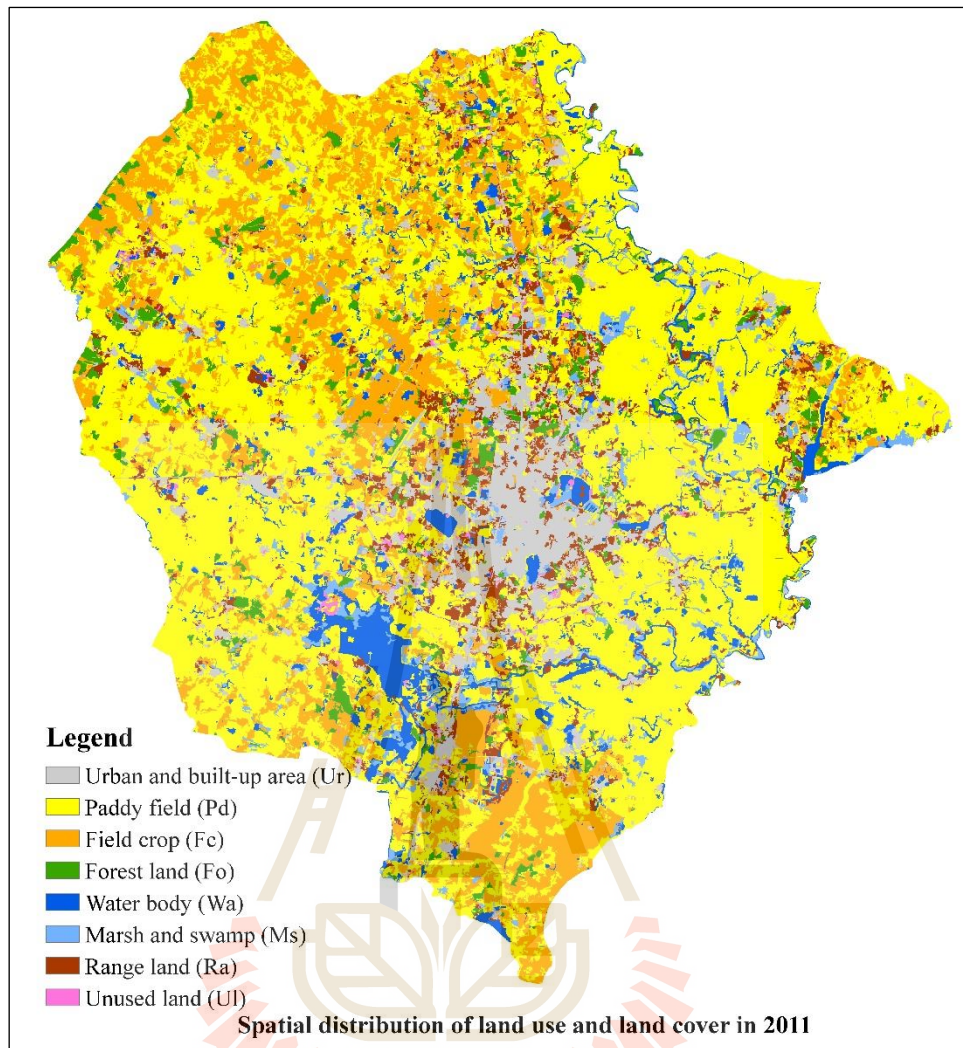
Figure 4.9 Spatial distribution of land use and land cover in 2011.

In addition, the classified LULC in 2011 was compared with ground information in 2011 from Google earth image for accuracy assessment using overall accuracy and kappa hat coefficient of agreement. In practice, error matrix between LULC type in 2011 and the reference LULC types from Google earth image in 2011 is firstly constructed and then evaluated accuracy. In this study, 757 randomly stratified sampling points based on multinomial distribution theory with desired level of confident 95 percent and a precision of 5 percent were used for accuracy assessment

(Figure 4.10). The error matrix between the classified LULC in 2011 and the reference

LULC from Google earth image in 2011 is shown in Table 4.5.

Table 4.5 Error matrix between land use and land cover in 2011 and ground reference
data from Google earth in 2011.

LULC in 2006	Ground reference data in 2006								
LULC type	Ur	Pd	Fc	Fo	Wa	Ms	Ra	Ul	Total
Urban and Built-Up area (Ur)	63	3		1					67
Paddy field (Pd)	9	338	28	2	4	5	10	3	399
Field crop (Fc)	9		127	2			8		146
Forest land (Fo)	2	4	6	20					32
Water body (Wa)	0		1	1	37	1	1		41
Marsh and swamp (Ma)	0	9	1			10	5		25
Range land (Ra)	0	12	8				16	5	41
Unused land (Ul)	2				0			4	6
Total	85	366	171	26	41	16	40	12	757
Producer's accuracy (%)	74.12	92.35	74.27	76.92	90.24	62.50	40.00	33.33	
User's accuracy (%)	94.03	84.71	86.99	62.50	90.24	40.00	39.02	66.67	
Overall accuracy (%)	81.24								
Kappa hat coefficient (%)	72.56								

Figure 4.10 Spatial distribution of LULC sampling point in 2011.

As result, it was found that the overall accuracy is 81.24% and Kappa hat coefficient of agreement is 72.56%. Meanwhile producer's accuracy (PA), which represents omission error, varies between 33.33% for unused land and 92.35% for paddy field while user's accuracy (UA), which represents commission error, varies between 39.02% for marsh and swamp and 94.03% for urban and built-up area. Based on Fitzpatrick-Lins (1981), Kappa hat coefficient between 40 and 80 percent represents moderate agreement or accuracy between the classified map and the reference map.

4.1.3   LULC status in 2011 and accuracy assessment

The most significant LULC type of Mueang Khon Kaen district, Khon Kaen province in 2016 is still paddy field covering an area of 451.39 km^2 or 45.96% of the study area. The second dominant LULC type is field crop accounting for 148.04 km^2 or 15.07% of the study area. The third important LULC category is urban and built-up area covering area of 131.75 km^2 or 13.41% of the study area. Other LULC types include forest land, water body, range land, marsh and swamp, and unused land (bare land, pit and marsh) distribute around the central of Mueang Khon Kaen district. These categories cover area of 251.04 km^2 or 25.55% of the study area. (Table 4.6 and Figure 4.11).

Table 4.6 Area and percentage of land use and land cover in 2016.

Land use and land cover type	Area in km^2	Percent
1. Urban and built-up area (Ur)	131.75	13.41
2. Paddy field (Pd)	451.39	45.96
3. Field crop (Fc)	148.04	15.07
4. Forest land (Fo)	40.21	4.09
5. Water body (Wa)	52.45	5.34
6. Marsh and swamp (Ms)	32.32	3.29
7. Range land (Ra)	109.24	11.12
8. Unused land (Ul)	16.82	1.71
Total	**982.21**	**100.00**

In addition, the classified LULC in 2016 was compared with ground information in 2017 for accuracy assessment using overall accuracy and kappa hat coefficient of agreement. In practice, error matrix between LULC type in 2016 and the reference LULC types from field survey in 2017 is firstly constructed and then assessed

accuracy. In this study, 757 randomly stratified sampling points based on multinomial distribution theory with desired level of confident 95 percent and a precision of 5 percent were used for accuracy assessment (Figure 4.12). The error matrix between the classified LULC in 2016 and the reference LULC from field survey in 2017 is shown in Table 4.7.
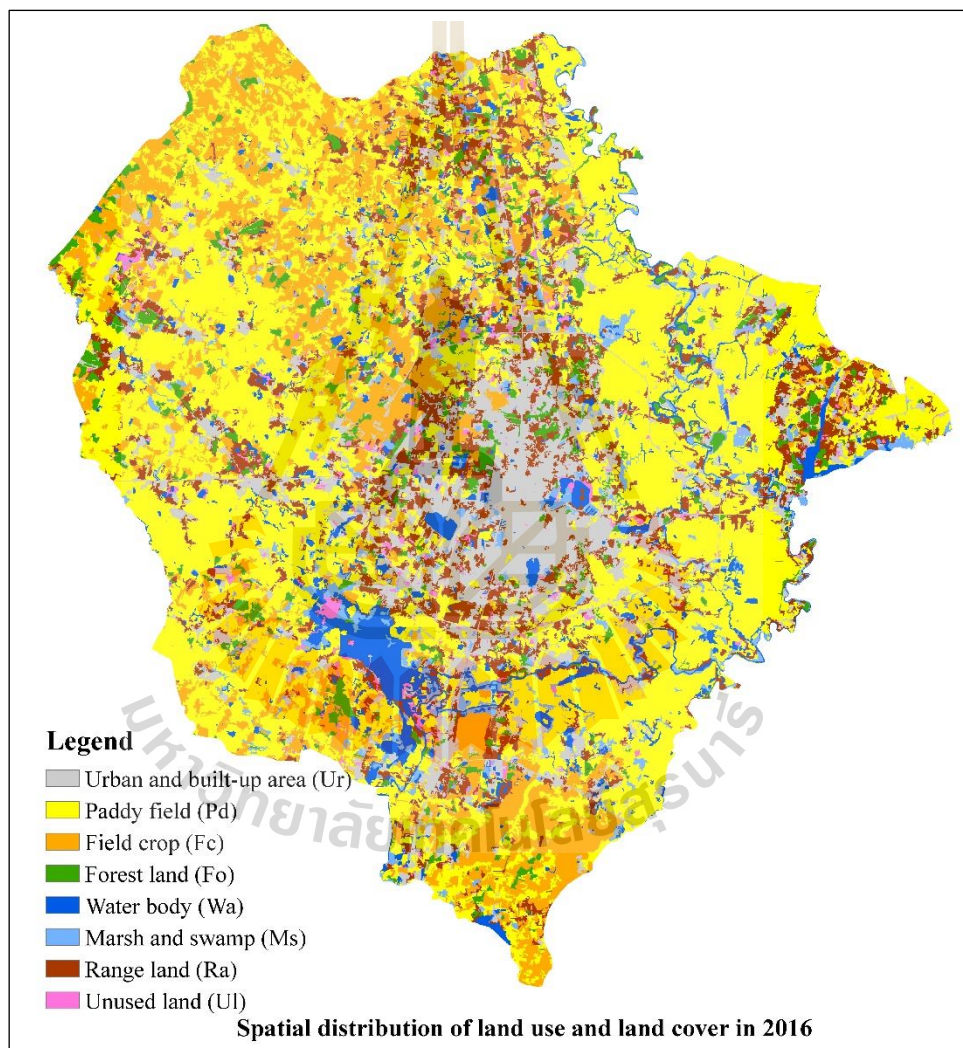
Figure 4.11 Spatial distribution of land use and land cover in 2016.
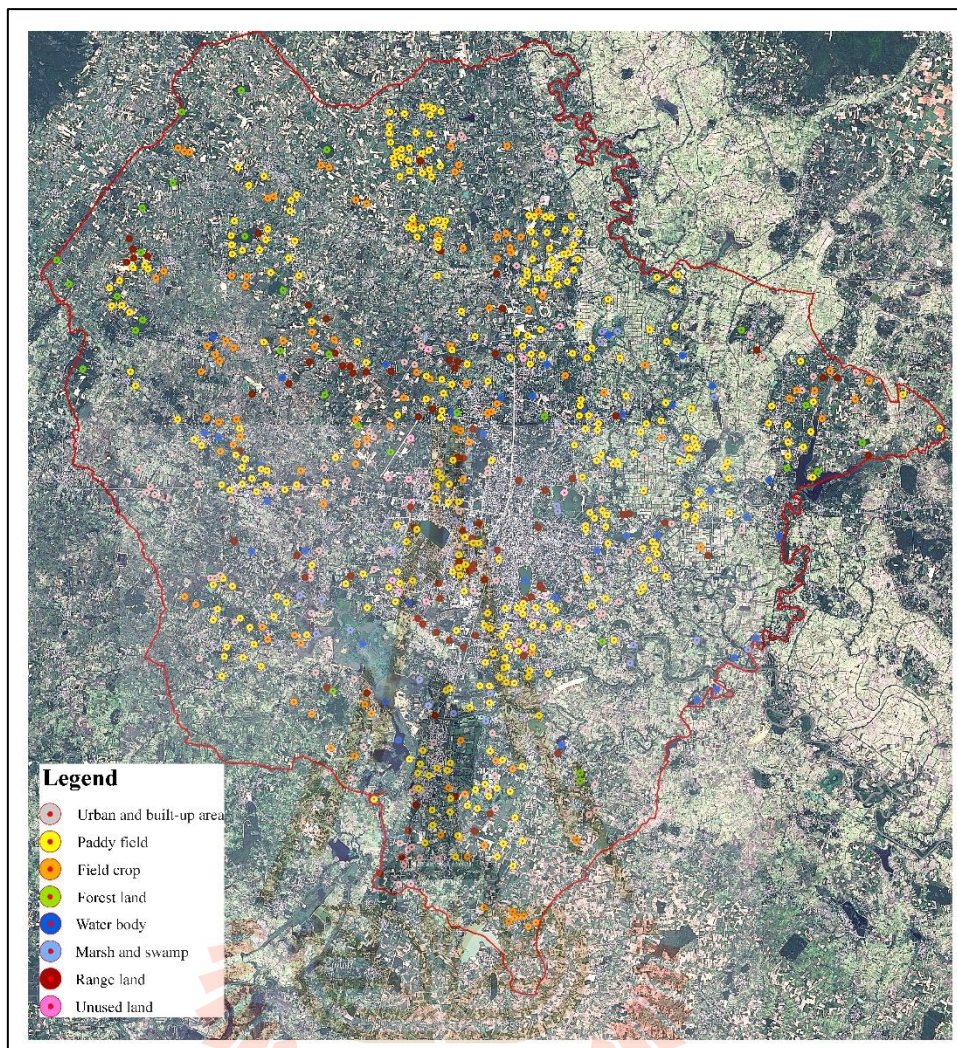
Figure 4.12 Spatial distribution of LULC sampling point in 2017.

Table 4.7 Error matrix between land use and land cover in 2016 and ground reference data in 2017.

LULC in 2016	Ground reference data in 2017								
LULC type	Ur	Pd	Fc	Fo	Wa	Ms	Ra	Ul	Total
Urban and Built-Up area (Ur)	97	2	1	0	0	1	1	0	102
Paddy field (Pd)	15	293	13	5	2	2	15	3	348
Field crop (Fc)	3	14	90	1	0	0	6	0	114
Forest land (Fo)	0	0	1	30	0	0	0	0	31
Water body (Wa)	1	3	0	0	36	0	0	0	40
Marsh and swamp (Ma)	0	0	0	0	2	22	1	0	25
Range land (Ra)	7	8	1	0	1	1	66	0	84
Unused land (Ul)	1	0	0	0	0	0	0	12	13
Total	124	320	106	36	41	26	89	15	757
Producer's accuracy (%)	78.23	91.56	84.91	83.33	87.80	84.62	74.16	80.00	
User's accuracy (%)	95.10	84.20	78.95	97.00	90.00	88.00	78.57	92.31	
Overall accuracy (%)	85.34								
Kappa hat coefficient (%)	80.24								

As results, it was found that the overall accuracy is 85.34% and Kappa hat coefficient of agreement was 80.24%. Meanwhile producer's accuracy (PA), which represents omission error, varies between 74.16% for range land and 91.56% for paddy field while user's accuracy (UA), which represents commission error, varies between 78.57% for range land and 96.77% for forest area.

Based on Fitzpatrick-Lins (1981), Kappa hat coefficient more than 80 percent represents strong agreement or accuracy between the classified map and the reference map. The derived accuracy assessment using OBIA in the current study is consistent with the previous study by Van Ninh and Waisurasingha in 2018, who applied support vector machine (SVM) to classify LULC from Landsat TM in 1990, Landsat ETM in 1999 and Landsat OLI in 2015. They found that the overall accuracy levels range from 94% to 98% and the Kappa index is 0.9. The results satisfy the

minimum 85% accuracy stipulated by the Anderson classification scheme, indicating the reliability of the LULC maps.

In addition, it can be observed that the significant omission error of range land with value of 25.84% mostly comes from paddy field and field crops because the spectral signature from Landsat 8 OLI image of range land is similar with paddy field and field crop. Meanwhile, the significant commission error of range land comes from paddy field and urban and built-up area because spectral signature from Landsat 8 OLI image of paddy field and urban and built-up area is similar with range land.

4.2   LULC simulation in 2026 and its status

Under this section, main results from major task of LULC simulation are here reported and discussed include (1) driving force on LULC change (2) optimum parameter for CLUE-S model (3) LULC prediction on Scenario I: Historical land use development (4) LULC prediction on Scenario II: Planning and policy as details in the following sections.

4.2.1   Driving force on LULC change

Driving factors are the factors that influence the allocation of land use changes. The main result of this part is logistic regression analysis to quantify a specific LULC type allocation according to driving force on LULC change. In this study, biophysical and socio-economic factors on LULC change include (1) elevation, (2) slope, (3) distance to existing urban area, (4) distance to road network, (5) distance to stream, (6) average income per capita at sub-district level, (7) land value in each land value zone and (8) population density at sub-district level (Table 4.8 and Figure 4.13)

are here applied for LULC prediction of 2 scenarios. Brief information of driving factors on LULC are summarizes below.

Elevation. Elevation was calculated from digital elevation model (DEM) which was interpolated from contour line of topographic map at scale 1:50,000. The domain value of elevation varies between 148 and 235 m above mean sea level.

Slope. Slope in percent was calculated from DEM and its domain value varies between 0 and 28 percent.

Distance to existing urban area. Distance to existing urban area is distance between each cell and the nearest of a set of urban cells. This distance was calculated from village to village using Euclidean distance method. The domain value of distance to existing urban area varies between 0 and 3,783 m.

Distance to road network. Distance to road network was computed from existing road network using Euclidean distance method. The domain value of distance to road network varies between 0 and 1,523 m.

Distance to stream. Distance to stream was computed from stream and river network using Euclidean distance method and its domain value varies between 0 and 3,020 m.

Average income per capita at sub-district level. Average income per capita at sub-district level was computed from Basic Minimum Need data (BMN) by average income per capita at sub-district level. The average income per capita at sub-district level in 2015 varies between 188,266 and 353,129 Baht/year.

Land value in each land value zone. Land value in each land value zone was calculated from maximum land value in each zone based on land appraisal

price from Treasury Department in 2012. The domain value of average land value in each land value zone varies between 0 to 80,000,000 Baht/Rai.

Population density at sub-district level. Population density of each district was calculated based on population data from Department of Provincial Administration in 2015. The population density of each district diverges between 61 and 1,264 persons/km^2.

Table 4.8 List of driving factors for LULC simulation by CLUE-S model.

Driving factors	Value	Unit	Remark
Elevation: ELE	148 - 235	Above mean sea level (AMSL).	Interval 20 m.
Slope: SLO	0 - 28	%	Interval 20 m.
Distance to existing urban area: D2Ur	0 - 3783	Meters	Euclidean distance
Distance to road network: D2R	0 - 1523	Meters	Euclidean distance
Distance to stream: D2STR	0 - 3020	Meters	Euclidean distance
Average income per capita at sub-district level: CAP	188,266 - 353,129	Baht/year.	BMN in 2015
Land value in each land value zone: LP	0 - 80,000,000	Baht/rai	Maximum value
Population density at sub-district level: POP	61 - 1,264.	Person/ km^2	BMN in 2015

Elevation

Slope
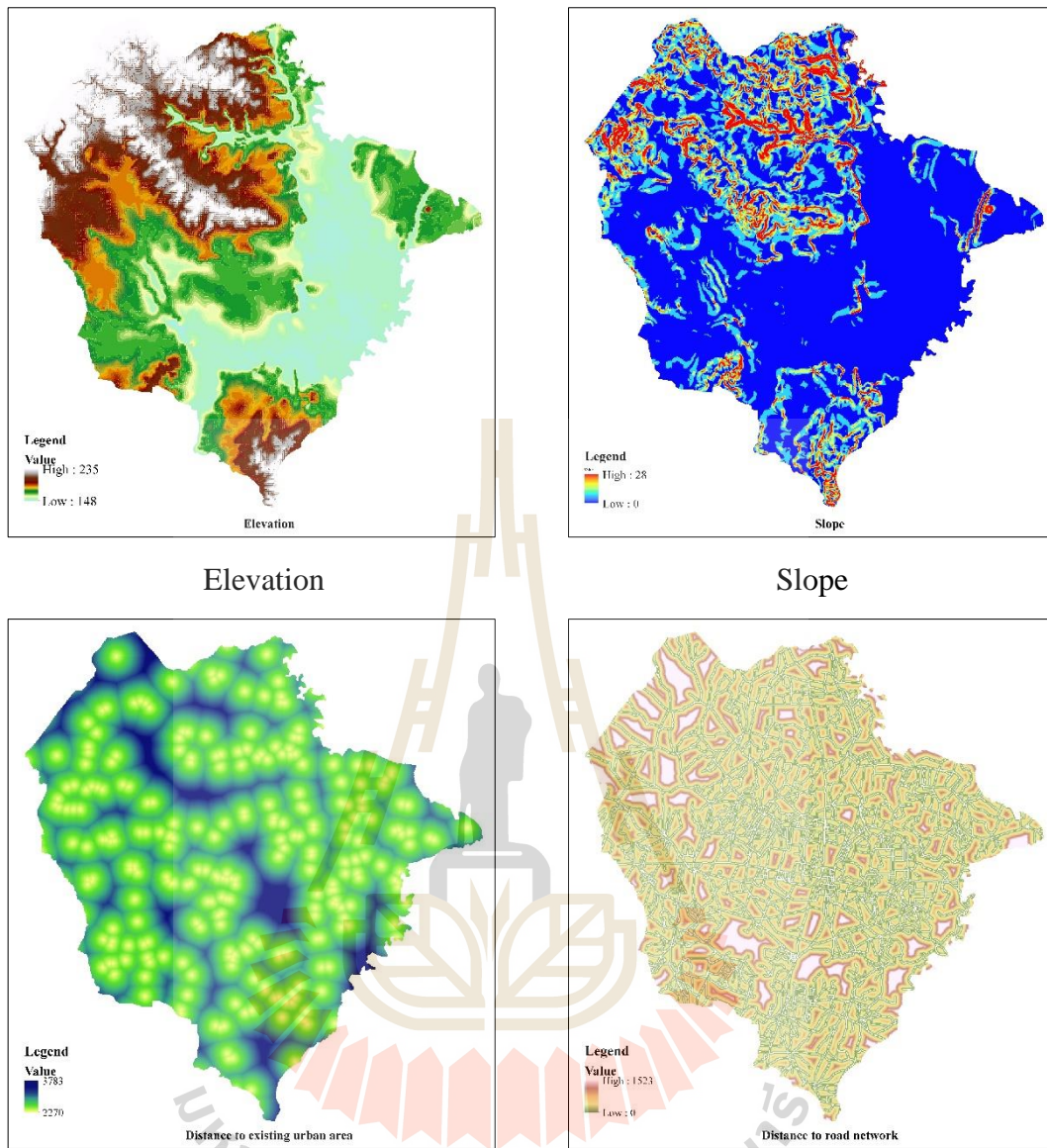
Distance to existing urban area

Distance to road network

Figure 4.13 Spatial distribution of driving factor on LULC change.

Distance to streams

Average income per capita at sub district level

Land value in each land value zone

Population density at sub-district level
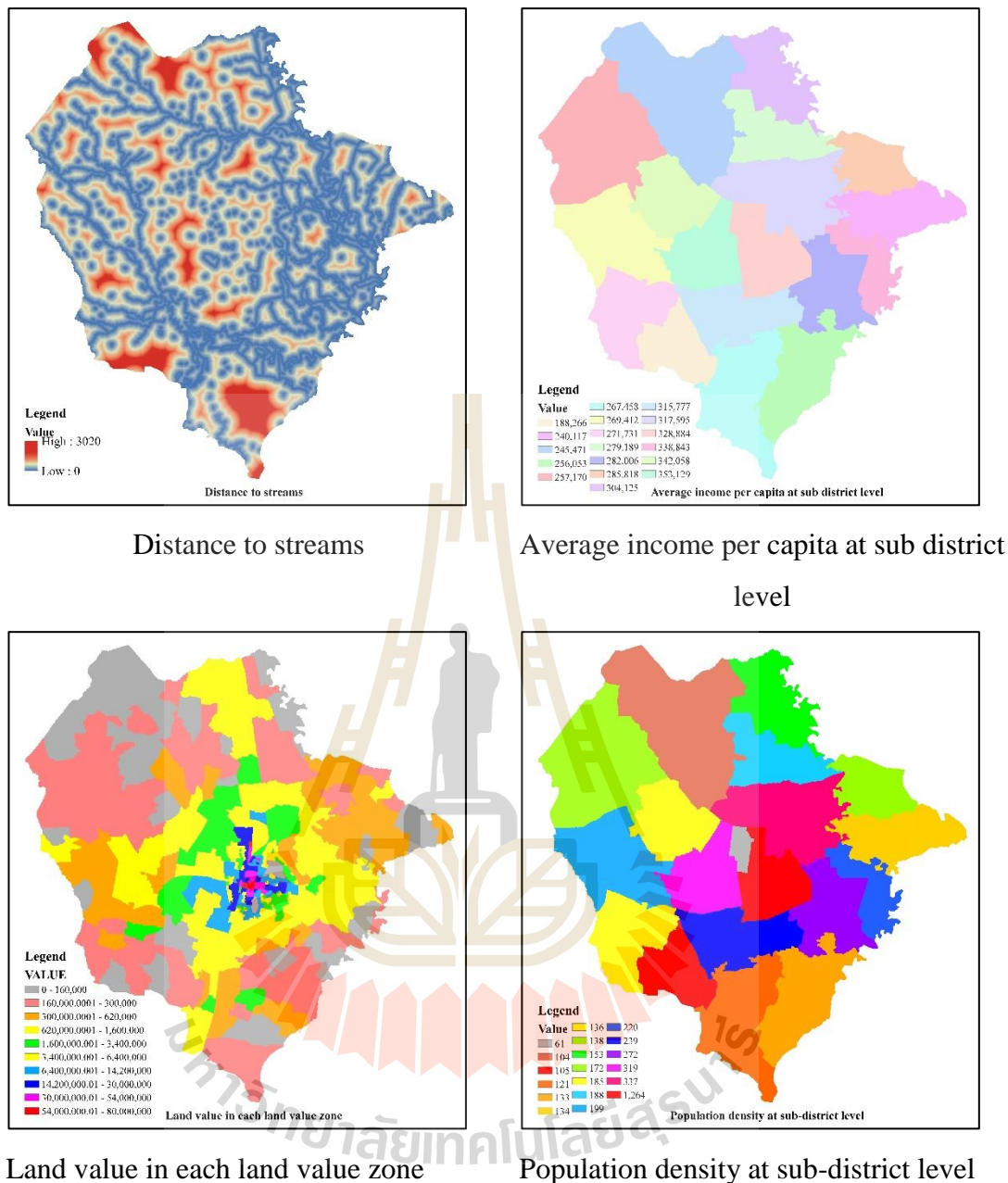
Figure 4.13 (Continued).

The result of multicollinearity test among independent variable with correlation coefficient and VIF values is summarized in Table 4.9 and 4.10, respectively. It was found that the correlation between a pair of covariates is very low whereas the VIF value that are calculate to examine the correlation among driving

factors is lower than 10. This implies that they are uncorrelated among driving factors and it is reasonable to use them for logistic regression analysis for a specific LULC type allocation. Meanwhile, result of multiple linear regression equation by logistic regression analysis of each LULC type for its location preference with AUC value is summarized in Table 4.11.

Table 4.9 Correlation coefficient among driving factors.

Driving factor	Correlation coefficient							
	X1	**X2**	**X3**	**X4**	**X5**	**X6**	**X7**	**X8**
Elevation (X1)	**1.000**	-0.282	-0.200	-0.009	-0.333	0.120	-0.023	0.143
Slope (X2)	-0.282	**1.000**	-0.015	0.012	0.101	0.003	-0.001	0.043
Distance to existing urban area (X3)	-0.200	-0.015	**1.000**	-0.179	-0.171	0.061	-0.039	-0.200
Distance to road network (X4)	-0.009	0.012	-0.179	**1.000**	0.085	0.084	0.045	0.044
Distance to stream (X5)	-0.333	0.101	-0.171	0.085	**1.000**	0.014	-0.034	0.043
Average income per capita at sub-district level (X6)	0.120	0.003	0.061	0.084	0.014	**1.000**	-0.053	-0.309
Land value in each land value zone (X7)	-0.023	-0.001	-0.039	0.045	-0.034	-0.053	**1.000**	-0.554
Population density at sub-district level (X8)	0.143	0.043	-0.200	0.044	0.043	-0.309	-0.554	**1.000**

Table 4.10 Variance inflation value of multicollinearity test.

Driving factors	VIF value
Elevation (X1)	1.060
Slope (X2)	1.223
Distance to existing urban area (X3)	1.214
Distance to road network (X4)	1.427
Distance to stream (X5)	1.111
Average income per capita at sub-district level (X6)	1.301
Land value in each land value zone (X7)	1.978
Population density at sub-district level (X8)	1.666

Table 4.11 Identified driving force for each LULC type allocation as equation form with AUC using binary logistic regression analysis.

| LULC | Constant | Driving Factors | | | | | | | | AUC |
| | | ELE | SLO | D2Ur | D2R | D2STR | INCAP | LP | POP | |
		X_1	X_2	X_3	X_4	X_5	X_6	X_7	X_8	
1. Urban and Built-Up area (Ur)	-4.35838	0.00448	n.s	-0.00081	-0.00375	0.00028	0.00001	n.s.	0.00307	0.821
2. Paddy field (Pd)	3.76717	-0.02129	-0.07755	0.00015	0.00101	-0.00019	n.s.	n.s.	-0.00256	0.814
3. Field crop (Fc)	-7.04359	0.03491	0.07137	0.00017	-0.00024	0.00075	n.s.	n.s.	-0.00891	0.852
4. Forest land (Fo)	-6.27343	0.01847	0.06303	n.s.	-0.00082	n.s.	n.s.	n.s.	n.s.	0.638
5. Water body (Wa)	3.02175	-0.03635	-0.05361	0.00034	0.00163	-0.00219	n.s.	n.s.	n.s.	0.779
6. Marsh and swamp (Ms)	2.25337	-0.03215	n.s	0.00031	0.00086	-0.00124	n.s.	n.s.	n.s.	0.708
7. Range land (Ra)	-3.49416	n.s.	0.05407	-0.00031	-0.00133	n.s	0.00001	n.s.	n.s.	0.659
8. Unused land (Ul)	-5.11792	n.s.	0.0580	n.s.	n.s.	n.s.	n.s.	n.s.	n.s.	0.600

Remark   n.s. is not-significant

4.2.1.1 Driving factor for urban and built-up area allocation

The multiple linear equation of the binomial logit regression model for urban and built-up area allocation after multicollinearity test is as follows:

$$Log\left(\frac{P_i}{1-P_i}\right) = \text{-4.35838} +0.00448X_1 -0.00081X_3 +0.00375X_4$$

$$+0.00028X_5 +0.00001X_6 +0.00307X_8 \qquad (4.1)$$

Where, X_1 is elevation (m)

X_3 is distance to existing urban area (m)

X_4 is distance to road network (m)

X_5 is distance to streams (m)

X_6 is average income per capita at sub-district level (Baht/year

X_8 is population density at sub-district level (persons/km2)

According to Eq. 4.1, it is found that four driving factors: (1) elevation, (2) distance to stream, (3) average income per capita at sub-district and (4) population density at sub-district level have positive relationship to a probability of urban and built-up area occurrence while two driving factors: (1) distance from existing urban area and (2) distance to road network area have negative relationship to its probability. The most importance factors for urban and built-up area occurrence are elevation, distance to road network and population density at sub-district level. This implies that when distance to road network decreases and elevation and population density at sub-district level increases, the probability of urban and built-up area occurrence increases. In the study area most of urban and built-up areas situates at upland area and spreads along road network from urban center at high population density to suburbs area.

In addition, the AUC value for urban and built-up area allocation is 0.82, it suggests good fit between the predicted and real LULC transition (Pontius and Schneider, 2001).

4.2.1.2 Driving factor for paddy field allocation

Multivariate linear regression equation as a binomial logit model for paddy field allocation is as follows:

$$Log\left(\frac{P_i}{1-P_i}\right) = 3.76717 - 0.02129X_1 - 0.07755X_2 + 0.00015X_3$$

$$+0.00101X_4 - 0.00019X_5 - 0.00256X_8 \qquad (4.2)$$

Where, X_1 is elevation (m)

X_2 is slope (%)

X_3 is distance to existing urban area (m)

X_4 is distance to road network (m)

X_5 is distance to streams (m)

X_8 is population density at sub-district level (persons/km2)

According to Eq. 4.2, two driving factors: (1) distance to existing urban area and (2) distance to road network have positive relationship to a probability of paddy field occurrence while four driving factors:(1) elevation, (2) slope, (3) distance to stream, and (4) population density at sub-district level have negative relationship to its probability. The most important factors for paddy field occurrence are slope and elevation. This implies that when slope and elevation decreases, the probability of paddy field occurrence increases. In study site, most of paddy field situates in lowland.

In addition, the AUC value for paddy field allocation is 0.81, it suggests good fit between the predicted and real LULC transition (Pontius and Schneider, 2001).

4.2.1.3 Driving factor for field crop allocation

Multivariate linear regression equation as a binomial logit model for field crop allocation is as follows

$$Log\left(\frac{P_i}{1-P_i}\right) = -7.04359 + 0.03491X_1 + 0.07137X_2 + 0.00017X_3 -$$

$$0.00024X_4 + 0.00075X_5 - 0.00891X_8 \qquad (4.3)$$

Where, X_1 is elevation (m)

            X_2 is slope (%)

            X_3 is distance to existing urban (m)

            X_4 is distance to road network (m)

            X_5 is distance to streams (m)

            X_8 is population density at sub-district level (persons/km2)

According to Eq. 4.3, it discloses that four driving factors: (1) elevation, (2) slope, (3) distance from existing urban area and (4) distance to stream have positive relationship to a probability of field crop occurrence meanwhile two driving factors: (1) distance to road network and (2) population density at sub-district have negative relationship to its probability. This infers that when distance to slope and elevation increases, the probability of field crop occurrence increases. In the study area, field crop is frequently found in upland area and far from main road.

In addition, the AUC value for field crop allocation is 0.85, it suggests good fit between the predicted and real LULC transition (Pontius and Schneider, 2001).

4.2.1.4 Driving factor for forest land allocation

Multivariate linear regression equation as a binomial logit model for forest land allocation is as follows:

$$Log\left(\frac{P_i}{1-P_i}\right)= -6.27343 +0.01847X_1 +0.06303X_2 -0.00082X_4 \qquad (4.4)$$

Where, X_1 is elevation (m)

X_2 is slope (%)

X_4 is distance to road network (m)

According to Eq. 4.4, It reveals that two driving factors: (1) elevation and (2) slope have positive relationship to a probability of forest area occurrence whilst distance to road network have negative relationship to its probability. This indicates that when elevation and slope increases, the probability of forest area occurrence increases. In the study area, most of forest land situates in upland area.

In addition, the AUC value for forest land allocation is 0.64, it suggests poor fit between the predicted and real LULC transition (Pontius and Schneider, 2001).

4.2.1.5 Driving factor for water body allocation

Multivariate linear regression equation as a binomial logit model for waterbody allocation is as follows:

$$Log\left(\frac{P_i}{1-P_i}\right) = 3.02175 -0.03635X_1 -0.05361X_2 +0.00034X_3$$

$$+0.00163X_4 -0.00219X_5 \qquad (4.5)$$

Where, X_1 is elevation (m)

X_2 is slope (%)

X_3 is distance to existing urban area (m)

X_4 is distance to road network (m)

X_5 is distance to streams (m)

According to Eq. 4.5, it is found that distance to existing urban area and distance to road network have positive relationship to a probability of water body

occurrence whilst three driving factors: (1) elevation, (2) slope and (3) distance to stream have negative relationship to its probability. The most importance factors of waterbody occurrence are slope, and elevation and distance to stream. This implies that when elevation, slope and distance to stream decrease, the probability of waterbody occurrence increases. In the study site most of water bodies locate in lowland and near stream.

In addition, the AUC value for water body allocation is 0.78, it suggests fair fit between the predicted and real LULC transition (Pontius and Schneider, 2001).

4.2.1.6 Driving factor for marsh and swamp allocation

Multivariate linear regression equation as a binomial logit model for marsh and swamp allocation is as follows:

$$Log\left(\frac{P_i}{1-P_i}\right) = 2.25337 -0.03215X_1 +0.00031X_3 +0.00089X_4 -0.00124X_5$$

$$(4.6)$$

Where, X_1 is elevation (m)

X_3 is distance to existing urban area (m)

X_4 is distance to road network (m)

X_5 is distance to streams (m)

According to Eq. 4.6, distance to existing urban area and road network have positive relationship to a probability of marsh and swamp occurrence while two driving factors: (1) elevation and (2) distance to stream have negative relationship to its probability. The most importance factors of range land occurrence are elevation and distance to stream. This implies that when elevation and distance to stream decrease, the probability of marsh and swamp occurrence increases. In the study site most of marsh and swamp locates in lowland area and close to stream network and water bodies.

In addition, the AUC value for marsh and swamp allocation is 0.71, it suggests fair fit between the predicted and real LULC transition (Pontius and Schneider, 2001).

4.2.1.7 Driving factor for range land allocation

Multivariate linear regression equation as a binomial logit model for range land allocation is as follows:

$$Log \left(\frac{P_i}{1-P_i}\right)= -3.49416 +0.05407X_2 -0.00031X_3 -0.0013X_4 +0.00001X_6$$

(4.7)

Where, X_2 is slope (%)

X_3 is distance to existing urban (m)

X_4 is distance to road network (m)

X_6 is average income per capita at sub-district level (baht/km2)

According to Eq. 4.7, It is found that slope and average income per capita at sub-district level have positive relationship to a probability of range land occurrence while distance to existing urban area and distance to road network have negative relationship to its probability. The most importance factors for range land occurrence are slope and distance to road network. This implies that when slope increases and distance to road network decreases, the probability of range land occurrence increases. In the study site most of range land situates in upland area and close to road network.

In addition, the AUC value for range land allocation is 0.66, it suggests poor fit between the predicted and real LULC transition (Pontius and Schneider, 2001).

4.2.1.8 Driving factor for unused land allocation

Multivariate linear regression equation as a binomial logit model unused land allocation is as follows:

$$Log\left(\frac{P_i}{1-P_i}\right) = -5.1179 + 0.0580X_2 \qquad (4.8)$$

Where, X_2 is slope (%)

According to Eq. 4.8, it is found that only one driving factor, namely slope, has positive relationship to a probability of unused land occurrence. This implies that when slope increases, the probability of unused land occurrence increases. In the study site most of unused land locates at high sloping area.

In addition, the AUC value for unused land allocation is 0.60, it suggests poor fit between the predicted and real LULC transition (Pontius and Schneider, 2001).

In summary, it can be here concluded that the most significant driving factor for all LULC type allocation except unused land in the study area is distance to road network. Meanwhile the second important driving factors for LULC type allocation are elevation, slope, distance to existing urban area whereas the third important driving factors for LULC type allocation area is distance to stream. Furthermore, it can be observed that land value in each land value zone is insignificant for each LULC type allocation since land value is mostly evaluated based on road networks and it is indirect relate with LULC types.

4.2.2 Optimum parameter for CLUE-S model

Under this section, two required parameters include land use type conversion matrix, land use type resistance (elasticity) are firstly defined and assigned the land requirement to predict LULC in 2016 for validation CLUE-S model using wall-to-wall accuracy assessment with the classified LULC in 2016 by OBIA.

In this study, if the overall accuracy and kappa hat coefficient equal or more than 80 percent, the assigned parameter values of conversion matrix and elasticity are acceptance as optimum local parameter of CLUE-S model. The brief information of two predefine parameter are summarized below.

(1) Land use type conversion matrix

Land use type specific conversion settings represents the behavior of one specific land use type. For each land use type a value needs to be specified that represents the relative conversion resistance, ranging from 0 (easy conversion) to 1 (irreversible change). The modeler decides on this factor based on expert knowledge or observed behavior in the recent past. In this study, the conversion matrix for each LULC type possibly change between 2011 and 2016 is set up based on transitional LULC change between 2006 and 2011 as summary in Table 4.12. It can be observed that urban and built-up area and forest land in 2006 do not change to other LULC types in 2016.

Table 4.12 Conversion matrix of possible change between 2006 and 2011.

	LULC type	Ur	Pd	Fc	Fo	Wa	Ms	Ra	Ul
	LULC type possible change in 2011								
LULC2006	Urban and built-up area (Ur)	1	0	0	0	0	0	0	0
	Paddy field (Pd)	1	0	0	1	0	1	1	1
	Field crop (Fc)	0	1	0	1	0	1	1	1
	Forest land (Fo)	0	0	1	0	0	0	0	0
	Water body (Wa)	0	0	0	0	0	1	1	1
	Marsh and swamp (Ms)	0	0	0	0	1	1	1	1
	Range land (Ra)	1	1	0	1	0	1	1	1
	Unused land (Ul)	0	0	0	0	0	1	0	1

(2) Land use type resistance (elasticity)

The conversion resistance is one of the land-use type specific settings that determine the temporal dynamics of the simulation. The conversion resistance or

elasticity relates to the reversibility of land-use changes. In the principle, land use type resistance represents the relative elasticity to conversion, ranging from 0 (easy conversion) to 1 (irreversible change) (van Asselen and Verburg, 2013). In this study, transition probability matrix of LULC change between 2006 and 2011 from Markov Chain model are here applied to assign elasticity value as suggested by Iamchuen (2014). Herewith, elasticity value of urban and built-up area (Ur), paddy field (Pd), field crop (Fc), forest land (Fo), water body (Wa), marsh and swamp (Ms), range land (Ra) and unused land (Ul) are 1.00, 0.40, 0.50, 1.00, 1.00, 0.80, 0.30 and 0.20, respectively

(3) Land requirement (Land demand)

Land demands indicate the need for specific land uses, or specific products or services provides by land uses that ultimately drive land use changes. These demands constrain the simulation by defining the totally required change (van Asselen and Verburg, 2013). Herein, land demand of LULC in 2016 is based on the rate of LULC change occurring between 2006 and 2011 from Markov Chain model as summary in Table 4.13. Finally, annual land demand of each LULC type in 2016 is calculated as shown Table 4.14. Figure 4.14 displays the result of LULC prediction in 2016 with predefined parameter and its land requirement.

Table 4.13 Transition area matrix between LULC 2011-2016 form Markov Chain model.

LULC type	Ur	Pd	Fc	Fo	Wa	Ms	Ra	Ul	Total
				LULC2016_demand in pixel					
Urban and built-up area (Ur)	34,731	6	0	0	0	0	3	6	**34,746**
Paddy field (Pd)	6,972	192,732	0	0	2	0	6,480	851	**207,037**
Field crop (Fc)	3,032	1	69,615	0	0	0	2,846	486	**75,980**
Forest land (Fo)	0	0	0	16,086	0	0	0	0	**16,086**
Water body (Wa)	4	0	0	0	21,034	0	0	114	**21,152**
Marsh and swamp (Ms)	0	0	0	0	0	12,805	0	317	**13,122**
Range land (Ra)	9	0	2	0	0	0	21,838	0	**21,849**
Unused land (Ul)	1,131	0	0	0	0	0	309	1,408	**2,848**
Total	**45,879**	**192,739**	**69,617**	**16,086**	**21,036**	**12,805**	**31,476**	**3,182**	**392,820**

(row label: LULC2011_OBIA)

Table 4.14 Annual land requirement for LULC 2016 by each LULC type.

Year	LULC type: Area in km^2								
	Ur	Pd	Fc	Fo	Wa	Ms	Ra	Ul	Total
2011	86.87	517.59	189.95	40.22	52.88	32.81	54.62	7.12	**982.05**
2012	92.43	510.44	186.77	40.22	52.82	32.65	59.44	7.29	**982.05**
2013	98.00	503.30	183.59	40.22	52.76	32.49	64.25	7.45	**982.05**
2014	103.57	496.15	180.41	40.22	52.71	32.33	69.06	7.62	**982.05**
2015	109.13	489.00	177.22	40.22	52.65	32.17	73.88	7.79	**982.05**
2016	114.70	481.85	174.04	40.22	52.59	32.01	78.69	7.96	**982.05**
Annual rate	**5.57**	**-7.15**	**-3.18**	**0.00**	**-0.06**	**-0.16**	**4.81**	**0.17**	

In addition, the error matrix between the classified LULC in 2016 by OBIA and the predicted LULC in 2016 by CLUE-S model is reported in Table 4.15. As results, it was found that overall accuracy and Kappa hat coefficient of predicted LULC in 2016 map when it was compared with the classified LULC in 2016 map are 86.83 and 81.51%, respectively. Both accuracy values are more than 80% as requirement. Therefore, predefine parameters (land use type conversion matrix, land

use type resistance (elasticity) can be accept for LULC prediction in 2026 of 2 scenarios

using CLUE-S model.
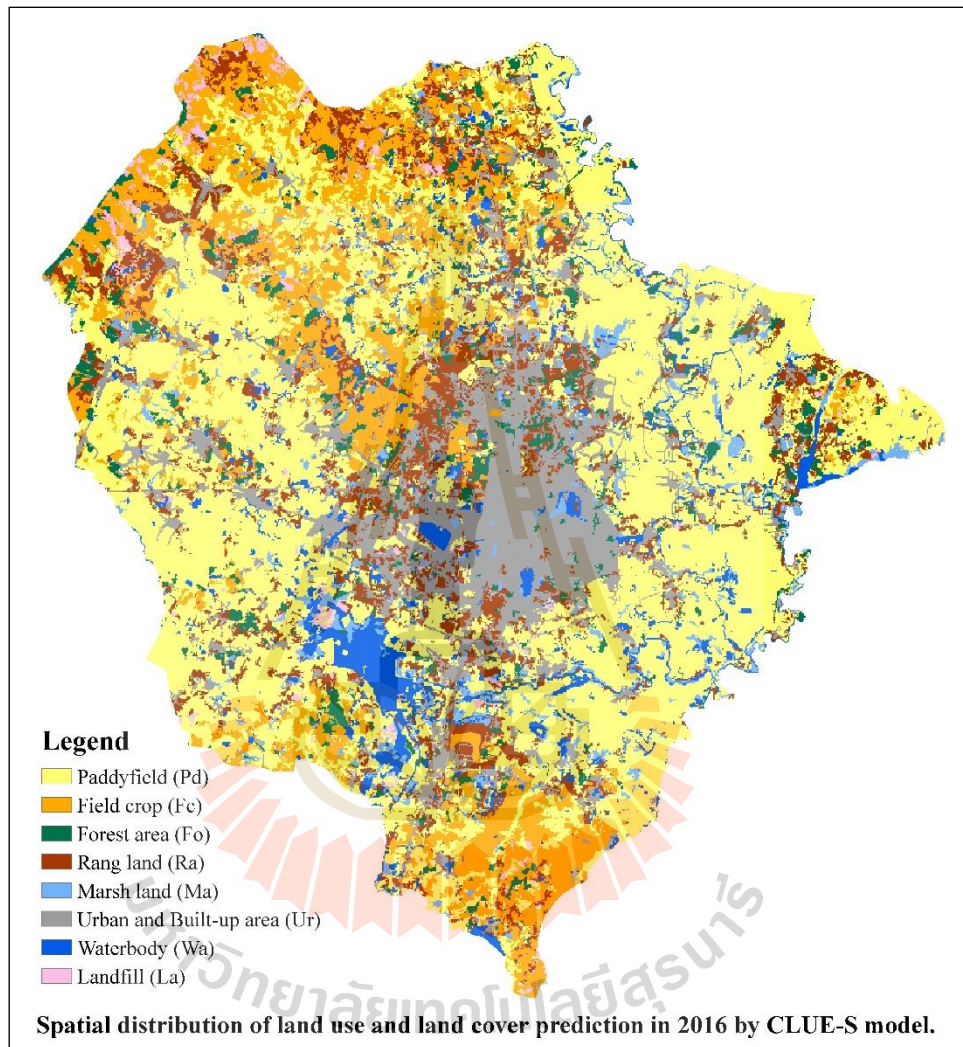
Figure 4.14 Spatial distribution of land use and land cover prediction in 2016 by

CLUE-S model.

Table 4.15 Error matrix between of LULC in 2016 using OBIA and LULC in 2016 prediction.

LULC2016_OBIA in pixel	LULC2016_Prediction in pixel								
LULC type	Ur	Pd	Fc	Fo	Wa	Ms	Ra	Ul	Total
Urban and built-up area (Ur)	36,190	9,391	3,823	43	1		2,891	212	52,551
Paddy field (Pd)	1,975	174,411	178		4	2	3,574	405	180,549
Field crop (Fc)	364		58,095		4	1	686	47	59,197
Forest land(Fo)				16,008					16,008
Water body (Wa)	232	15	4	35	20,791	24	2		21,103
Marsh and swamp (Ms)	313	3			2	12,610			12,928
Range land (Ra)	2,036	12,617	8,448			1	20,674	6	43,782
Unused land (Ul)	453	1,977	1,424		116	165	255	2,312	6,702
Total	41,563	198,414	71,972	16,086	20,918	12,803	28,082	2,982	392,820
Producer's accuracy in %	87.07	87.90	80.72	99.52	99.39	98.49	73.62	77.53	
User's accuracy in %	68.87	96.60	98.14	100.00	98.52	97.54	47.22	34.50	
Overall accuracy in %	86.83								
Kappa hat coefficient in %	81.51								

4.2.3 LULC prediction on Scenario I: Historical land use development

To predict LULC in 2026 of Scenario I: Historical land use development, the derived optimum parameter of CLUE-S model from the previous section were here applied while specific land demand was calculated based on the annual change rate of LULC between 2016 and 2026 by Markov Chain model (Table 4.16). The result of annual land demand of Scenario I between 2016 and 2026 is presented in Table 4.17.

Table 4.16 Transition area matrix between LULC 2016-2026 form Markov Chain model.

	LULC type	Ur	Pd	Fc	Fo	Wa	Ms	Ra	Ul	Total
				LULC2026 SC1_ land demand in pixel (50 m.)						
	Urban and built-up area (Ur)	52,533	0	0	0	15	0	0	3	52,551
	Paddy field (Pd)	18,640	137,296	0	0	27	5	21,166	3,415	180,549
LULC2016 in pixel	Field crop (Fc)	7,690	0	35,928	0	7	0	13,442	2,130	59,197
	Forest land (Fo)	85	0	0	15,853	69	0	0	0	16,007
	Water body (Wa)	14	7	7	0	20,836	4	1	234	21,103
	Marsh and swamp (Ms)	16	4	2	0	47	12,539	2	319	12,929
	Range land (Ra)	6,886	4	0	0	8	0	36,884	0	43,782
	Unused land (Ul)	1,176	0	0	0	0	0	0	5,526	6,702
	Total	87,040	137,311	35,937	15,853	21,009	12,548	71,495	11,627	392,820

Table 4.17 Annual land requirement for Scenario I by each LULC type.

Year	LULC type: Area in km^2								
	Ur	Pd	Fc	Fo	Wa	Ms	Ra	Ul	Total
2016	131.38	451.37	147.99	40.02	52.76	32.32	109.46	16.76	**982.05**
2017	140.00	440.56	142.18	39.98	52.73	32.23	116.38	17.99	**982.05**
2018	148.62	429.75	136.36	39.94	52.71	32.13	123.31	19.22	**982.05**
2019	157.24	418.94	130.55	39.90	52.69	32.04	130.24	20.45	**982.05**
2020	165.87	408.14	124.73	39.86	52.66	31.94	137.17	21.68	**982.05**
2021	174.49	397.33	118.92	39.83	52.64	31.85	144.10	22.91	**982.05**
2022	183.11	386.52	113.10	39.79	52.62	31.75	151.03	24.14	**982.05**
2023	191.73	375.71	107.29	39.75	52.59	31.66	157.95	25.37	**982.05**
2024	200.36	364.90	101.47	39.71	52.57	31.56	164.88	26.61	**982.05**
2025	208.98	354.09	95.66	39.67	52.55	31.47	171.81	27.84	**982.05**
2026	217.60	343.28	89.84	39.63	52.52	31.37	178.74	29.07	**982.05**
Annual rate	**8.62**	**-10.81**	**-5.82**	**-0.04**	**-0.02**	**-0.09**	**6.93**	**1.23**	

The result of LULC prediction in 2026 of Scenario I: LULC historical development is presented in Figure 4.15 and area and percentage of predictive LULC in 2026 of Scenario I is summarized in Table 4.18.

Legend
- Paddy field (Pd)
- Field crop (Fc)
- Forest area (Fo)
- Rang land (Ra)
- Marsh land (Ma)
- Urban and Built-up area (Ur)
- Waterbody (Wa)
- Landfill (La)

Spatial distribution of land use and land cover in 2026 prediction on Scenario I: Historical land use development
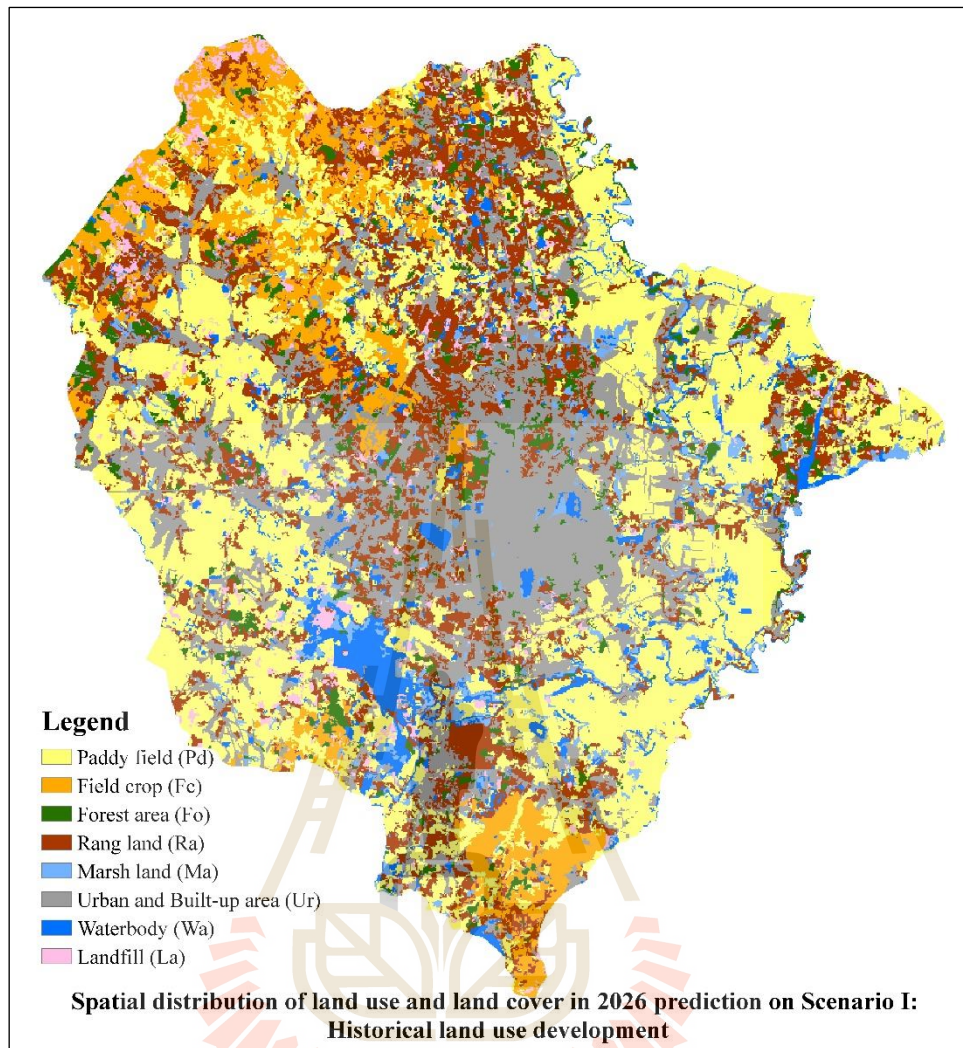
Figure 4.15 Spatial distribution of land use and land cover in 2026 prediction on Scenario I: Historical land use development.

Table 4.18 Area and percentage of land use and land cover in 2026 Scenario I.

Land use and land cover type	Area in km^2	Percent
1. Urban and Built-Up area (Ur)	217.27	22.12
2. Paddy field (Pd)	342.84	34.91
3. Field crop (Fc)	90.70	9.24
4. Forest land (Fo)	40.03	4.08
5. Water body (Wa)	52.07	5.30
6. Marsh and swamp (Ms)	31.34	3.19
7. Range land (Ra)	178.70	18.20
8. Unused land (Ul)	29.10	2.96
Total	**982.05**	**100.00**

As results, the most significant LULC type in 2026 of Scenario I is paddy field covering an area of 342.84 km or 34.91% of the study area. The second dominant LULC type is urban and built-up area accounting for 217.27 km^2 or 22.12% of the study area and situates around middle part of the study area. The third important LULC category is range land covering area of 178.70 km^2 or 18.20% of the total area. This area situates in northern and southern parts of the study area. Other LULC types include field crop, forest land, marsh and swamp, water body and unused land are distributed around the Mueang Khon Kaen district. These categories cover area of 243.24 km^2 or 24.77% of the study area.

Refer to van Asselen and Verburg (2013), the land demands dictate the final area of each LULC type in the future under CLUE-S model. In this study it reveals that areas of LULC types including field crop, forest land, and unused land have increased from their land demands with the increasing area of 0.86, 0.40 and 0.03 km^2, respectively. On the contrary areas of water body, paddy field, urban and built-up area, range land, and marsh and swamp have decreased from their land demands with the

decreasing area of 0.45, 0.44, 0.33, 0.04 and 0.03 km^2, respectively. However, area of each predictive LULC type in 2026 of Scenario I is rather small (less than 1 km^2 or 0.001% of the study area).

4.2.4 LULC prediction on Scenario II: Planning and policy

Under this scenario, area of predictive urban and built-up area in 2026 was transformed from government policy on urban development plan and prevention and solving on crowded communities in Khon Kaen province by National Housing Authority (Figure 4.16). At the same time, Department of Public Works and Town & Country Planning was published new city planning of Khon Kaen district in 2017, it was declared to conserve some agricultural area, thus this area must be excluded under LULC prediction by CLUE-S model (Figure 4.17).

For land demand of Scenario II, the classified LULC data in 2016 which was firstly updated with urban and built-up area from Plan of National Housing Authority and new annual change rates of LULC types between 2006 and 2016 were then calculated using Markov Chain model as shown in Table 4.19. Finally, annual land demand of LULC type in 2026 was then assigned as summary in Table 4.20. In addition, conservation agriculture area under city plan of Department of Public Works and Town & Country Planning in 2017 was applied as exclusion area under prediction processing of CLUE-S model.

132
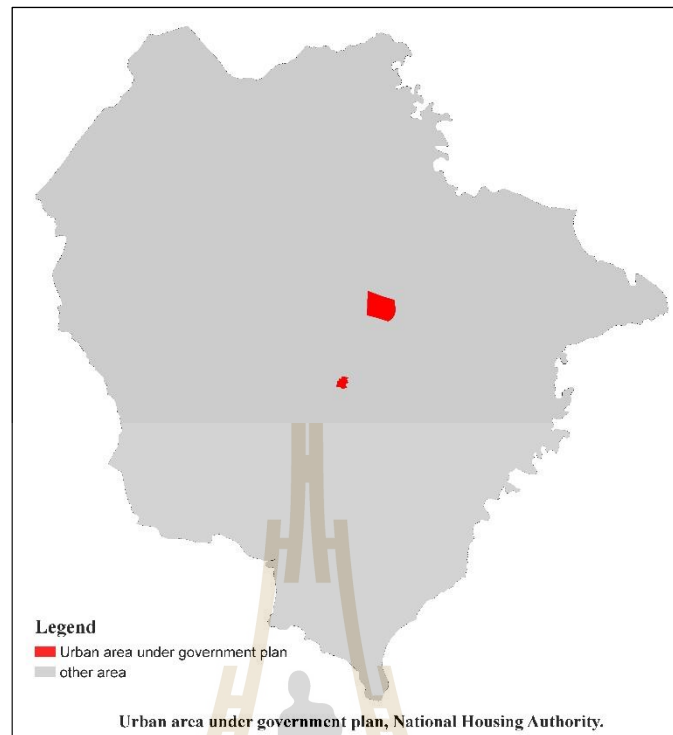
Figure 4.16 Urban area under government plan, National Housing Authority.

Figure 4.17 Conservation agriculture area under city plan of Department of Public

Works and Town & Country Planning in 2017.

133

Table 4.19 Transition area matrix between LULC 2016-2026 scenario II from Markov Chain model (Unit: pixel).

	LULC type	Ur	Pd	Fc	Fo	Wa	Ms	Ra	Ul	Total
					LULC2026 SC1I_ land demand in pixel (50 m.)					
LULC2016 in pixel	Urban and built-up area (Ur)	53,282	0	0	0	15	0	0	3	**53,300**
	Paddy field (Pd)	18,988	137,091	0	0	27	5	20,943	3,405	**180,459**
	Field crop (Fc)	7,840	0	35,928	0	7	0	13,300	2,122	**59,197**
	Forest land (Fo)	632	0	0	15,024	67	0	0	0	**15,723**
	Water body (Wa)	76	7	7	0	20,745	4	1	232	**21,072**
	Marsh and swamp (Ms)	28	4	2	0	47	12,521	2	318	**12,922**
	Range land (Ra)	7638	4	0	0	8	0	35,808	0	**43,458**
	Unused land (Ul)	1224	0	0	0	0	0	0	5,463	**6,687**
	Total	**89,708**	**137,106**	**35,937**	**15,024**	**20,916**	**12,530**	**70,054**	**11,543**	**392,818**

Table 4.20 Annual land requirement for Scenario II by each LULC type.

Year	Ur	Pd	Fc	Fo	Wa	Ms	Ra	Ul	Total
				LULC type: Area in km2					
2016	133.25	451.15	147.99	39.31	52.68	32.31	108.65	16.72	**982.05**
2017	142.35	440.31	142.18	39.13	52.64	32.21	115.29	17.93	**982.05**
2018	151.45	429.47	136.36	38.96	52.6	32.11	121.94	19.15	**982.05**
2019	160.56	418.63	130.55	38.78	52.56	32.01	128.59	20.36	**982.05**
2020	169.66	407.79	124.73	38.61	52.52	31.91	135.24	21.57	**982.05**
2021	178.76	396.96	118.92	38.43	52.49	31.82	141.89	22.79	**982.05**
2022	187.86	386.12	113.1	38.26	52.45	31.72	148.54	24	**982.05**
2023	196.96	375.28	107.29	38.08	52.41	31.62	155.19	25.22	**982.05**
2024	206.07	364.44	101.47	37.91	52.37	31.52	161.84	26.43	**982.05**
2025	215.17	353.6	95.66	37.73	52.33	31.42	168.49	27.64	**982.05**
2026	224.27	342.77	89.84	37.56	52.29	31.33	175.14	28.86	**982.05**
Annual rate	9.10	-10.84	-5.82	-0.18	-0.04	-0.10	6.65	1.21	

The result of LULC prediction in 2026 of Scenario II: Policy and planning is presented in Figure 4.18 and area and percentage of predictive LULC in 2026 of Scenario II is summarized in Table 4.21.

As results, the most significant LULC type in 2026 of scenario II is paddy field covering an area of 342.33 km^2 or 34.86% of the study area. The second

dominant LULC type is urban and built-up areas accounting for 223.99 km^2 or 22.81% of the study area. These areas are found spread form the center except the eastern part of the study area. The third important LULC category is range land covering area of 174.99 km^2 or 17.82% of the study area. This area situates in northern and southern parts of the study area. Other LULC types include field crop, forest land, marsh and swamp, water body and unused land distribute around Mueang Khon Kaen district. These categories cover area of 240.74 km^2 or 24.51% of the study area.

Table 4.21 Area and percentage of land use and land cover in 2026 Scenario II.

Land use and land cover type	Area in km^2	Percentage
1. Urban and Built-Up area (Ur)	223.99	22.81
2. Paddy field (Pd)	342.33	34.86
3. Field crop (Fc)	90.33	9.20
4. Forest land (Fo)	37.94	3.86
5. Water body (Wa)	52.13	5.31
6. Marsh and swamp (Ms)	31.48	3.21
7. Range land (Ra)	174.99	17.82
8. Unused land (Ul)	28.86	2.94
Total	982.05	100.00

Legend
Paddf field (Pd)
Field crop (Fc)
Forest area (Fo)
Rang land (Ra)
Marsh land (Ma)
Urban and built-up area (Ur)
Waterbody (Wa)
Landfill (La)

Spatial distribution of land use and land cover in 2026 prediction on Scenario II: Planning and policy.
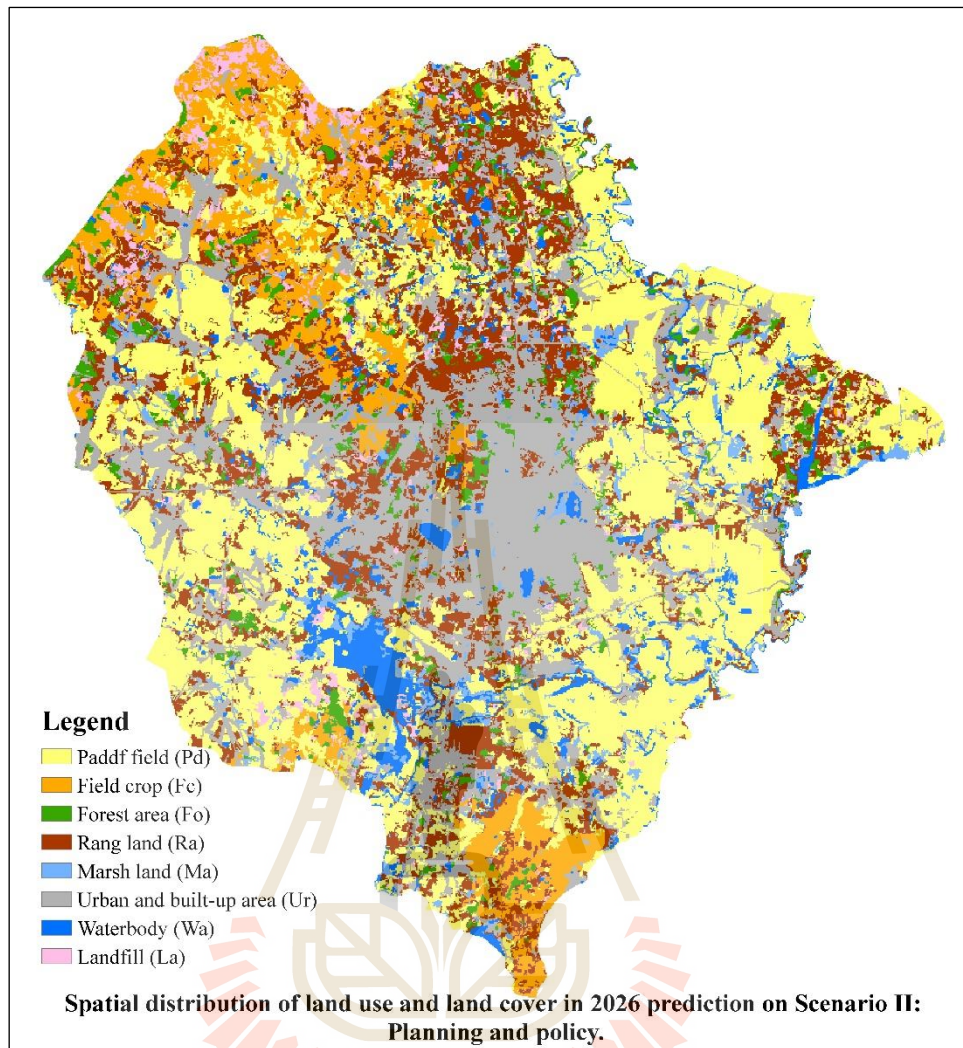
Figure 4.18 Spatial distribution of land use and land cover in 2026 prediction on Scenario II: Planning and policy.

4.3   Change of land use and land cover during 2006 to 2026

Simple change detection of extracted and predicted LULC data during 2006 to 2026 (Scenario I and II) were compared for LULC change (Table 4.22 and Figure 4.19). It was found that the main LULC types with decreasing area in Mueang Khon Kaen district, Khon Kaen province during 2006 to 2026 (Scenario I and II) is paddy field and field crop. This result shows transfiguration activity from local society to urbanization

society in Mueang Khon Kaen district. This finding is agreed with the study of Ninh and Waisurasingha (2018), who found that most of agriculture were converted to urban and built-up area during 1990-2015.

On contrary, urban and built-up area in the same period continuously increase. This result shows effect of policy on city development, particularly signing a memorandum of understanding between Thailand Convention and Exhibition Bureau (TCEB) and Khon Kaen Municipality in 2013 to promote Khon Kaen province as Thailand's fifth MICE (Meetings, Incentives, Conferencing, Exhibitions) City. Meanwhile, it can be observed that area of range land has been continuously increased in this period, it increases from 28.82 km^2 in 2006 to 109.24 km^2 in 2016. Since paddy field and field crop areas are sold by farmers to business men and they abandoned them for highly return in the future. This observation is consistent with the previous study of Phomphakping and Phothaworn (2014), who found that agricultural land in suburb area were sold to land lord.

Table 4.22 Allocation of the extracted LULC categories in 2006, 2011 and 2016 and the predicted LULC in 2026 (Scenario I and II).

LULC type	LULC 2006		LULC 2011		LULC 2016		LULC 2026 of Scenario I		LULC 2026 of Scenario II	
	Km^2	Percent	Km^2	Percent	Km^2	Percent	Km^2	Percent	Km^2	Percent
Urban and built-up area (Ur)	58.033	5.91	87.14	8.87	131.39	13.38	217.27	22.12	223.99	22.81
Paddy field (Pd)	556.2	56.63	517.84	52.72	451.64	45.99	342.84	34.91	342.33	34.86
Field crop (Fc)	207.4	21.12	189.81	19.32	147.73	15.04	90.7	9.24	90.33	9.20
Forest land (Fo)	40.42	4.12	40.41	4.12	40.21	4.09	40.03	4.08	37.94	3.86
Water body (Wa)	52.81	5.38	52.52	5.35	52.34	5.33	52.07	5.3	52.13	5.31
Marsh and swamp (Ms)	33.64	3.43	32.81	3.34	32.48	3.31	31.34	3.19	31.48	3.21
Range land (Ra)	28.82	2.94	54.47	5.55	109.74	11.17	178.7	18.2	174.99	17.82
Unused land (Ul)	4.89	0.5	7.21	0.73	16.52	1.68	29.1	2.96	28.86	2.94
Total	**982.21**	**100**	**982.21**	**100**	**982.05**	**100**	**982.05**	**100**	**982.05**	**100**
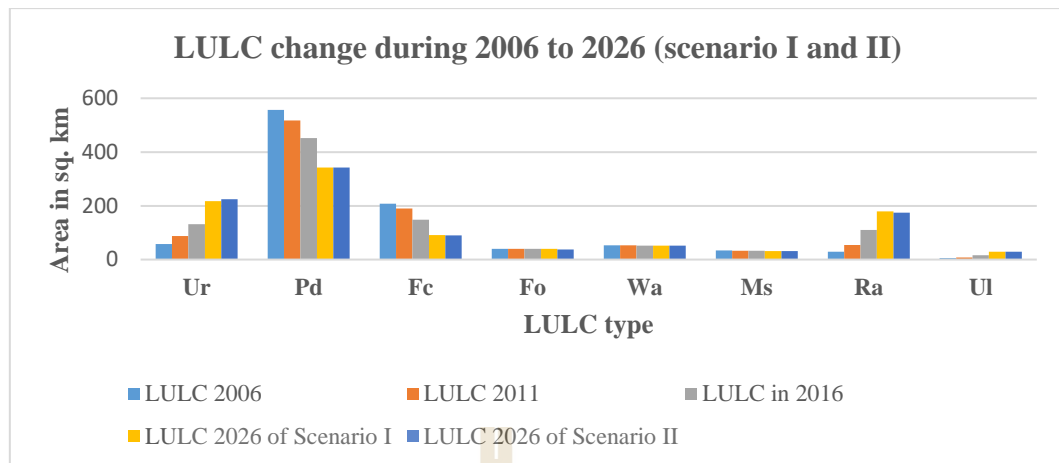
Figure 4.19 Comparison of land use and land cover type in 2006, 2011, 2016 and 2026 (Scenario I and II).

Furthermore, post-classification comparison change detection algorithm which explain from-to change was here applied for LULC change in three periods: 2006–2011, 2011–2016 and 2016–2026 (Scenario I and II) as describing in the following sections.

4.3.1 Land use and land cover change between 2006 and 2011

During this period, urban and built-up area is the most increasing LULC type with area of 29.10 km^2 or 2.96% of the study area. Most of this increased area comes from paddy field, field crop. At the same time, range land, and unused land (bare land, pit and landfill) has also increased with area of 25.65 and 2.33 km^2 or 2.61 and 0.24% of the study area, respectively.

For the most decreasing LULC class, paddy field has been decreased with 38.35 km^2 or 3.90% of the study area. It is changed into range land, urban and built-up area and unused land. At the same time, field crop, marsh and swamp and water

body had also decreased with area of 17.59, 0.84 and 0.29 km^2 or 1.79, 0.09 and 0.03%, respectively.

Detail of LULC change between 2006 and 2011 is presented in Table 4.23 and Figure 4.20. Highlight of urban and build up area change between 2006 and 2011 is presented in Figure 4.21.

Table 4.23 Land use and land cover change matrix of Meuang Khon Kaen district, Khon Kaen province in 2006 - 2011.

Landuse land cover type in 2006	Land use land cover type in 2011 (Area in km^2)								
	Ur	Pd	Fc	Fo	Wa	Ms	Ra	Ul	Total
Urban and built-up area (Ur)	58.00	0.01	0.00	0.00	0.00	0.00	0.00	0.02	**58.03**
Paddy field (Pd)	18.70	517.83	0.00	0.00	0.00	0.00	17.41	2.25	**556.20**
Field crop (Fc)	8.51	0.00	189.80	0.00	0.00	0.00	7.72	1.36	**207.40**
Forest area (Fo)	0.00	0.00	0.00	40.41	0.00	0.00	0.00	0.00	**40.41**
Water body (Wa)	0.01	0.00	0.00	0.00	52.52	0.00	0.00	0.29	**52.81**
Marsh and swamp (Ms)	0.00	0.00	0.00	0.00	0.00	32.81	0.00	0.83	**33.64**
Range land (Ra)	0.01	0.00	0.00	0.00	0.00	0.00	28.81	0.00	**28.82**
Unused land (Ul)	1.89	0.00	0.00	0.00	0.00	0.00	0.53	2.47	**4.89**
Total	**87.14**	**517.84**	**189.81**	**40.41**	**52.52**	**32.81**	**54.47**	**7.21**	**982.21**
Area change (km^2)	29.10	-38.35	-17.59	0.00	-0.29	-0.84	25.65	2.33	
Percent change of study area (%)	2.96	-3.90	-1.79	0.00	-0.03	-0.09	2.61	0.24	
Area of annual change (km^2)	5.82	-7.67	-3.52	0.00	-0.06	-0.17	5.13	0.47	

Legend

☐ Ur	☐ FC	☐ MS			
☐ Pd to Ur	☐ Fc to Ra	☐ Ms to Ul			
☐ Pd	☐ Fc to Ul	☐ Ra			
☐ Pd to Ra	☐ Fo	☐ Ra to Ur			
☐ Pd to Ul	☐ Wa	☐ Ul to Ra			
☐ Fc to Ur	☐ Wa to Ul	☐ Ul			

Spatial distribution of land use and land cover change of Mueang Khon Kaen district, Khon Kaen province between 2006 and 2011.
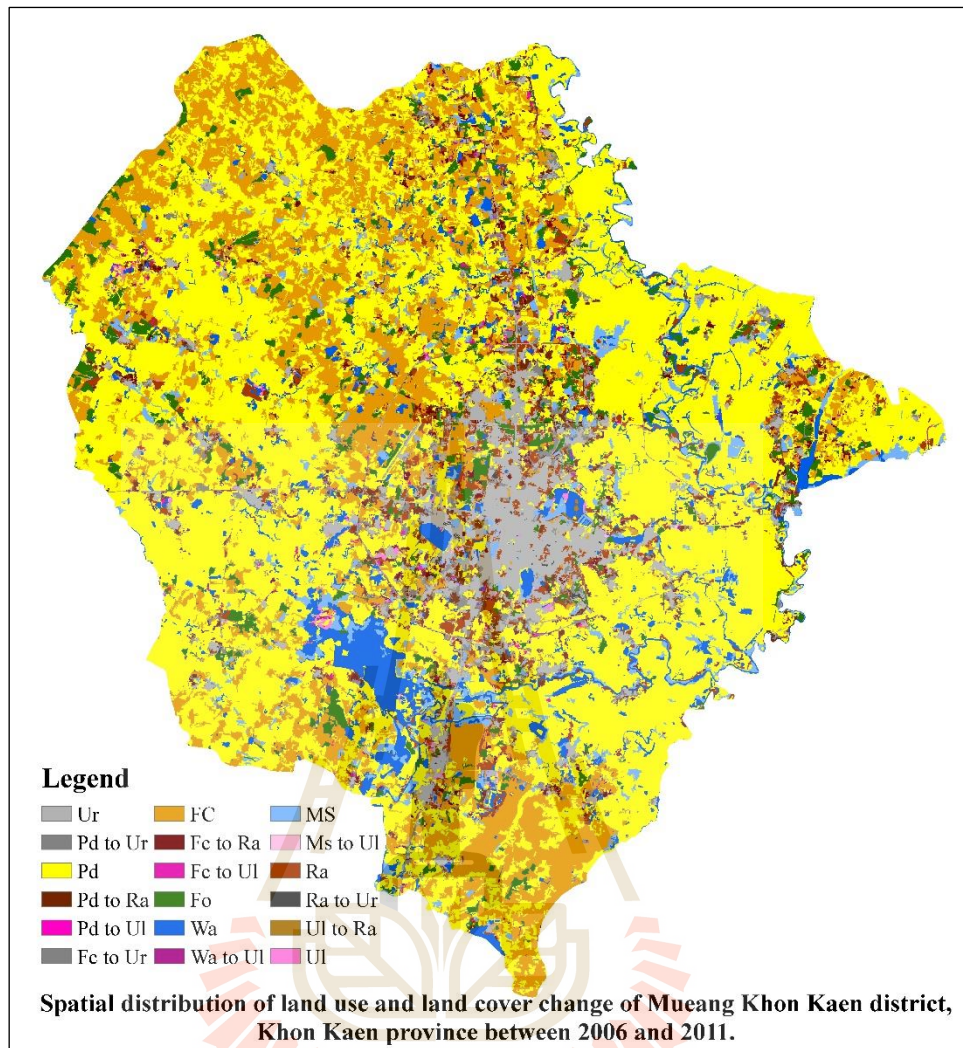
Figure 4.20 Spatial distribution of LULC change between 2006 and 2011.
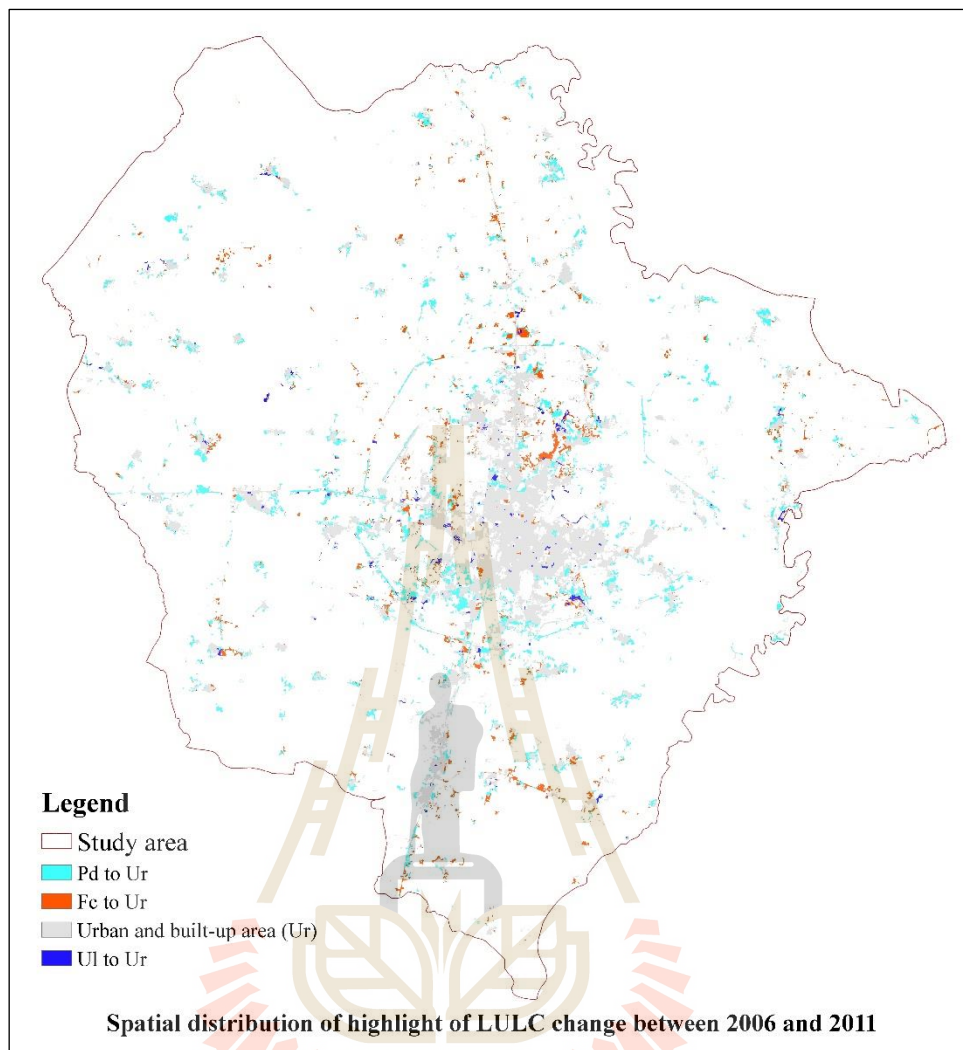
Figure 4.21 Spatial distribution of highlight of LULC change between 2006 and 2011.

4.3.2 Land use and land cover change between 2011 and 2016

During this period, range land is the most increased LULC type with area of 54.77 km^2 or 5.58% of the study area. Most of this increased area comes from paddy field and field crop. At the same time, urban and built-up area, and unused land (bare land, pit and landfill) had also increased with area of 44.62 and 9.60 km^2 or 4.54 and 0.98% of the study area, respectively.

For decreased LULC class, paddy field is the most decreased LULC type with area of 66.45 km^2 or 6.77% of the study area. It is changed into range land, urban and built-up area and range land. At the same time, field crop, marsh and swamp and forest land had also decreased having area of 41.77, 0.49 and 0.21 km^2 or 4.25, 0.05 and 0.02%, respectively. Detail of LULC change between 2011 and 2016 was presented in Table 4.24 and Figure 4.22. In addition, highlight of urban and build up area change between 2006 and 2011 is presented in Figure 4.23.
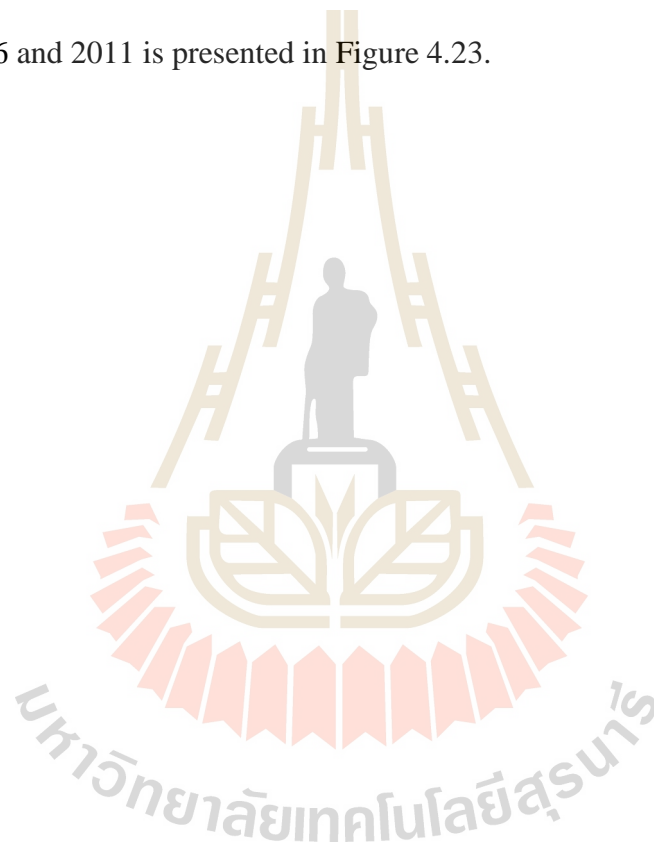
Table 4.24 Land use and land cover change matrix of Mueang Khon Kaen district, Khon Kaen province in 2011 – 2016.

Landuse land cover type in 2011	Land use land cover type in 2016								
	Ur	Pd	Fc	Fo	Wa	Ms	Ra	Ul	Total
Urban and built-up area (Ur)	87.10	0.00	0.00	0.00	0.03	0.00	0.00	0.00	**87.14**
Paddy field (Pd)	26.99	451.36	0.00	0.00	0.04	0.01	33.96	5.48	**517.84**
Field crop (Fc)	12.54	0.00	148.02	0.00	0.01	0.00	25.19	4.04	**189.81**
Forest area (Fo)	0.10	0.00	0.00	40.21	0.10	0.00	0.00	0.00	**40.41**
Water body (Wa)	0.01	0.02	0.01	0.00	52.20	0.00	0.00	0.29	**52.52**
Marsh and swamp (Ms)	0.00	0.00	0.00	0.00	0.06	32.30	0.00	0.44	**32.81**
Range land (Ra)	4.37	0.00	0.00	0.00	0.00	0.00	50.09	0.00	**54.47**
Unused land (Ul)	0.64	0.00	0.00	0.00	0.00	0.00	0.00	6.57	**7.21**
Total	**131.75**	**451.39**	**148.04**	**40.21**	**52.45**	**32.32**	**109.24**	**16.82**	**982.21**
Area change (km^2)	44.62	-66.45	-41.77	-0.21	-0.08	-0.49	54.77	9.60	
Percent change of study area (%)	4.54	-6.77	-4.25	-0.02	-0.01	-0.05	5.58	0.98	
Area of annual change (km^2)	8.92	-13.29	-8.35	-0.04	-0.02	-0.10	10.95	1.92	
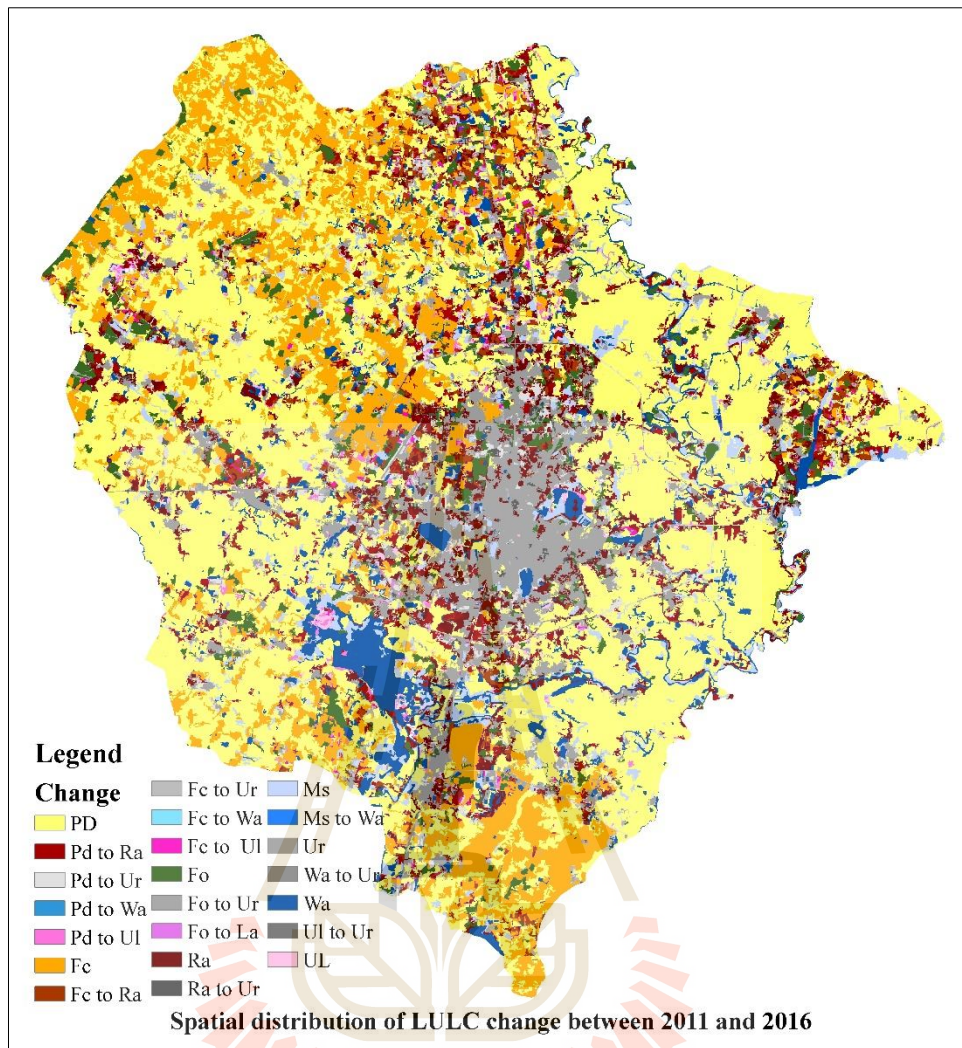
Figure 4.22 Spatial distribution of LULC change between 2011 and 2016.
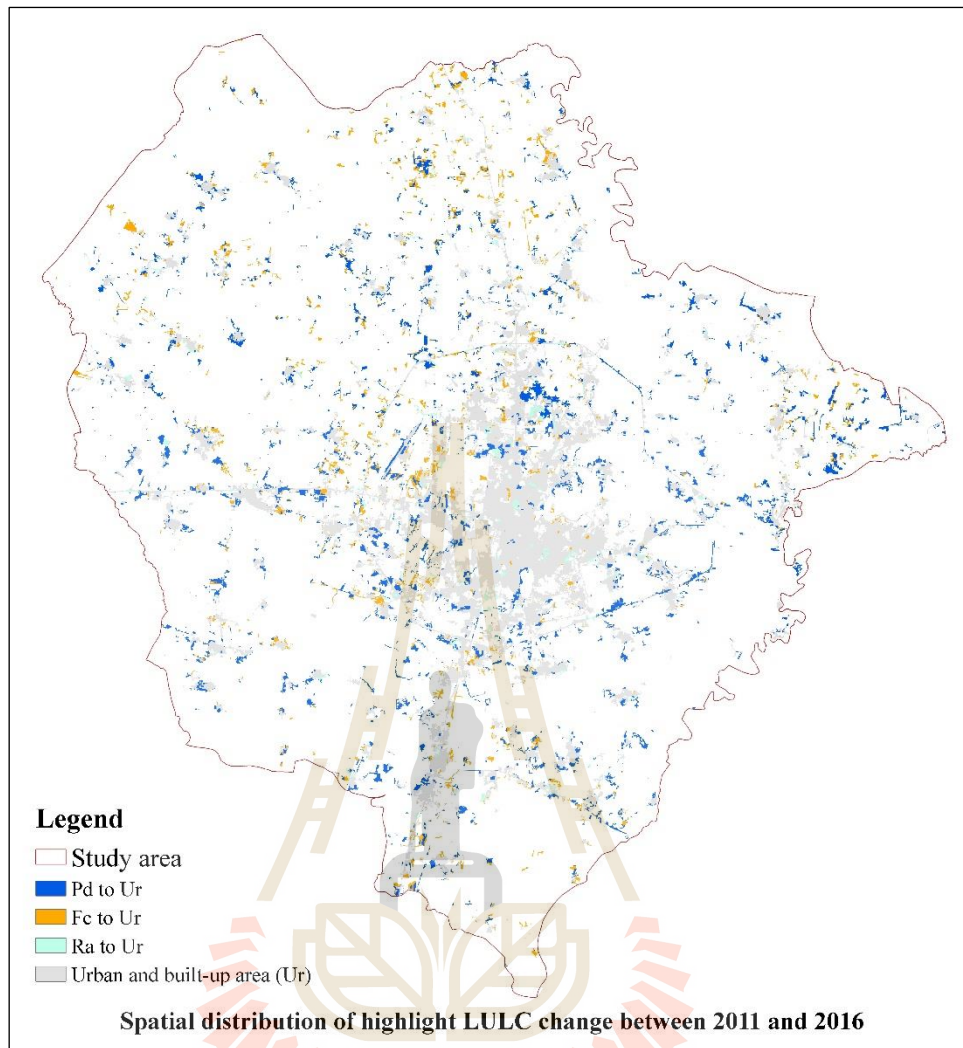
Figure 4.23 Spatial distribution of highlight of LULC change between 2011 and 2016.

4.3.3 Land use and land cover change between 2016 and 2026 (Scenario I)

According LULC change matrix between LULC in 2016 and LULC in 2026 of Scenario I (Table 4.25), decreasing LULC classes from LULC in 2016 are paddy field, field crop, forest land, water body and marsh and swamp with a decreasing rate of 10.88, 5.70, 0.02, 0.03 and 0.11 km^2 per year, respectively. On the other hand, the increasing LULC classes are urban and built-up area, range land, and unused land with an increasing rate of 8.59, 6.90 and 1.26 km^2 per year, respectively. Herein, the increased area of urban and built-up area comes from paddy field, field crop and range land and the increase of range land and unused land come from paddy field and field crop (Figure 4.24).

The pattern of LULC change between LULC in 2016 and predictive LULC in 2026 of Scenario I is identical to historical LULC change in three different periods (2006-2011 and 2011-2016) since the predictive LULC in 2026 of Scenario I is based on transformation LULC development in the past (2006-2016). This finding confirms that CLUE-S model can provides the good result for LULC prediction according historical land use development in the past.

Table 4.25 Transition matrix of LULCC between 2016 and 2026 of Scenario I.

LULC type		LULC 2026 Scenario I: Area in km²								
		Ur	Pd	Fc	Fo	Wa	Ms	Ra	Ul	Total
LULC 2016	Urban and built-up area (Ur)	114.95	3.95	0.53	1.3	1.34	1.05	7.38	0.89	131.39
	Paddy field (Pd)	65.25	319.29	4.78	2.43	4.31	3.19	43.21	9.18	451.64
	Field crop (Fc)	14.25	5.3	83.45	1.01	0.58	0.51	35.79	6.84	147.73
	Forest land (Fo)	2.2	1.47	0.52	33.23	0.38	0.21	1.93	0.27	40.21
	Water body (Wa)	2.57	3.94	0.2	0.26	42.22	1.07	1.62	0.46	52.34
	Marsh and swamp (Ms)	2.36	2.86	0.14	0.21	1.46	24.34	0.96	0.15	32.48
	Range land (Ra)	12.73	5.01	0.94	1.41	1.38	0.82	86.39	1.06	109.74
	Unused land (Ul)	2.96	1.02	0.14	0.18	0.4	0.15	1.42	10.25	16.52
Total		217.27	342.84	90.7	40.03	52.07	31.34	178.7	29.1	982.05
Land demand		217.60	343.28	89.84	39.63	52.52	31.37	178.74	29.07	
Area deviation (km²)		-0.33	-0.44	0.86	0.40	-0.45	-0.03	-0.04	0.03	
Area change (km²)		85.88	-108.80	-57.03	-0.18	-0.27	-1.14	68.96	12.58	
Annual change (km²)		8.59	-10.88	-5.70	-0.02	-0.03	-0.11	6.90	1.26	

Legend
- ☐ Study area
- ▮ Pd to Ur
- ▮ Fe to Ur
- ▮ Ra to Ur
- ▮ Urban and built-up area (Ur)
- ☐ Ul to Ur

Spatial distribution of LULC change between actual LULC in 2016 and the predicted LULC in 2026 of Scenario I.
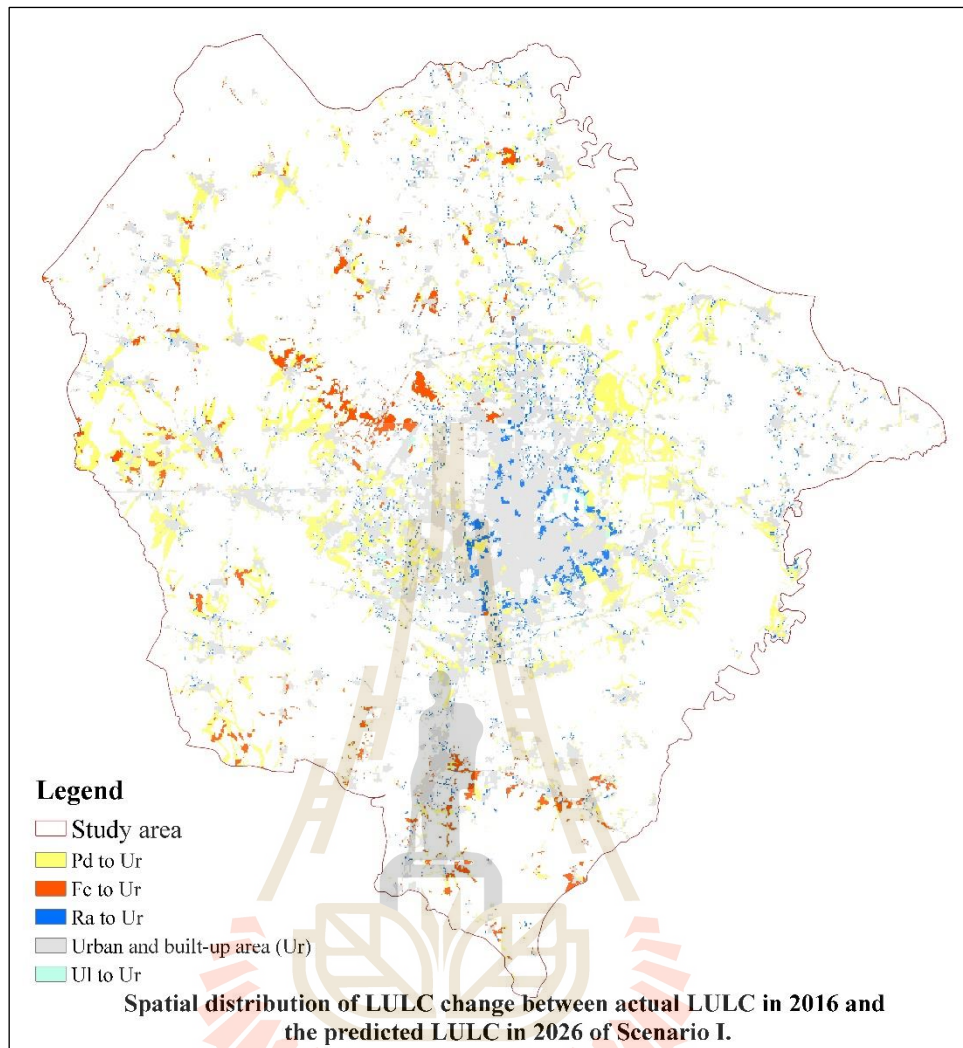
Figure 4.24 Spatial distribution of LULC change between actual LULC in 2016 and the predicted LULC in 2026 of Scenario I.

4.3.4   Land use and land cover change between 2016 and 2026 (Scenario II)

According LULC change matrix between LULC in 2016 and LULC in 2026 of Scenario II (Table 4.26), the decreasing LULC classes from LULC in 2016 are paddy field, field crop, forest land, water body and marsh and swamp with a decreasing rate of 10.93, 5.74, 0.23, 0.02 and 0.10 km^2 per year, respectively. On the other hand, increasing LULC classes are urban and built-up area, range land, and unused land with an increasing rate of 9.26, 6.53 and 1.23 km^2 per year, respectively (Figure 4.25). Herein, the increased area of urban and built-up area comes from major LULC class include paddy field, field crop and range land and the increase of range land and unused land comes from paddy field and field crop. The main pattern of LULC change between 2016 and 2026 of Scenario II is also identical to historical LULC change in three different periods (2006-2011 and 2011-2016).

Table 4.26 Transition matrix of LULCC between 2016 and 2026 of Scenario II.

LULC type		LULC 2026 Scenario II: Area in km^2								
		Ur	Pd	Fc	Fo	Wa	Ms	Ra	Ul	**Total**
LULC 2016	Urban and built-up area (Ur)	115.51	4.43	0.52	1.25	1.34	1.06	6.54	0.74	131.39
	Paddy field (Pd)	60.82	313.81	4.73	2.29	4.31	3.2	48.54	13.94	451.64
	Field crop (Fc)	19.47	7.29	83.16	1	0.58	0.51	31.77	3.95	147.73
	Forest land (Fo)	2.89	2.55	0.51	31.53	0.38	0.21	1.9	0.24	40.21
	Water body (Wa)	2.58	3.98	0.2	0.21	42.28	1.08	1.68	0.33	52.34
	Marsh and swamp (Ms)	2.13	3.06	0.14	0.2	1.47	24.43	0.97	0.08	32.48
	Range land (Ra)	16.65	5.44	0.92	1.28	1.37	0.84	82.23	1.01	109.74
	Unused land (Ul)	3.94	1.77	0.15	0.18	0.4	0.15	1.36	8.57	16.52
Total		223.99	342.33	90.33	37.94	52.13	31.48	174.99	28.86	982.05
Land demand		224.27	342.77	89.84	37.56	52.29	31.33	175.14	28.86	
Area deviation (km^2)		-0.28	-0.44	0.49	0.38	-0.16	0.15	-0.15	0.00	
Area change (km^2)		92.60	-109.31	-57.40	-2.27	-0.21	-1.00	65.25	12.34	
Annual change (km^2)		9.26	-10.93	-5.74	-0.23	-0.02	-0.10	6.53	1.23	
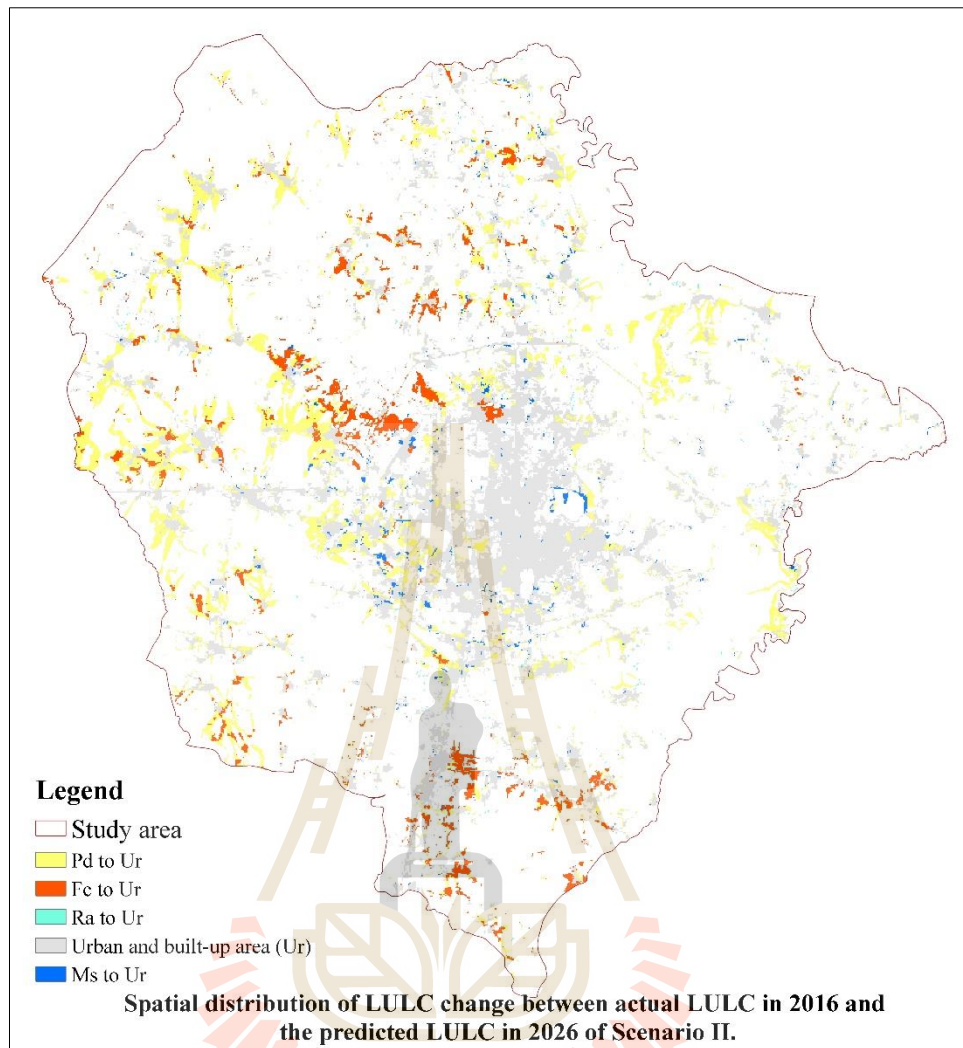
Figure 4.25 Spatial distribution of LULC change between actual LULC in 2016 and
the predicted LULC in 2026 of Scenario II.

Similar to Scenario I, it was also found that areas of LULC type
including field crop, forest area, and marsh and swamp have increased from their land
demands with the increasing area of 0.49, 0.38 and 0.15 km^2, respectively. On the
contrary area of LULC classes including paddy field, urban and built-up area, water
body, range land and unused land have decreased from their land demand with the
decreasing area of 0.44, 0.28, 0.16, 0.15 and 0.00 km^2, respectively. Like Scenario I,

area of each predictive LULC type in 2026 of Scenario II is rather small (less than 1 km^2 or 0.001% of the study area).

4.4   Characteristic of urban growth during 2006 and 2026

Based on the extracted and predicted urban and built-up area during 2006 and 2026 (Scenario I and II) as summary in Table 4.27 and shown in Figure 4.26, urban growth which is defined as spatial and demographic processes (Yu, 2013) can be here characterized using (1) Annual Expansion Intensity index (AEII), (2) Urban land percentage (PU) and (3) Urban land expansion index (SI) as details in the following sections.

153
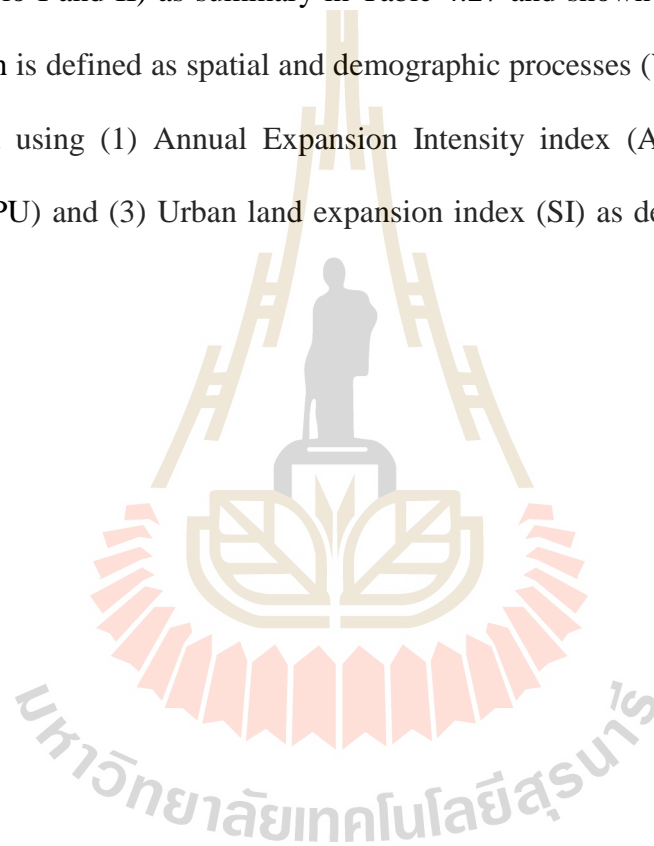
Table 4.27 Area and percentage of urban areas at sub-district and district during 2006 to 2026.

Sub-district/District	Urban area (km^2)				
	2006	2011	2016	2026 of Scenario I	2026 of Scenario II
Ban Kho	1.10	2.36	6.58	10.48	12.58
Ban Pet	6.36	10.38	15.09	22.58	24.93
Ban Thum	2.11	3.72	6.43	16.08	17.48
Ban Wa	0.83	1.56	2.81	7.97	8.95
Bueng Niam	0.85	1.27	2.49	5.71	5.03
Daeng Yai	0.62	1.46	3.57	11.14	13.91
Don Chang	0.33	0.88	2.11	3.01	2.59
Don Han	1.05	2.03	3.86	5.58	5.93
Khok Si	0.87	1.93	4.50	4.50	4.50
Mueang Kao	4.85	8.02	10.89	13.15	14.30
Nai Mueang	22.23	24.53	27.58	36.90	35.69
Non Thon	0.87	1.90	3.77	6.15	7.58
Nong Tum	0.63	1.40	2.47	3.91	4.18
Phra Lap	2.26	3.70	5.53	10.43	6.44
Samran	1.35	2.46	4.26	6.92	7.65
Sawathi	1.54	2.98	6.16	11.28	14.06
Sila	6.96	11.41	15.47	30.36	25.34
Tha Phra	3.22	5.14	8.16	11.08	12.74
District	**58.03**	**87.13**	**131.74**	**217.23**	**223.90**

(a) Urban area in 2006

(b) Urban area in 2011

(c) Urban area in 2016

(d) Urban area in 2026 of Scenario I
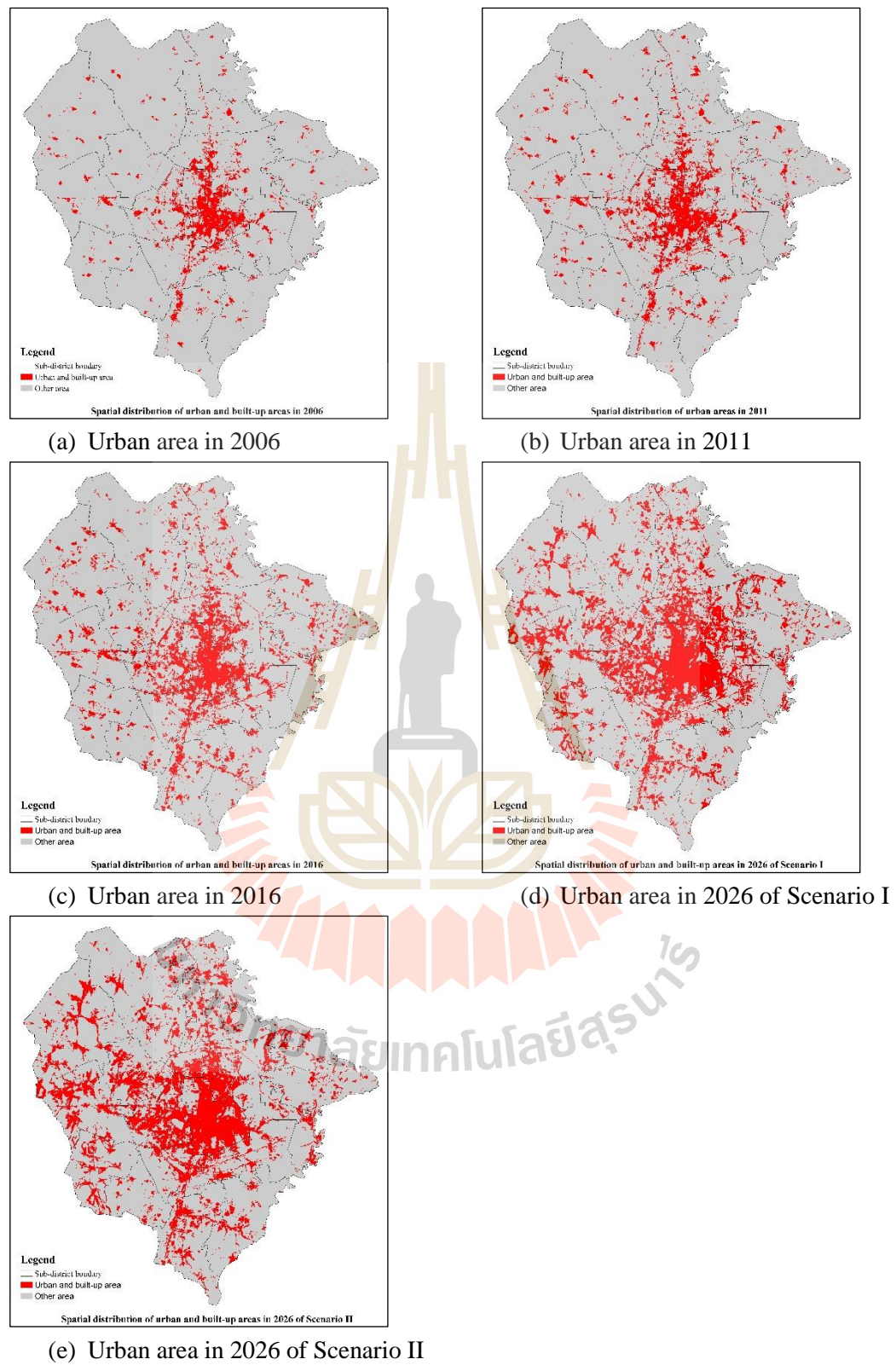
(e) Urban area in 2026 of Scenario II

Figure 4.26 Spatial distribution of urban areas during 2006 and 2026 (Scenario I and

II).

4.4.1 Annual expansion intensity index

Urban expansion intensity index (AEII) by sub-district in the study area was here calculated to identify expansion stage of urban growth by using Eq. 3.1 as suggestion by Zhao-ling et al. (2007). Table 4.28 presents the statistics of the AEII for 18 sub-districts in different periods (2006-2011, 2011-2016, 2016-2026 (scenario I and II). In the meantime, Figure 4.27 shows spatial distribution of AEII classification at sub-district level in each period as follows:

(1) AEII < 0.25% represents an area with slow expansion;

(2) 0.25% ≤ AEII < 0.5% represents an area with slow-speed expansion;

(3) 0.5% ≤ AEII < 0.75% represents an area with medium-speed expansion.

(4) 0.75% ≤ AEII < 1.0% represents an area with fair-speed expansion;

(5) 1.0% ≤ AEII represents an area with high-speed expansion.

Table 4.28 Annual expansion intensity index (AEII) in each sub-district.

Sub-district	Annual expansion intensity index (AEII) (%)			
	2006-2011	2011-2016	2016-2026 scenario I	2016-2026 scenario II
Mueang Kao	1.29	1.17	1.69	1.93
Daeng Yai	0.39	0.98	2.42	3.06
Khok Si	0.44	1.07	0.75	0.76
Non Thon	0.44	0.79	1.12	1.43
Nai Mueang	1.00	1.32	3.18	2.92
Don Chang	0.31	0.69	0.76	0.64
Don Han	0.34	0.63	0.78	0.84
Tha Phra	0.59	0.93	1.21	1.47
Ban Pet	1.89	2.21	3.81	4.36
Ban Kho	0.21	0.71	0.79	0.97
Ban Thum	0.49	0.83	2.15	2.36
Ban Wa	0.31	0.52	1.49	1.70
Bueng Niam	0.30	0.86	1.71	1.47
Phra Lap	0.63	0.81	1.80	0.92
Sila	1.30	1.18	3.41	2.68
Sawathi	0.29	0.65	0.99	1.27
Samran	0.54	0.87	1.35	1.53
Nong Tum	0.45	0.63	0.96	1.04
District	**0.59**	**0.91**	**1.62**	**1.69**

(a) Period 2006-2011

(b) Period 2011-2016

(c) Period 2016-2026 (Scenario I)

(d) Period 2016-2026 (Scenario II)
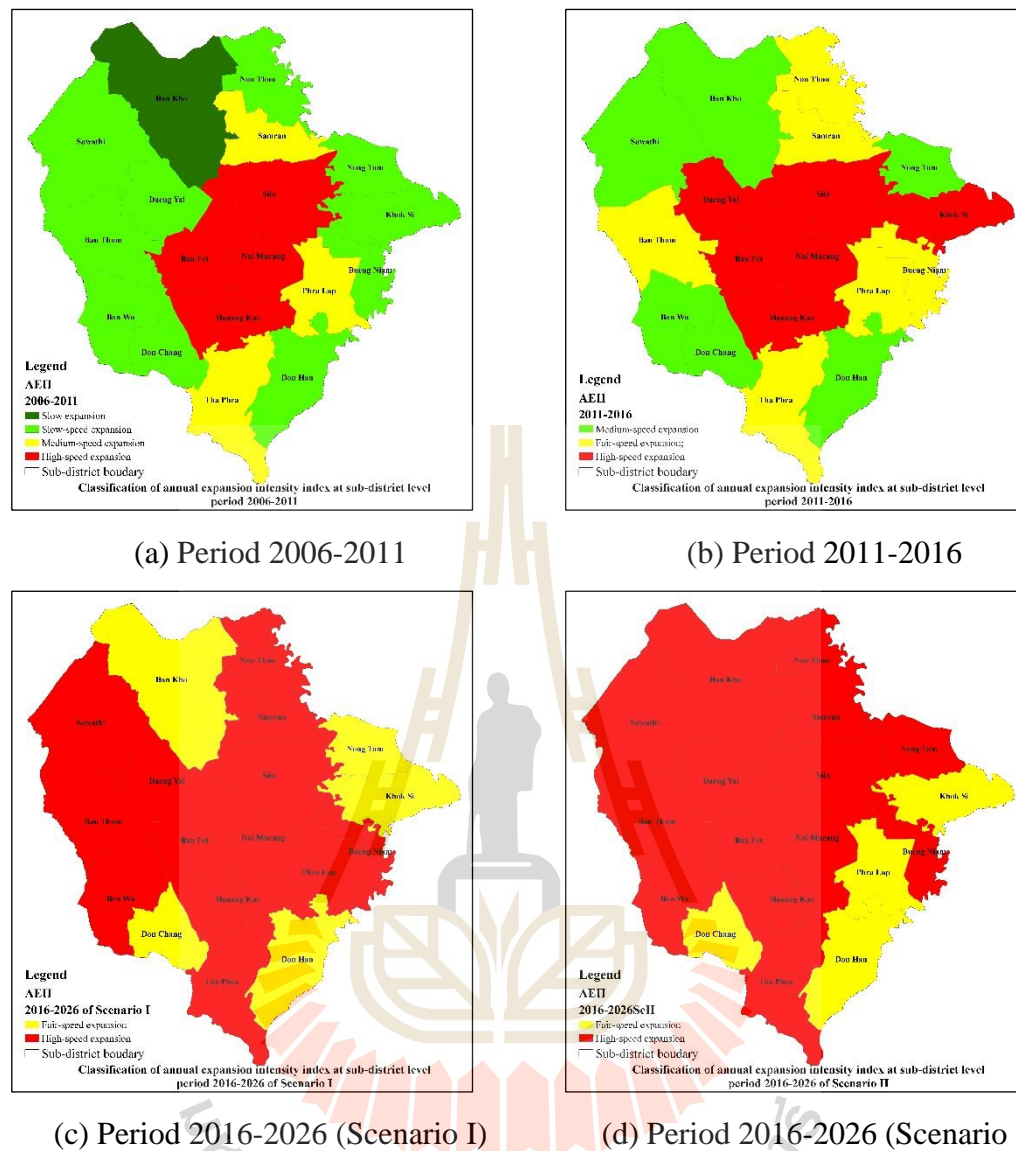
Figure 4.27 Classification of annual expansion intensity index at sub-district level during 2006 to 2026 (Scenario I and II).

At sub-district level, during 2006 to 2011, it was found that 4 sub-districts have AEII with high-speed expansion, 3 sub-districts have AEII with medium-speed expansion, 10 sub-districts have AEII with slow-speed expansion, and 1 sub-districts have AEII with slow expansion. On contrary, during 2011 and 2016, 5 sub-

districts have AEII with high-speed expansion, 7 sub-districts have AEII with fair-speed expansion and 6 sub-districts have AEII with medium-speed expansion.

Meanwhile, during 2016 to 2026 of Scenario I, it was found that 12 sub-districts have AEII with high-speed expansion and 6 sub-districts have AEII with fair-speed expansion. In the meantime, during 2016 to 2026 of Scenario II, 13 sub-districts have AEII with high-speed expansion and 5 sub-districts have AEII with fair-speed expansion.

In addition, it can be observed that during 2006 to 2026 (Scenario I and II), 4 sub-districts, namely Mueang Kao, Nai Mueang, Ban Pet, and Sila, have annual expansion intensity index at high speed expansion level with value from 1.00% to 4.36%.

Moreover, most of AEII values at district level during 2006 and 2011 show medium speed expansion while most of AEII values show fair speed expansion during 2011 to 2016. Meanwhile, most of AEII values show high speed expansion during 2016 to 2026 (Scenario I and II). This find infers that urban area will increase more in the future.

4.4.2 Urban land percentage

Urban land percentage (PU), which represents the proportion of urban area to a total area, was here extracted by sub-district boundary using Eq. 3.2 and reclassified into 5 grades based on Tian et al. (2005) as:

(1) PU < 0.001% represents an area with very low urbanization;

(2) 0.001% ≤ PU < 1% represents an area with low urbanization;

(3) 1% ≤ PU < 5% represents an area with moderate urbanization;

(4) 5% ≤ PU < 10% represents an area with high urbanization;

(5) 10% ≤ PU represents an area with very high urbanization.

The result of PU in each sub-district in the study area was summarized as shown in Table 4.29 while distribution of PU classification during 2006 to 2026 (Scenario I and II) is presented in Figure 4.28.

Table 4.29 Urban land percentage (PU) in each sub-district during 2006 to 2026 (Scenario I and II).

Sub-district	Urban land percentage (PU) in				
	2006	2011	2016	2026 scenario I	2021 scenario II
Mueang Kao	9.88	16.34	22.19	26.80	29.16
Daeng Yai	1.43	3.36	8.24	25.67	32.05
Khok Si	1.80	4.01	9.36	9.33	9.36
Non Thon	1.86	4.05	8.03	13.09	16.12
Nai Mueang	48.17	53.16	59.77	79.96	77.33
Don Chang	0.94	2.50	5.97	8.49	7.33
Don Han	1.80	3.48	6.62	9.58	10.18
Tha Phra)	4.97	7.93	12.59	17.09	19.65
Ban Pet	14.95	24.39	35.45	53.05	58.58
Ban Kho	0.93	2.00	5.56	8.87	10.64
Ban Thum	3.25	5.71	9.88	24.72	26.88
Ban Wa	1.74	3.26	5.88	16.66	18.72
Bueng Niam	2.98	4.47	8.77	20.07	17.67
Phra Lap	4.98	8.16	12.19	23.00	14.21
Sila	10.14	16.63	22.55	44.26	36.94
Sawathi	1.57	3.03	6.26	11.46	14.27
Samran	3.29	5.98	10.34	16.79	18.58
Nong Tum	1.85	4.10	7.26	11.50	12.27
District	**5.91**	**8.87**	**13.42**	**22.12**	**22.80**

(a) 2006   (b) 2011

(c) 2016   (d) 2026 (Scenario I)
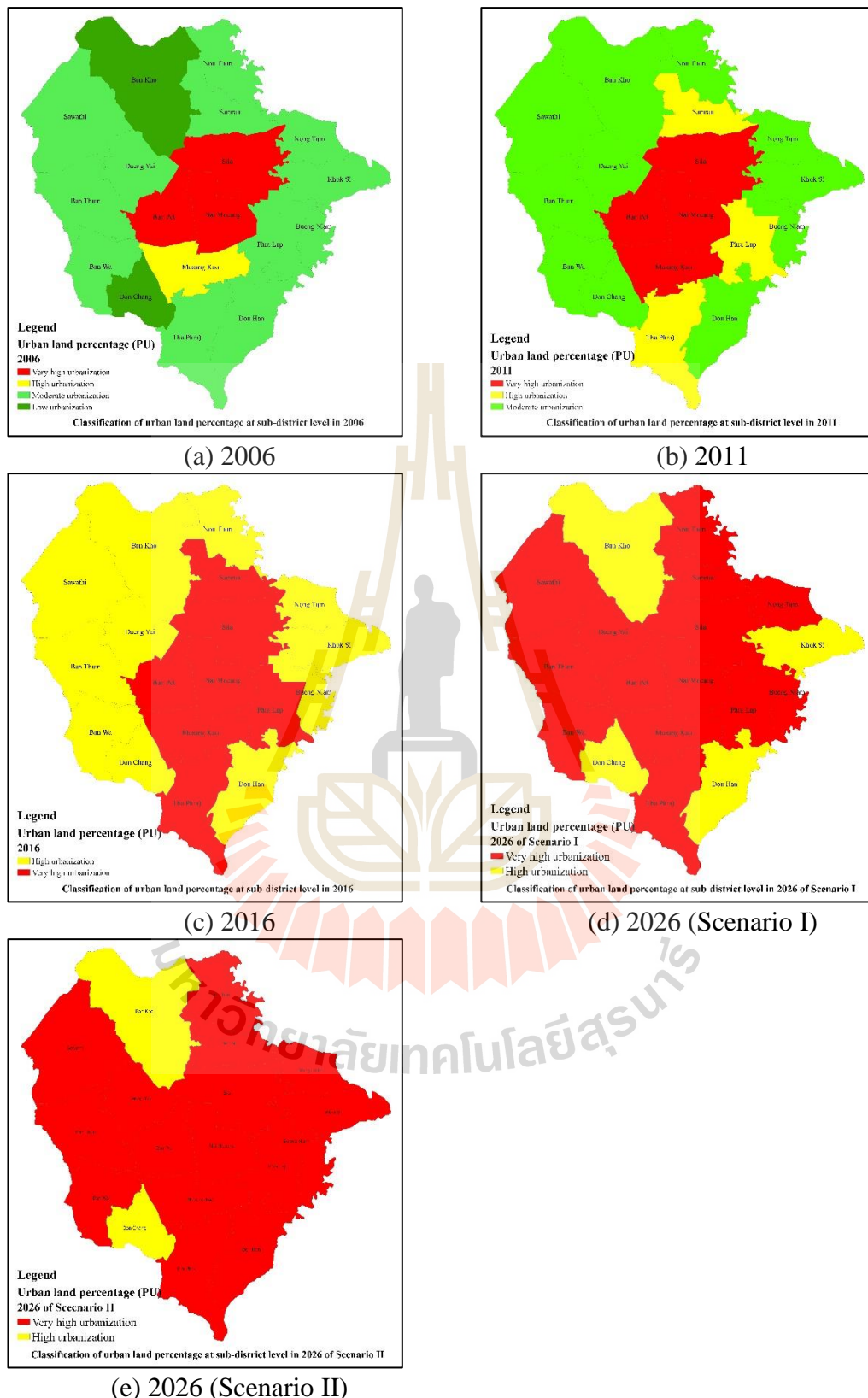
(e) 2026 (Scenario II)

Figure 4.28 Classification of urban land percentage at sub-district level during 2006 to

2026 (Scenario I and II).

At sub-district level, it was found that 2 sub-districts have low urbanization, 12 sub-districts have moderate urbanization, 1 sub-district has high urbanization and 3 sub-districts have very high urbanization (Nai Mueang, Ban Pet, and Sila sub-districts) in 2006. Later in 2011, 10 sub-districts have moderate urbanization, 4 sub-districts have high urbanization and 4 sub-districts have very high urbanization (Nai Mueang, Ban Pet, and Sila, Mueang Kao sub-districts). Meanwhile 11 sub-districts have high urbanization and 7 sub-districts have very high urbanization (Nai Mueang, Ban Pet, and Sila, Mueang Kao, Tha Phra, Phralap, Sam Ran sub-districts) in 2016.

In the meantime, in 2026 of Scenario I, 4 sub-districts have high urbanization and 14 sub-districts have very high urbanization while 2 sub-districts have high urbanization and 16 sub-districts have very high urbanization in 2026 (Scenario II). This finding shows future trend of urbanization due to transformation of planning and policy on urban growth under Scenario II.

In addition, it can be observed that during 2006 to 2026 (Scenario I and II), 3 sub-districts, namely Nai Mueang, Ban Pet, and Sila, have very high urban land percentage (PU) at very high urbanization level with value from 10.14% to 79.96%.

Moreover, at district level, urban land percentage in 2006 and 2011 shows high urbanization while urban land percentage 2016 and 2026 (scenario I and II) reveals very high urbanization. This indicates the trend of urbanization in the study area in the near future.

4.4.3 Urban land expansion index

Similar to AEII, urban land expansion index (SI) was here extracted in each sub-district in different periods during 2006 to 2026 (Scenario I and II) using Eq. 3.3 to explain about urban growth. Herewith, standard SI classification which was suggested by Tian et al. (2005) was here applied to characterize urban development as following.

(1) SI < 0.001% represents an area with no change;

(2) 0.001% ≤SI < 0.1% represents an area with low development;

(3) 0.1% ≤SI < 1.0% represents an area with rapid development;

(4) 1.0% ≤SI < 5.0% represents an area with more rapid development;

(5) 5.0% ≤SI represents an area with dramatic development.

Result of urban land expansion index (SI) and classification of urban land expansion in each sub-district in four periods was displayed in Table 4.30 and Figure 4.28, respectively.

At sub-district level, urban land expansion index between 2006 and 2011 reveals that 15 sub-districts have more rapid development, 3 sub-districts have dramatic development. While, between 2011 and 2016 urban land expansion index shows that 13 sub-districts have more rapid development and 5 sub-districts have dramatic development.

In the meantime, urban land expansion index between 2016 and 2026 of Scenario I reveals that 1 sub-district (Khok Si) has no change, 6 sub-districts have more rapid development and 11 sub-districts have dramatic development. Meanwhile, urban land expansion index between 2016 and 2026 of Scenario II shows that 1 sub-district (Khok Si) has no change, 3 sub-districts have more rapid development and 14 sub-

districts have dramatic development. This finding shows effect of planning and policy under Scenario II on land development.

Moreover, at district level, urban land expansion index between 2006 and 2011 and between 2011 and 2016 shows more rapid development. Meanwhile, urban land expansion index between 2016 and 2026 (Scenarios I and II) shows dramatic development in the study area. This finding also infers more land development into urban area in the future.

Table 4.30 Land expansion index (SI) in each sub–district.

Sub-district	Land expansion index (SI)			
	2006-2011	2011-2016	2016-2026 scenario I	2016-2026 scenario II
Mueang Kao	6.46	5.85	4.60	6.96
Daeng Yai	1.93	4.88	17.44	23.81
Khok Si	2.21	5.35	0.00	0.00
Non Thon	2.20	3.97	5.07	8.10
Nai Mueang	4.99	6.61	20.19	17.56
Don Chang	1.56	3.47	2.52	1.36
Don Han	1.69	3.14	2.96	3.56
Tha Phra	2.96	4.66	4.50	7.07
Ban Pet	9.44	11.06	17.60	23.13
Ban Kho	1.07	3.57	3.30	5.08
Ban Thum	2.46	4.17	14.84	16.99
Ban Wa	1.53	2.61	10.79	12.84
Bueng Niam	1.49	4.30	11.31	8.90
Phra Lap	3.17	4.03	10.81	2.02
Sila	6.49	5.92	21.70	14.38
Sawathi	1.46	3.23	5.20	8.02
Samran	2.70	4.35	6.45	8.25
Nong Tum	2.25	3.16	4.24	5.01
Total	**2.96**	**4.54**	**8.70**	**9.38**

(a) Period 2006-2011

(b) Period 2011-2016

(c) Period 2016-2026 (Scenario I)

(d) Period 2016-2026 (Scenario II)
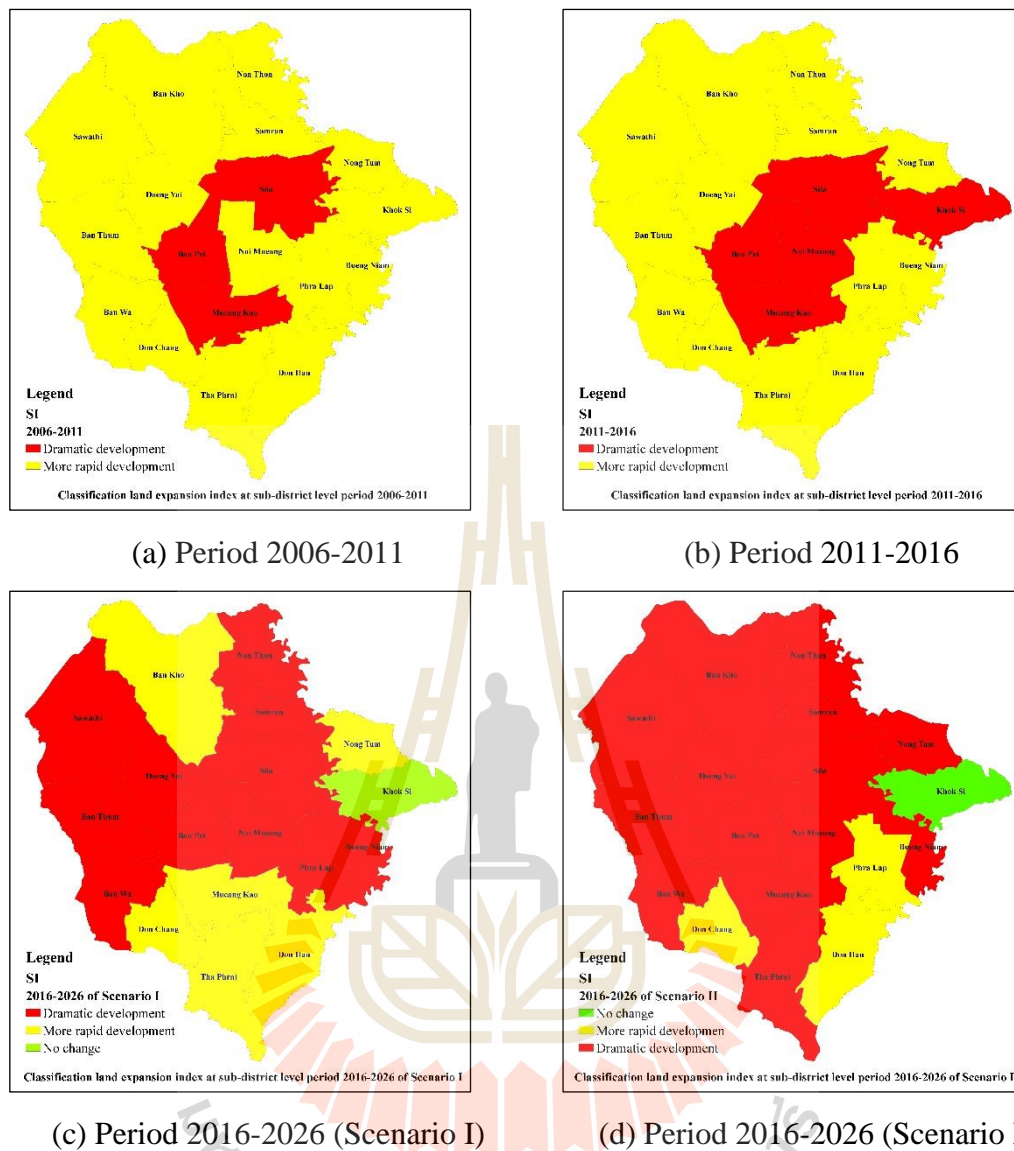
Figure 4.29 Classification land expansion index at sub-district level during 2006 to 2026 (Scenario I and II).

In summary, urban growth characteristics which is here described using (1) AEII, (2) PU and (3) SI based on urban area in each year or period show repeatable phenomena in specific sub-districts during 2006 to 2026 (2 scenarios). Herein, 3 sub-districts include Ban Pet, Sila, and Mueang Kao have AEII with high-speed expansion, PU with very high urbanization, and SI with dramatic development in each year or period.

CHAPTER V

URBAN GROWTH IMPACT ON URBAN LANDSCAPE

ECOLOGY

This chapter presents results of the second objective focusing on urban growth impact on urban landscape ecology. Herein, the derived urban landscape data (LULC data in 2006, 2010, 2016 and 2026 (Scenario I and II) are quantified to assess status and its change due to urban growth at class and landscape levels by using landscape pattern analysis with landscape metrics. The main results of this chapter include (1) status and change of urban landscape (2) status and change of urban and built-up area and (3) landscape metrics and urban growth pattern relationship.

5.1   Status and change of urban landscape

Status and change of urban landscape which includes all LULC type in the past, present and future and their changes at class and landscape levels are here separately assessed landscape pattern and described based on various landscape metrics measurement.

5.1.1   Status and change of urban landscape at class level

At class level, landscape metrics included edge density (ED), total edge (TE) percent of landscape (PLAND), class area (CA), area-weighted fractal dimension (FRAC_AM), area-weighted mean shape index (SHAPE_AM), number of patches

(NP), patch density (PD), landscape shape index (LSI) and interspersion and juxtaposition index (IJI) were here applied to calculate landscape metrics value for each LULC type in Mueang Khon Khaen district, Khon Khon province. The characteristic of each index can be separately described in the following sections.

(1) Class area (CA). Class area is a measure of landscape composition; specifically, how much of the landscape is comprised of a particular patch type. By definition, class area equals the sum of area of all patches of the corresponding patch type. In this study, area of paddy field, field crop, forest land, and water body decreases during 20 years (2006–2026 (Scenario I and II)). In the same period, area of urban and built-up area, range land, and unused land has continuously increased while area of marsh and swamp is stable (Table 5.1 and Figure 5.1). These results imply that interchange occurs among landscape types (LULC types) in these periods. In fact, the value of CA of each landscape type directly relates with area of LULC type and pattern landscape change by CA also related with LULC change during these periods.

Table 5.1 Class area values of each landscape type during 2006 to 2026 (Scenario I and II).

Landscape class level	Class area (km^2)				
	2006	2011	2016	2026 of Scenario I	2026 of Scenario II
Urban and built -up area (Ur)	57.9425	86.865	131.3775	217.28	223.96
Paddy field (Pd)	555.995	517.5925	451.3725	342.855	342.31
Field crop (Fc)	207.31	189.9475	147.9925	90.72	90.3275
Forest land (Fo)	40.215	40.215	40.02	40.02	37.9175
Water body (Wa)	53.1725	52.88	52.7575	52.055	52.1075
Marsh and swamp (Ms)	33.6175	32.805	32.32	31.3375	31.4825
Range land (Ra)	28.9375	54.6225	109.455	178.69	175.105
Unused land (Ul)	4.86	7.1225	16.755	29.0925	28.84
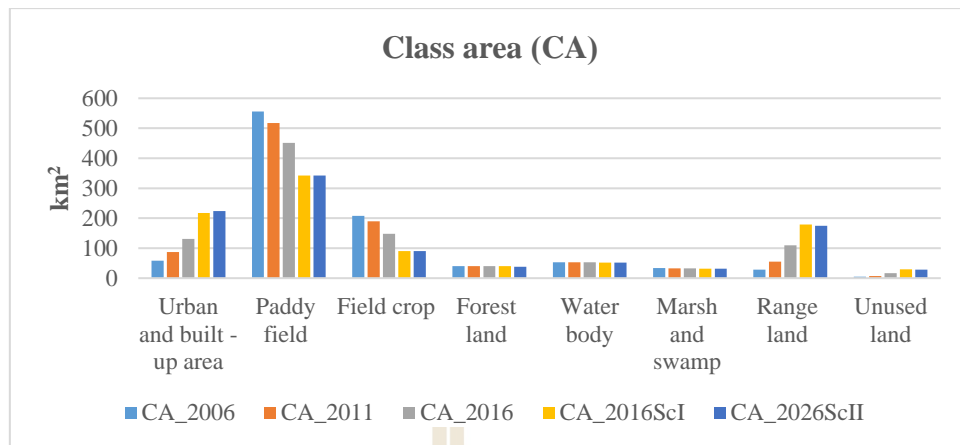
Figure 5.1 Comparison of class area values of each landscape type during 2006 to 2026 (Scenario I and II).

(2) Percent of landscape (PLAND). Percentage of landscape quantifies the proportional abundance of each patch type in the landscape. In this study, percent of paddy field, field crop, forest land, marsh and swamp, and water body have continuously decreased between 2006 and 2026 (Scenario I and II). This infers that fragmentation occurs in these landscape types. In the same period, percent of urban and built-up area, range land, and unused land have continuously increased (Table 5.2 and Figure 5.2). This result implies the expansion of urban and built-up area during these periods. This finding is similar with the previous work of Shetty, Gowda, Gururaja and Sudhira (2012) who studied effect of landscape metrics on varied spatial extent of Bangalore, India, they found that the percent of built-up had increased doubled (11.88 to 22.59) between 2000 and 2009. Because, vegetation was the dominant patch type in 2000 it changed to built-up in 2009. Additionally, this indicates that the proportional change in land cover over the years, whether the open spaces, vegetation and water bodies, all have succumbed due to rapid urban growth.

In addition, percentage of landscape like class area, it is a measure of landscape composition important in many ecological applications. However, because percentage of landscape is a relative measure, it may be a more appropriate measure of landscape composition than class area for comparing among landscapes of varying sizes (Shetty et al., 2012).

Table 5.2 Percent of landscape values of each landscape type during 2006 to 2026 (Scenario I and II).

Landscape class level	Percent of landscape (Percent)				
	2006	2011	2016	2026 of Scenario I	2026 of Scenario II
Urban and built -up area (Ur)	5.90	8.85	13.38	22.13	22.81
Paddy field (Pd)	56.62	52.71	45.96	34.91	34.86
Field crop (Fc)	21.11	19.34	15.07	9.24	9.20
Forest land (Fo)	4.10	4.10	4.08	4.08	3.86
Water body (Wa)	5.41	5.38	5.37	5.30	5.31
Marsh and swamp (Ms)	3.42	3.34	3.29	3.19	3.21
Range land (Ra)	2.95	5.56	11.15	18.20	17.83
Unused land (Ul)	0.49	0.73	1.71	2.96	2.94
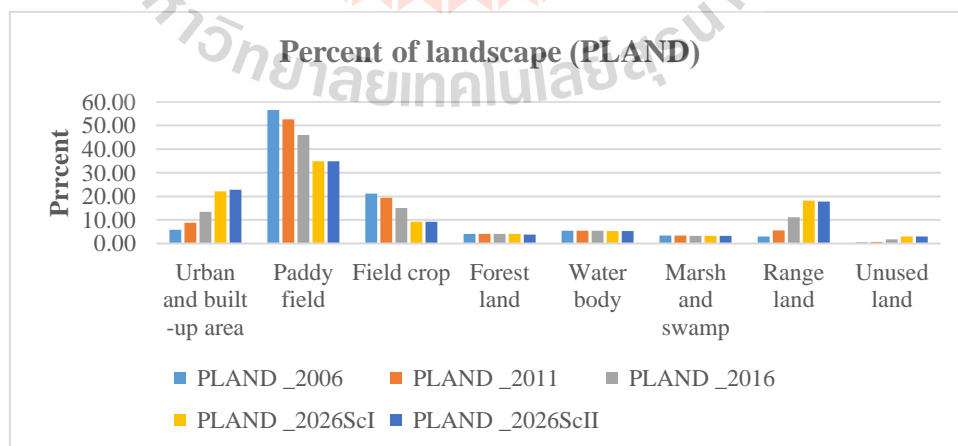
Figure 5.2 Comparison of percent of landscape values of each landscape type during 2006 to 2026 (Scenario I and II).

(3) Edge density (ED). It is standardizes edge per unit area basis that facilitates comparison among landscapes of varying size. The edge density (ED) is a measure of total length of edges of the landscape type patches or reports edge length per unit area. During 2006 to 2026 (Scenario I and II), edge density of paddy field, field crop, forest land, marsh and swamp and water body decreases. This infers that reduction of edge density occurs in these landscape type, particularly paddy field and field crop. In contrast, edge density of urban and built up area, range land, and unused land increases in these periods. This infers that area of these landscape types is expanded in these periods, particularly urban and built-up area and range land (Table 5.3 and Figure 5.3). This finding is similar with the previous work of Megahed, Cabral, Silva and Caetano (2015) who found that edge density of urban area increased in 2014 was almost four times of what had been in 1984, indicating that urban area had become more fragmented over time.

Table 5.3 Edge density values of each landscape type during 2006 to 2026 (Scenario I and II).

Landscape class level	Edge density (m/ha)				
	2006	2011	2016	2026 of Scenario I	2026 of Scenario II
Urban and Built-Up area (Ur)	12.85	19.09	28.11	36.85	35.36
Paddy field (Pd)	58.17	56.39	51.22	40.38	38.22
Field crop (Fc)	39.66	35.04	25.07	14.16	14.04
Forest land (Fo)	9.92	9.92	9.83	9.83	9.42
Water body (Wa)	13.29	13.19	13.20	13.09	13.08
Marsh and swamp (Ms)	10.02	9.59	9.38	9.15	9.19
Range land (Ra)	10.77	18.87	28.68	41.40	40.31
Unused land (Ul)	2.30	3.42	6.84	10.15	9.65
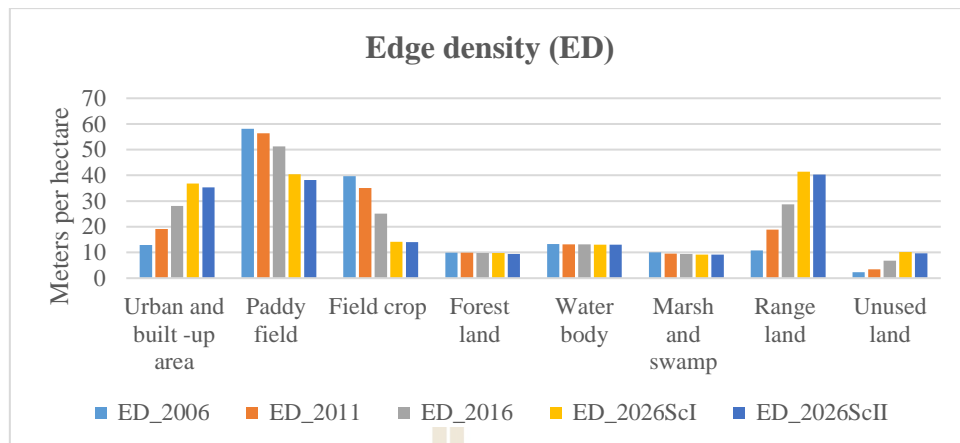
Figure 5.3 Comparison of edge density values of each landscape type during 2006 to
2026 (Scenario I and II).

　　　　　(4) Total edge (TE). It is an absolute measure of total edge length of a
particular patch type. Pattern of status and change of all landscape types based on total
edge are similar to edge density (ED). During 2006 to 2026 (Scenario I and II), total
edge of paddy field, field crop, forest land, marsh and swamp and water body decreases.
This infers that total edge of these landscape types reduces in these periods. Meanwhile,
total edge of urban and built up area, range land, and unused land increases in these
periods. This implies that these landscape types expand in these periods. In contrast,
during 2016 to 2026 of Scenario I periods total edge of forest land, marsh and swamp
and water body increases. This infers about expansion of these landscape type in the
future of two scenarios (Table 5.4 and Figure 5.4). This finding is consistent with Liu
and Yang (2015) who found that total edge of residential land from 2000 to 2010
increased rapidly, indicating that residential land had become more fragmented over
time.

Table 5.4 Total edge values of each landscape type during 2006 to 2026 (Scenario I and II).

Landscape class level	Total edge (m)				
	2006	2011	2016	2026 of Scenario I	2026 of Scenario II
Urban and Built-Up area (Ur)	1,261,450	1,874,300	2,760,250	3,629,700	3,472,100
Paddy field (Pd)	5,712,300	5,538,250	5,029,700	4,036,600	3,753,750
Field crop (Fc)	3,895,000	3,441,000	2,462,450	1,415,750	1,379,100
Forest land (Fo)	974,000	974,000	965,500	981,200	924,700
Water body (Wa)	1,305,600	1,295,800	1,296,750	1,337,700	1,284,750
Marsh and swamp (Ms)	984,150	942,150	921,350	924,100	902,850
Range land (Ra)	1,057,400	1,853,350	2,817,000	4,089,900	3,958,600
Unused land (Ul)	225,800	335,650	671,600	1,008,050	948,150
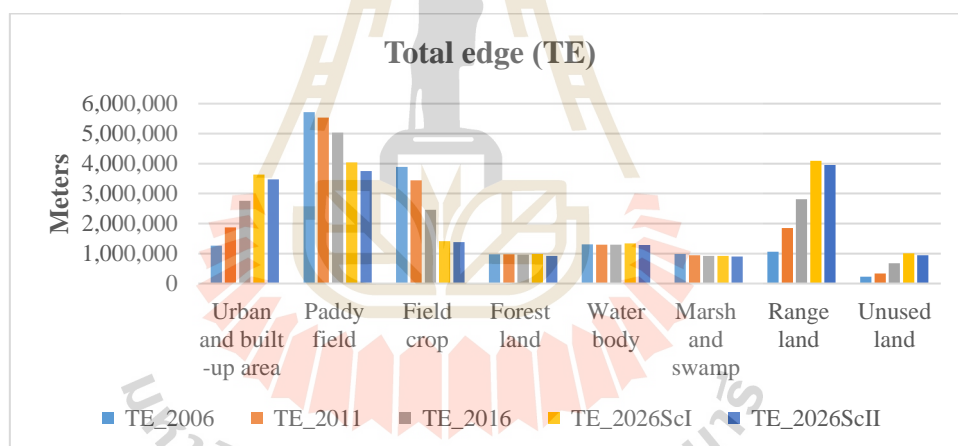
Figure 5.4 Comparison of total edge values of each landscape type during 2006 to 2026 (Scenario I and II).

(5) Area-weighted fractal dimension (FRAC_AM). By definition, area-weighted fractal dimension measure of complexity of the shapes of class boundaries, ranging from 1 to 2. It uses class area as a weighting factor. FRAC _AM value closes to 1 for shapes with very simple perimeters such as squares while FRAC_AM value closes to 2 for shapes with highly convoluted, plane-filling

perimeters (McGarigal et al., 2002). During 2006 to 2026 (Scenario I and II), area-weighted fractal dimension of paddy field and field crop forest land and water body shows a very slightly decrease approach to 1. This infers that less modification and shapes with very simple perimeters occur in these landscape types. In the same periods, area-weighted fractal dimension of marsh and swamp and unused land slightly increases. This refers that they become larger and more complex. Meanwhile, area-weighted fractal dimension of urban and built-up area and range land increases approach to 2. This infers that fragmentation occurs in these landscape type and shape with highly convoluted in these landscape types (Table 5.5 and Figure 5.5). This finding is consistent with Padmanaban, Bhowmik, Cabral, Zamyatin, Almegdadi and Wang (2017) who found the area-weighted fractal dimension value of urban area increased, it indicates a result of contained urban growth with reasonable shape complexity.

Table 5.5 Area-weighted fractal dimension values of each landscape type during 2006 to 2026 (Scenario I and II).

Landscape class level	Area-weighted fractal dimension (Unitless)				
	2006	2011	2016	2026 of Scenario I	2026 of Scenario II
Urban and Built-Up area (Ur)	1.214	1.230	1.233	1.269	1.254
Paddy field (Pd)	1.364	1.329	1.294	1.238	1.248
Field crop (Fc)	1.228	1.223	1.214	1.233	1.233
Forest land (Fo)	1.108	1.108	1.108	1.108	1.108
Water body (Wa)	1.139	1.139	1.139	1.140	1.139
Marsh and swamp (Ms)	1.117	1.118	1.119	1.119	1.119
Range land (Ra)	1.105	1.121	1.152	1.186	1.185
Unused land (Ul)	1.077	1.073	1.087	1.104	1.117
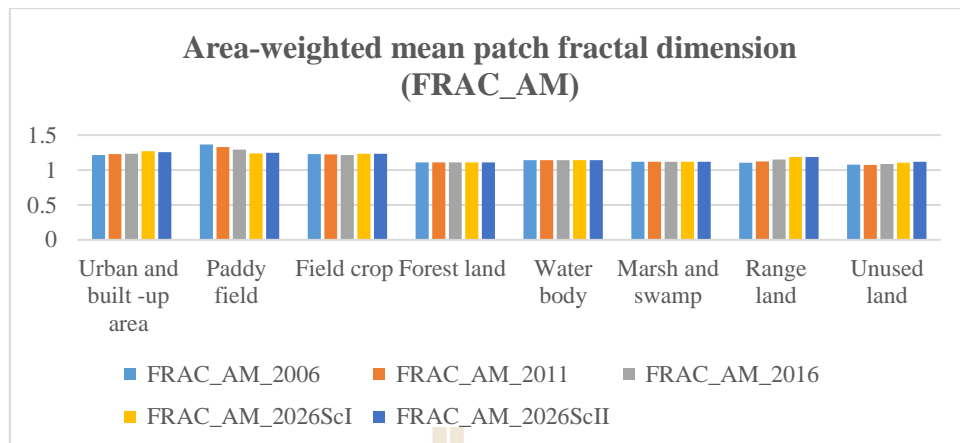
Figure 5.5 Comparison of area-weighted fractal dimension values of each landscape type during 2006 to 2026 (Scenario I and II).

(6) Area-weighted mean shape index (SHAPE_AM). It generally uses to measure the urban morphology of the district in terms of the irregularity in patch shape. During 2006 to 2026 (Scenario I and II), area-weighted mean shape index of paddy field has dramatically decreased. This reflects a decreasing complexity in irregularity in the spatial pattern of landscape type in these periods. Meanwhile, area-weighted mean shape index of field crop, forest land, range land, marsh and swamp and water body are rather stable. It implies that complexity in irregularity in the spatial pattern of these landscape types in these periods is stable. At the same time, area-weighted mean shape index of urban and built–up area and unused land is increasing. This reflects an increasing complexity in irregularity in the spatial pattern of two landscape types in these periods (Table 5.6 and Figure 5.6). The finding is similar with the previous work of Su, Xiao and Jiang (2012) who found the increase of area-weighted mean shape index of built-up, they suggested that build-up presented more

irregular shape. Conversely, forest has become more regular in shape, as evidenced by the declining values of area-weighted mean shape index.

Table 5.6 Area-weighted fractal dimension values of each landscape type during 2006 to 2026 (Scenario I and II).

Landscape class level	Area-weighted mean shape index (Unitless)				
	2006	2011	2016	2026 of Scenario I	2026 of Scenario II
Urban and Built-Up area (Ur)	8.13	10.13	10.99	14.75	11.28
Paddy field (Pd)	43.29	27.21	17.12	8.63	10.12
Field crop (Fc)	7.56	7.20	6.58	7.46	7.47
Forest land (Fo)	1.93	1.93	1.93	1.93	1.92
Water body (Wa)	2.02	2.03	2.04	2.04	2.04
Marsh and swamp (Ms)	2.02	2.03	2.04	2.04	2.04
Range land (Ra)	1.86	2.13	2.80	4.59	4.67
Unused land (Ul)	1.53	1.51	1.63	1.89	2.20
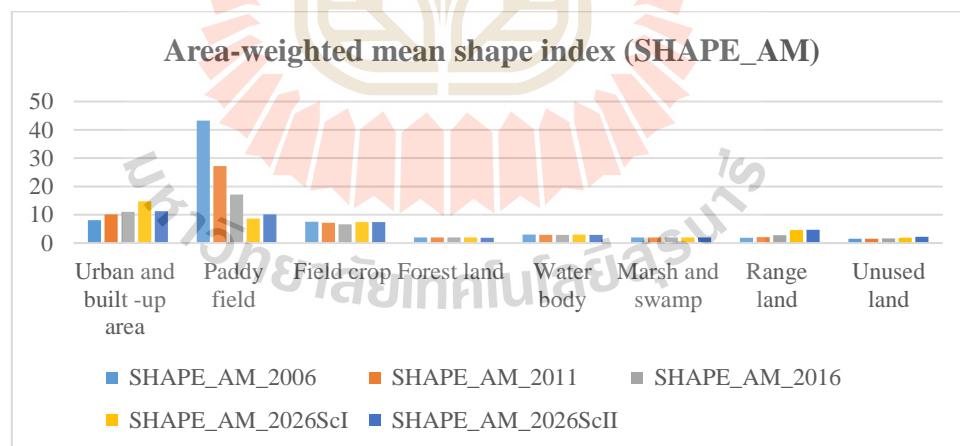
Figure 5.6 Comparison of area-weighted mean shape index values of each landscape type during 2006 to 2026 (Scenario I and II).

(7) Interspersion and juxtaposition index (IJI). The interspersion index measures the extent to which patch types are interspersed; higher values result

from landscapes in which the patch types are well interspersed, whereas lower values characterize landscapes in which the patch types are poorly interspersed. During 2006 to 2016, interspersion and juxtaposition index of all landscape types has continuously increased. This represents that these landscape types become more landscape configuration. However, interspersion and juxtaposition index of urban and built-up area, field crop, forest land, marsh and swamp, range land and unused land decreases in 2026 of both Scenario-I and II. This means that these landscape type distribute less landscape configuration than the earlier periods (2006–2016). In contrast, interspersion and juxtaposition index of paddy field and water bodies increases in 2026 of both Scenario-I and II. This means that this landscape type distributes more landscape configuration than the earlier periods (2006–2016) (Table 5.7 and Figure 5.7). Likewise, Linh, Erasmi and Kappas (2012) who studied on quantifying LULC change and landscape fragmentation in Danang City, Vietnam: 1979-2009 and they found the increases of the IJI of urban class from 1979 to 2009 indicated that urban class distributed a more landscape configuration in 2009 than in 1979.

Table 5.7 Interspersion and juxtaposition index values of each landscape type during 2006 to 2026 (Scenario I and II).

Landscape class level	Interspersion and juxtaposition index (Unitless)				
	2006	2011	2016	2026 of Scenario I	2026 of Scenario II
Urban and Built-Up area (Ur)	79.21	80.58	82.65	74.06	80.61
Paddy field (Pd)	78.95	85.08	90.97	87.69	88.87
Field crop (Fc)	53.79	59.63	67.75	79.82	85.08
Forest land (Fo)	69.19	77.11	84.79	82.10	84.27
Water body (Wa)	66.49	72.64	82.80	82.58	81.14
Marsh and swamp (Ms)	67.94	72.75	80.32	81.26	79.70
Range land (Ra)	79.69	79.54	82.37	78.99	83.72
Unused land (Ul)	86.19	86.94	87.37	83.99	85.32
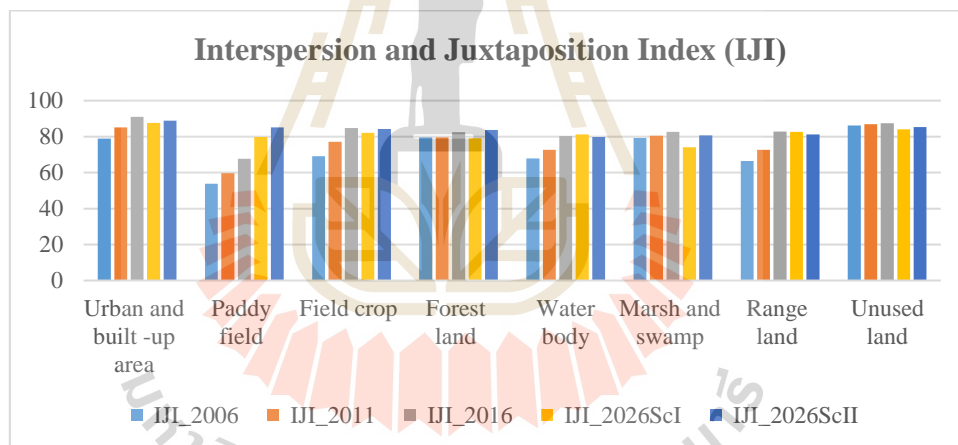
Figure 5.7 Comparison of interspersion and juxtaposition index values of each landscape type during 2006 to 2026 (Scenario I and II).

(8) Landscape shape index (LSI). Landscape shape index measures the shape of the class in the landscape and LSI equals 1, when the landscape consists of a single square patch of the corresponding type and landscape shape index increases as landscape shape becomes more irregular. During 2006 to 2026 (Scenario I and II) landscape shape index of all landscape type is irregular shape. Herewith landscape

shape index of paddy field, field crop, forest land, marsh and swamp and water body landscapes continuously decreases in these periods. This reflects a decrease irregular shape of these landscape types. In contrast, landscape shape index of urban and built–up area, range land and unused land continuous increases. This indicates that shape of these landscape types becomes more irregular. (Table 5.8 and Figure 5.8). This finding is consistent with the previous work of Sha and Tian (2010) who mentioned that landscape shape index of urban area from 1912 to 2000 kept growing, indicating during the large- scale of urbanization, urban area kept expand and its shape complexity increased.

Table 5.8 Landscape shape index values of each landscape type during 2006 to 2026 (Scenario I and II).

Landscape class level	Landscape shape index (unitless)				
	2006	2011	2016	2026 of Scenario I	2026 of Scenario II
Urban and Built-Up area (Ur)	41.37	50.28	60.24	61.52	60.81
Paddy field (Pd)	61.56	61.83	60.18	54.48	51.67
Field crop (Fc)	68.31	63.05	51.27	37.17	36.86
Forest land (Fo)	38.97	38.97	38.64	38.64	37.96
Water body (Wa)	46.50	46.32	46.36	46.29	46.26
Marsh and swamp (Ms)	43.52	42.07	41.53	41.25	41.26
Range land (Ra)	49.12	62.88	67.62	76.45	75.15
Unused land (Ul)	25.46	31.45	41.09	46.67	44.56

Landscape Shape Index (LSI)
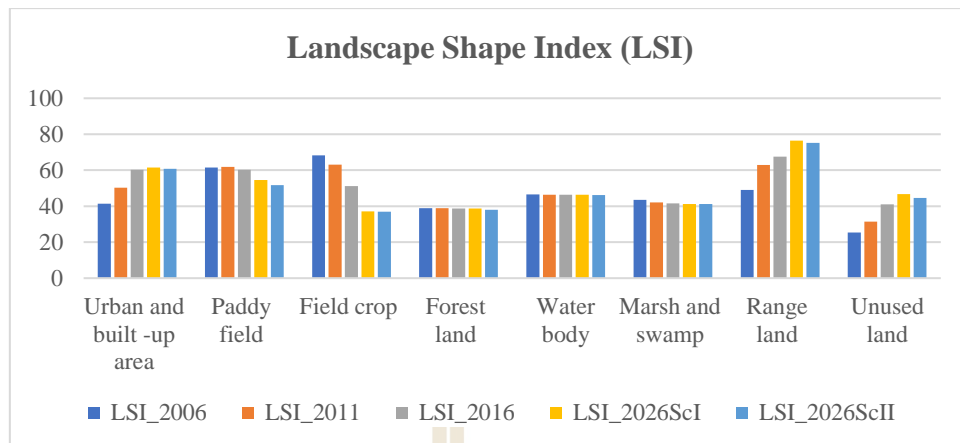
Figure 5.8 Comparison of landscape shape index values of each landscape type during 2006 to 2026 (Scenario I and II).

(9) Number of patches (NP). Number of patches is, in general, used to measure the extent fragmentation of patch type of each land class. Number of patches is a simple measure of subdivision and fragmentation of different patch type (McGarigal et al., 2002). During 2006 to 2016, number of patch of paddy field, field crop, forest land, marsh and swamp, and water bodies has been decreased. This infers that these landscape types become more compact. Meanwhile, in 2026 of Scenario I and II, number of patches of these landscape type except paddy field tends to decrease and becomes more compact. This finding is consistent with the previous of Fan and Ding (2016) who found that the number of patches of cultivated land decreases from 3871 to 2078 indicates that the distribution of cultivated land is gradually concentrated from 1990 to 2013.

In opposite, during 2006 to 2016, number of patches of urban and built-up area, range land, and unused land has been continuously increased. This infers that these landscape types become more fragmentation. Meanwhile, in 2026 of Scenario I

and II, number of patches of urban and built-up area tends to decrease and becomes more compact in the future. In contrast, number of patches of range land and unused land in 2026 of Scenario I and II tends to increase and becomes more fragmentation in the future (Table 5.9 and Figure 5.9). This finding is similar with the previous work of Lal, Kumar and Kumar (2017) who found that the number of patches increased from 1972-2011, indicating sparse growth and more fragmented development of new urban nuclei.

Table 5.9 Number of patches values of each landscape type during 2006 to 2026 (Scenario I and II).

Landscape class level	Number of patches metrics (patches)				
	2006	**2011**	**2016**	**2026 of Scenario I**	**2026 of Scenario II**
Urban and Built-Up area (Ur)	1,252	1,640	1,914	1,853	1,762
Paddy field (Pd)	1,328	1,366	1,109	1,309	1,224
Field crop (Fc)	2,280	1,843	952	491	488
Forest land (Fo)	729	729	717	717	708
Water body (Wa)	1,218	1,199	1,197	1,190	1,188
Marsh and swamp (Ms)	909	797	752	745	748
Range land (Ra)	1,543	2,186	1,739	2,196	2,240
Unused land (Ul)	503	771	1,161	1,435	1,327
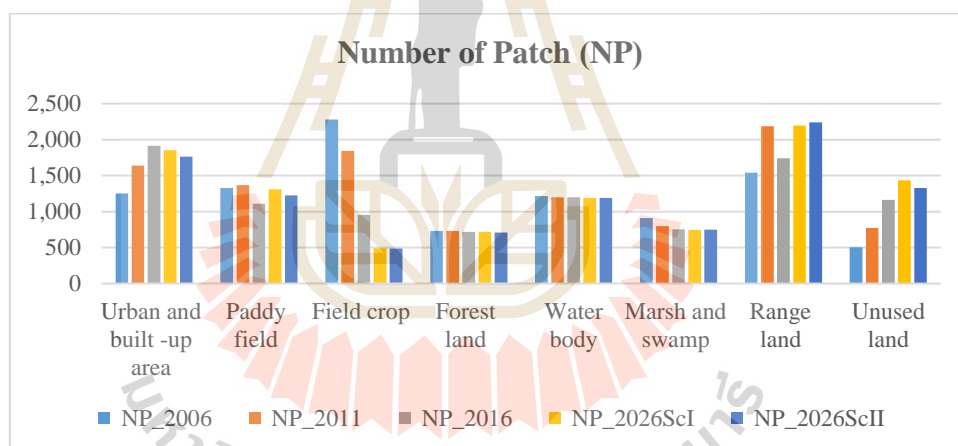
Figure 5.9 Comparison of number of patches values of each landscape type during 2006 to 2026 (Scenario I and II).

(10) Patch density (PD). The patch density equals the number of patches of the corresponding land cover type divided by total area of interest. Pattern of status and change of landscape type based on patch density are similar with number of patch. During 2006 to 2016, patch density of paddy field, field crop, forest land, marsh and swamp, and waterbodies has been decreased. This infers that these landscape

types become more compact. Meanwhile, in 2026 of Scenario I and II, patch density of these landscape types tends to decrease and these landscape types become more compact. This finding is similar with the previous work of Zhou and Wang (2011) found that under the urbanization pressure, patch density declined for forest land, suggesting that the area of forest land have reduced in size but not fragmented.

In opposite, during 2006 to 2016, patch density of urban and built-up area, range land, and unused land has been continuously increased. This infers that these landscape types become more fragmentation. Meanwhile, in 2026 of Scenario I and II, patch density of urban and built-up area tends to decrease and becomes more compact in the future. In contrast, patch density of range land and unused land in 2026 of Scenario I and II, tends to increase and becomes more fragmentation in the future (Table 5.10 and Figure 5.10). This finding is similar with the previous work of Subasinghe, Estoque and Murayama (2016) who found that the patch density of built-up class from 1993 to 2014 increased, it indicates that the built-up lands have become more fragmented.

Table 5.10 Patches density values of each landscape type during 2006 to 2026 (Scenario I and II).

Landscape class level	Patch density (Patch/100ha)				
	2006	**2011**	**2016**	**2026 of Scenario I**	**2026 of Scenario II**
Urban and Built-Up area (Ur)	1.27	1.67	1.95	1.89	1.79
Paddy field (Pd)	1.35	1.39	1.13	1.33	1.25
Field crop (Fc)	2.32	1.88	0.97	0.50	0.50
Forest land (Fo)	0.74	0.74	0.73	0.73	0.72
Water body (Wa)	1.24	1.22	1.22	1.21	1.21
Marsh and swamp (Ms)	0.93	0.81	0.77	0.76	0.76
Range land (Ra)	1.57	2.23	1.77	2.24	2.28
Unused land (Ul)	0.51	0.79	1.18	1.46	1.35
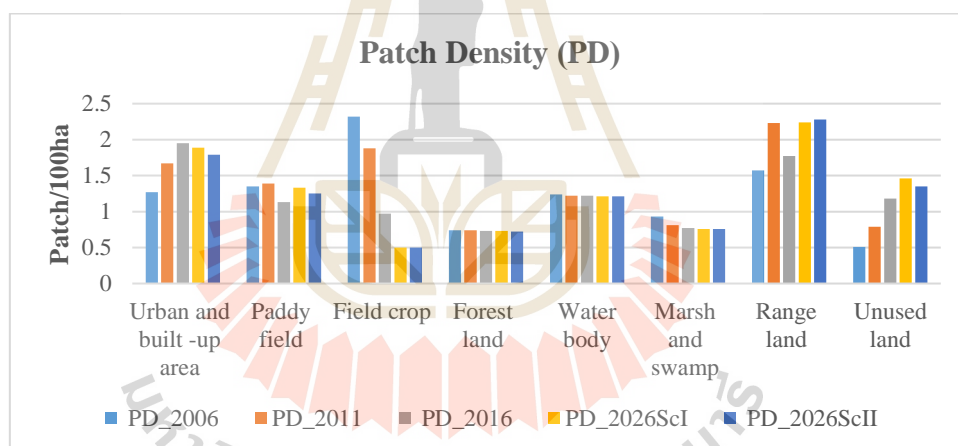
Figure 5.10 Comparison of patches density values of each landscape type during 2006 to 2026 (Scenario I and II).

5.1.2 Status and change of urban landscape at landscape level

At landscape level, Contagion (C), Shannon's Evenness Index (SHEI) and Shannon's Diversity Index (SHDI) were here calculated to describe the whole landscape status (all LULC type) during 2006 and 2026 of Scenario I and II. The

characteristics of each landscape metric are separately summarized in the following sections.

(1) **Contagion (C).** A contagion as an information theory-based index measures the extent to which patches are spatially aggregated in a landscape. During 2006 to 2016, contagion value has been continuously declined and it indicates that the landscape shape complexity and the degree of fragmentation considerably increases in these periods. This finding is consistent with the previous of Padmanaban et al. (2017) who found that the decrease in the contagion value indicated a high fragmentation of the landscape. However, contagion value in 2026 of Scenario I and II continuously decreases, it also indicates that the landscape shape complexity and the degree of fragmentation decreases (Table 5.11). This finding is consistent with the previous work of Cao et al. (2017) who found that contagion value decreased from 1976 to 2015, which indicated that land use types became more disaggregated and the degree of land fragmentation increased in the past 40 years.

Table 5.11 Contagion value of landscape during 2006 to 2026 (Scenario I and II).

YEAR	Contagion (Percent)
2006	49.6605
2011	45.5948
2016	40.4483
2026 of Scenario I	37.4482
2026 of Scenario II	38.0964

(2) **Shannon's Diversity Index (SHDI).** Shannon's diversity index is used to measure the degree of diversity of the landscape. It is zero when there is only one patch in the landscape and increases with the number of patch types and as the

proportional distribution of patch types increases. During 2006 to 2016 Shannon's diversity index has been increased, and it indicates that landscape becomes more fragmentation among landscape types. Meanwhile Shannon's diversity index value in 2026 of Scenario I and II continuously increases and it also indicates that the landscape tends to more fragmentation (Table 5.12). Likewise, Wu, Jenerette, Buyantuyev and Redman (2010) who studies on quantifying spatiotemporal patterns of urbanization: the case of the two fastest growing metropolitan regions in the United States and they found that Shannon's diversity index increased with urbanization due largely to the increasing uneven areal distribution of land use types. That is as urbanization unfolded, the two metropolitan landscape become more fragmented and more evenly distributed among land use type.

Table 5.12 Shannon's diversity index value of landscape during 2006 to 2026 (Scenario I and II).

YEAR	Shannon's Diversity Index (Information)
2006	1.3518
2011	1.468
2016	1.6254
2026 of Scenario I	1.7315
2026 of Scenario II	1.7267

(3) Shannon's Evenness Index (SHEI). SHEI measures the other aspect of landscape composition-the distribution of area among patch types. There are numerous ways to quantify evenness and most diversity indices have a corresponding evenness index derived from them. SHEI approaches 0 from above, the landscape is

185

increasingly dominated by particular land cover/land use types, whereas as SHEI approaches 1 from below, the distribution of landscape types becomes increasingly more even. During 2006 to 2016, SHEI value has been continuously increased and it indicates more distribution of patch types. However, SHEI value in 2026 of Scenario I and II continuously decreases and it also indicates that more distribution of patch types in this scenario (Table 5.13). Likewise, Deng, Wang and Qi (2009) who studies on spatio-temporal dynamics and evolution of land use change and landscape pattern in response to rapid urbanization and they found that SHEI increased constantly indicating that the landscape composition became more even and land use type were more equally distributed. In contrast the subsequent slight decline in SHEI reflected the fact that the continual increased in urban land use curtailed the heterogeneity and made landscape uneven again.

Table 5.13 Shannon's evenness index value of landscape during 2006 to 2026 (Scenario I and II).

YEAR	Shannon's Evenness Index (Unitless)
2006	0.6501
2011	0.706
2016	0.7817
2026 of Scenario I	0.8327
2026 of Scenario II	0.8304

In summary, the simulated LULC change in Khon Kaen district has resulted in principal change of landscape pattern. The agriculture landscape has gradually converted into urban and built-up area landscape. It can be seen the percentage of landscape (Table 5.2) of paddy field and field crop decrease greatly from 56.62% and

21.11% in 2006 to 52.71% and 19.34% in 2011 and to 45.96% and 15.07% in 2016 and to 34.91% and 9.24% in 2026 of Scenario I and to 34.86% and 9.20% in 2026 of Scenario II. In contrast, the percentage of landscape of urban and built-up area increases sharply from 5.90% in 2006 to 8.85% in 2011, to 13.38% in 2016, to 22.13% in 2026 of Scenario I and to 22.81% in 2026 of Scenario II. During 2006 to 2026 (Scenario I and II), the Shannon's Diversity Index (Table 5.12) continuously increases, it indicates that the landscape composition becomes more even and LULC types are more equally distributed. This trend is confirmed by the increase of the Shannon's Evenness Index (Table 5.13).

5.2   Status and change of urban and built-up area

Under this section, status and change of urban and built–up area at class levels with various landscape metrics are quantified and described in details in term of influence of urban growth in the past, present and future (Scenario I and II).

(1) Class area (CA). During 2006 to 2016, class area of urban and built-up area landscape type has continuously increased. Meanwhile, class area of urban and built-up area landscape type in 2026 of both scenarios (I and II) tends to continuously increase (Table 5.14). This result implies that urban and built-up area landscape type in the future of both scenarios is more expansion. Under this study, the expansion of urban and built-up area under Scenario-II (Planning and policy) is higher than Scenario-I (Historical LULC development). Since urban and built-up area of Scenario II will be added up by housing under National Housing Authority's plan.

Table 5.14 Class area value of urban and built-up landscape during 2006 to 2026 (Scenario I and II).

YEAR	Class area (km^2)
2006	57.9425
2011	86.865
2016	131.3775
2026 of Scenario I	217.28
2026 of Scenario II	223.96

(2) Percent of landscape (PLAND). Similar to class area metric, during 2006 to 2016, percent of landscape of urban and built-up area landscape type has continuously increased. Meanwhile, percent of landscape of urban and built-up area landscape type in 2026 of both scenarios (I and II) tends to continuously increase (Table 5.15). This result implies that urban and built-up area landscape type in the future of both scenarios is more expansion. The phenomena is consistent with Linh et al. (2012) who found that when percent of urban land increased, expansion of urban area concentrated on existent urban. Under this study, the expansion of urban and built-up area under Scenario-II (Planning and policy) is higher than Scenario-I (Historical LULC development). Since urban and built-up area of Scenario II is added up under National Housing Authority's plan.

Table 5.15 Percent of landscape value of urban and built-up landscape during 2006 to 2026 (Scenario I and II).

YEAR	Percent of landscape (Percent)
2006	5.90
2011	8.85
2016	13.38
2026 of Scenario I	22.13
2026 of Scenario II	22.81

(3) Edge density (ED). Similar to class area metric, during 2006 to 2016, edge density of urban and built-up area landscape type has continuously increased. Meanwhile, edge density of urban and built-up area landscape type in 2026 of both scenarios (I and II) tends to continuously increase (Table 5.16). This result implies that urban and built–up area landscape type in the future of both scenarios is more expansion as mentioned earlier by Megahed et al. (2015) in the previous section. Under this study, the expansion of urban and built-up area under Scenario-II (Planning and policy) is higher than Scenario-I (Historical LULC development).

Table 5.16 Edge density value of urban and built-up landscape during 2006 to 2026 (Scenario I and II).

YEAR	Edge density (m/ha)
2006	12.85
2011	19.09
2016	28.11
2026 of Scenario I	36.85
2026 of Scenario II	35.36

(4) Total edge (TE). Similar to edge density metric, during 2006 to 2016, total edge of urban and built-up area landscape type has continuously increased. Meanwhile, total edge of urban and built-up area landscape type in 2026 of both scenarios (I and II) tends to continuously increase (Table 5.17). This result implies that urban and built–up area landscape type in the future of both scenarios is more expansion. However, absolute total edge of Scenario I (Historical LULC development) with value of 3,629,700 m is higher than absolute total edge of Scenario II (Planning and policy) with value of 3,472,100 m. This finding suggests that number of urban and built-up area landscape type (patch) with larger size under Scenario II is less than Scenario I, since the urban and built-up area under Scenario-I is expanded without specific policy and plan as Scenario II.

Table 5.17 Total edge value of urban and built-up landscape during 2006 to 2026 (Scenario I and II).

YEAR	Total edge (m)
2006	1,261,450
2011	1,874,300
2016	2,760,250
2026 of Scenario I	3,629,700
2026 of Scenario II	3,472,100

(5) Area-weighted fractal dimension (FRAC_AM). Similar to total edge metric, during 2006 to 2016, area-weighted fractal dimension of urban and built-up area landscape type has slightly increased. Meanwhile, area-weighted fractal dimension of urban and built-up area landscape type in 2026 of both scenarios (I and II) tends to abruptly increase (Table 5.18). This result implies that shape of urban and built–up area

landscape type in the future of both scenarios has highly convoluted in the future. Herein, area-weighted fractal dimension of Scenario I (Historical LULC development) with value of 1.2693 is higher than Scenario II (Planning and policy) with value of 1.2544. This finding suggests that urban and built-up area landscape of Scenario I is more modification than Scenario II, since the urban and built-up area under Scenario-II is modified with specific policy and plan.

Table 5.18 Area-weighted fractal dimension (FRAC_AM) value of urban and built-up landscape during 2006 to 2026 (Scenario I and II).

YEAR	Area-weighted fractal dimension (Unitless)
2006	1.214
2011	1.230
2016	1.233
2026 of Scenario I	1.269
2026 of Scenario II	1.254

(6) **Area-weighted mean shape index (SHAPE_AM).** Similar to total edge metric area-weighted fractal dimension, during 2006 to 2016 area-weighted mean shape index of urban and built-up area landscape type has continuously increased. In the meantime, area-weighted mean shape index of urban and built-up area landscape type in 2026 of both scenarios (I and II) tends to continuously increase (Table 5.19). This result implies that shape of urban and built-up area landscape type in the future of both scenarios is more complexity in irregularity in the spatial pattern in the future. Herein, area-weighted mean shape index of Scenario I (Historical LULC development) with value of 14.754 is higher than Scenario II (Planning and policy) with value of 11.2797. This finding suggests that shape of urban and built-up area landscape of Scenario I is

more complex than Scenario II, since the urban and built-up area under Scenario-II is modified with specific policy and plan.

Table 5.19 Area-weighted mean shape index (SHAPE_AM) value of urban and built-up landscape during 2006 to 2026 (Scenario I and II).

YEAR	Area-weighted mean shape index (Unitless)
2006	8.13
2011	10.13
2016	10.99
2026 of Scenario I	14.75
2026 of Scenario II	11.28

(7) Interspersion and juxtaposition index (IJI). During 2006 to 2016, interspersion and juxtaposition index of urban and built-up area landscape type has continuously increased. In the meantime, interspersion and juxtaposition index of urban and built-up area landscape type in 2026 of Scenarios I and II decreases (Table 5.20). This result implies that urban and built-up area landscape in 2026 is less uniform configuration than the previous periods. Herein, IJI of Scenario I (Historical LULC development) with value of 74.0625 is lower than Scenario II (Planning and policy) with value of 80.612. This finding suggests that extent of urban and built-up area landscape of Scenario II is more complex than Scenario I, since the urban and built-up area under Scenario II with specific policy and plan is well dispersed than Scenario I.

Table 5.20 Interspersion and juxtaposition index (IJI) value of urban and built-up landscape during 2006 to 2026 (Scenario I and II).

YEAR	Interspersion and juxtaposition index (Unitless)
2006	79.21
2011	80.58
2016	82.65
2026 of Scenario I	74.06
2026 of Scenario II	80.61

       (8) Landscape shape index (LSI). During 2006 to 2016, landscape shape index of urban and built-up area landscape type has continuously increased. In the meantime, landscape shape index of urban and built-up area landscape type in 2026 of Scenarios I increases when it compares with urban and built-up area landscape type in 2016. In contrary, landscape shape index of urban and built-up area landscape type in 2026 of Scenarios II decreases when it compares with urban and built-up area landscape type in 2016 (Table 5.21). This result implies that urban and built–up area landscape of Scenario II becomes more simplified irregular shape than Scenario I, since the urban and built-up area under Scenario II with specific policy and plan is well dispersed than Scenario I.

Table 5.21 Landscape shape index (LSI) value of urban and built-up landscape during 2006 to 2026 (Scenario I and II).

YEAR	Landscape shape index (unitless).
2006	41.37
2011	50.28
2016	60.24
2026 of Scenario I	61.52
2026 of Scenario II	58.17

(9) Number of patches (NP). During 2006 to 2016, number of patches of urban and built-up area landscape type has continuously increased. In the meantime, number of patches of urban and built-up area landscape type in 2026 of both scenarios (I and II) decreases when it compares with urban and built-up area landscape type in 2016 (Table 5.22). This result implies that urban and built–up area landscape of both scenarios becomes more aggregation than the previous period (2016). In addition, number of patches of Scenario II with value of 1,765 patches is less than Scenario I with value of 1,853 patches. This finding suggest that size of urban and built-up area of Scenario II is larger than Scenario I since the urban and built-up area under Scenario-II is allocated with specific policy and plan. In other word, it also indicates that numerous small urban patches are found more under Scenario I than Scenario II.

Table 5.22 Number of patches metrics value of urban and built-up landscape during 2006 to 2026 (Scenario I and II).

YEAR	Number of patches metrics (patches)
2006	1,252
2011	1,640
2016	1,914
2026 of Scenario I	1,853
2026 of Scenario II	1,762

(10) Patch density (PD). Similar to number of patches metrics (NP), during 2006 to 2016, patch density of urban and built-up area landscape type has continuously increased. In the meantime, patch density of urban and built-up area landscape type in 2026 of both scenarios (I and II) decreases when it compares with urban and built-up area landscape type in 2016 (Table 5.23). This result implies that urban and built–up

area landscape of both scenarios becomes more aggregation than the previous period (2016). In addition, patch density of Scenario II with value of 0.9719 is less than Scenario I with value of 1.0221. This finding suggests that size of urban and built-up area of Scenario II is larger than Scenario I since the urban and built-up area under Scenario-II is allocated with specific policy and plan.

Table 5.23 Patch density (PD) value of urban and built-up landscape during 2006 to 2026 (Scenario I and II).

YEAR	Patch density (Patch/100ha)
2006	1.27
2011	1.67
2016	1.95
2026 of Scenario I	1.89
2026 of Scenario II	1.79

5.3   Landscape metrics and urban growth pattern relationship

The percent of urban and built-up area in 2016 as dependent variable and relevant landscape metrics in 2016 as independent variables are displayed in Figures 5.11 and 5.18. Basic statistical data of dependent and independent variables is summarized in Table 5.24. The relationship between urban growth pattern in 2016 (PLAND) and selected landscape metrics is separately described in following sections.

195
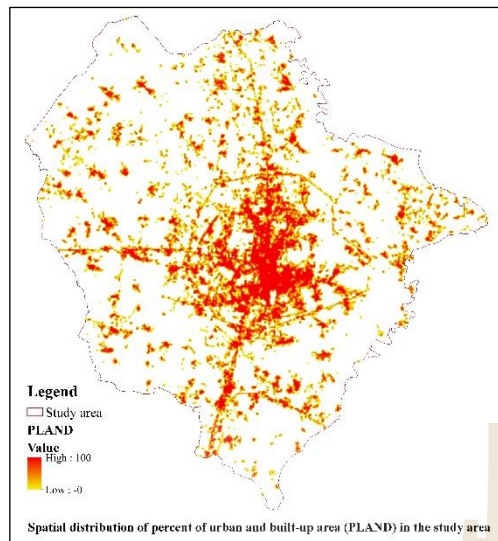
Figure 5.11 Spatial distribution of
percent of urban and built-up area
(PLAND) in the study area.
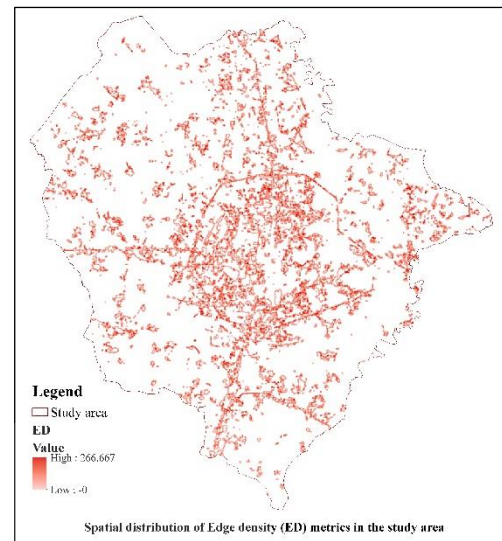
Figure 5.12 Spatial distribution of Edge
density (ED) metrics in the study area.
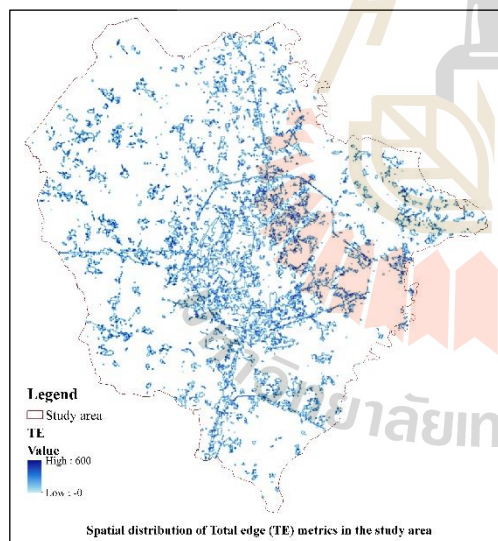
Figure 5.13 Spatial distribution of Total
edge (TE) metrics in the study area.
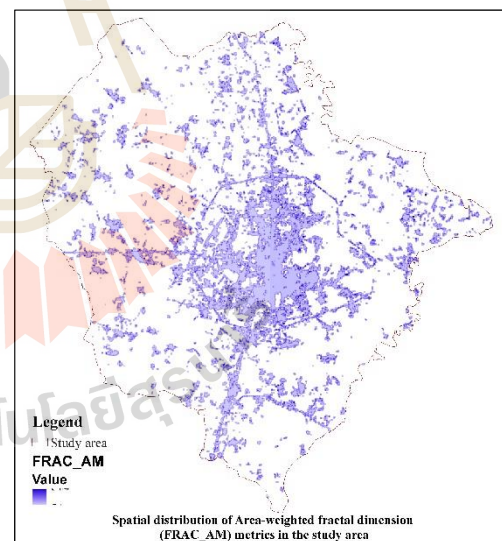
Figure 5.14 Spatial distribution of Area-
weighted fractal dimension (FRAC_AM)
metrics in the study area.
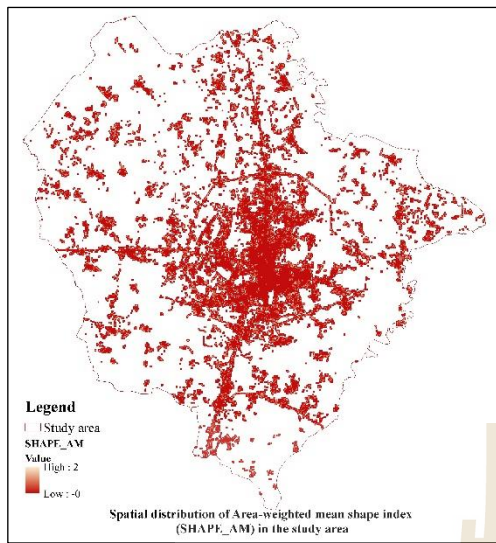
Figure 5.15 Spatial distribution of Area-weighted mean shape index (SHAPE_AM) in the study area.
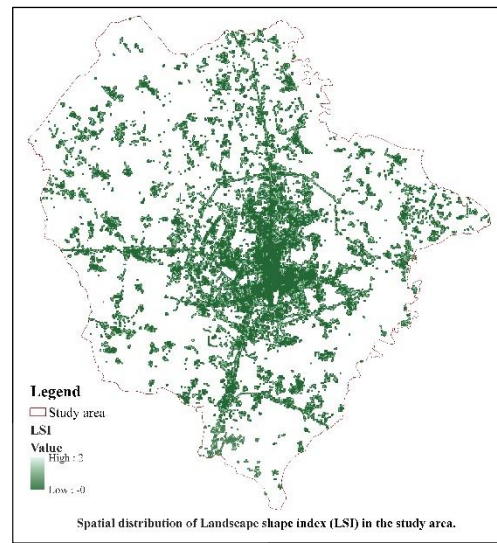
Figure 5.16 Spatial distribution of Landscape shape index (LSI) in the study area.
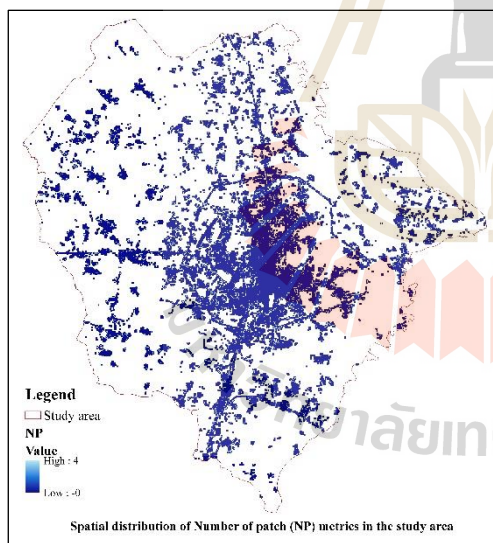
Figure 5.17 Spatial distribution of Number of patch (NP) metrics in the study area.
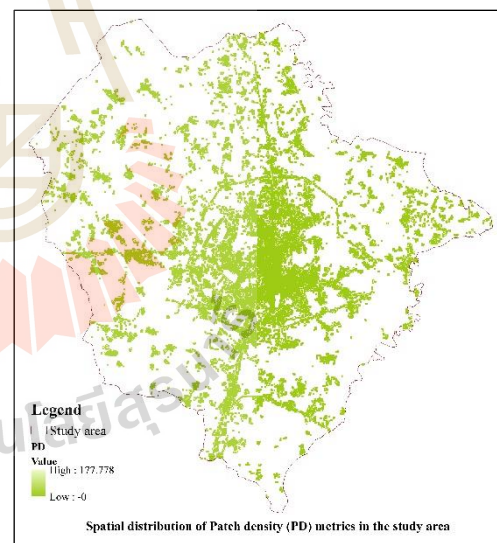
Figure 5.18 Spatial distribution of Patch density (PD) metrics in the study area.

Table 5.24 Basic statistical data of dependent and independent variables.

Landscape metric	Value		
Class level	**Min**	**Max**	**Mean**
Percent of urban and built-up area (PLAND)	11.111	100	13.368
Edge density (ED) metrics	0	266.667	18.724
Total edge (TE) metrics	0	600	22.836
Area-weighted fractal dimension (FRAC_AM) metrics	1	1.710	0.149
Weighted mean shape index (SHAPE_AM)	1	2	0.154
Landscape shape index (LSI)	1	2	0.158
Number of patch (NP) metrics	1	4	0.156
Patch density (PD) metrics	44.444	177.778	6.923

(1) Edge density (ED). The simple linear regression equation to quantify spatial pattern relationship between percent of urban and built-up area in 2016 (Y) and its edge density (X) is as follows:

$$Y = 4.443 + 0.353X \tag{5.1}$$

According to Eq. 5.1, it was found that edge density has positive correlation with percent of urban and built-up area. It shows that when edge density increases, percent of urban and built-up area increases. This finding is consistent with the definition of edge density (ED) as the total length of all edge segments per unit area for land cover class or landscape of consideration. (Buyantuyev et al., 2010).

In addition, result of bivariate correlation analysis with r value of 0.614 and r^2 value of 0.377 (Table 5.24) shows fair degree of relationship between edge density and urban growth pattern. Herewith, edge density can be applied to explain pattern of urban and built-up area in 2016 (urban growth) about 38%.

Table 5.25 Coefficient (r) and coefficient of determination (r^2) between Edge density (ED) and urban growth pattern (PLAND).

Urban growth pattern	Landscape metric	r	r^2	sig(2-tailed)
PLAND	ED	0.614	0.377	.000

**. Correlation is significant at the 0.01 level (2-tailed).

(2). Total edge (TE). The simple linear regression equation to quantify spatial pattern relationship between percent of urban and built-up area in 2016 (Y) and its total edge (X) is as follows:

$$Y = 0.443 + 0.157X \tag{5.2}$$

According to Eq. 5.2, it is found that total edge has positive correlation with percent of urban and built-up area. Similar to edge density, when total edge increases, percent of urban and built-up area increases. In other words, when total edge increases, urban and built-up area is expanded. The total edge is the absolute measure of the total length (perimeter) of the built-up areas of a particular patch in a landscape in meters (Aburas, As'shari, Abdullah and Ramli, 2016), large values of total edge indicates large, continuous urban patches.

In addition, result of bivariate correlation analysis with r value of 0.614 and r^2 value of 0.377 (Table 5.25) shows the moderate to good relationship between edge density and urban growth pattern. Herewith, total edge can be applied to explain pattern of urban and built-up area in 2016 (urban growth) about 38%.

Table 5.26 Coefficient (r) and coefficient of determination (r^2) between Total edge (TE) and urban growth pattern (PLAND).

Urban growth pattern	Landscape metric	r	r^2	sig(2-tailed)
PLAND	TE	0.614	0.377	.000

**. Correlation is significant at the 0.01 level (2-tailed).

(3). Area-weighted fractal dimension (FRAC_AM). The simple linear regression equation to quantify spatial pattern relationship between percent of urban and built-up area in 2016 (Y) and its area-weighted fractal dimension (X) is as follows:

$$Y = 0.230 + 56.350X \qquad (5.3)$$

According to Eq. 5.3, it is found that area-weighted fractal dimension has positive correlation with percent of urban and built-up area. This implies that when area-weighted fractal dimension increases, percent of urban and built-up area increases. In other words, when area-weighted fractal dimension increases, urban and built-up area is more complexity in irregularity in the spatial pattern. Subasinghe et al. (2016) stated that the size and shape of the patches of built-up lands have also become larger and more complex, as indicated by the increase in the values of area-weighted fractal dimension.

In addition, result of bivariate correlation analysis with r value of 0.843 and r^2 value of 0.711 (Table 5.26). The result shows the good to strong relationship between area-weighted fractal dimension and urban growth pattern. Herewith, area-weighted fractal dimension can be applied to explain pattern of urban and built-up area in 2016 (urban growth) about 71%.

Table 5.27 Coefficient (r) and coefficient of determination (r^2) between Area-weighted fractal dimension (FRAC_AM) and urban growth pattern (PLAND).

Urban growth pattern	Landscape metric	r	r^2	sig(2-tailed)
PLAND	FRAC_AM	0.843	0.711	.000

**. Correlation is significant at the 0.01 level (2-tailed).

(4) Area-weighted mean shape index (SHAPE_AM). The simple linear regression equation to quantify spatial pattern relationship between percent of urban and built-up area in 2016 (Y) and its area-weighted mean shape index (X) is as follows:

$$Y = 0.356 + 41.794X \tag{5.4}$$

According to Eq. 5.4, it is found that area-weighted mean shape index has positive correlation with percent of urban and built-up area. This implies that when area-weighted mean shape index increases, percent of urban and built-up area increases. In other words, when area-weighted mean shape index increases, shape of urban and built-up area is more complexity in irregularity in the spatial pattern. Su, Xiao, Jiang and Zhang (2012) stated that patch shapes tends to be more regular and less complicated, evidenced by the decline in area-weighted mean shape index values.

In addition, result of bivariate correlation analysis with r value of 0.831 and r^2 value of 0.690 (Table 5.27). The result shows the good to strong relationship between area-weighted mean shape index and urban growth pattern. Herewith, area-weighted mean shape index can be applied to explain pattern of urban and built-up area in 2016 (urban growth) about 69%.

Table 5.28 Coefficient (r) and coefficient of determination (r^2) between Area-weighted mean shape index (SHAPE_AM) and urban growth pattern (PLAND).

Urban growth pattern	Landscape metric	r	r^2	sig(2-tailed)
PLAND	SHAPE_AM	0.831	0.690	.000

**. Correlation is significant at the 0.01 level (2-tailed).

(5) Landscape shape index (LSI). The simple linear regression equation to quantify spatial pattern relationship between percent of urban and built-up area in 2016 (Y) and its landscape shape index (X) is as follows:

$$Y = 0.530 + 39.594X \tag{5.5}$$

According to Eq. 5.5, it is found that landscape shape index has positive correlation with percent of urban and built-up area. This implies that when landscape shape index increases, percent of urban and built-up area increases. In other words, when landscape shape index increases, shape of urban and built-up area is more expansion. Wan (2015) stated that landscape shape index value increases, it suggested that scattered urban areas are merged into larger area, decreasing the fragmentation of urban areas.

In addition, result of bivariate correlation analysis with r value of 0.821 and r^2 value of 0.674 (Table 5.28). The result shows the good to strong relationship between landscape shape index and urban growth pattern. Herewith, landscape shape index can be applied to explain pattern of urban and built-up area in 2016 (urban growth) about 67%.

Table 5.29 Coefficient (r) and coefficient of determination (r^2) between Landscape shape index (LSI) and urban growth pattern (PLAND).

Urban growth pattern	Landscape matric	r	r^2	sig(2-tailed)
PLAND	LSI	0.821	0.674	0.000

**. Correlation is significant at the 0.01 level (2-tailed).

(6) Number of patches (NP). The simple linear regression equation to quantify spatial pattern relationship between percent of urban and built-up area in 2016 (Y) and its number of patches (X) is as follows:

$$Y = 1.434 + 37.956X \tag{5.6}$$

According to Eq. 5.6 m it is found that number of patches has positive correlation with percent of urban and built-up area. This implies that when number of patches increases, percent of urban and built-up area increases. In other words, when number of patches increases, urban and built-up area is more fragmentation. Wan (2015) stated that number of patch reflects landscape fragmentation, number of patch ranks highest indicating patches are small, highly heterogeneous, scattered and highly fragmentation.

In addition, result of bivariate correlation analysis with r value of 0.783 and r^2 value of 0.613 (Table 5.29). The result shows the good to strong relationship between number of patches and urban growth pattern. Herewith, number of patches can be applied to explain pattern of urban and built-up area in 2016 (urban growth) about 61%.

Table 5.30 Coefficient (r) and coefficient of determination (r^2) between Number of patch (NP) and urban growth pattern (PLAND).

Urban growth pattern	Landscape matric	r	r^2	sig(2-tailed)
PLAND	NP	0.783	0.613	0.000

**. Correlation is significant at the 0.01 level (2-tailed).

(7) Patch density (PD). The simple linear regression equation to quantify spatial pattern relationship between percent of urban and built-up area in 2016 (Y) and its patch density (X) is as follows:

$$Y = 1.434 + 0.854X \tag{5.7}$$

According to Eq. 5.7, it is found that patch density has positive correlation with percent of urban and built-up area. This implies that when patch density increases, the percent of urban and built-up area increases. In other words, when patch density increases, urban and built-up area is more fragmentation. Change in fragmentation metrics (PD) also implies a decrease in spatial heterogeneity due to the increasing dominance of the built-up land (Kong, Yin, Nakagoshi and James, 2012).

In addition, result of bivariate correlation analysis with r value of 0.783 and r^2 value of 0.613 (Table 5.30). The result shows the good to strong relationship between number of patches and urban growth pattern. Herewith, patch density can be applied to explain pattern of urban and built-up area in 2016 (urban growth) about 61%.

Table 5.31 Coefficient (r) and coefficient of determination (r^2) between Patch density (PD) and urban growth pattern (PLAND).

Urban growth pattern	Landscape matric	r	r^2	sig(2-tailed)
PLAND	PD	0.783	0.613	0.000

**. Correlation is significant at the 0.01 level (2-tailed).

In summary, by comparison the derived correlation coefficient (r) and coefficient of determination (r^2) from simple linear regression analysis between landscape metrics and urban growth pattern (PLAND in 2016), it can be here concluded that area-weighted mean fractal dimension (FRAC_AM) metrics is the optimum landscape metrics to characterize urban growth pattern (pattern of urban and built-up area) in the current study (Table 5.31). Since the area-weighted mean fractal dimension metrics can provide the highest correlation coefficient (r) and coefficient of determination (r^2). These imply that pattern of urban and built-up area (PLAND) is strongly positive correlation with the area-weighted mean fractal dimension (FRAC_AM) with r value of 0.842 whereas the proportion of the total variation in the value of urban and built-up area pattern (PLAND) can be explained by a linear relationship with the value of the area-weighted mean fractal dimension pattern (FRAC_AM) about 71%.

Table 5.32 Ranking of correlation coefficient (r) and coefficient of determination (r^2) from simple linear regression analysis.

No.	Landscape metrics	r	r^2	Meaning of relationship	Rank
1	Edge density	0.614	0.377	Moderate to good	6
2	Total edge	0.614	0.377	Moderate to Good	6
3	Area-weighted fractal dimension	0.843	0.711	Strong	1
4	Area-weighted mean shape index	0.831	0.690	Strong	2
5	Landscape shape index	0.821	0.674	Strong	3
6	Number of patches	0.783	0.613	good to strong	4
7	Patch density	0.783	0.613	good to strong	4
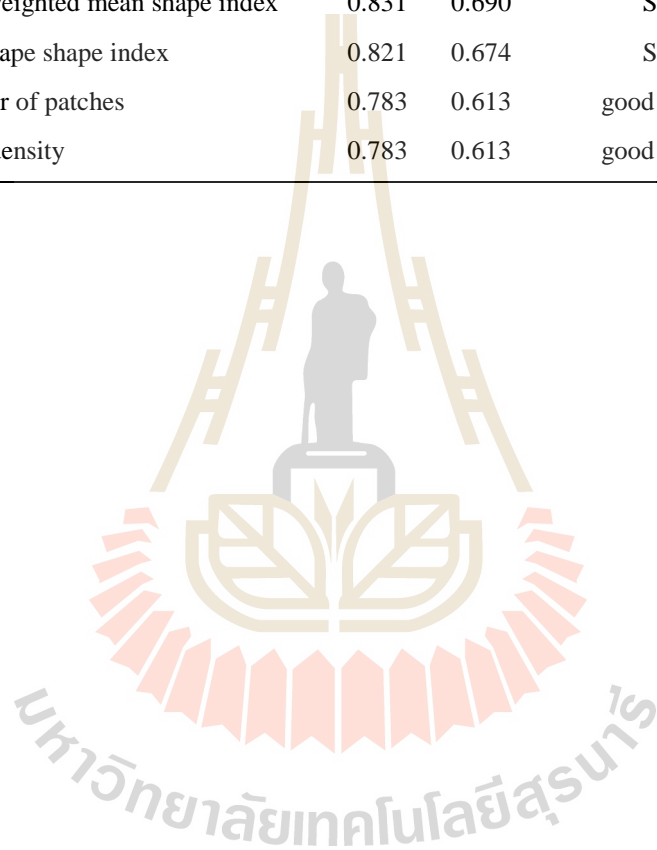
CHAPTER VI

URBAN GROWTH IMPACT ON ECOSYSTEM SERVICE

FUNCTION VALUE

This chapter presents results of the second objective focusing on impact of urban growth on ecosystem service value. Herein, the dynamic LULC data during 2006 and 2026 (Scenario I and II) which represent urban growth in each period were applied to quantify ecosystem service value of ecosystem service function based on simple benefit transfer method of Costanza (1997). The major results include (1) valuation of ecosystem services function, (2) change of ecosystem service function values and (3) degree of ecosystem service function values change in the future are reported and discussed under this chapter.

6.1   Valuation of ecosystem service function

The derived LULC data in 2006, 2011, 2016 and predictive LULC in 2026 of two scenarios were here used as input data to valuate ecosystem service function and its change during 2006 and 2026 (two scenarios) based on coefficients of ecosystem service values for LULC categories (Table 3.5) using Eq. 3.1. The status of ecosystem service values in each period is separately described according to ecosystem service functions of ecosystem service categories (regulating, supporting, provision, cultural services) in the following sections.

6.1.1   Ecosystem service function values in 2006

Result of ecosystem service function values (ESFV) in 2006 based on coefficients of ecosystem service values of each LULC category is presented in Table 6.1. As results, it revealed that paddy field can provide the highest ESFV under gas regulation, soil formation, biodiversity protection, and food production service functions with values of 4.15, 12.13, 5.90 and 8.31 million USD in 2006. Meanwhile, water body provides the highest ESFV under waste treatment, water supply, and recreation and culture service functions with value of 14.36, 16.09 and 3.42 million USD. Likewise, marsh and swamp in 2006 provides the highest ESFV under climate regulation service function with value of 8.59 million USD. Meanwhile paddy field and forest land can serve raw material service function at the highest ESFV of 0.83 million USD.

In addition, according to LULC type it was found that top three dominant LULC types that provide the highest total ESFV in 2006 are paddy field, water body, and marsh and swamp with value of 57.40, 36.30 and 31.52 million USD, respectively. Moreover, it can be observed that LULC in 2006 can contribute three dominant ecosystem functions: waste treatment, water supply, and climate regulation with ESFV of 42.96, 32.18 and 20.57 million USD or 27.39%, 20.50% and 13.10% of total ESFV, respectively (Figure 6.1).

Table 6.1 Ecosystem services values of ecosystem service functions in 2006 (unit: million USD).

Ecosystem services category	Ecosystem services function	ESFV of LULC type in million USD/ha/year								Total	Percent
		Ur	Pd	Fc	Fo	Wa	Ms	Ra	Ul		
	1.1 Gas regulation	0.00	4.15	1.55	1.21	0.00	0.90	0.30	0.00	8.12	5.17
1.Regulating services	1.2 Climate regulation	0.00	7.40	2.76	1.14	0.36	8.59	0.31	0.00	20.57	13.10
	1.3 Waste treatment	0.00	13.63	5.08	0.48	14.36	9.14	0.26	0.01	42.96	27.37
	2.1 Soil formation	0.00	12.13	4.52	1.13	0.01	0.86	0.45	0.01	19.10	12.17
2.Supporting services	2.2 Biodiversity protection	0.00	5.90	2.20	1.26	1.96	1.26	0.37	0.01	12.97	8.27
	3.1 Water supply	0.00	4.98	1.86	1.15	16.09	7.79	0.30	0.00	32.18	20.50
3.Provision services	3.2 Food production	0.00	8.31	3.10	0.09	0.08	0.15	0.09	0.00	11.82	7.53
	3.3 Raw materials	0.00	0.83	0.31	0.83	0.01	0.04	0.07	0.00	2.09	1.33
4.Cultural services	4.1 Recreation and culture	0.07	0.08	0.03	0.58	3.42	2.79	0.17	0.01	7.17	4.57
Total		0.07	57.42	21.41	7.88	36.30	31.52	2.33	0.05	156.97	100.00

Figure 6.1 Contribution of ecosystem services function value in 2006.

6.1.2 Ecosystem service function values in 2011

Result of ecosystem service function values in 2011 based on coefficients of ecosystem service values of each LULC category is presented in Table 6.2. As results, it revealed that paddy field can provide the highest ESFV under gas regulation, waste treatment, soil formation, biodiversity protection, and food production service functions with values of 3.87, 12.69, 11.29, 5.49 and 7.74 million USD in 2011. Meanwhile, water body provides the highest ESFV under water supply and recreation and culture service functions with value of 16.01 and 3.41 million USD, respectively. Likewise, only forest land in 2011 provides the highest ESFV under raw materials service function with value of 0.83 million USD. Meanwhile marsh and swamp can supply climate regulation service function at the highest ESFV of 8.38 million USD.

In addition, according to LULC type it was found that top three dominant LULC types that provide the highest total ESFV in 2011 are paddy field, water body, and marsh and swamp with value of 53.46, 36.10 and 30.74 million USD,

210

respectively. Moreover, it can be observed that LULC in 2011 can contribute three dominant ecosystem functions: waste treatment, water supply and climate regulation with ESFV of 41.52, 31.67 and 19.89 million USD or 27.25%, 20.78% and 13.05% of total ESFV, respectively (Figure 6.2).

Table 6.2 Ecosystem services values of ecosystem services functions in 2011 (unit: million USD).

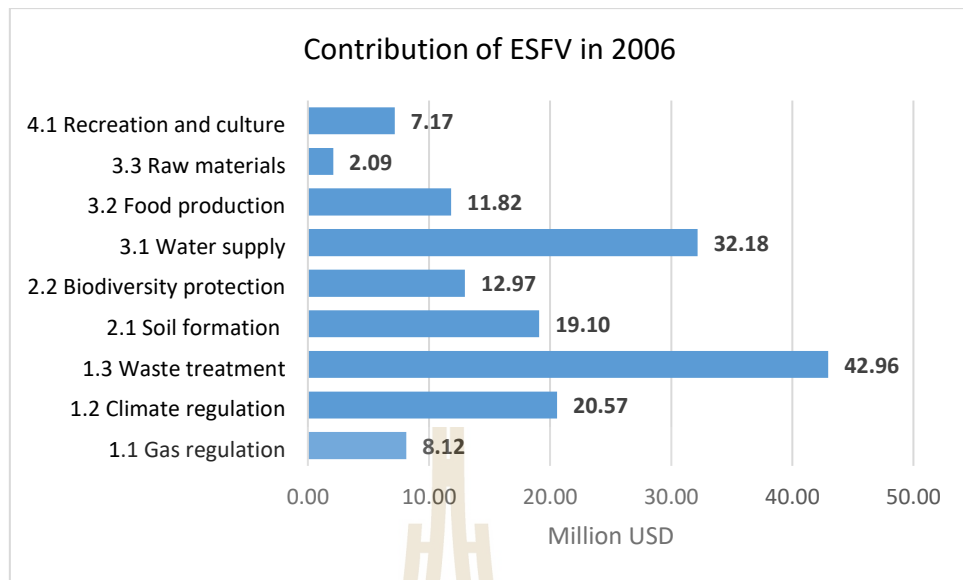| Ecosystem services category	Ecosystem services function	ESFV of LULC type in million USD/ha/year								Total	Percent
		Ur	Pd	Fc	Fo	Wa	Ms	Ra	Ul		
	1.1 Gas regulation	0.00	3.87	1.42	1.21	0.00	0.88	0.57	0.00	7.95	5.22
1.Regulating services	1.2 Climate regulation	0.00	6.89	2.52	1.14	0.36	8.38	0.59	0.01	19.89	13.05
	1.3 Waste treatment	0.00	12.69	4.65	0.48	14.28	8.91	0.50	0.01	41.52	27.25
	2.1 Soil formation	0.00	11.29	4.14	1.13	0.01	0.84	0.84	0.01	18.26	11.98
2.Supporting services	2.2 Biodiversity protection	0.00	5.49	2.01	1.26	1.95	1.23	0.71	0.02	12.68	8.32
	3.1 Water supply	0.00	4.64	1.70	1.15	16.01	7.60	0.57	0.00	31.67	20.78
3.Provision services	3.2 Food production	0.00	7.74	2.84	0.09	0.08	0.15	0.16	0.00	11.05	7.26
	3.3 Raw materials	0.00	0.77	0.28	0.83	0.01	0.03	0.14	0.00	2.07	1.36
4.Cultural services	4.1 Recreation and culture	0.11	0.08	0.03	0.58	3.41	2.72	0.33	0.01	7.27	4.77
Total		**0.11**	**53.46**	**19.59**	**7.88**	**36.10**	**30.74**	**4.40**	**0.07**	**152.35**	**100.00**

Figure 6.2 Contribution of ecosystem services function value in 2011.

6.1.3 Ecosystem service function values in 2016

Result of ecosystem service value in 2016 based on coefficients of ecosystem service values of each LULC type is presented in Table 6.3. As results, it revealed that paddy field can provide the highest ESFV under gas regulation, waste treatment, soil formation, biodiversity protection, and food production service functions with values of 3.37, 11.06, 9.84, 4.79 and 6.74 million USD in 2016. Meanwhile, water body provides the highest ESFV under water supply and recreation and culture service functions with value of 15.99 and 3.40 million USD, respectively. Likewise, forest land in 2016 only provides the highest ESFV under raw materials service function with value of 0.83 million USD. Meanwhile marsh and swamp can provide climate regulation service function at the highest ESFV of 8.26 million USD.

In addition, according to LULC type it was found that top three dominant LULC types that provide the highest total ESFV in 2016 are paddy field, water body and marsh and swamp with value of 46.60, 36.05 and 30.28 million USD,

respectively. Moreover, it can be observed that LULC in 2016 can contribute three dominant ecosystem functions: waste treatment, water supply and climate regulation with ESFV of 39.32, 31.14 and 18.92 million USD or 27.02%, 21.44% and 13.03% of total ESFV, respectively (Figure 6.3).

Table 6.3 Ecosystem services values of ecosystem services functions in 2016 (unit: million USD).

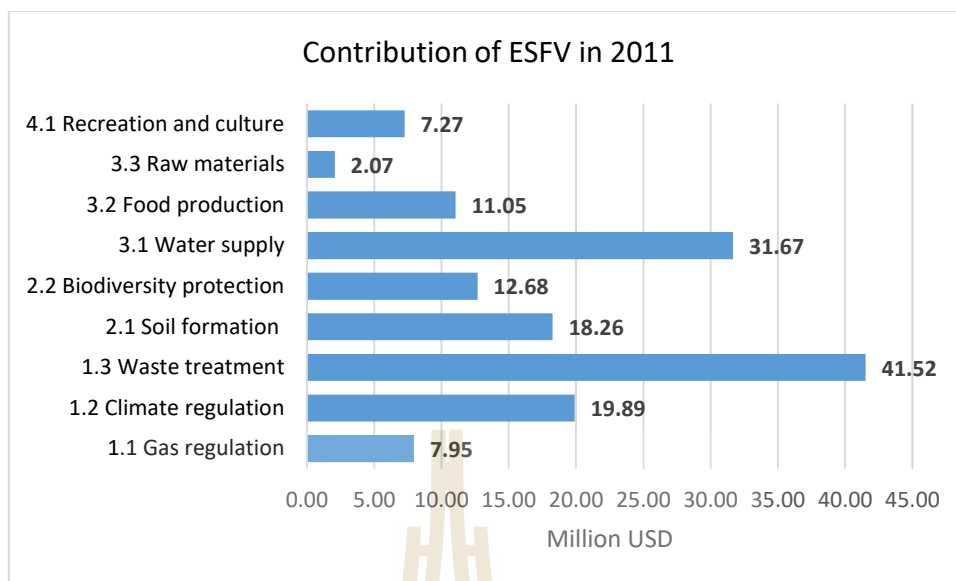| Ecosystem services category	Ecosystem services function	ESFV of LULC type in million USD/ha/year								Total	Percent
		Ur	Pd	Fc	Fo	Wa	Ms	Ra	Ul		
	1.1 Gas regulation	0.00	3.37	1.11	1.20	0.00	0.87	1.14	0.01	7.69	5.30
1.Regulating services	1.2 Climate regulation	0.00	6.00	1.97	1.13	0.36	8.26	1.18	0.02	18.92	13.03
	1.3 Waste treatment	0.00	11.06	3.63	0.48	14.26	8.78	1.00	0.03	39.23	27.02
	2.1 Soil formation	0.00	9.84	3.23	1.12	0.01	0.83	1.69	0.02	16.74	11.53
2.Supporting services	2.2 Biodiversity protection	0.00	4.79	1.57	1.26	1.95	1.21	1.42	0.05	12.24	8.43
	3.1 Water supply	0.00	4.04	1.33	1.14	15.99	7.48	1.15	0.01	31.14	21.44
3.Provision services	3.2 Food production	0.00	6.74	2.21	0.09	0.08	0.14	0.33	0.00	9.60	6.61
	3.3 Raw materials	0.00	0.67	0.22	0.83	0.01	0.03	0.27	0.00	2.04	1.41
4.Cultural services	4.1 Recreation and culture	0.17	0.07	0.02	0.58	3.40	2.68	0.66	0.03	7.60	5.24
Total		0.17	46.60	15.28	7.84	36.05	30.28	8.83	0.16	145.21	100.00

Figure 6.3 Contribution of ecosystem services function value in 2016.

6.1.4 Ecosystem service function values in 2026 of Scenario I

Result of ecosystem service value in 2026 of Scenario I (Historical land development) based on coefficients of ecosystem service values of each LULC category is presented in Table 6.4 As results, it revealed that paddy field can provide the highest ESFV under gas regulation, soil formation, biodiversity protection, and food production service functions with values of 2.56, 7.48, 3.64 and 5.12 million USD in 2026 of Scenario I, respectively. Meanwhile, water body provides the highest ESFV under water supply and recreation and culture service functions with value of 15.87 and 3.38 million USD. Likewise, marsh and swamp in 2026 of Scenario I provides the highest ESFV under climate regulation and waste treatment service functions with value of 8.01 and 8.51 million USD, respectively. Meanwhile forest land can provide raw materials service function at the highest ESFV of 0.83 million USD.

In addition, according LULC type it was found that top three dominant LULC types that provide the highest total ESFV in 2026 of Scenario I are water body,

paddy field and marsh and swamp with value of 35.78, 35.39 and 29.36 million USD, respectively. Moreover, it can be observed that LULC in 2026 of Scenario I can contribute three dominant ecosystem functions: waste treatment, water supply, and climate regulation with ESFV of 35.45, 30.03 and 17.22 million USD or 26.72%, 22.63% and 12.97% of total ESFV, respectively (Figure 6.4).

Table 6.4 Ecosystem services values of ecosystem services functions in 2026 of Scenario I (unit: million USD).

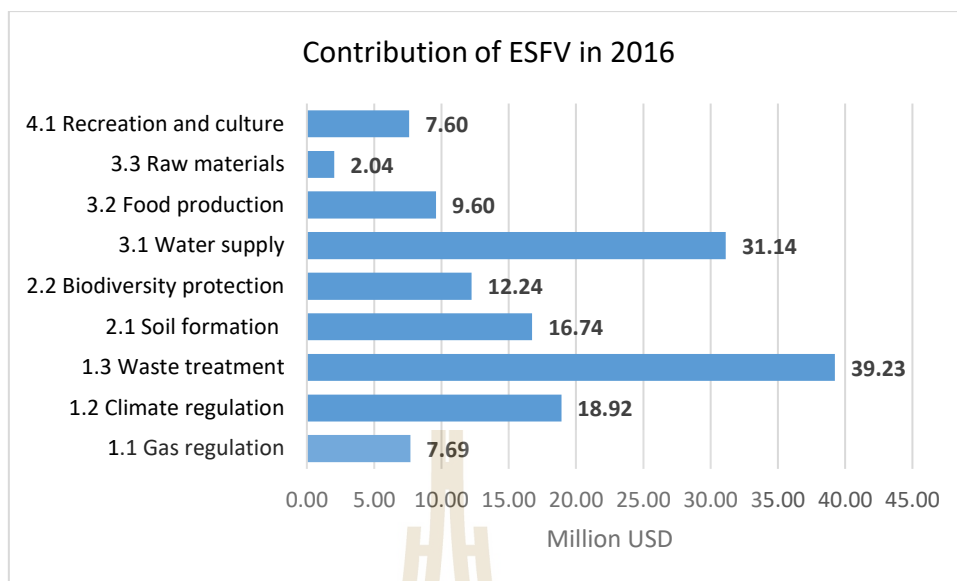| Ecosystem services category	Ecosystem services function	ESFV of LULC type in million USD/ha/year								Total	Percent
		Ur	Pd	Fc	Fo	Wa	Ms	Ra	Ul		
1.Regulating services	1.1 Gas regulation	0.00	2.56	0.68	1.20	0.00	0.84	1.86	0.01	7.15	5.39
	1.2 Climate regulation	0.00	4.56	1.21	1.13	0.36	8.01	1.93	0.03	17.22	12.97
	1.3 Waste treatment	0.00	8.40	2.22	0.48	14.16	8.51	1.64	0.05	35.45	26.72
2.Supporting services	2.1 Soil formation	0.00	7.48	1.98	1.11	0.01	0.80	2.77	0.03	14.18	10.69
	2.2 Biodiversity protection	0.00	3.64	0.96	1.25	1.94	1.17	2.32	0.08	11.36	8.56
3.Provision services	3.1 Water supply	0.00	3.07	0.81	1.13	15.87	7.26	1.88	0.01	30.03	22.63
	3.2 Food production	0.00	5.12	1.36	0.09	0.08	0.14	0.53	0.00	7.32	5.52
	3.3 Raw materials	0.00	0.51	0.14	0.83	0.01	0.03	0.45	0.01	1.97	1.48
4.Cultural services	4.1 Recreation and culture	0.28	0.05	0.01	0.58	3.38	2.60	1.08	0.05	8.02	6.04
Total		**0.28**	**35.39**	**9.37**	**7.80**	**35.78**	**29.36**	**14.45**	**0.28**	**132.71**	**100.00**
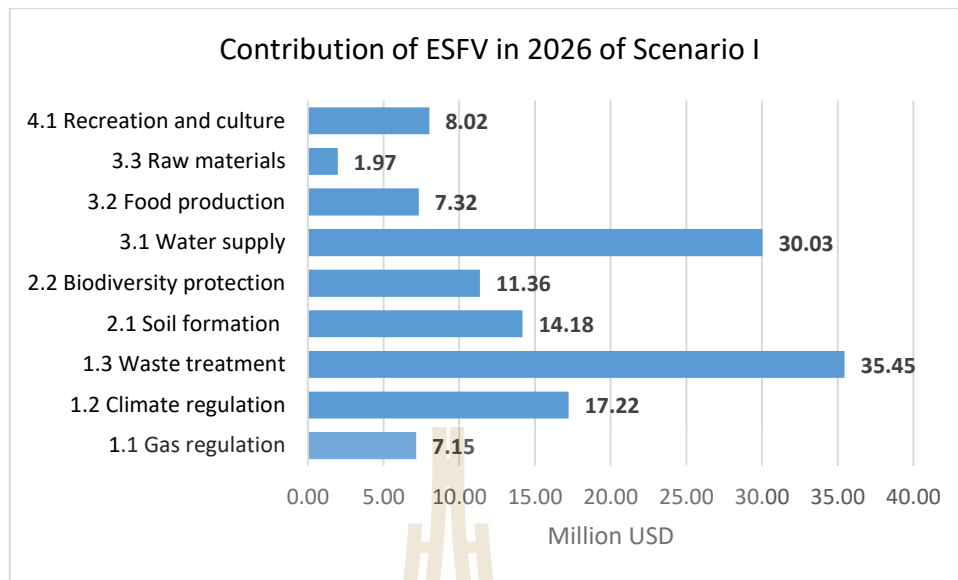
Figure 6.4 Contribution of ecosystem services function value in 2026 scenario I.

6.1.5 Ecosystem service function values in 2026 of Scenario II

Result of ecosystem service value in 2026 of Scenario II based on coefficients of ecosystem service values of each LULC category is presented in Table 6.5 As results, it revealed that paddy field can provide the highest ESFV under gas regulation, soil formation, biodiversity protection, and food production service functions with values of 2.56, 7.47, 3.63 and 5.11 million USD in 2026 of Scenario II. Meanwhile, water body provides the highest ESFV under water supply and recreation and culture service functions with value of 15.88 and 3.38 million USD. Likewise, marsh and swamp in 2026 of Scenario II provides the highest ESFV under climate regulation and waste treatment service functions with value of 8.04 and 8.55 million USD, respectively. Meanwhile forest land can provide raw materials service function at the highest ESFV of 0.78 million USD.

In addition, according to LULC type it was found that top three dominant LULC types that provide the highest total ESFV in 2026 of Scenario II are

water body, paddy field and marsh and swamp with value of 35.82, 35.34 and 29.49

million USD, respectively. Moreover, it can be observed that LULC in 2026 of Scenario

II can contribute three dominant ecosystem functions: waste treatment, water supply,

and climate regulation with ESFV of 35.42, 29.98 and 17.14 million USD or 26.82%,

22.69% and 12.98% of total ESFV, respectively (Figure 6.5).
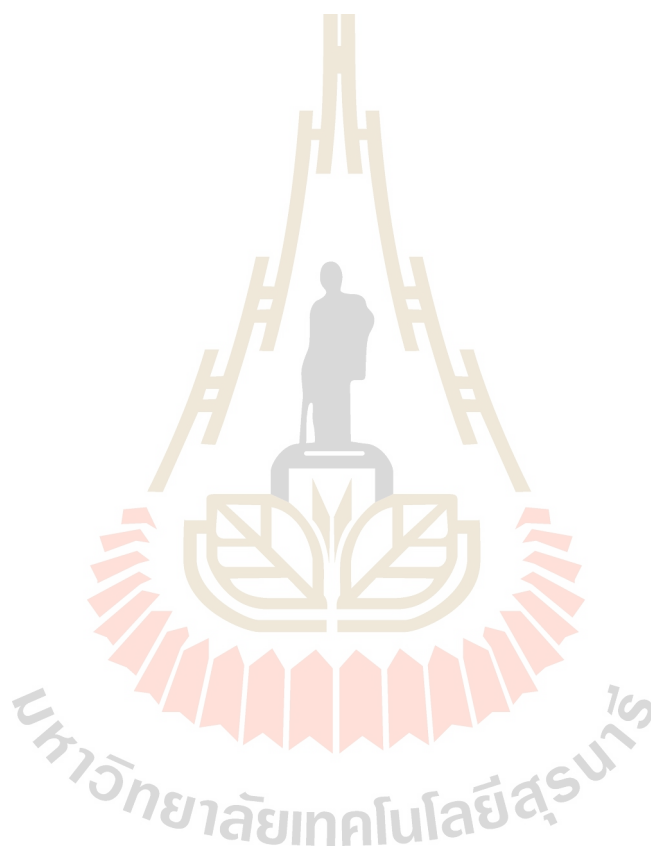
Table 6.5 Ecosystem services values of ecosystem services functions in 2026 of Scenario II (unit: million USD).

Ecosystem services category	Ecosystem services function	ESFV of LULC type in million USD/ha/year								Total	Percent
		Ur	Pd	Fc	Fo	Wa	Ms	Ra	Ul		
	1.1 Gas regulation	0.00	2.56	0.67	1.14	0.00	0.85	1.82	0.01	7.05	5.34
1.Regulating services	2 Climate regulation	0.00	4.55	1.20	1.07	0.36	8.04	1.89	0.03	17.14	12.98
	1.3 Waste treatment	0.00	8.39	2.21	0.45	14.17	8.55	1.60	0.05	35.42	26.82
	2.1 Soil formation	0.00	7.47	1.97	1.06	0.01	0.80	2.71	0.03	14.05	10.64
2.Supporting services	2 Biodiversity protection	0.00	3.63	0.96	1.19	1.94	1.18	2.28	0.08	11.25	8.51
	3.1 Water supply	0.00	3.07	0.81	1.08	15.88	7.29	1.84	0.01	29.98	22.69
3.Provision services	3.2 Food production	0.00	5.11	1.35	0.09	0.08	0.14	0.52	0.00	7.30	5.52
	3.3 Raw materials	0.00	0.51	0.13	0.78	0.01	0.03	0.44	0.01	1.91	1.45
4.Cultural services	1 Recreation and culture	0.28	0.05	0.01	0.55	3.38	2.61	1.06	0.05	7.99	6.05
Total		**0.28**	**35.34**	**9.32**	**7.39**	**35.82**	**29.49**	**14.16**	**0.28**	**132.09**	**100.00**
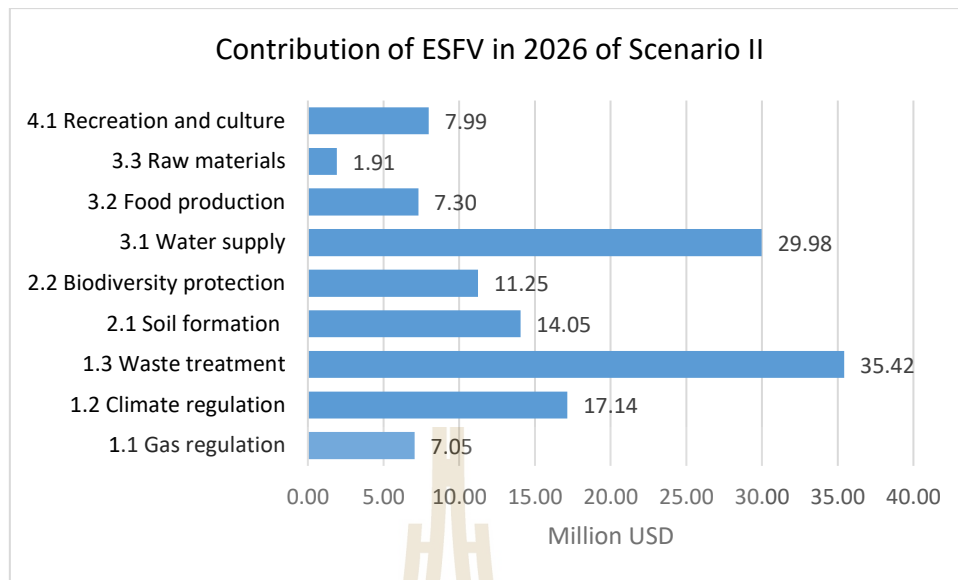
Figure 6.5 Contribution of ecosystem services function value in 2026 scenario II.

In summary, during 2006 to 2026 (scenario I and II) it was found that top three dominant LULC types that provide the highest total ESFV are paddy field, water body and marsh and swamp. In the meantime, top three dominant ecosystem functions in the same period are waste treatment, water supply, and climate regulation. However, ESFV of three dominant services had continuously decreased since areas of paddy field, water body and marsh and swamp that plays important role on these services have continuously decreased. The high rate of decline of these LULC types would have considerably negative ecological consequences.

In addition, according ecosystem service category (regulating, supporting, provision and cultural services), the total regulating ecosystem service value in 2006, 2011, 2016, 2026 of scenario I and 2026 of scenario II are 71.65, 69.36, 65.84, 59.82 and 59.61 million USD, respectively. Meanwhile, the total supporting ecosystem service value in these periods are 32.07, 30.94, 28.98, 25.54 and 25.3 million USD, and the total provision ecosystem service value in the same periods are 46.09, 44.79, 42.78, 39.32

and 39.19 million USD. These three ecosystem service categories show trend of decreasing. On contrary, the total cultural ecosystem service value in the same periods show trend of increasing. Its value is 7.27, 7.6, 8.02 and 7.99 million USD in 2011, 2016, 2026 of scenario I and 2026 of scenario II, respectively. (Table 6.6 and Figure 6.6).

Table 6.6 Total ecosystem services values between 2006 and 2026 Scenario I and II (unit: million USD).

Ecosystem services category	Ecosystem services values million USD				
	2006	2011	2016	2026 of scenario I	2026 of scenario II
1. Regulating services	71.65	69.36	65.84	59.82	59.61
2. Supporting services	32.07	30.94	28.98	25.54	25.3
3. Provision services	46.09	44.79	42.78	39.32	39.19
4. Cultural services	7.17	7.27	7.6	8.02	7.99
Total	**156.97**	**152.35**	**145.21**	**132.71**	**132.09**
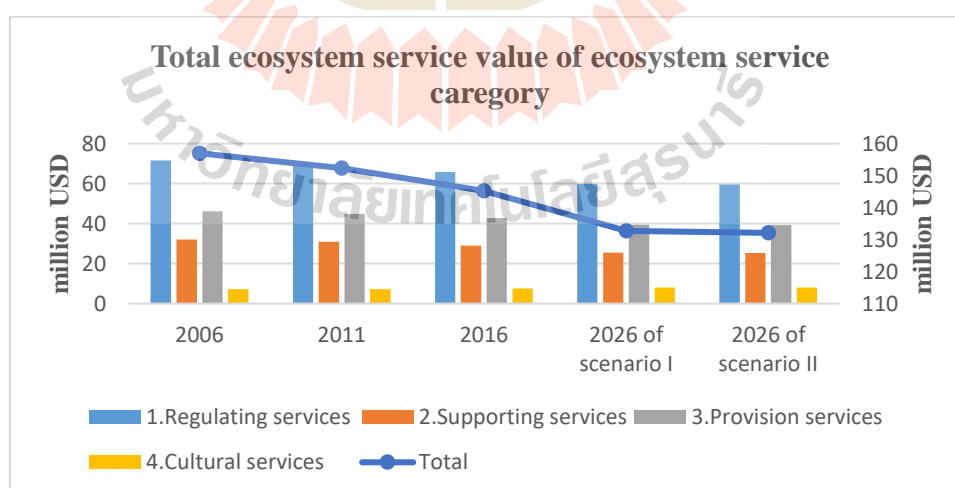
Figure 6.6 Total ecosystem services values between 2006 and 2026 Scenario I and II (unit: million USD).

6.2   Change of ecosystem service function values

Change of ecosystem services values in different periods (2006 – 2011, 2011 – 2016, 2016 – 2026 of Scenario I and 2016 – 2026 of Scenario II) was here described and discussed in this section.

6.2.1   Ecosystem service function values change between 2006 and 2011

During 2006 to 2011, the total ecosystem service function values in 2011 decreases from in 2006 with value of 4.62 million USD or 2.94%. Herein, waste treatment service function is the most decreased ecosystem service function with value of 1.44 million USD or 3.34%. At the same time, soil formation, food production, climate regulation, water supply, biodiversity protection, gas regulation, and raw materials service functions have also deceased with value of 0.84, 0.76, 0.68, 0.51, 0.30, 0.17, and 0.02 million USD, respectively. The major cause of declining of ecosystem service function value is LULC change that is associate with the coefficient of ecosystem service value for each LULC type (See Table 3.5).

On contrary, recreation and culture service function has increased during 2006 to 2011 with value of 0.10 million USD or 1.39%. Because urban and built-up area in 2011 that plays an important role on recreation and culture service function increases 1.89 km^2 from 2006. Detail of ecosystem services function values change between 2006 and 2011 is presented in Table 6.7 and Figure 6.7.

Table 6.7 Ecosystem services function values change between 2006 and 2011.

Ecosystem service function	ESFV in million USD in			ESFV Change	
	2006	**2011**	**Gain (+)/Loss (-)**	**By index**	**By %**
1.1 Gas regulation	8.12	7.95	-0.17	-0.0213	-2.13
1.2 Climate regulation	20.57	19.89	-0.68	-0.0330	-3.30
1.3 Waste treatment	42.96	41.52	-1.44	-0.0334	-3.34
2.1 Soil formation	19.10	18.26	-0.84	-0.0441	-4.41
2.2 Biodiversity protection	12.97	12.68	-0.30	-0.0228	-2.28
3.1 Water supply	32.18	31.67	-0.51	-0.0159	-1.59
3.2 Food production	11.82	11.05	-0.76	-0.0646	-6.46
3.3 Raw materials	2.09	2.07	-0.02	-0.0094	-0.94
4.1 Recreation and culture	7.17	7.27	0.10	0.0139	1.39
Total	**156.97**	**152.35**	**-4.62**	**-0.0294**	**-2.94**

Figure 6.7 Ecosystem services function values change between 2006 and 2011.
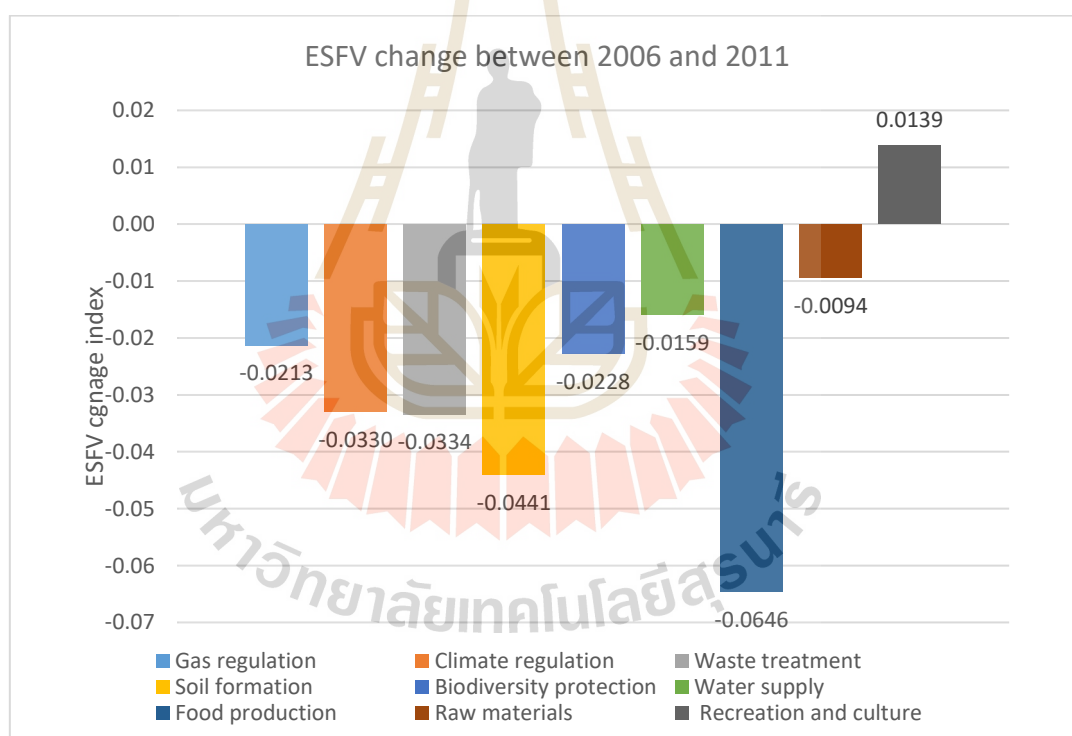
6.2.2 Ecosystem services function values change between 2011 and 2016

During 2011 to 2016, the total ecosystem services function value in 2016 decreases from in 2011 with value of 7.14 million USD or 4.69%. Herein, waste treatment service function is the most decreased ecosystem services function with value of 2.29 million USD or 5.51%. Since areas of water body and marsh and swamp in 2011 that play an important role on waste treatment service function were converted to unused land in 2016. At the same time, soil formation, food production, climate regulation, water supply, biodiversity protection, gas regulation, and raw materials service functions have also deceased with value of 1.52, 1.46, 0.97, 0.53, 0.44, 0.25 and 0.03 million USD, respectively. Herewith, the major cause of declining of ecosystem service function value is LULC change in this period as mentioned in the previous section.

On contrary, recreation and culture service function has increased during 2011 to 2016 with value of 0.34 million USD or 4.66%. Because urban and built-up area in 2016 that plays an important role on recreation and culture service function increases 1.89 km^2 from 2011. Detail of ecosystem service function values change between 2011 and 2016 is presented in Table 6.8 and Figure 6.8.

Table 6.8 Ecosystem service function values change between 2011 and 2016.

Ecosystem service function	ESFV in million USD in			ESFV Change	
	2011	**2016**	**Gain (+)/Loss (-)**	**By index**	**By %**
1.1 Gas regulation	7.95	7.69	-0.25	-0.0319	-3.19
1.2 Climate regulation	19.89	18.92	-0.97	-0.0488	-4.88
1.3 Waste treatment	41.52	39.23	-2.29	-0.0551	-5.51
2.1 Soil formation	18.26	16.74	-1.52	-0.0831	-8.31
2.2 Biodiversity protection	12.68	12.24	-0.44	-0.0344	-3.44
3.1 Water supply	31.67	31.14	-0.53	-0.0168	-1.68
3.2 Food production	11.05	9.60	-1.46	-0.1316	-13.16
3.3 Raw materials	2.07	2.04	-0.03	-0.0127	-1.27
4.1 Recreation and culture	7.27	7.60	0.34	0.0466	4.66
Total	**152.35**	**145.21**	**-7.14**	**-0.0469**	**-4.69**
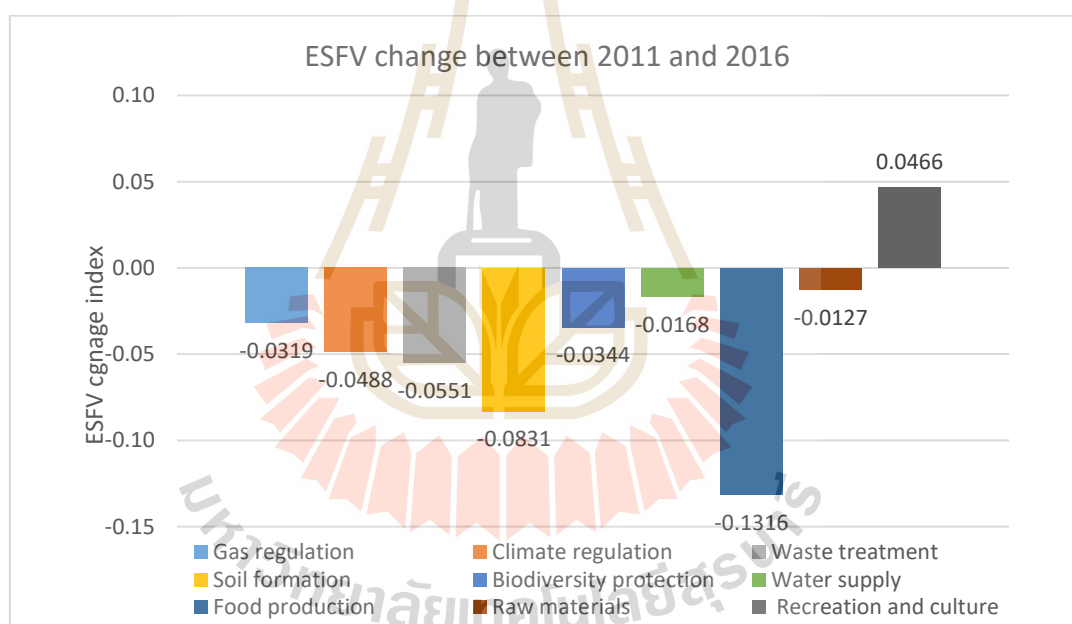
Figure 6.8 Ecosystem services function values change between 2011 and 2016.

6.2.3 Ecosystem service function values change between 2016 and 2026 of Scenario I

During 2016 to 2026 of Scenario I, the total ecosystem services function value in 2026 of Scenario I decreases from in 2016 with value of 12.50 million USD or 8.61%. Herein, waste treatment service function is the most decreased with value of with 3.78 million USD or 9.64%. At the same time, soil formation, food production, climate regulation, water supply, biodiversity protection, gas regulation, and raw materials service functions will be reduced with value of 2.56, 2.27, 1.70, 1.10, 0.88, 0.54 and 0.08 million USD, respectively. The major cause of reduction of ecosystem service function values is LULC change in the future.

On contrary, recreation and culture service functions has increased during 2016 to 2026 of scenario I with value of 0.41 million USD or 5.44% due to increasing of urban and built-up area in 2026. Detail of ecosystem service function values change between 2016 and 2026 of Scenario I is presented in Table 6.9 and Figure 6.9.

Table 6.9 Ecosystem service function values change between 2016 and 2026 of Scenario I.

Ecosystem service function	ESFV in million USD in			ESFV Change	
	2016	2026-Scenario I	Gain (+)/Loss (-)	By index	By %
1.1 Gas regulation	7.69	7.15	-0.54	-0.0706	-7.06
1.2 Climate regulation	18.92	17.22	-1.70	-0.0900	-9.00
1.3 Waste treatment	39.23	35.45	-3.78	-0.0964	-9.64
2.1 Soil formation	16.74	14.18	-2.56	-0.1527	-15.27
2.2 Biodiversity protection	12.24	11.36	-0.88	-0.0719	-7.19
3.1 Water supply	31.14	30.03	-1.10	-0.0354	-3.54
3.2 Food production	9.60	7.32	-2.27	-0.2370	-23.70
3.3 Raw materials	2.04	1.97	-0.08	-0.0367	-3.67
4.1 Recreation and culture	7.60	8.02	0.41	0.0544	5.44
Total	**145.21**	**132.71**	**-12.50**	**-0.0861**	**-8.61**
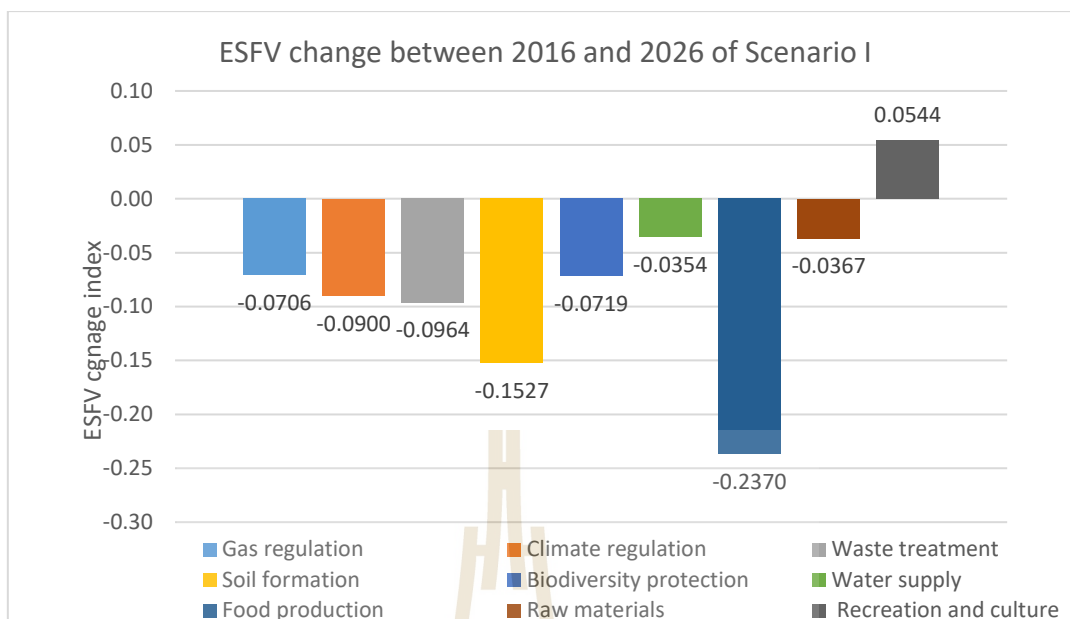
Figure 6.9 ESFV change of ecosystem service function between LULC data in 2016 and 2026 of Scenario I.

6.2.4 Ecosystem service function values change between 2016 and 2026 of Scenario II

During 2016 to 2026 of Scenario II, the total ecosystem services value in 2026 of Scenario II decreases from in 2016 with value of 13.13 million USD or 9.04%. Herein, waste treatment service function is the most decreased ecosystem services with value of 3.81 million USD or 9.71%. At the same time, soil formation, food production, climate regulation, water supply, biodiversity protection, gas regulation, and raw materials service functions have also deceased with value of 2.69, 2.30, 1.78, 1.16, 1.00, 0.65 and 0.13 million USD, respectively. Like Scenario I, the major cause of reduction of ecosystem service function values is LULC change in the future.

On contrary, recreation and culture service function has increased during 2026 of Scenario II to 2016 with value of 0.38 million USD or 5.06% due to increasing of urban and built-up area in 2026. Detail of ecosystem service function values change between 2016 and 2026 of Scenario I is presented in Table 6.10 and Figure 6.10.

Table 6.10 Ecosystem service function values change between 2016 and 2026 of Scenario II.

| Ecosystem service function	ESFV in million USD in			ESFV Change	
	2016	2026-Scenario II	Gain (+)/Loss (-)	By index	By %
1.1 Gas regulation	7.69	7.05	-0.65	-0.0841	-8.41
1.2 Climate regulation	18.92	17.14	-1.78	-0.0940	-9.40
1.3 Waste treatment	39.23	35.42	-3.81	-0.0971	-9.71
2.1 Soil formation	16.74	14.05	-2.69	-0.1606	-16.06
2.2 Biodiversity protection	12.24	11.25	-1.00	-0.0813	-8.13
3.1 Water supply	31.14	29.98	-1.16	-0.0373	-3.73
3.2 Food production	9.60	7.30	-2.30	-0.2400	-24.00
3.3 Raw materials	2.04	1.91	-0.13	-0.0630	-6.30
4.1 Recreation and culture	7.60	7.99	0.38	0.0506	5.06
Total	**145.21**	**132.09**	**-13.13**	**-0.0904**	**-9.04**
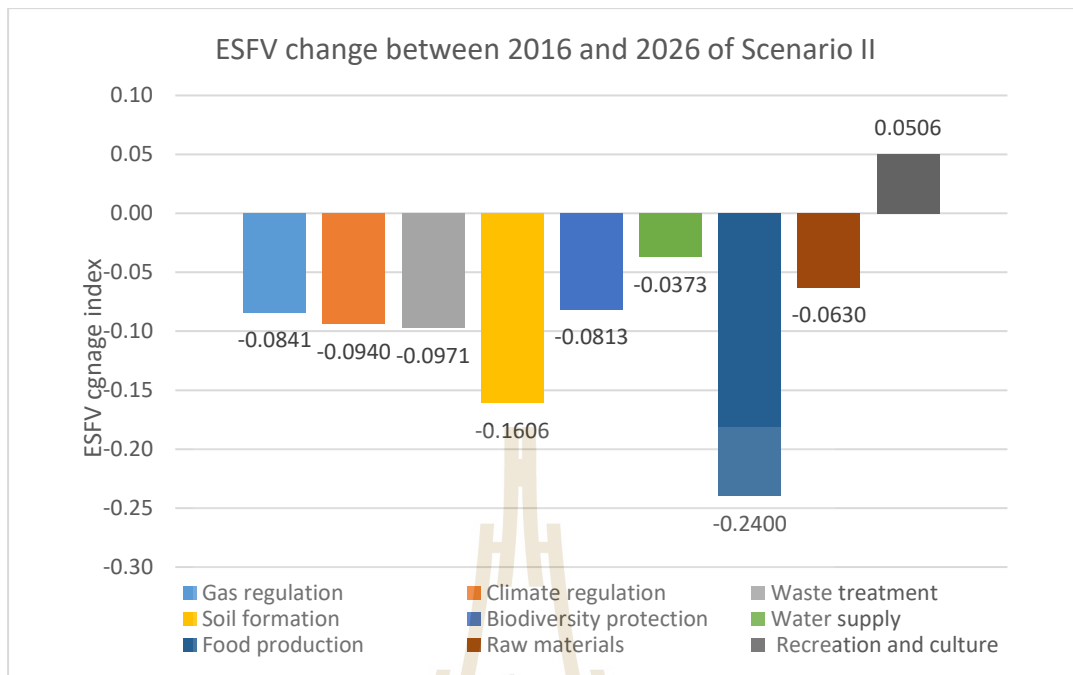
Figure 6.10 ESFV change of ecosystem service function between LULC data in 2011 and 2026 of Scenario II.

6.3 Degree of ecosystem service function values change in the future

A general description of ecosystem services values changes mainly relies on the transitional change among difference LULC types (Kreuter et al., 2001 and Su et al., 2012). Degree of future ecosystem services function values change between 2016 and 2026 of two scenarios is here summarized and discussed again as summary in Table 6.11 and shown in Figure 6.11.

As results, it was found that total ecosystem service function values during 2016 to 2026 of Scenario I and Scenario II have decreased with values of 12.50 and 13.31 million USD, respectively. In addition, all of ecosystem service function values decrease except recreation and culture service function with the increased value of 0.41% in Scenario I and 0.38% in Scenario II.

Moreover, it was found that under Scenario II (Planning and policy) all ecosystem service function values are lower than Scenario I (Historical land use development). This finding shows the effect of planning and policy on ecosystem service function in the future.

Table 6.11 Degree of future ecosystem services values change in 2026 Scenario I and II (unit: million USD).

Ecosystem service	Ecosystem service function	ESFV 2026 of		Degree of Future Change	
		Scenario I	Scenario II	2026 scenario I	2026 scenario II
	Gas regulation	7.15	7.05	-0.54	-0.65
1. Regulating services	Climate regulation	17.22	17.14	-1.70	-1.78
	Waste treatment	35.45	35.42	-3.78	-3.81
	Soil formation	14.18	14.05	-2.56	-2.69
2. Supporting services	Biodiversity protection	11.36	11.25	-0.88	-1.00
	Water supply	30.03	29.98	-1.10	-1.16
3. Provision services	Food production	7.32	7.30	-2.27	-2.30
	Raw materials	1.97	1.91	-0.08	-0.13
4. Cultural services	Recreation and culture	8.02	7.99	0.41	0.38
Total		132.71	132.09	-12.50	-13.13
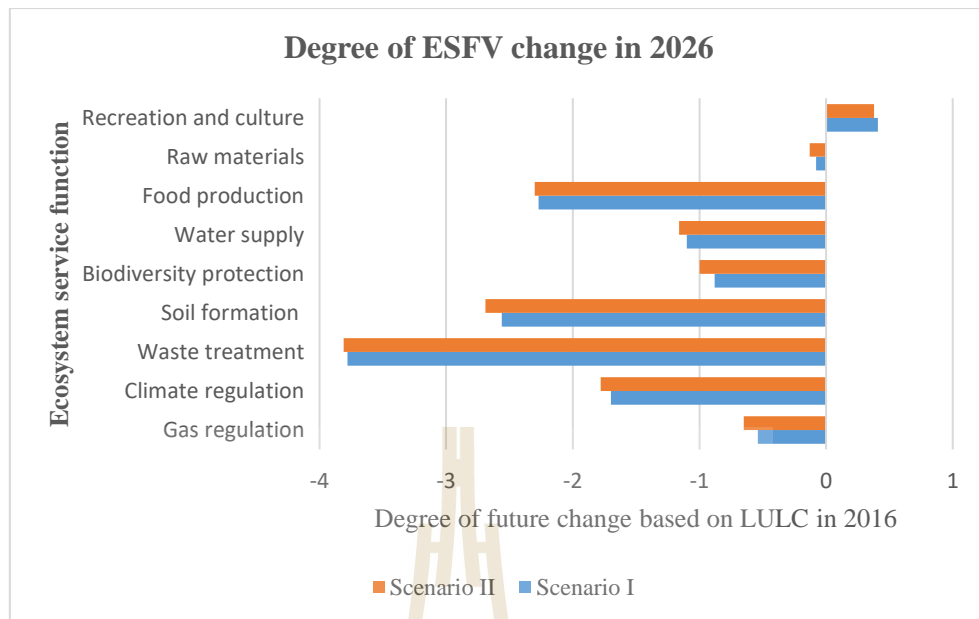
Figure 6.11 Degree of future ESFV change of two scenarios.

In summary, LULC change plays important role on an overall ecosystem services function value with variation in the spatial distribution and temporal change in the ecosystem services. In the current study, an increasing of urban and built up areas, range land and unused land and decreasing of paddy field, field crop, forest land, water body, and marsh and swamp lead to decrease total ecosystem service function value in the future. In addition, Scenario II (Planning and policy) will provide total ecosystem service function value less than Scenario I (Historical land use development). Consequently, land use planner or city planner who responsible for land use planning or city planning should try to minimize the effect of LULC change on ecosystem service function by balancing ESFV during planning process.

CHAPTER VII

ECOSYSTEM SERVICE FUNCTION VALUE AND

URBAN LANDSCAPE METRICS RELATIONSHIP

This chapter presents results of the third objective focusing on the relationship between ecosystem services function value and landscape metrics. Herein, the derived ecosystem service function value data were regressed against landscape metrics at class and landscape levels using stepwise multiple linear regression analysis. The major results includes (1) basic information of ecosystem service function values in 2016 (2) basic information of urban landscape metrics in 2016, (3) ecosystem service function value and urban landscape metrics relationship are reported and discussed under this chapter

7.1   Basic information of ecosystem service function values in 2016

In this study, ecosystem service function values (ESFV) as dependent variables include (1) gas regulation, (2) climate regulation, (3) waste treatment, (4) soil formation, (5) biodiversity protection, (6) water supply, (7) food production, (8) raw materials and (9) recreation and culture were separately prepared according to coefficients of ecosystem service function value of each LULC type (Table 7.1) for multiple linear regression analysis with selected landscape metrics. Spatial distribution

of ESFV at pixel level in 2016 is presented in Figures 7.1. Herewith, basic statistical

value of ecosystem service functions at pixel level is summarized in Table 7.2.

Table 7.1 Coefficient of ecosystem service function value of each LULC type.

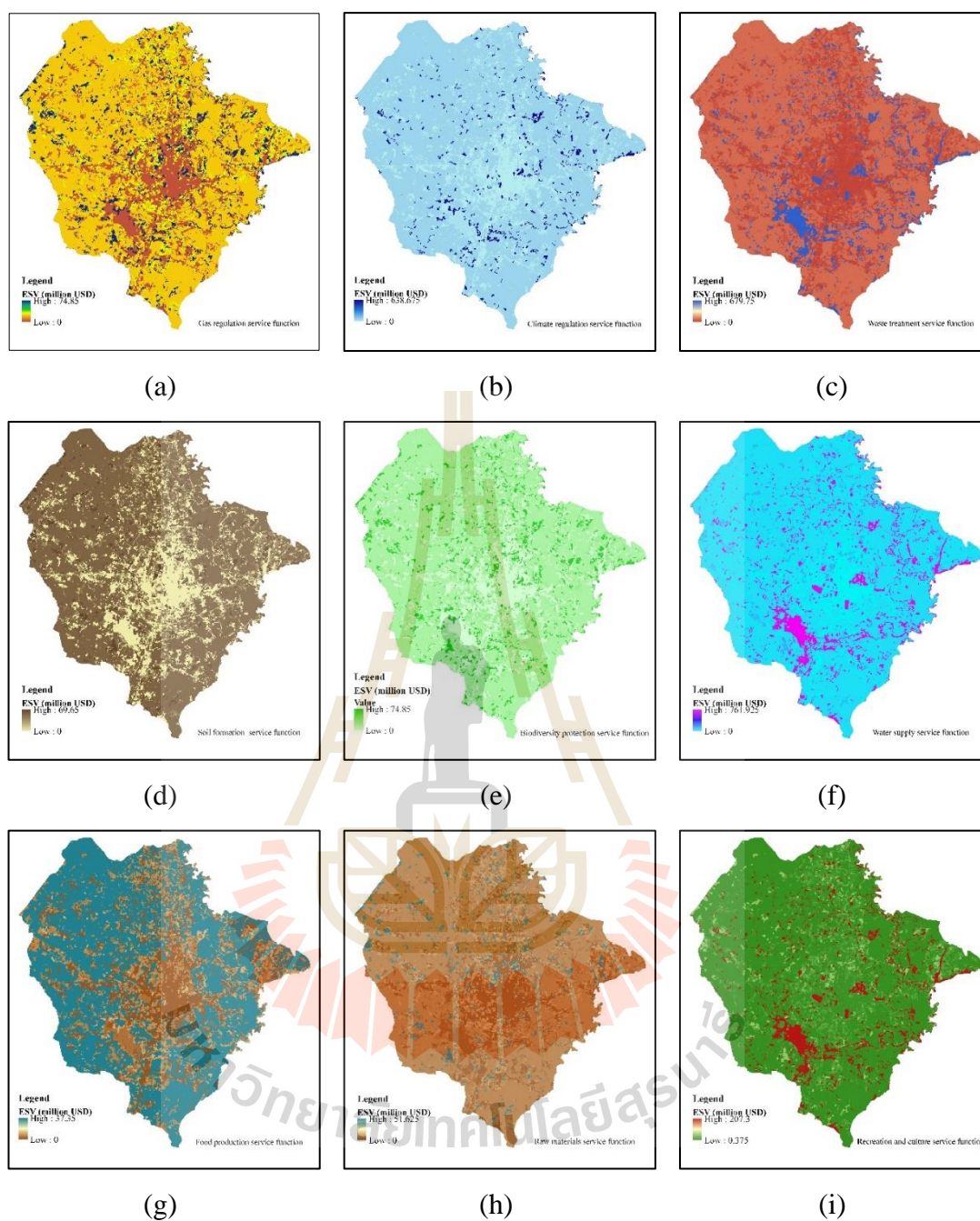| Ecosystem services function	Ecosystem service value in million USD/pixel/year							
	Ur	**Pd**	**Fc**	**Fo**	**Wa**	**Ms**	**Ra**	**Ul**
1 Gas regulation	0.00	18.68	18.68	74.85	0.00	67.23	26.00	1.05
2 Climate regulation	0.00	33.25	33.25	70.53	17.18	638.68	27.00	2.25
3 Waste treatment	0.00	61.25	61.25	29.80	679.75	679.00	22.88	4.50
4 Soil formation	0.00	54.53	54.53	69.65	0.38	63.88	38.75	2.95
5 Biodiversity protection	0.00	26.53	26.53	78.15	93.00	93.38	32.50	6.93
6 Water supply	0.00	22.40	22.40	70.88	761.93	578.90	26.25	1.20
7 Food production	0.00	37.35	37.35	5.73	3.73	11.20	7.45	0.35
8 Raw materials	0.00	3.73	3.73	51.63	0.38	2.63	6.25	0.70
9 Recreation and culture	3.18	0.38	0.38	36.05	162.10	207.30	15.08	4.15
Total	3.18	258.1	258.1	487.27	1718.45	2342.2	202.16	24.08
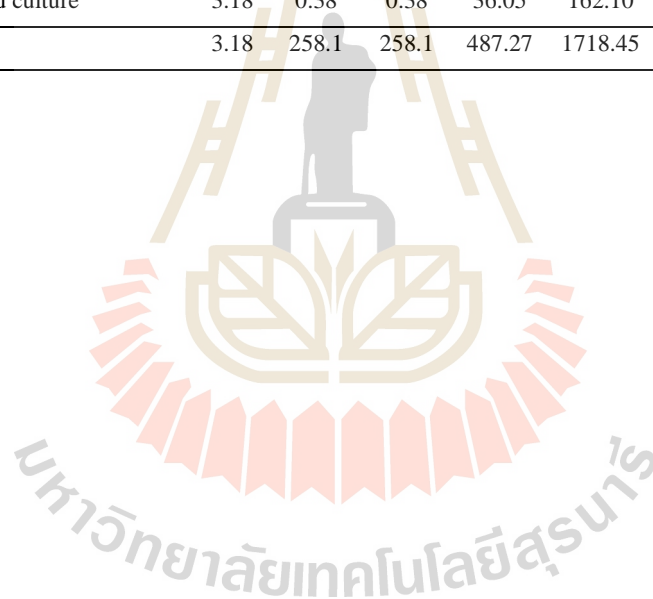
Figure 7.1 Spatial distribution of ecosystem service function value in 2016: (a) gas regulation, (b) climate regulation, (c) waste treatment, (d) soil formation, (e) biodiversity protection, (f) water supply, (g) food production, (h) raw materials, and (i) recreation and culture.

Table 7.2 Basic statistical of ecosystem service function value at pixel level.

Ecosystem services function	Basic statistical value		
	Minimum	Maximum	Range
1 Gas regulation	0.00	74.85	74.85
2 Climate regulations	0.00	638.68	638.68
3 Waste treatment	0.00	679.75	679.75
4 Soil formation	0.00	69.65	69.65
5 Biodiversity protection	0.00	93.38	93.38
6 Water supply	0.00	761.93	761.93
7 Food production	0.00	37.35	37.35
8 Raw materials	0.00	51.63	51.63
9 Recreation and culture	0.38	207.30	206.92

7.2   Basic information of urban landscape metrics in 2016

To identify the relationship between nine ecosystem services function value as mentioned in section 7.1 and urban landscape metrics using stepwise multiple linear regression analysis, the selected landscape metric at class level include (1) percent of landscape (PLAND), (2) area weighted mean shape index (SHAPE_AM) (3) patch density (PD) of each of LULC type as independent variables were separately prepared in advance. In the meantime, three selected landscape metric at landscape level include (1) Shannon's diversity index (SHDI), Shannon's evenness index (SHEI), and Contagion (CONTAG) as independent variables were also separately prepared in advance to examine the relation with nine ecosystem services function value using stepwise multiple linear regression analysis. The characteristic of each landscape metric are separately described below.

Percent of landscape (PLAND). Percent of landscape reflects the dominance of specific LULC type in the landscape, it is a measure of landscape composition

important in many ecological applications. In 2016, percent of landscape of paddy field covering an area of 24.90% is the most dominant LULC type in the study area. The second dominant LULC type is field crop accounting for 8.16% of the study area. The third important LULC category is urban and built-up area covering area of 7.25% of the study area. Other LULC types include forest land, range land, marsh and swamp, water body and unused land (bare land, pit and marsh) and cover area of 13.86% of the study area (Table 7.3). Spatial distribution of percent of landscape of each LULC type is displayed in Figure 7.2.

Area-weighted mean shape index (SHAPE_AM). Area-weighted mean shape index shows the fragmentation of landscape, and it is the simplest and perhaps most straightforward measure of shape complexity. In 2016, area-weighted mean shape index of paddy field shows the highest complexity in term of spatial irregularity. Likewise, urban and built–up area and field crop is the second and third complexity in term of spatial irregularity. In contrast, area-weighted mean shape index of forest land, water body, marsh and swamp, marsh land and swamp and unused land shows less complexity in term of spatial irregularity (Table 7.3). Spatial distribution of area-weighted mean shape index of each LULC type is displayed in Figure 7.3.

Patch density (PD). The patch density equals the number of patches of the corresponding land cover type divided by total area of interest, patch density is a limited, but it reflects about landscape pattern. In 2016, urban and built-up area provides the highest patch density with value of 1.06 patches/100 ha. The second patch density dominance is range land with value of 0.96 patch/100 ha. At the same time, water body, unused land, paddy field, field crop, marsh and swamp and forest land provide lower

patch density (Table 7.3). Spatial distribution of patch density of each LULC type is displayed in Figure 7.4.

Shannon's Diversity Index (SHDI). Shannon's diversity index is used to measure the degree of diversity of the landscape and it is a popular measure of diversity in community ecology. In 2016, value of Shannon's diversity index of the whole landscape is 1.6254, it indicates that landscape become more diverse in landscape. Spatial distribution of Shannon's diversity index of landscape is displayed in Figure 7.5a.

Shannon's Evenness Index (SHEI). Shannon's evenness index is expressed as an even distribution of area among patch types resulting in maximum evenness. As such, evenness is the complement of dominance at landscapes level. In 2016, value of Shannon's evenness index is 0.782, it indicates that the distribution of area among patch types in landscape is nearly perfectly even. Spatial distribution of Shannon's evenness index of landscape is displayed in Figure 7.5b.

Contagion (CONTAG). Contagion considers all patch types present on the whole landscape including any present in the landscape border, it presents and considers like adjacencies. In addition, contagion is affected by both the dispersion and interspersion of patch types. In 2016, value of contagion is 40.448, it indicates that all patch types in landscape become more aggregate. Spatial distribution of contagion of landscape is displayed in Figure 7.5c.

Table 7.3 Landscape metrics values of each landscape type in 2016.

LULC type	Class level metrics in %			Landscape metric		
	PLAND	SHAPE_AM	PD	SHDI	SHEI	CONTAG
Urban and built -up area (Ur)	7.25	10.99	1.06			
Paddy field (Pd)	24.9	17.12	0.61			
Field crop (Fc)	8.16	6.58	0.53			
Forest land (Fo)	2.21	1.93	0.4	1.6254	0.782	40.448
Water body (Wa)	2.91	2.04	0.66			
Marsh and swamp (Ms)	1.78	2.04	0.41			
Range land (Ra)	6.04	2.8	0.96			
Unused land (Ul)	0.92	1.63	0.64			

(a)

(b)

(c)

(d)
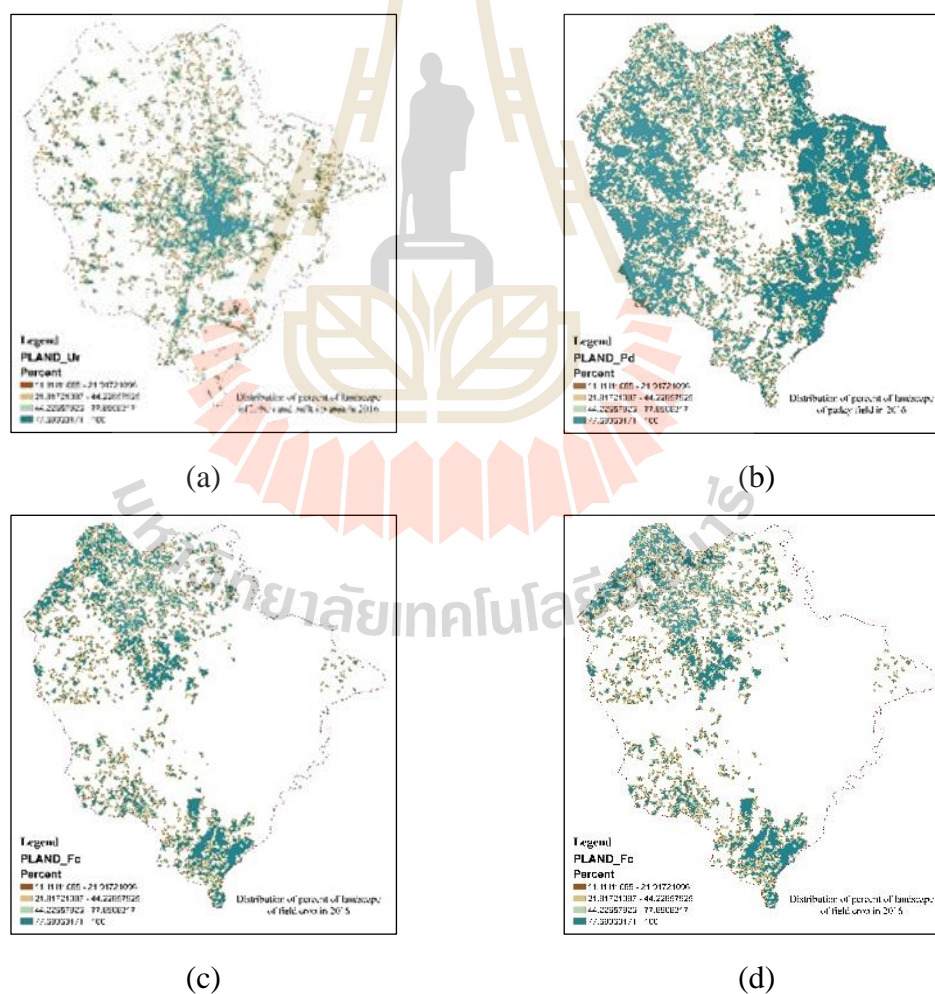
Figure 7.2 Spatial distribution of percent of landscape (PLAND) at class level in 2016:

(a) PLAND_Ur, (b) PLAND_Pd, (c) PLAND_Fc, (d) PLAND_Fo,

(e)

(f)

(g)

(h)
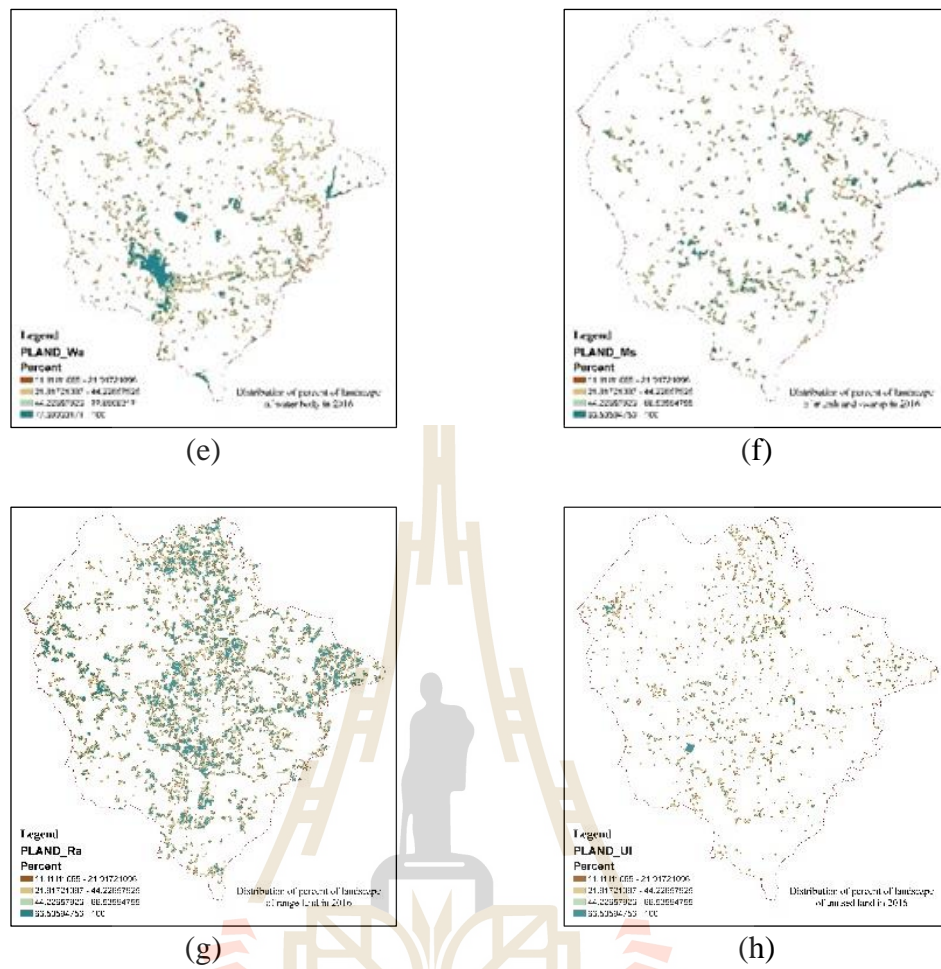
Figure 7.2 (Continued): (e) PLAND_Wa, (f) PLAND_Ms, (g) PLAND_Ra and (h)

PLAND_Ul.

(a)

(b)

(c)

(d)

(e)

(f)
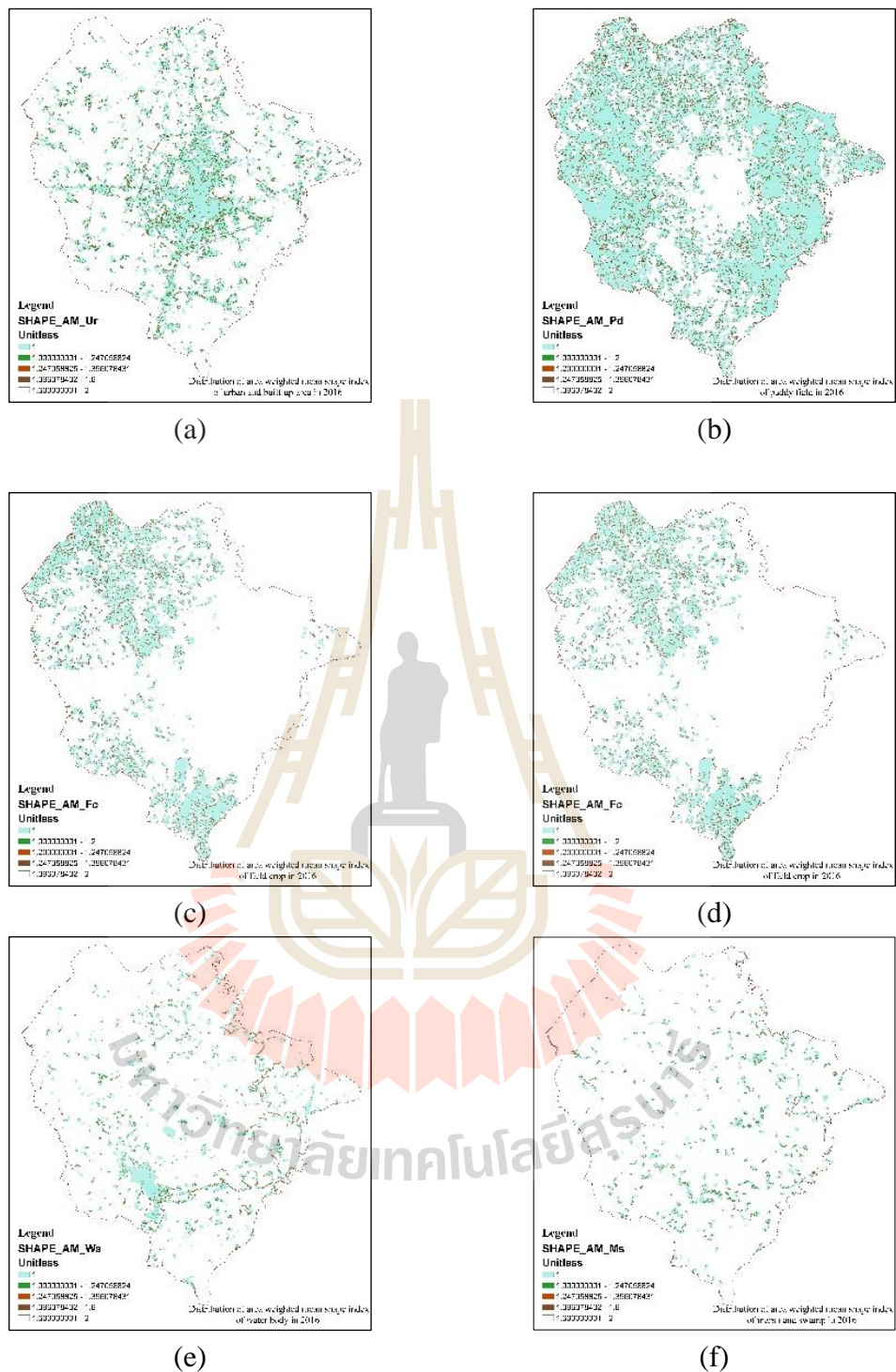
Figure 7.3 Spatial distribution of area-weighted mean shape index (SHAPE_AM) at

class level in 2016: (a) SHAPE_AM_Ur, (b) SHAPE_AM_Pd, (c) SHAPE_AM_Fc,

(d) SHAPE_AM_Fo, (e) SHAPE_AM_Wa, (f) SHAPE_AM_Ms,

(g)   (h)
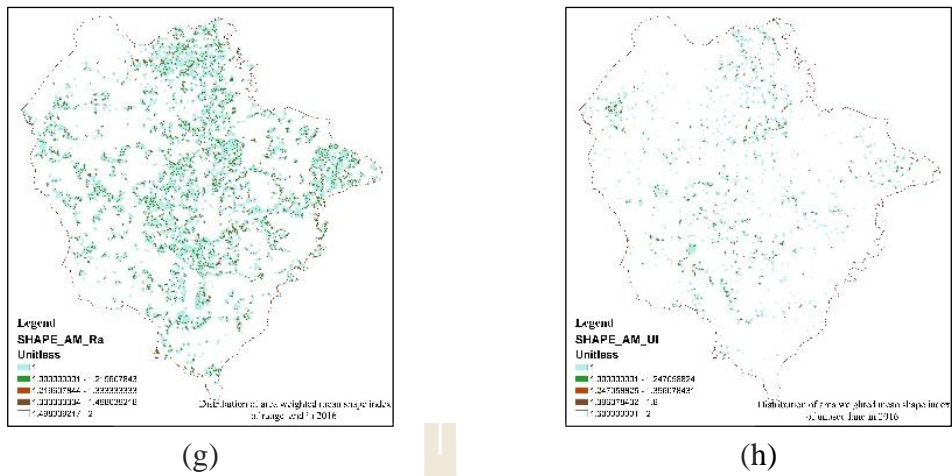
Figure 7.3 (Continued): (g) SHAPE_AM_Ra and (h) SHAPE_AM_Ul.

(a)   (b)
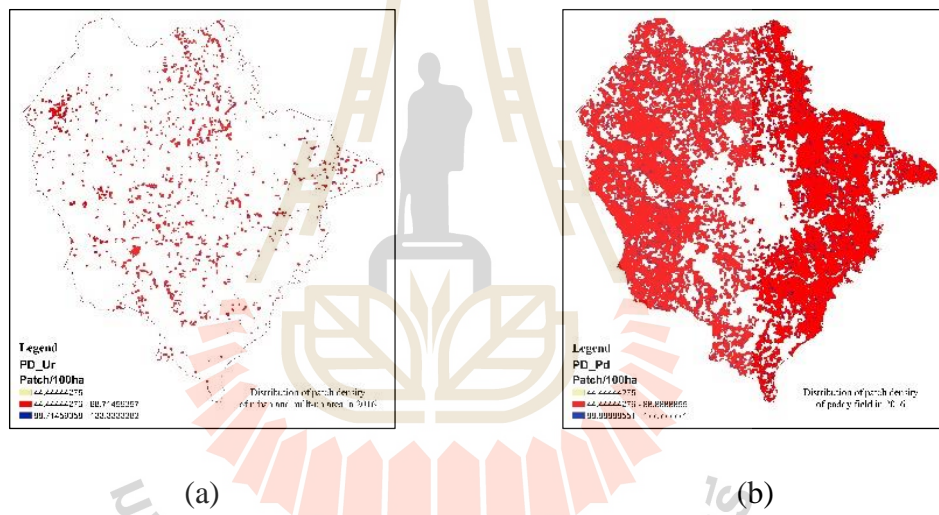
Figure 7.4 Spatial distribution of patch density index (PD) at class level in 2016:

(a) PD_Ur, (b) PD_Pd.

243
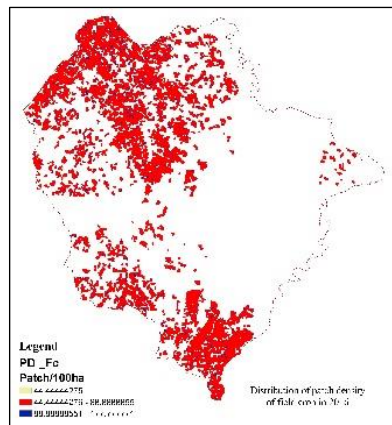
(c)
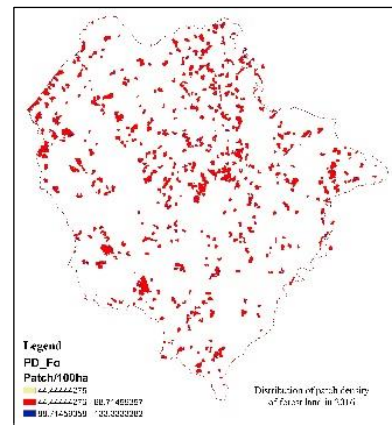
(d)
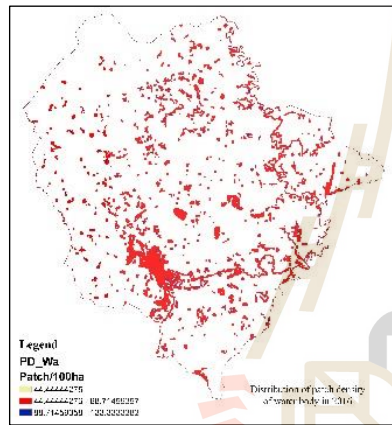
(e)
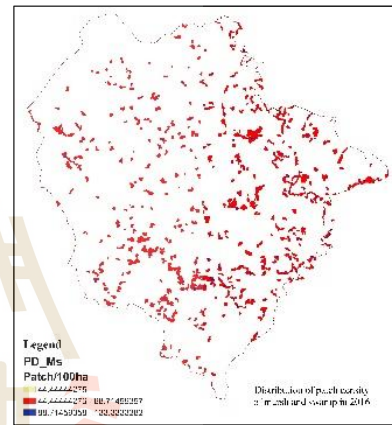
(f)
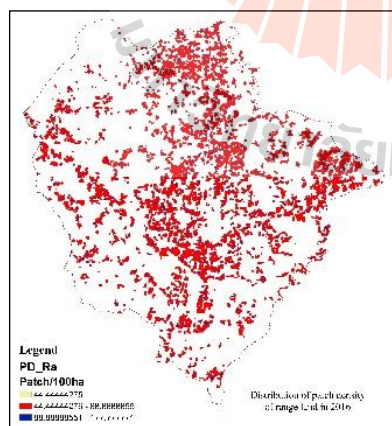
(g)
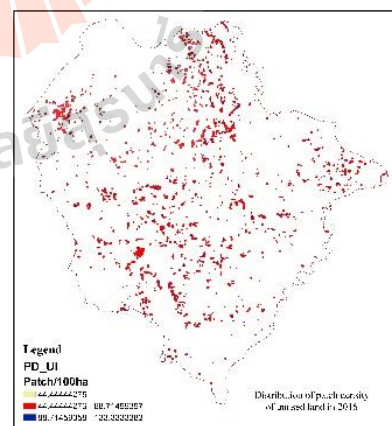
(h)

Figure 7.4 (Continued): (c) PD_Fc, (d) PD_Fo, (e) PD_Wa, (f) PD_MS, (g) PD_Ra (h)

PD_Ul.

| (a) | (b) | (c) |
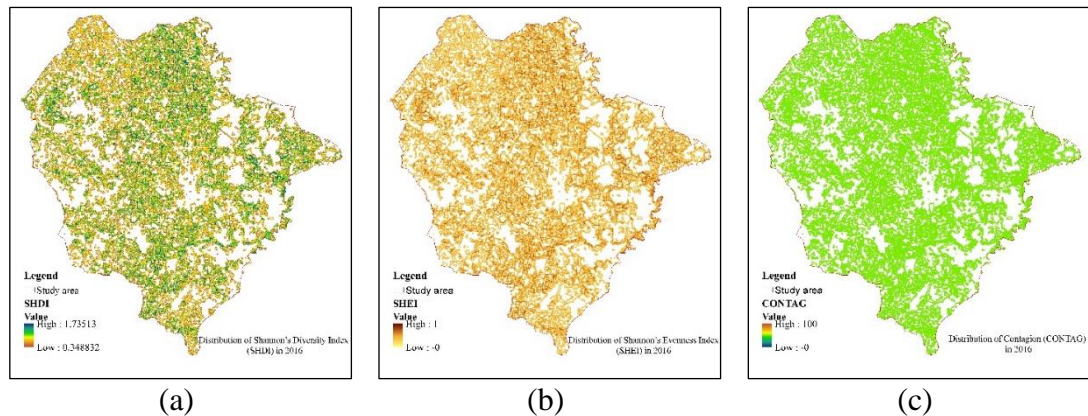
Figure 7.5 Spatial distribution of metrics value in 2016 at landscape level: (a) Shannon's diversity index, (b) Shannon's evenness index and (c) contagion.

7.3   Ecosystem service function value and urban landscape metrics relationship

The prepared data from section 7.1 and 7.2 were here used to analyze the relationship between ecosystem service function and landscape metrics at class level and landscape levels using stepwise multiple linear regression analysis under SPSS statistic software. The relationship ecosystem service function value and landscape metrics is separately described according to ecosystem service function at class and landscape levels.

7.3.1   Class level

7.3.1.1 Gas regulation

The multiple linear equation between ESFV of gas regulation and landscape metrics at class level is as follows:

Gas regulation = 0.689(PLAND_Fo) + 0.536(PLAND_Ms) - 0.382(PLAND_Ur) -

0.268(PLAND_Wa) + 0.142(PLAND_Ra) - 0.102(PLAND_Ul) -

$$0.162 \, (PD\_Fo) - 0.232(PD\_Ms) + 0.181(PD\_Ur) + 0.068(PD\_Wa) -$$

$$0.102(SHAPE\_AM\_Ur) - 0.044(PD\_Ra) + 0.100(SHAPE\_AM\_Ms)$$

$$(7.1)$$

According to Eq. 7.1, it was found that six independent variables: (1) percent of landscape of forest land, (2) percent of landscape of marsh and swamp, (3) percent of landscape of range land, (4) patch density of urban and built-up area, (5) patch density of water body and (6) area-weighted mean shape index of marsh and swamp have positive relationship with gas regulation service function. In contrast, seven independent variables: (1) percent of landscape of urban and built-up area, (2) percent of landscape of water body (3) percent of landscape of unused land (4) patch density of forest land, (5) patch density of marsh and swamp, (6) area-weighted mean shape index of urban and built-up area and (7) patch density of range land have negative relationship with gas regulation service function. The most important positive variable for gas regulation is percent of landscape of forest land while the most significant negative variable for this function is percent of landscape of urban and built-up area. This implies that when percent of landscape of forest land increases 1 standard unit, the ESFV of gas regulation increases 0.689 unit. In opposite way, when percent of landscape of paddy field increases 1 standard unit, the ESFV of gas regulation decreases 0.382 unit. The finding is similar with the previous work of Fang, Tang, Li and Han (2014) who found that the significant positive variables on gas regulation service function value are percentage of forest land and orchard whereas the significant negative variables on this service function value are percentage of cropland and the Interspersion and Juxtaposition index (IJI) of cropland.

In addition, the derived coefficient of correlation (r) and coefficient of determination (r^2) between dependent variable and independent variables from multiple linear regression analysis are 0.856 and 0.733, respectively. These findings imply that these significant landscape metrics provide very strong correlation with gas regulation service function and they can be applied to predict ecosystem service function value on gas regulation about 73%.

7.3.1.2 Climate regulation

The multiple linear equation between ESFV of climate regulation and landscape metrics at class level is as follows:

Climate regulation = 0.999(PLAND_Ms) - 0.414(PD_Ms) - 0.100(PLAND_Ur) + 0.185(SHAPE_AM_Ms) + 0.025(PD_Pd) - 0.026(PLAND_Ul) - 0.050(PLAND_Wa) + 0.037(PD_Wa) + 0.029(PD_Ur)   (7.2)

According to Eq. 7.2, it was found that five independent variables: (1) percent of landscape of marsh and swamp, (2) area-weighted mean shape index of marsh and swamp, (3) patch density of paddy field, (4) patch density of water body and (5) patch density of urban and built-up area have positive relationship with climate regulation service function. In contrast, four independent variables:(1) patch density of marsh and swamp, (2) percent of landscape of urban and built-up area, (3) percent of landscape of unused land and (4) percent of landscape of water body have negative relationship with climate regulation service function. The most important positive variable for climate regulation is percent of landscape of marsh and swamp while the most significant negative variable for this function is patch density of marsh and swamp. This implies that when percent of landscape of marsh and swamp increases 1 standardized unit, the ESFV of climate regulation increases 0.999 unit. In opposite way,

when patch density of marsh and swamp increases 1 standard unit, the ESFV of gas regulation decreases 0.414 unit. The finding is similar with the previous work of Fang et al. (2014) who found that the significant positive variables on climate regulation service function value are percentage of forest land and orchard whereas the significant negative variables on this service function value are percentage of unused land and Land Use Intensity Index (LUII).

In addition, the derived coefficient of correlation (r) and coefficient of determination (r^2) between dependent variable and independent variables from multiple linear regression analysis are 0.847 and 0.717, respectively. These findings imply that these significant landscape metrics provide very strong correlation with climate regulation function and they can be used to predict ecosystem service function value on climate regulation about 72%.

7.3.1.3 Waste treatment

The multiple linear equation between ESFV of waste treatment and landscape metrics at class level is as follows:

$$
\begin{aligned}
\text{Waste treatment} = {} & 0.481(\text{PLAND\_Wa}) + 0.399(\text{PLAND\_Ms}) - 0.536(\text{PLAND\_Ur}) - \\
& 0.309(\text{PD\_Wa}) - 0.206(\text{PD\_Ms}) + 0.056(\text{PD\_Pd}) + \\
& 0.193(\text{SHAPE\_AM\_Wa}) - 0.418(\text{PLAND\_Fc}) - \\
& 0.644(\text{PLAND\_Pd}) + 0.038(\text{PD\_Ur}) + 0.088(\text{SHAPE\_AM\_Ms}) - \\
& 0.157(\text{PLAND\_Ul}) - 0.426(\text{PLAND\_Ra}) - 0.254(\text{PLAND\_Fo}) + \\
& 0.030(\text{PD\_Ra}) \qquad\qquad\qquad\qquad\qquad\qquad\qquad (7.3)
\end{aligned}
$$

According to Eq. 7.3, it was found that seven independent variables: (1) percent of landscape of water body, (2) percent of landscape of marsh and swamp, (3) patch density of paddy field, (4) area weighted mean shape index of water body, (5)

patch density of urban and build-up area, (6) area weighted mean shape index of marsh and swamp and (7) patch density of range land have positive relationship with waste treatment function. In contrast, eight independent variables: (1) percent of landscape of urban and built-up area, (2) patch density of water body, (3) patch density of marsh and swamp (4) percent of landscape of field crop, (5) percent of landscape of paddy field, (6) percent of landscape of unused land (7) percent of landscape of range land and (8) percent of landscape of forest land have negative relationship with waste regulation service function. The most important positive variable for waste treatment service function is percent of landscape of water body whereas the most significant negative variable for this function is percent of landscape of urban and built-up area. This implies that when percent of landscape of water body increases 1 standardized unit, the ESFV of waste treatment increases 0.481 unit. In opposite way, when percent of landscape of urban and built-up area increases 1 standard unit, the ESFV of waste treatment decreases 0.536 unit. The finding is similar with the previous work of Fang et al. (2014) who found that the significant positive variables on waste treatment service function value are percentage of water body, forest land, orchard and residential land whereas the significant negative variable on this service function value is percentage of unused land.

In addition, the derived coefficient of correlation (r) and coefficient of determination (r^2) between dependent variable and independent variables from multiple linear regression analysis are 0.870 and 0.758, respectively. These findings suggest that these significant landscape metrics provide very strong correlation with waste treatment service function and they can be applied to predict ecosystem service function value on waste treatment about 76%.

7.3.1.4 Soil formation

The multiple linear equation between ESFV of soil formation and landscape metrics at class level is as follows:

Soil information = -0.580(PLAND_Ur) - 0.383(PLAND_Wa) - 0.187(PLAND_Ul) +

0.003(PLAND_Ra) + 0.287(PLAND_Fo) + 0.242(PD_Ur) +

0.222(PLAND_Ms) - 0.092(PD_Pd) + 0.187(PD_Wa) -

0.068(PD_Fo) - 0.131(SHAPE_AM_Ur) - 0.060(PD_Ms) +

0.385(PLAND_Pd) + 0.047(PD_Ul) - 0.110(SHAPE_AM_Wa) +

0.222(PLAND_Fc)   (7.4)

According to Eq. 7.4, it was found that nine independent variables: (1) percent of landscape of urban and built-up area, (2) percent of landscape of range land, (3) percent of landscape of forest land, (4) patch density of urban and built-up area, (5) percent of landscape of marsh and swamp, (6) patch density of water body, (7) percent of landscape of paddy field, (8) patch density of unused land and (9) percent of landscape of field crop have positive relationship with soil formation service function. In contrast, seven independent variables: (1) percent of landscape of water body, (2) percent of landscape of unused land, (3) patch density of paddy field, (4) patch density of forest land, (5) area-weighted mean shape index of urban and built-up area, (6) patch density of marsh and swamp and (7) area-weighted mean shape index of water body have negative relationship with soil formation service function. The most important positive variable for soil formation service function is percent of landscape of forest land while the most significant negative variable for this function is percent of landscape of urban and built-up area. This implies that when percent of landscape of forest land increases 1 standardized unit, the ESFV of soil formation increases 0.287

unit. In opposite way, when percent of landscape of urban and built-up area increases 1 standard unit, the ESFV of soil formation decreases 0.580 unit. The finding is similar with the previous work of Fang et al. (2014) who found that the significant positive variables on soil formation service function value are percentage of forest land and orchard whereas the significant negative variables on this service function value are percentage of unused land and LUII.

In addition, the derived coefficient of correlation (r) and coefficient of determination (r^2) between dependent variable and independent variables from multiple linear regression analysis are 0.881 and 0.776, respectively. These findings suggest that these significant landscape metrics provide very strong correlation with soil formation service function and they can apply to predict ecosystem service function value on soil formation about 88%.

7.3.1.5 Biodiversity protection

The multiple linear equation between ESFV of biodiversity protection and landscape metrics at class level is as follows:

Biodiversity protection = 0.363(PLAND_Wa) + 0.316 (PLAND_Ms) +

0.230(PLAND_Fo) - 0.750(PLAND_Ur) -

0.194(PLAND_Ul) + 0.196(PD_Ur) - 0.252(PD_Wa) -

0.109(PD_Ms) - 0.099(PD_Fo) - 0.257(PLAND_Ra) +

0.158(SHAPE_AM_Wa) - 0.118(SHAPE_AM_Ur) +

0.051(PD_Pd) -0.588(PLAND_Pd) +0.382(PLAND_Fc)

(7.5)

According to Eq. 7.5, it was found that seven independent variables: (1) percent of landscape of water body, (2) percent of landscape of marsh and swamp, (3)

percent of landscape of forest land, (4) patch density of urban and built up area, (5) area weight mean shape index of water body, (6) patch density of paddy field and (7) percent of landscape of field crop have positive relationship with biodiversity protection service function. In the other hand, eight independent variables: (1) percent of landscape of urban and built-up area, (2) percent of landscape of unused land, (3) patch density of water body, (4) patch density of marsh and swamp, (5) patch density of forest land (6) percent of landscape of range land, (7) area-weighted mean shape index of urban and built-up area and (8) percent of landscape of paddy field have negative relationship with biodiversity protection function. The most important variable for biodiversity protection is percent of landscape of forest land while the most significant negative variable for this function is percent of landscape of urban and built-up area. This implies that when percent of landscape of forest land increases 1 standardized unit, the ESFV of biodiversity protection increases 0.3823 unit. In opposite way, when percent of landscape of urban and built-up area increases 1 standard unit, the ESFV of biodiversity protection decreases 0.750 unit. The finding is similar with the previous work of Fang et al. (2014) who found that the significant positive variables on biodiversity protection service function value are percentage of forest land and crop land and Shannon's diversity index (SHDI) whereas the significant negative variables on this service function value is area weighted mean shape index of forest land.

In addition, the derived coefficient of correlation (r) and coefficient of determination (r^2) between dependent variable and independent variables from multiple linear regression analysis are 0.866 and 0.750, respectively. These findings suggest that these significant landscape metrics provide very strong correlation with biodiversity

protection service function and they can be used to predict ecosystem service function value on biodiversity protection about 87%.

7.3.1.6 Water supply

The multiple linear equation between ESFV of water supply and landscape metrics at class level is as follows:

$$
\begin{aligned}
\text{Water supply} = {} & 0.835(\text{PLAND\_Wa}) + 0.509(\text{PLAND\_Ms}) - 0.348(\text{PD\_Wa}) - \\
& 0.099(\text{PD\_Ms}) + 0.221(\text{SHAPE\_AM\_Wa}) + 0.072(\text{PD\_Pd}) + \\
& 0.041(\text{PLAND\_Fo}) - 0.048(\text{PLAND\_Pd}) - 0.053(\text{PLAND\_Ur}) + \\
& 0.029(\text{PD\_Ur}) \quad\quad\quad\quad\quad\quad\quad\quad\quad\quad\quad\quad (7.6)
\end{aligned}
$$

According to Eq. 7.6, it was found that six independent variables: (1) percent of landscape of water body, (2) percent of landscape of marsh and swamp, (3) area-weighted mean shape index of water body (4) patch density of paddy field, (5) percent of landscape of forest land, and (6) patch density of urban and built-up area have positive relationship with water supply service function. In the other hand, four independent variables: (1) patch density of water body, (2) patch density of marsh and swamp, (3) percent of landscape of paddy field, and (4) percent of landscape of urban and built-up area have negative relationship with water supply service function. The most important variable for water supply service function is percent of landscape of water. While the most significant negative variable for this function is patch density of water. This implies that when percent of landscape of water body increases 1 standardized unit, the ESFV of water supply increases 0.835 unit. In opposite way, when patch density of water body increases 1 standard unit, the ESFV of water supply decreases 0.348 unit. The finding is similar with the previous work of Fang et al. (2014) who found that the significant positive variables on water supply service function value

are percentage of forest land and orchard whereas the significant negative variables on this service function value are percentage of unused land and LUII.

In addition, the derived coefficient of correlation (r) and coefficient of determination (r^2) between dependent variable and independent variables from multiple linear regression analysis are 0.870 and 0.757, respectively. These findings suggest that these significant landscape metrics provide very strong correlation with water supply service function and they can apply to predict ecosystem service function value on water supply about 76%.

7.3.1.7 Food production

The multiple linear equation between ESFV of food production and landscape metrics at class level is as follows:

Food production= 1.005(PLAND_Pd) + 0.663(PLAND_Fc) - 0.138(PLAND_Ur) -

$$0.133(PD\_Pd) + 0.091(PD\_Ur) + 0.033(PD\_Ms) + 0.061(PD\_Ra) -$$

$$0.052(PLAND\_Ul) - 0.043(PD\_Fc) + 0.036(PD\_Ul) +$$

$$0.027(PD\_Fo) + 0.042(PLAND\_Ms) \qquad\qquad (7.7)$$

According to Eq. 7.7, it is found that eight independent variables: (1) percent of landscape of paddy field, (2) percent of landscape of field crop, (3) patch density of urban and built-up area, (4) patch density of marsh and swamp, (5) patch density of range land, (6) patch density of unused land (7) patch density of forest land and (8) percent of landscape of marsh and swamp have positive relationship with food production service function. In the other hand four independent variables: (1) percent of landscape of urban and built up area, (2) patch density of paddy field, (3) percent of landscape of unused land and (4) patch density of field crop have negative relationship with food production services function. The most important variable for food

production service function is percent of landscape of paddy field while the most significant negative variable for this function is percent of urban and built-up area. This implies that when percent of landscape of paddy field increases 1 standardized unit, the ESFV of food production increases 1.005 unit. In opposite way, when percent of urban and built-up area increases 1 standard unit, the ESFV of food production decreases 0.138 unit. The finding is similar with the previous work of Fang et al. (2014) who found that the significant positive variables on food production service function value are percentage of cropland and LUII whereas the significant negative variable on this service function values are percentage of forest land and SHDI.

In addition, the derived coefficient of correlation (r) and coefficient of determination (r^2) between dependent variable and independent variables from multiple linear regression analysis are 0.903 and 0.815, respectively. These findings suggest that these significant landscape metrics provide very strong correlation with food production service function and they can be applied to predict ecosystem service value function on water supply about 82%.

7.3.1.8 Raw materials

The multiple linear equation between ESFV of raw materials and landscape metrics at class level is as follows:

Raw material = 1.007(PLAND_Fo) - 0.344(PD_Fo) - 0.155(PLAND_Ur) + 0.064

(PLAND_Ra) - 0.068 (PLAND_Wa) + 0.052(PD_Ur) -

0.032(PLAND_Ul) + 0.128(SHAPE_AM_Fo) - 0.018(PLAND_Ms)

(7.8)

According to Eq. 7.8, it was found that four independent variables: (1) percent of landscape of forest land, (2) percent of landscape of range land, (3) patch

density of urban and built-up area and (4) area weight mean shape index of forest land have positive relationship with raw materials service function. In the other hand, five independent variables: (1) patch density of forest land, (2) percent of landscape of urban and built-up area, (3) percent of landscape of water body, (4) percent of landscape of unused land and (5) percent of landscape of marsh and swamp have negative relationship with raw materials service function. The most important variable for raw materials service function is percent of landscape of forest land while the most significant negative variable for this function is patch density of forest land. This implies that when percent of landscape of forest land increase 1 standardized unit, the ESFV of raw materials increases 1.007 unit. In opposite way, when patch density of forest land increases 1 standard unit, the ESFV of raw materials decreases 0.344 unit. The finding is similar with the previous work of Fang et al. (2014) who found that the significant positive variables on raw materials service function value are percentage of forest land, SHDI, and LUII.

In addition, the derived coefficient of correlation (r) and coefficient of determination (r^2) between dependent variable and independent variables from multiple linear regression analysis are 0.874 and 0.764, respectively. These findings suggest that these significant landscape metrics provide very strong correlation with raw materials service function and they can be used to predict ecosystem service function value on raw materials about 76%.

7.3.1.9 Recreation and culture

The multiple linear equation between ESFV of recreation and culture and landscape metrics at class level is as follows:

Recreation and culture = 0.677(PLAND_Wa) + 0.711(PLAND_Ms) +

0.110(PLAND_Fo) - 0.250(PD_Ms) + 0.063(PLAND_Ra) -

0.264(PD_Wa) + 0.171(SHAPE_AM_Wa) + 0.083(PD_Pd)

- 0.073(PLAND_Pd) + 0.109(SHAPE_AM_Ms)   (7.9)

According to Eq. 7.9, it is found that seven independent variables: (1) percent of landscape of water body, (2) percent of landscape of marsh and swamp, (3) percent of landscape of forest land, (4) percent of landscape of range land, (5) area weighted mean shape index of marsh and swamp, (6) patch density of paddy field and (7) area weighted mean shape index of marsh and swamp have positive relationship with recreation and culture service function. In the other hand, three independent variables: (1) patch density of marsh and swamp, (2) patch density of water body, and (3) percent of landscape of paddy field have negative relationship with recreation and culture service function. The most important positive variable for recreation and culture services function is percent of landscape of marsh and swamp while the most significant negative variable for this function is patch density of water body. This implies that when percent of landscape of marsh and swamp increases 1 standardized unit, the ESFV of raw materials increases 0.711 unit. In opposite way, when patch density of water body increases 1 standard unit, the ESFV of recreation and culture decreases 0.264 unit. The finding is similar with the previous work of Fang et al. (2014) who found that the significant positive variable on recreation and culture service function value is IJI of cropland whereas the significant negative variables on this service function is percent of cropland.

In addition, the derived coefficient of correlation (r) and coefficient of determination (r^2) between dependent variable and independent variables from multiple

linear regression analysis are 0.869 and 0.755, respectively. These findings suggest that these significant landscape metrics provide very strong correlation with recreation and culture service function and they can be applied to predict ecosystem service function value on recreation and culture about 76%.

7.3.1.10 Total

The multiple linear equation between total ESFV and landscape metrics at class level is as follows:

Total = 0.534(PLAND_Ms) + 0.370(PLAND_Wa) - 0.558(PLAND_Ur)-

0.263(PD_Ms) -0.247(PD_Wa) - 0.151(PLAND_Fo) +0.56(PD_Pd) -

0.180(PLAND_Ul) +0.156(SHAPE_AM_Wa) +0.104(PD_Ur) +

1.113(SHAPE_AM_Ms) -0.396(PLAND_Fc) + 0.021(PD_Ul) -

0.37(PLAND_Ra) - 0.612(PLAND_Pd) + 0.021(PD_Ra)   (7.10)

According to Eq. 7.10, it is found that eight independent variables: (1) percent of landscape of marsh and swamp, (2) percent of landscape of water body, (3) patch density of paddy field, (4) area weighted mean shape index of water body, (5) patch density of urban and built-up area (6) area weighted mean shape index of marsh and swamp (7) patch density of unused land and (8) patch density of range land have positive relationship with total ecosystem service function value. In the other hand, eight independent variables: (1) percent of landscape of urban and built-up area, (2) patch density of marsh and swamp, (3) patch density of water body, (4) percent of landscape of forest land, (5) percent of landscape of unused land, (6) percent of landscape of field crop, (7) percent of landscape of range land, and (8) patch density of range land have negative relationship with total ESFV. The most important positive variable for total ESFV is patch density of paddy field while the most significant

negative variable for percent of landscape of paddy field. This implies that when patch density of paddy field increases 1 standardized unit, the total ESFV increases 0.56 unit. In opposite way, when percent of landscape of paddy field increases 1 standard unit, the ESFV value decreases 0.612 unit. The finding is similar with the previous work of Fang et al. (2014) who found that the significant positive on total ecosystem service function value is the area weighted of forest land whereas the significant negative variable on this service function values are percentage of crop land and SHDI.

In addition, the derived coefficient of correlation (r) and coefficient of determination (r^2) between dependent variable and independent variables from multiple linear regression analysis are 0.878 and 0.753, respectively. These findings suggest that these significant landscape metrics provide very strong correlation with total ESFV and they can be applied to predict total ecosystem service function value about 75%.

In summary, refer to the derived multiple linear equations 7.1 to 7.10, which show relationship between ESFV and urban landscape metrics, it can be here summarized that dominant landscape metric both positive and negative independent variables, namely percent of landscape (PLAND) of different LULC types are the most dominant independent variables to describe ESFV, except food production service function that is dominant by patch density (PD) (Table 7.1).

In addition, the significant landscape metrics can provide very strong correlation with all ecosystem service function values and they can be applied to predict ecosystem service function value varies from 73% to 88%.

Table 7.4 Summary of dominant landscape metric of ecosystem service function value from multiple linear regression analysis.

Ecosystem service function	Group	Metric	Number	Total
Gas regulation	Area and edge metric	PLAND	6	13
Climate regulation	Area and edge metric	PLAND	4	9
Waste treatment	Area and edge metric	PLAND	8	15
Soil formation	Area and edge metric	PLAND	8	16
Biodiversity protection	Area and edge metric	PLAND	8	15
Water supply	Area and edge metric	PLAND	5	10
Food production	Aggregation metric	PD	7	12
Raw materials	Area and edge metric	PLAND	6	9
Recreation and culture	Area and edge metric	PLAND	5	10
Total	**Area and edge metric**	**PLAND**	**8**	**16**

7.3.2 Landscape level

7.3.2.1 Gas regulation

The multiple linear equation between ESFV of gas regulation and landscape metrics at landscape level is as follows:

$$\text{Gas regulation} = 0.039(\text{SHEI}) + 0.039(\text{SHDI}) + 0.015(\text{CONTAG}) \tag{7.11}$$

According to Eq. 7.11, it was found that all independent variables includes Shannon's evenness index, Shannon's diversity index and contagion have positive relationship with gas regulation service function. The importance positive variable for gas regulation service function is Shannon's evenness index and Shannon's diversity index. This implies that when Shannon's evenness index or Shannon's diversity index increases 1 standard unit, the ESFV of gas regulation increases 0.039 unit.

In addition, the derived coefficient of correlation (r) and coefficient of determination (r^2) between dependent variable and independent variables from multiple

linear regression analysis are 0.084 and 0.007, respectively. These findings suggest that these selected landscape metrics provide weak correlation with gas regulation ESFV at landscape level and they can explain the relationship with gas regulation service function value only 1%.

7.3.2.2 Climate regulation

The multiple linear equation between ESFV of climate regulation and landscape metrics at landscape level is as follows:

Climate regulation = 0.077(SHDI) +0.030(SHEI)-0.010(CONTAG)   (7.12)

According to Eq. 7.12, it was found that two independent variables: Shannon's diversity index and Shannon's evenness index have positive relationship with climate regulation service function. In contrast, contagion has negative relationship with climate regulation service function. The most importance positive variable for climate regulation is Shannon's diversity index. This implies that when Shannon's diversity index increases 1 standardized unit, the ESFV of climate regulation increases 0.077 unit. In opposite way, when contagion increases 1 standard unit, the ESFV of gas regulation decreases 0.010 unit.

In addition, the derived coefficient of correlation (r) and coefficient of determination (r^2) between dependent variable and independent variables from multiple linear regression analysis are 0.102 and 0.010, respectively. These findings suggest that these selected landscape metrics provide weak correlation with climate regulation service function at landscape level and they can explain the relationship with climate regulation service function value only 1%.

7.3.2.3 Waste treatment

The multiple linear equation between ESFV of waste treatment and landscape metrics at landscape level is as follows:

Waste treatment = 0.132(SHDI)-0.037(CONTAG) (7.13)

According to Eq. 7.13, it was found that Shannon's diversity index has positive relationship to waste treatment service function. In contrast, contagion has negative relationship with waste regulation service function. This implies that when Shannon's diversity index increases 1 standardized unit, the ESFV of waste treatment increases 0.132 unit. In opposite way, when contagion increases 1 standard unit, the ESFV of waste treatment decreases 0.037 unit.

In addition, the derived coefficient of correlation (r) and coefficient of determination (r^2) between dependent variable and independent variables from multiple linear regression analysis are 0.123 and 0.015, respectively. These findings suggest that these selected landscape metrics provide weak correlation with waste treatment service function at landscape level and they can explain the relationship with waste treatment service function value only 2%.

7.3.2.4 Soil formation

The multiple linear equation between ESFV of soil formation and landscape metrics at landscape level is as follows:

Soil information = 0.198(SHDI)+0.027(CONTAG)+0.025(SHEI) (7.14)

According to Eq. 7.14, it was found that all independent variables includes Shannon's diversity index, contagion and Shannon's evenness index have positive relationship with soil information function. The importance positive variable for soil information is Shannon's diversity index. This implies that when Shannon's

diversity index increases 1 standard unit, the ESFV of soil formation increases 0.198 unit.

In addition, the derived coefficient of correlation (r) and coefficient of determination (r^2) between dependent variable and independent variables from multiple linear regression analysis are 0.166 and 0.028, respectively. These findings suggest that these selected landscape metrics provide weak correlation with soil formation service function at landscape level and they can explain the relationship with soil formation service function value only 3%.

7.3.2.5 Biodiversity protection

The multiple linear equation between ESFV of biodiversity protection and landscape metrics at landscape level is as follows:

Biodiversity protection = 0.124(SHDI)-0.022(CONTAG)+0.017(SHEI)   (7.15)

According to Eq. 7.15, it was found that two independent variables: Shannon's diversity index and Shannon's evenness index have positive relationship with biodiversity protection service function. In contrast, contagion has negative relationship with biodiversity protection service function. The most importance positive variable for biodiversity protection service function is Shannon's diversity index. This implies that when Shannon's diversity index increases 1 standardized unit, the ESFV of biodiversity protection increases 0.124 unit. In opposite way, when contagion increases 1 standard unit, the ESFV of biodiversity protection decreases 0.022 unit.

In addition, the derived coefficient of correlation (r) and coefficient of determination (r^2) between dependent variable and independent variables from multiple linear regression analysis are 0.133 and 0.018, respectively. These findings suggest that these selected landscape metrics provide weak correlation with biodiversity protection

service function at landscape level and they can explain the relationship with biodiversity protection service function value only 2%.

7.3.2.6 Water supply

The multiple linear equation between ESFV of water supply and landscape metrics at landscape level is as follows:

Water supply = 0.159(SHDI)-0.038(CONTAG)   (7.16)

According to Eq. 7.16, it was found that Shannon's diversity index has positive relationship with water supply service function. In contrast, contagion has negative relationship with water supply service function. This implies that when Shannon's diversity index increases 1 standardized unit, the ESFV of water supply increases 0.159 unit. In opposite way, when contagion increases 1 standard unit, the ESFV of water supply decreases 0.038 unit.

In addition, the derived coefficient of correlation (r) and coefficient of determination (r^2) between dependent variable and independent variables from multiple linear regression analysis are 0.149 and 0.002, respectively. These findings suggest that these selected landscape metrics provide weak correlation with water supply service function at landscape level and they can explain the relationship with water supply service function value only 0.2%.

7.3.2.7 Food production

The multiple linear equation between ESFV of food production and landscape metrics at landscape level is as follows:

Food production = 0.304(SHDI)+0.019(CONTAG)-0.012(SHEI)   (7.17)

According to Eq. 7.17, it was found that Shannon's diversity index and contagion have positive relationship with food production service function. In contrast,

Shannon's evenness index has negative relationship with food production service function. The most important independent variable for food production service function is Shannon's diversity index. This implies that when Shannon's diversity index increases 1 standardized unit, the ESFV of food production increases 0.304 unit. In opposite way, when contagion increases 1 standard unit, the ESFV of food production decreases 0.012 unit.

In addition, the derived coefficient of correlation (r) and coefficient of determination (r^2) between dependent variable and independent variables from multiple linear regression analysis are 0.309 and 0.095, respectively. These findings suggest that these selected landscape metrics provide weak correlation with food production service function at landscape level and they can explain the relationship with food production service function value only 1%.

7.3.2.8 Raw materials

The multiple linear equation between ESFV of raw materials and landscape metrics at landscape level is as follows:

$$\text{Raw material} = 0.076(\text{SHDI})+0.015(\text{CONTAG}) \tag{7.18}$$

According to Eq. 7.18, it was found that Shannon's diversity index and contagion have positive relationship with raw material function. The most important variable for raw materials function is Shannon's diversity index. This implies that when Shannon's diversity index increases 1 standardized unit, the ESFV of raw material increases 0.076 unit.

In addition, the derived coefficient of correlation (r) and coefficient of determination (r^2) between dependent variable and independent variables from multiple linear regression analysis are 0.083 and 0.007, respectively. These findings suggest that

these selected landscape metrics provide weak correlation with raw material service function at landscape level and they can explain the relationship with raw material service function value only 1%.

7.3.2.9 Recreation and culture

The multiple linear equation between ESFV of recreation and culture and landscape metrics at landscape level is as follows:

Recreation and culture = 0.188(SHDI)-0.034(CONTAG)+0.013(SHEI)   (7.19)

According to Eq. 7.19, it was found that two independent variables: Shannon's diversity index and Shannon's evenness index have positive relationship with recreation and culture service function. In contrast, contagion has negative relationship with recreation and culture service function. The most importance positive variable for recreation and culture service function is Shannon's diversity index. This implies that when Shannon's diversity index increases 1 standardized unit, the ESFV of recreation and culture increases 0.188 unit. In opposite way, when contagion increases 1 standard unit, the ESFV of recreation and culture decreases 0.034 unit.

In addition, the derived coefficient of correlation (r) and coefficient of determination (r^2) between dependent variable and independent variables from multiple linear regression analysis are 0.190 and 0.036, respectively. These findings suggest that these selected landscape metrics provide weak correlation with recreation and culture service function at landscape level and they can explain the relationship with recreation and culture service function value only 4%.

In summary, the derived multiple linear equations for identifying the relationship between the ESFV and the selected landscape metrics at landscape level including Shannon's diversity index, Shannon's evenness index and contagion provide

very low correlation coefficient (r) and coefficient of determination (r^2). As results, it can be here concluded that landscape metrics at landscape level cannot be used to predict ESFV of any function since ESFV of all functions is estimated from LULC type at class level.

CHAPTER VIII

IMPACT OF URBAN GROWTH ON LAND SURFACE
TEMPERATURE EVALUATION AND PREDICTION

This chapter presents results of the fourth objective focusing impact of urban growth on land surface temperature evaluation and prediction. Herein LST was firstly extracted from Landsat-8 using standard single channel window method, and then it used to identify relationship with urban landscape metrics for LST prediction of two different scenarios. The main results which consist of (1) extraction of land surface temperature data in 2016, (2) land surface temperature and landscape metrics relationship, and (3) prediction of land surface temperature in 2026 of 2 Scenarios are described and discussed in detail.

8.1 Extraction of land surface temperature in 2016

Land surface temperature (LST) in 2016 was here extracted based on standard conversion method as suggestion by USGS (2015). In practice, digital numbers of Landsat TIR band firstly convert to spectral radiance and spectral radiance is then transformed to at-satellite brightness temperature (T_B) in kelvin. After that, spectral emissivity (ε) values that relate to difference land features are used to convert T_B to LST. In this study, the NDVI threshold method was used to estimate spectral emissivity of difference land surface type due to their electromagnetic reflectance. This method

categorizes various LULC type through a NDVI classification scheme to obtain land surface spectral emissivity (Afrakhteh, Asgarian, Sakieh and Soffianian, 2016).

Results of LST data in 2016 that was analyzed from Landsat 8 OLI, date 15 November 2016 is shown in Figure 8.1. As result, temperature ranges from 18.799 to 34.468°C and mean temperature is 27.07°C. In addition, it was found that the lowest temperature is located at water bodies while the highest temperature is mostly found at urban and built-up area such as airport or CBD at the center of the study area as expectation.

Distribution of land surface temperature in 2016 from Landsat 8 OLI
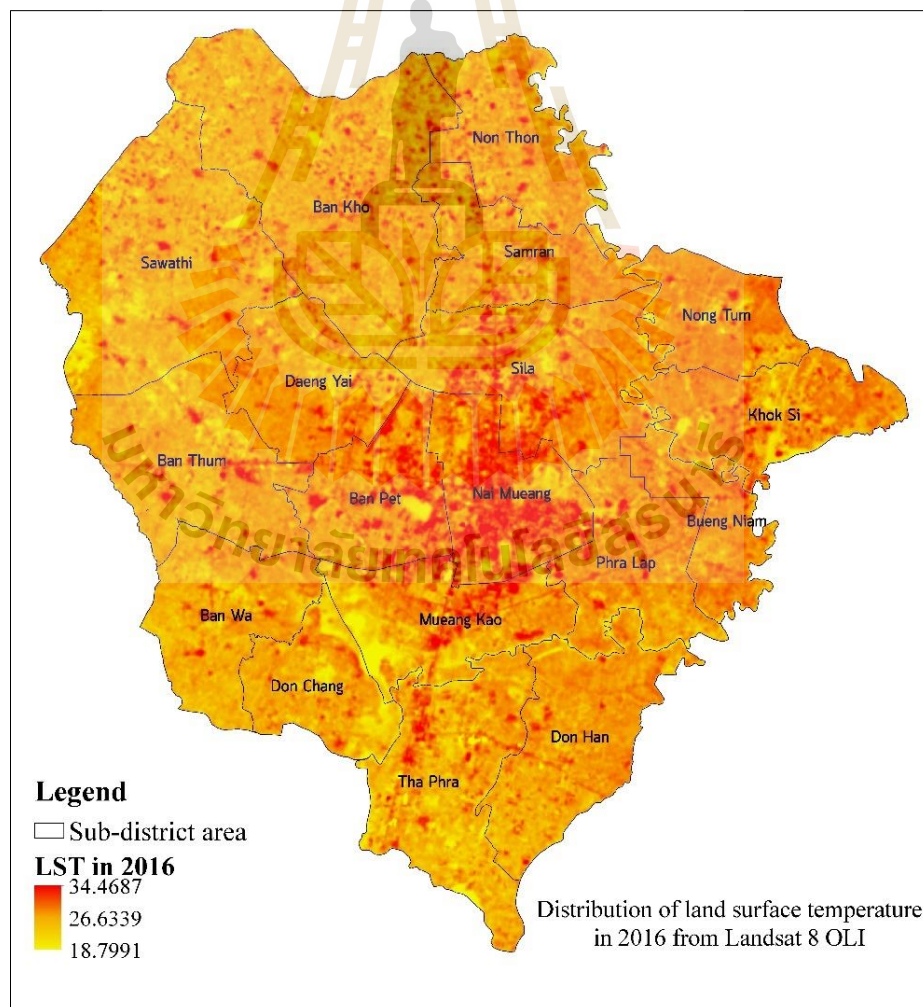
Figure 8.1 Spatial distribution of land surface temperature in 2016.

8.2   Land surface temperature and landscape metrics relationship

An attempt was here made to quantify and analyze the relationship between LST and landscape metrics in this study. In this study, multiple linear regression analysis was employed to model the statistical relationship between LST data in 2016 and the selected single and multiple landscape metrics. Herein, class area (CA) metric of each LULC type as single metric was examined the relationship with the LST data of the whole study area and zonal areas based on urbanization grade at sub-district level. In the meantime, the representative metric at class from 3 groups including percent of landscape (PLAND), area weighted fractal dimension (FRAG_AM), and patch density (PD) of each LULC type were examined the relationship with the LST data of the whole study area. The relationship between land surface temperature and its landscape metric is separately described in the following sections.

8.2.1   Relationship between overall LST and class area metric

The relationship between overall LST and class area metric of LULC type in 2016 as multiple linear equation is as follows:

$$LST_{2016} = 26.099 + 1.149\ CA_{UR} - 0.044\ CA_{WA} - 0.076\ CA_{FO} + 0.907\ CA_{UL}$$
$$+ 0.063\ CA_{MS} + 0.303\ CA_{FC} + 0.394\ CA_{PD} + 0.358\ CA_{RA} \qquad (8.1)$$

Where, $LST2016$ is Overall land surface temperature in 2016

CA_{UR} is Class area of urban and built up area in 2016

CA_{PD} is Class area of paddy field in 2016

CA_{FC} is Class area of field crop in 2016

CA_{FO} is Class area of forest land in 2016

CA_{WA} is Class area of water body in 2016

CA_{MS} is Class area of marsh and swamp in 2016

CA_{RA} is Class area of range land in 2016

CA_{UL} is Class area of unused land in 2016

As results, it was found that six significant independent variables including (1) class area of urban and built-up area, (2) class area of unused land, (3) class area of marsh and swamp (4) class area of field crop, (5) class area of paddy field, and 6) class area of range land have positive relationship with overall LST. In contrast, two significant independent variables including class area of water body and forest land have negative relationship with overall LST. In reveals that the most important positive variable on overall LST is class area of urban and built-up area while the most significant negative variable on overall LST is class area of forest land. This finding shows an expected phenomena, when urban and built-up area increases, then LST increases while when forest land increases, then LST decreases.

In addition, the derived coefficient of correlation (r) and coefficient of determination (r2) between dependent variable and independent variables in regression are 0.651 and 0.424, respectively.

8.2.2 Relationship between zonal LST and class area metric

Two common urbanization grades of LULC data in 2026 and LULC data in 2026 of 2 scenarios which was classified based on urban land percentage (PU) at sub-district level include (1) high urbanization and (2) very high urbanization (Figure 8.2) was here used to extract zonal LST data for identifying relationship between CA metric and zonal LST data.

| (a) | (b) | (c) |
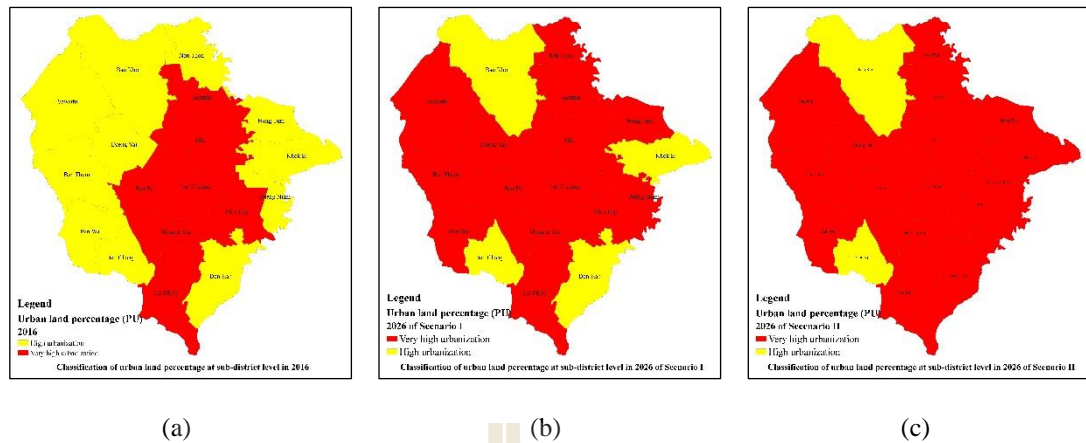
Figure 8.2 Urbanization grade at sub-district level based on urban land percentage in: (a) 2016, (b) 2026 of Scenario I and (c) 2026 of Scenario II.

The relationship between zonal LST of high urbanization sub-districts and class area metric of LULC type in 2016 as multiple linear equation is as follows:

$$\text{LST}_{\text{high urbanization}} = 26.785 - 0.051\text{CA}_{\text{Ms}} - 0.057\text{CA}_{\text{Wa}} - 0.024\text{CA}_{\text{Fc}} - 0.030\text{CA}_{\text{Fo}} \qquad (8.2)$$

Where, $\text{LST}2016$ is Zonal land surface temperature in high urbanization zone in 2016

CAFC is Class area of field crop in 2016

CA_{FO} is Class area of forest land in 2016

CA_{WA} is Class area of water body in 2016

CA_{MS} is Class area of marsh and swamp in 2016

As results, it is found that all four significant independent variables including (1) class area of marsh and swamp, (2) class area of water body, (3) class area of field crop and (4) class area of forest land have negative relationship with zonal LST. In reveals that the most important negative variable on zonal LST is class area of water body. This finding shows an expected phenomena, when water body in high urbanization sub-district increases, then LST decreases.

Herein, the derived coefficient of correlation (r) and coefficient of determination (r^2) between dependent variable and independent variables in regression are 0.612 and 0.374, respectively.

Meanwhile, the relationship between zonal LST of very high urbanization sub-districts and class area metric of LULC type in 2016 as multiple linear equation is as follows:

$$LST_{very\ high\ urbanization} = 27.210 + 0.217CA_{UR} - 0.190CA_{FC} + 0.229CA_{FO} \qquad (8.3)$$

Where,   LST2016 is Zonal land surface temperature in very high urbanization zone in 2016

CA_{UR} is Class area of urban and built up area in 2016

CA_{FC} is Class area of field crop in 2016

CA_{FO} is Class area of forest land in 2016

As results, it was found that two significant independent variables including (1) class area of urban and built-up area, and (2) class area of forest land have positive relationship with zonal LST. In contrast, one significant independent variable, field crop, has negative relationship with zonal LST. In reveals that the most important positive variable on zonal LST is class area of urban and built-up area while the most significant negative variable on zonal LST is class area of field crop. This finding shows an expected phenomena, when urban and built-up area increases, then LST increases while when field crop increases, then LST decreases.

Herein, the derived coefficient of correlation (r) and coefficient of determination (r^2) between dependent variable and independent variables in regression are 0.546 and 0.298, respectively.

8.2.3 Relationship between overall LST and multiple landscape metrics

The relationship between overall LST and multiple landscape metrics of LULC types in 2016 as multiple linear equation is as follows:

$$LST = 27.026 + 0.013 PLAND_{UR} - 0.522 FRAC\_AM_{WA} - 0.008 PLAND_{FO} +$$

$$0.010 PD_{UL} - 0.005 PLAND_{MS} - 0.003 PD_{FC} \tag{8.4}$$

Where,   LST is Overall land surface temperature

$PLAND_{UR}$ is percent of landscape of urban and built up area

$FRAC\_AM_{WA}$ is area weighted fractal dimension of water body

$PLAND_{FO}$ is percent of landscape of forest land

PD_{UL} is patch density of unused land in 2016

$PLAND_{MS}$ is percent of landscape of marsh and swamp

PD_{FC} is patch density of field crop

As results, it was found that two significant independent variables including (1) percent of landscape of urban and built up area and (2) patch density of unused land have positive relationship with overall LST. In contrast, four significant independent variables including (1) area weighted fractal dimension of water body, (2) percent of landscape of forest land, (3) patch density of unused land and (4) percent of landscape of marsh and swamp have negative relationship with overall LST. In reveals that the most important positive variable on overall LST is percent of landscape of urban and built-up area while the most significant negative variable on overall LST is area weighted fractal dimension of water body. This finding shows an expected phenomena, when urban and built-up area increases, then LST increases while when water body increases, then LST decreases. This finding is similar with the previous work of Connors, Galletti and Chow (2013) who found that in mesic areas there was a

strong positive relationship between LST and the PLAND of buildings ($r^2 = 0.42$, $p <$ 0.02) and a strong negative relationship ($r^2 = -0.63$, $p < 0.01$) between the PLAND of grass and LST. For mesic areas, class-level metrics for buildings were the only other metrics that displayed a significant relationship with LST: PD of buildings ($r^2 = 0.48$, $p < 0.01$), ED of buildings ($r^2 = 0.43$, $p < 0.01$), and LSI of buildings ($r^2 = 0.40$, $p < 0.05$). None of the landscape-level metrics were significantly correlated to LST for the residential land uses.

Herein, the derived coefficient of correlation (r) and coefficient of determination (r^2) between dependent variable and independent variables in regression are 0.766 and 0.586, respectively. Additionally, multicollinearity test result is summarized in Table 8.1.

Table 8.1 Multicollinearity statistics between independent and dependent variables.

Independent variable	Multicollinearity statistics	
	Tolerance	VIF
Percent of landscape of urban and built-up area	.888	1.126
Area weighted mean fractal dimension of water body	.910	1.098
Percent of landscape of forest land	.985	1.015
Patch density of unused land	.982	1.018
Percent of landscape of marsh and swamp	.957	1.045
Patch density of field crop	.847	1.181
Dependent Variable: Land surface temperature		

8.3   Prediction of land surface temperature in 2026 of 2 Scenarios

The derived relationships between land surface temperature and its landscape metric were separately applied to predict LST data in 2026 of 2 scenarios. Results of LST prediction of 2 scenarios based on relevant equations using Raster Calculator module of ArcGIS software is separately described in the following sections.

8.3.1   Prediction of LST data in 2026 based on the relationship between overall LST and class area metric in 2016

By applying the derived multiple linear equation based on the relationship between overall LST and class area metric in 2016 (Eq. 8.1), spatial distribution of predictive LST in 2026 of Scenario I and II is separately displayed Figure 8.3 and Figure 8.4, respectively and basic statistical data is summarized in Table 8.2.
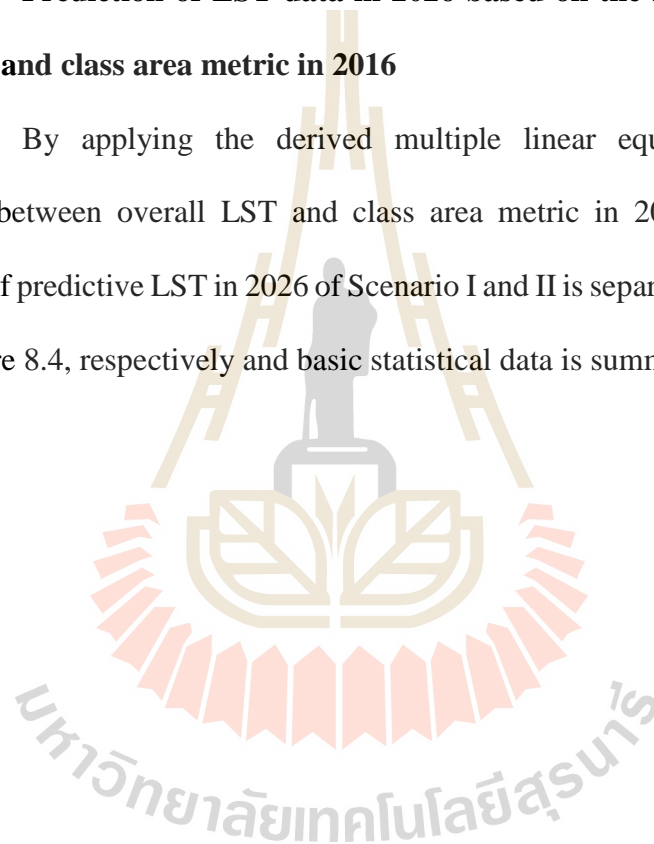
Figure 8.3 Spatial distribution of predicted LST data in 2026 of Scenario I based on the relationship between overall LST data and class area metric in 2016.

Figure 8.4 Spatial distribution of predicted LST data in 2026 of Scenario II based on the relationship between overall LST data and class area metric in 2016.

Table 8.2 Basic statistical data of the predicted LST data in 2026 of 2 scenarios based on the relationship between overall LST data and class area metric in 2016.

Year	Land surface temperature in °C		
	Min	Max	Mean
2026 scenario I	31.881	32.433	32.258
2026 scenario II	30.349	31.282	31.078

As results, it can be observed that LST data in 2026 of Scenario I ranges from 31.881 to 32.433°C and mean LST data is 32.258°C. In addition, the lowest temperature is mostly located over water bodies while the highest temperature is found at urban and built-up area.

In the meantime, LST data in 2026 of Scenario II varies from 30.349 to 31.282°C and mean LST data is 31.078°C. Like Scenario I, the lowest temperature is located over water bodies while the highest temperature is found at urban and built-up area.

In summary, it can be observed that range and mean of LST data in 2026 of LULC of Scenario II is higher than LST data of LULC of Scenario I (see Table 8.2). This finding shows influence of transformation of policy on LULC change, particularly urban growth on LST.

8.3.2 Prediction of LST data in 2026 based on the relationship between zonal LST and class area metric in 2016

By applying the derived multiple linear equation based on the relationship between zonal LST and class area metric in 2016 (Eq. 8.2 and 8.3), spatial distribution of predictive LST in 2026 of Scenario I and II is separately displayed Figure 8.5 and Figure 8.6, respectively and basic statistical data is summarized in Table 8.3.
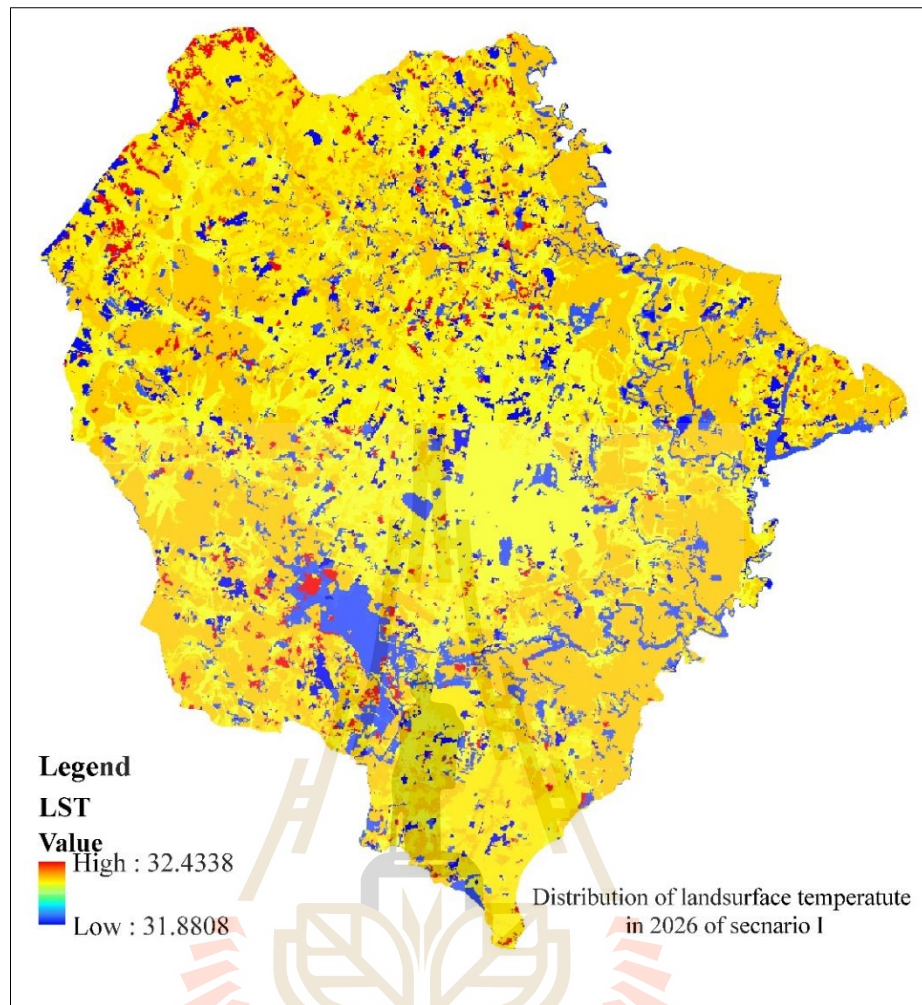
Figure 8.5 Spatial distribution of predicted LST data in 2026 of Scenario I based on the relationship between zonal LST data and class area metric in 2016.

Distribution of land surface temperature (LST)
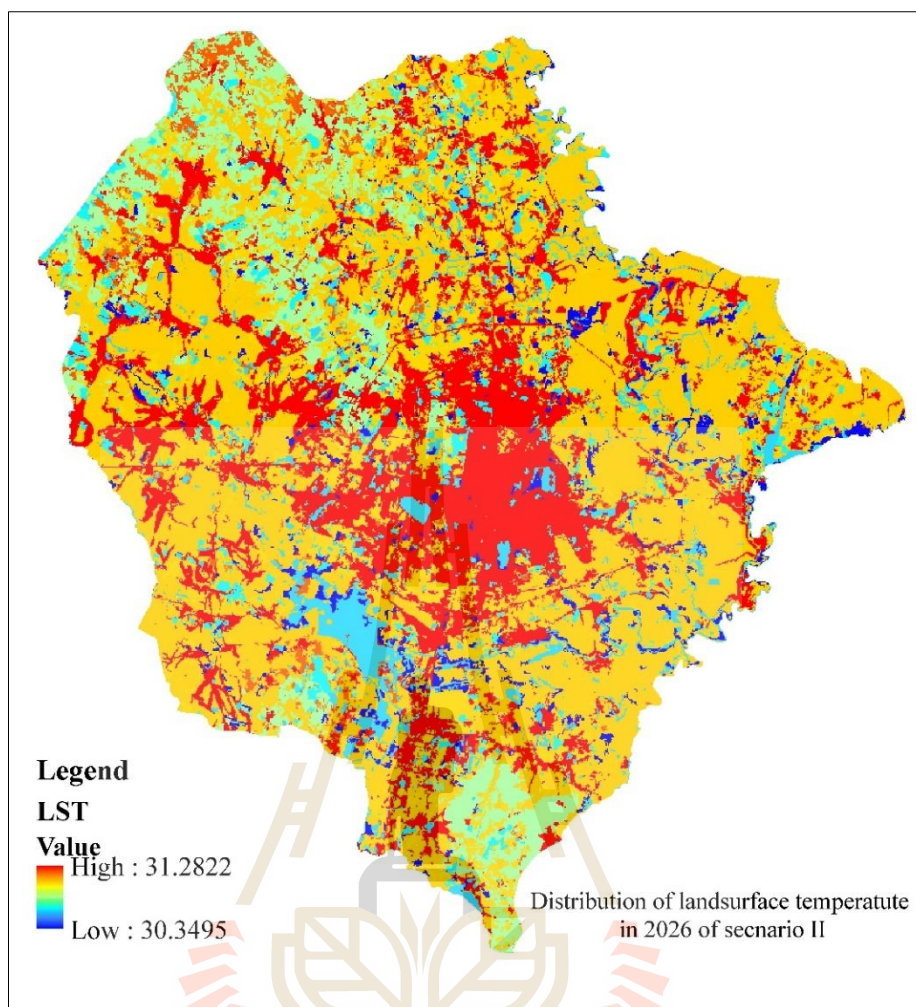in urban land percentage (PU) zone in 2016

Figure 8.6 Spatial distribution of predicted LST data in 2026 of Scenario II based on the relationship between zonal LST data and class area metric in 2016.

Table 8.3 Basic statistical data of the predicted LST data in 2026 of 2 scenarios based on the relationship between zonal LST data and class area metric in 2016.

Year	Land surface temperature in °C		
	Min	Max	Mean
2026 scenario I	26.616	27.725	27.185
2026 scenario II	26.656	27.725	27.239

As results, it can be observed that LST data in 2026 of Scenario I ranges from 26.616 to 27.725°C and mean LST data is 27.185°C. In addition, the lowest temperature is mostly located over water bodies while the highest temperature is found at urban and built-up area.

In the meantime, LST data in 2026 of Scenario II varies from 26.656 to 27.725°C and mean LST data is 27.239°C. Like Scenario I, the lowest temperature is located over water bodies while the highest temperature is found at urban and built-up area.

In summary, it can be observed that range and mean of LST data in 2026 of LULC of Scenario II is higher than LST data of LULC of Scenario I (Table 8.3). This finding shows influence of transformation of policy on LULC change, particularly urban growth on LST.

8.3.3 Prediction of LST data in 2026 based on the relationship between overall LST and multiple landscape metrics in 2016

By applying the derived multiple linear equation based on the relationship between overall LST and multiple landscape metrics in 2016 (Eq. 8.4), spatial distribution of predictive LST in 2026 of Scenario I and II is separately displayed Figure 8.7 and Figure 8.8, respectively and basic statistical data is summarized in Table 8.5.
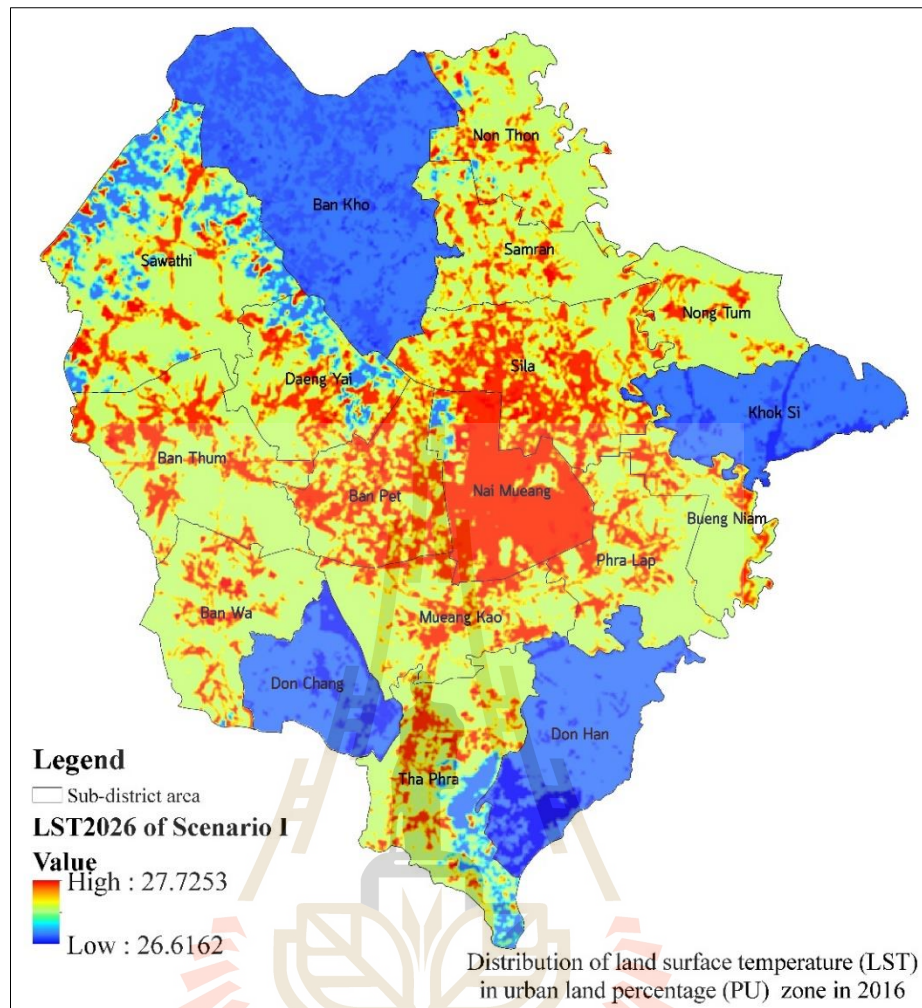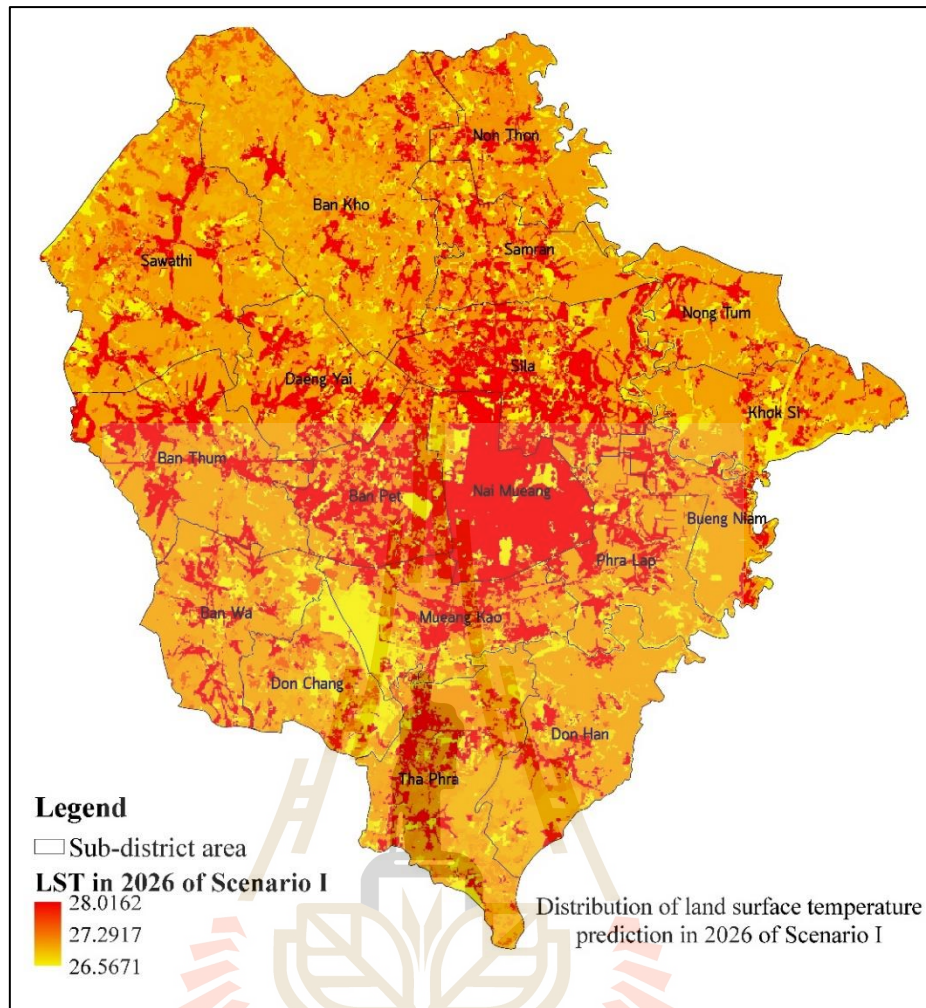
Figure 8.7 Spatial distribution of predicted LST data in 2026 of Scenario I based on the relationship between LST data and multiple landscape metrics in 2016.

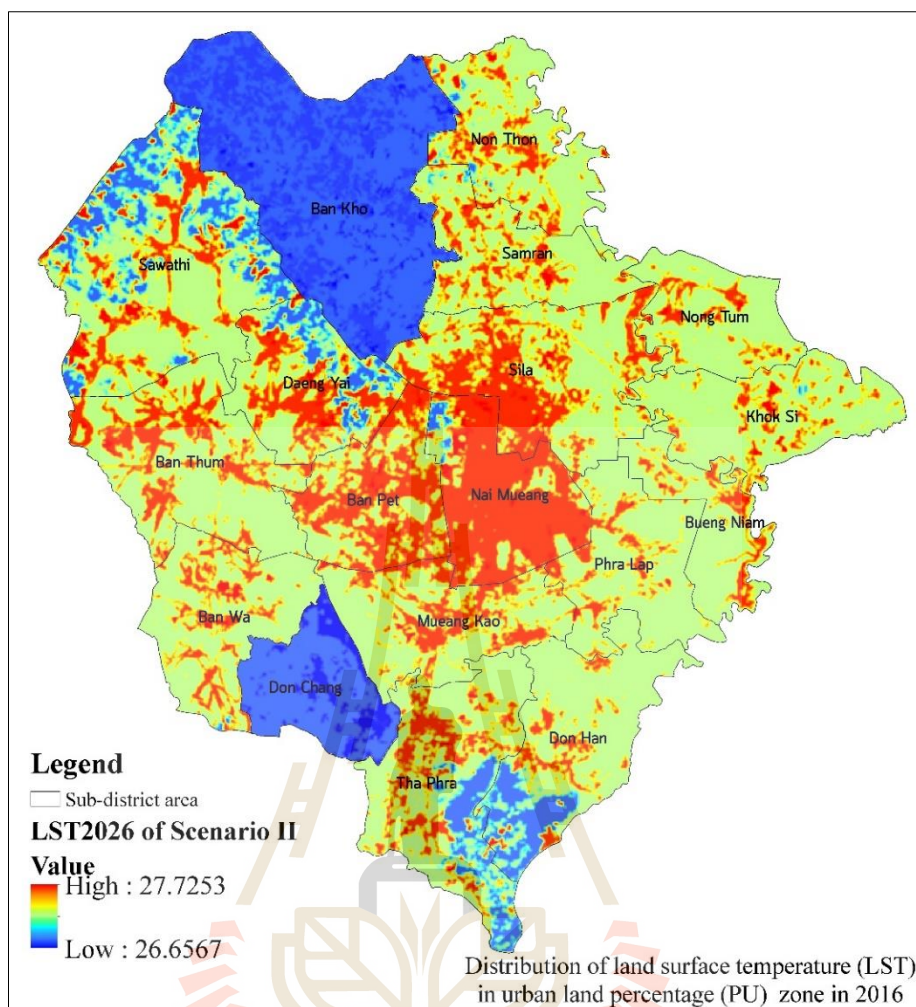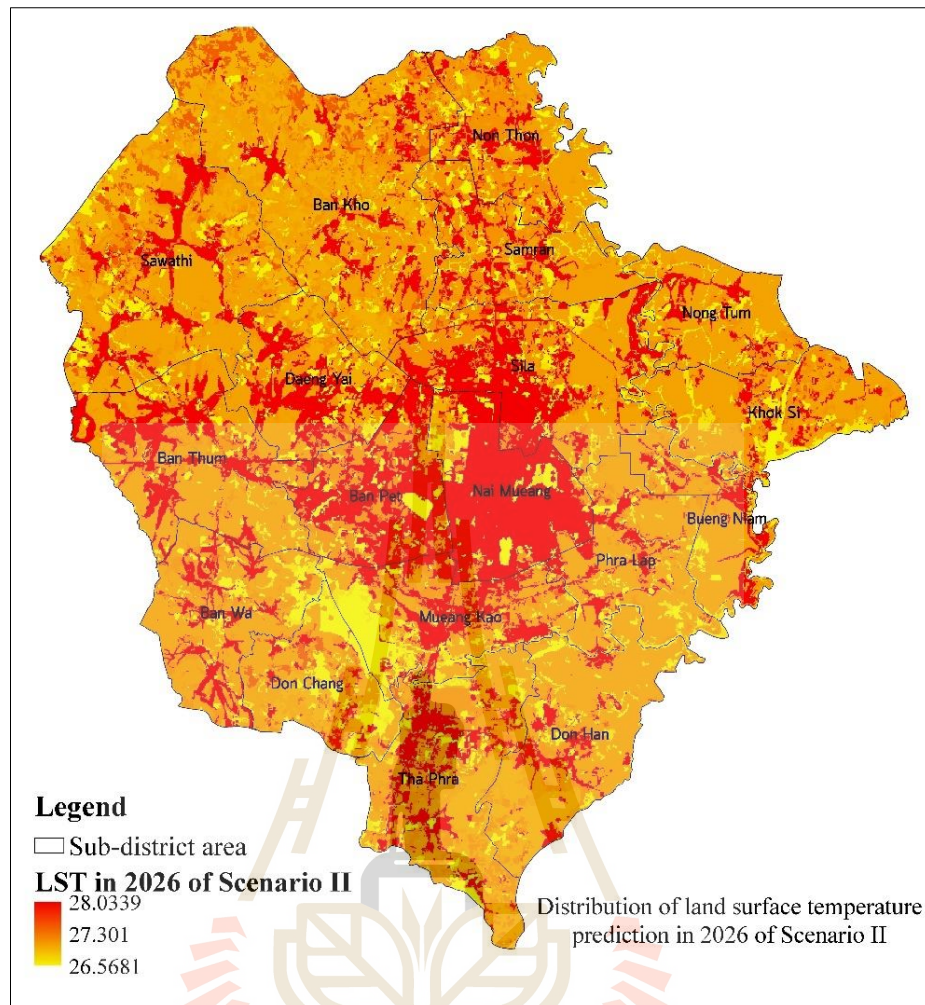**Figure 8.8** Spatial distribution of predicted LST data in 2026 of Scenario II based on the relationship between LST data and multiple landscape metrics in 2016.

Table 8.4 Basic statistical data of the predicted LST data in 2026 of 2 scenarios based on the relationship between overall LST data and multiple landscape metrics in 2016.

Year	Land surface temperature in $^{\circ}$C		
	Min	Max	Mean
2026 scenario I	26.567	28.016	27.291
2026 scenario II	26.568	28.039	27.301

As results, it can be observed that LST data in 2026 of Scenario I ranges from 26.567 to 28.016°C and mean LST data is 27.291°C. In addition, the lowest temperature is mostly located over water bodies while the highest temperature is found at urban and built-up area.

In the meantime, LST data in 2026 of Scenario II varies from 26.568 to 28.039°C and mean LST data is 27.301°C. Like Scenario I, the lowest temperature is located over water bodies while the highest temperature is found at urban and built-up area.

In summary, it can be observed that range and mean of LST data in 2026 of LULC of Scenario II is higher than LST data of LULC of Scenario I (Table 8.4). This finding shows influence of transformation of policy on LULC change, particularly urban growth on LST.

Finally, the derived predictive LST data of two scenarios from three different approaches based on (1) overall LST and class area metric in 2016, (2) zonal LST and class area metric in 2016 and (3) overall LST and multiple landscape metrics in 2016 were here compared and justified an optimum approach for LST prediction. Herewith, comparison of basic statistical data of predictive LST deriving from three different

methods is summarized in Table 8.5 and Table 8.6 presents correlation coefficient (r) and coefficient of determination (r2) values from multiple linear regression analysis.

Table 8.5 Basic statistical data of predictive LST deriving from three different methods.

Method	Scenario I				Scenario II			
	Min	Max	Range	Mean	Min	Max	Range	Mean
Overall LST and class area metric	31.881	32.433	0.552	32.258	30.349	31.282	0.993	31.078
Zonal LST and class area metric	26.616	27.725	1.065	27.185	26.656	27.725	1.069	27.239
Overall LST and multiple landscape metrics	26.567	28.016	1.449	27.291	26.568	28.039	1.471	27.301

Table 8.6 Correlation coefficient (r) and coefficient of determination (r^2) values of multiple linear regression analysis from three different methods.

Method	r	r2	Ranking
Overall LST and class area metric	0.651	0.424	2
Zonal LST and class area metric: High urbanization	0.612	0.374	3
Zonal LST and class area metric: Very high urbanization	0.546	0.298	4
Overall LST and multiple landscape metrics	0.766	0.586	1

As results, it can be observed that the predicted LST data from 2 LULC scenarios (Scenario I: Historical land use development and Scenario II: Planning and policy) based on overall LST data and multiple landscape metrics in 2016 can provide the highest range with amount of 1.449 and 1.471, respectively. Additionally, the relationship between overall LST data and multiple landscape metrics in 2016 can provide the highest correlation coefficient (r) and coefficient of determination (r^2) values with value of 0.766 and 0.586, respectively. Furthermore, the derived LST range of this approach is reasonable to apply for describing LST value of various LULC types which include (1) urban and built-up area, (2) paddy field, (3) field crop, (4), forest land, (5) water body (6), marsh and swamp, (7) range land and (8) unused land (bare

land and land fill, pits). The significant independent variables which can explain the relationship with overall LST about 60% include most of LULC type, i.e. landscape metrics of urban and built-up area, forest land, water body, marsh and swamp, and unused land. Consequently, overall LST and multiple landscape metrics approach is here chosen an optimum approach to predict LST in this study.

In addition, the optimum relationship between overall LST and multiple landscape metrics in this study indicates that both the composition and configuration of LULC features significantly affects the magnitude of LST. By explicitly describing the quantitative relationships of LST with the composition and configuration of LULC features; this study develops to understanding of the effects of LULC pattern on overall LST in urban landscapes. These results have important theoretical and management implications. Urban planners and natural resource managers attempting to mitigate the impact of urban development on UHI can gain insights into the importance of balancing the relative amount of various types of land cover features and optimizing their spatial distributions (Zhou, Huang and Cadenasso, 2011).

CHAPTER IX

CONCLUSION AND RECOMMENDATIONS

Under this chapter, five main results which were reported according to objectives in the study including (1) land use and land cover extraction and simulation (Chapter IV), (2) urban growth impact on urban landscape ecology (Chapter V), (3) impact of urban growth on ecosystem service value (Chapter VI) , (4) ecosystem service function value and urban landscape metrics relationship (Chapter VII) and (5) impact of urban landscape change on land surface temperature (Chapter VIII) are here separately concluded and some recommendations are suggested for future research and development.

9.1 Conclusion

9.1.1 Land use and land cover extraction and simulation

(1) Land use and land cover extraction

LULC types in 2006, 2011 and 2016 were here classified from Landsat -7 ETM+ and Landsat 8 OLI data using OBIA with standard nearest neighbor classifier and feature space optimization. The most significant LULC type in 2006, 2011, and 2016 was paddy field covering an area of 556.20, 517.84, 451.39 km^2 or 56.63, 52.72, 45.96% of the study area, respectively. At the same time, the second dominant LULC type was field crop accounting for 207.40, 189.81 and 148.04 km^2 or 21.12, 19.32 and

15.07% of the study area, respectively and the third important LULC category was urban and built-up area covering area of 58.03, 87.14 and 131.75 km^2 or 5.91, 8.87 and 13.41% of the study area, respectively. In addition, the classified LULC in 2006, 2011, and 2016 were compared with ground information for accuracy assessment, it was found that the overall accuracy were 83.88%, 81.24% and 85.34% and Kappa hat coefficient of agreement were 74.78%, 72.56% and 80.24% respectively.

(2) Land use and land cover simulation

Two scenarios of LULC change in 2026 including Scenario I: Historical land use development and Scenario II: Planning and policy were here simulated based on an optimum local parameters of CLUE-S model with a specific land use requirement for each scenario. It was found that the most significant LULC type of Scenario I and II was paddy field covering an area of 342.84 km^2 and 342.33 km^2 or 34.91% and 34.86% of the study area, respectively. Meanwhile, the second dominant LULC type of both scenarios was urban and built-up area accounting for 217.27 km^2 and 223.99 km^2 or 22.12% and 22.81% of the study area, respectively and the third important LULC category was range land covering area of 178.7 km^2 and 174.99 km^2 or 18.20% and 17.82% of the study area, respectively.

In addition, the most significant driving factor for all LULC type allocation except unused land in the study area was distance to road network. Meanwhile the second important driving factors for LULC type allocation were elevation, slope, and distance to existing urban area whereas the third important driving factors for LULC type allocation area was distance to stream.

Furthermore, major LULC types with decreasing areas during 2006 to 2026 of both scenarios were paddy field and field crop whereas areas of urban and built-

up area will continuously increase. This result shows effect of policy on city development, particularly a signing MOU between TCEB and Khon Kaen Municipality in 2013 to promote Khon Kaen province as Thailand's fifth MICE City.

(3) Characteristic of urban growth

According to AEII value at district level during 2006 to 2026 (Scenario I and II), most of AEII values at district level during 2006 and 2011 showed medium speed expansion while most of AEII values showed fair speed expansion during 2011 to 2016. Meanwhile, most of AEII values showed high speed expansion during 2016 to 2026 (Scenario I and II). This find infers that urban area will increase more in the future.

Likewise, according to PU values at district level during 2006 to 2026 (Scenario I and II), most of PU values in 2006 and 2011 showed moderate urbanization whereas PU values in 2016 showed high urbanization with number of 11 sub-districts and very high urbanization with number of 7 sub-districts. Meanwhile, PU values of Scenario I in 2026 showed high urbanization with number of 4 sub-districts and very high urbanization with number of 14 sub-districts whereas PU values of Scenario II in 2026 showed high urbanization with number of 2 sub-districts and very high urbanization with number of 16 sub-districts. This finding shows future trend of urbanization due to transformation of planning and policy on urban growth under Scenario II.

Meanwhile, according to SI values at district level during 2006 to 2026 (Scenario I and II) urban land expansion index of two periods (2006 - 2011 and 2011 - 2016) showed more rapid development whereas urban land expansion index between 2016 and 2026 (Scenarios I and II) showed dramatic development. This finding infers that more land will develop to urban area in the future.

9.1.2   Urban growth impact on urban landscape ecology

(1) Status and change of urban landscape

Under area and edge metrics group, class area (CA), percent of landscape (PLAND), edge density (ED), and total edge density (TE) of paddy field, field crop, forest land, marsh and swamp and water body landscape types had been decreased between 2006 and 2026 (Scenario I and II). This finding indicates that these landscape types will more fragment in the future, particularly paddy field and field crop. Meanwhile, CA, PLAND, ED and TE of urban and built-up area, range land and unused land had been increased during these times. This indicates that these landscape types will more expand in these periods, particularly urban and built-up area and range land.

Under shape metrics group, area-weighted fractal dimension (FRAC_AM) and area-weighted mean shape index (SHAPE_AM) of paddy field, field crop, forest land and water body landscape types had been decreased between 2006 and 2026 (Scenario I and II). This finding indicates that the regularity shape of these landscape types will decrease in the future. Meanwhile, FRAC-AM and SHAPE_AM of urban and built-up area, range land and unused land landscape types had been decreased during these periods. This finding indicates that these landscape types will be more growth and dispersed, especially urban and built-up area.

Under aggregation metric group, number of patch (NP), patch density (PD) and Contagion (C) of paddy field, field crop, forest land and water body landscape types had been decreased during 2006 to 2016 while interspersion and juxtaposition index (IJI) and landscape shape index (LSI) of them had been increased. This finding indicates that these landscape types became more compact and fragmentation. In contrast, NP, PD, C, interspersion and juxtaposition index (IJI) and landscape shape

index (LSI) of urban and built-up area, range land and unused land landscape types had been increased. This finding implies that that these landscape types become more fragmentation and landscape configuration. Additionally, during 2016 to 2026 of Scenario I, NP, PD, LSI, C of urban and built-up area, field crop, forest land, marsh and swamp, range land and unused land had been increased but IJI had been increased. These findings imply that these landscape types will be more fragmentation and less landscape configuration. Furthermore, during 2016 to 2026 Scenario II, urban and built-up area, field crop, forest land, marsh and swamp, range land and unused land had been exposed IJI and C had been decreased while NP, PD and LSI had been increased. This finding implies that these landscape types will more fragmentation, configuration and complexity and the degree of fragmentation will decrease.

Under diversity metric group, Shannon's diversity index (SHDI) and Shannon's Evenness Index (SHEI) of the whole landscape had been increased during 2006 to 2016, and it indicates that landscape becomes more fragmentation and more distribution of patch types among landscape types. Meanwhile, in 2026 of Scenario I SHDI had been increased but SHEI had been decreased, it indicates that less distribution and more fragmentation among landscape types will occur in the future. However, SHDI and SHEI of Scenario II had been increased, it indicates that more fragmentation and more distribution among landscape types will occur in the future.

(2) Status and change of urban and built-up area

Urban and built-up area had been continuously increased between 2006 and 2026 of two scenarios, this finding implies that this landscape will be more expansion and complexity in irregularity. In addition, by comparison between scenario I and II, it was found that urban and built-up area landscape of Scenario I is more

modification than Scenario II, since the urban and built-up area under Scenario-II is modified with specific policy and plan.

(3) Landscape metrics and urban growth pattern relationship

The relationship between urban growth pattern in 2016 which was represented by percent of urban and built–up area (PLAND) and selected landscape metrics at class level including ED, TE, FRAG_AM, SHAPE_AM, LSI, NP and PD was here analyzed the spatial linear relationship with bivariate correlation analysis. It can be concluded that area-weighted mean fractal dimension (FRAC_AM) metrics is the optimum landscape metrics to characterize urban growth pattern (pattern of urban and built-up area) since it can provide the highest r and r^2. This implies that pattern of urban and built-up area is strongly positive correlation with the area-weighted mean fractal dimension and the proportion of the total variation in the value of urban and built-up area pattern can be explained by a linear relationship with the value of the area-weighted mean fractal dimension pattern about 71%.

9.1.3 Impact of urban growth on ecosystem service value

(1) Valuation of ecosystem service function

Top three dominant ecosystem service functions from dynamic LULC data in the study area during 2006 and 2026 of Scenario I and II were waste treatment, water supply, and climate regulation with ESFV of 42.96, 32.18 and 20.57 million USD in 2006, 41.52, 31.67 and 19.89 million USD in 2011, 39.32, 31.14 and 18.92 million USD in 2016, 35.45, 30.03 and 17.22 million USD in 2026 of Scenario I and 35.42, 29.98 and 17.14 million USD in 2026 of Scenario II, respectively.

Meanwhile, according to LULC type it was found that top three dominant LULC types that provide the highest total ESFV during 2006 and 2026 of

two scenarios were paddy field, water body and marsh and swamp with value of 57.40, 36.30 and 31.52 million USD in 2006, 53.46, 36.10 and 30.74 million USD in 2011, 46.60, 36.05 and 30.28 million USD in 2016, 35.78, 35.39 and 29.36 million USD in 2026 of Scenario I, and 35.82, 35.34 and 29.49 million USD in 2026 of Scenario II, respectively.

(2) Change of ecosystem service function values

During 2006 to 2011, the total ecosystem service function values decreased with value of 4.62 million USD or 2.94%. Likewise, the total ecosystem service function values decreased with value of 7.14 million USD or 4.69% during 2011 to 2016. Meanwhile, the total ecosystem service function values decreased with value of 12.50 million USD or 8.61% during 2016 to 2026 of Scenario I and the total ecosystem service function values decreased with value of 13.13 million USD or 9.04% during 2011 to 2026 of Scenario II. Herein, waste treatment service function was the most decreased ecosystem service function during these periods. On contrary, recreation and culture service function had been increased during these periods. Additionally, all values of ecosystem service functions under Scenario II (Planning and policy) were lower than Scenario I (Historical land use development). This finding shows the effect of planning and policy on ecosystem service function in the future.

In summary, LULC change plays important role on an overall ecosystem services function value with variation in the spatial distribution and temporal change in the ecosystem services. In this study, an increasing of urban and built up areas, range land and unused land and decreasing of paddy field, field crop, forest land, water body, and marsh and swamp lead to decrease total ecosystem service function value in the future. In addition, Scenario II (Planning and policy) will provide total ecosystem service

function value less than Scenario I (Historical land use development). Consequently, land use planner or city planner who responsible for land use planning or city planning should try to minimize the effect of LULC change on ecosystem service function by balancing ESFV during planning process.

9.1.4 Ecosystem service function value and urban landscape metrics relationship

The relationship between ecosystem service function value and urban landscape metrics are defined from multiple linear regression analysis. It was found that, percent of landscape (PLAND) of different LULC types was the most dominant independent variables to describe ESV of ecosystem service function both positive and negative relationship, except food production service function that was dominant by patch density (PD).

In addition, the significant landscape metrics can provide very strong correlation with all ecosystem service function values and they can be applied to predict ecosystem service function value varies from 73% to 88%.

9.1.5 Impact of urban growth on land surface temperature evaluation and prediction

Land surface temperature (LST) in 2016 was here extracted based on standard conversion method. It was found that, temperature varied from 18.799 to 34.468ºC and mean temperature was 27.07ºC. In addition, it was found that the highest temperature is mostly found at urban and built-up area such as airport or CBD at the center of the study area.

In addition, multiple linear regression analysis was firstly employed to model the statistical relationship between overall and zonal LST in and single and

multiple landscape metrics using three approaches: (1) overall LST and class area (CA) metric, (2) zonal LST and class area (CA) metric and (3) overall LST and multiple landscape metrics (PLAND, FRAG_AM and PD) of each LULC type, then the derived relationships between LST and its landscape metric were separately applied to predict LST data in 2026 of 2 scenarios. As results of LST prediction, it can be observed that range and mean of LST data in 2026 from three different approaches of LULC of Scenario II was higher than LST data of LULC of Scenario I. This finding shows influence of transformation of policy on LULC change, particularly urban growth on LST. Additionally, it can be observed that the predicted LST data from 2 LULC scenarios (Scenario I: Historical land use development and Scenario II: Planning and policy) based on overall LST data and multiple landscape metrics relationship can provide the highest range with amount of 1.449 and 1.471, respectively and the derived relationship can provide the highest r and r^2 values with value of 0.766 and 0.586, respectively. Furthermore, the derived LST range of this approach is reasonable to apply for describing LST value of various LULC types which include (1) urban and built-up area, (2) paddy field, (3) field crop, (4), forest land, (5) water body (6), marsh and swamp, (7) range land and (8) unused land (bare land and land fill, pits). Consequently, overall LST and multiple landscape metrics relationship was here chosen an optimum approach to predict LST.

In conclusion, it appears that the integration of remote sensing technology, geospatial models (CLUE-S model) and landscape ecology and ecosystem service evaluation can be used as capable tools to quantify LULC status and its change and to assess urban growth impact on urban landscape ecology, ecosystem services and LST.

9.2   Recommendations

Many objectives were taken into account with assessment of LULC extraction and simulation, assess urban growth impact on urban landscape ecology and ecosystem services, identify relationship between ecosystem service function value and landscape pattern metrics and evaluate and predict impact of urban growth on land surface temperature, in Mueang Khon Kaen district, Khon Kaen province. The possibly expected recommendations could be made for further studies as follows:

(1) For LULC classification method, it should be considered another method to increase accuracy of thematic map, for example the Random Forests classifier.

(2) For study driving force for LULC change, it should be considered more significant factors at local scale (social factor and culture) since driving factor plays an important role for land allocation under CLUE-S model based on binary logistic regression analysis.

(3) For land surface temperature prediction, it should examine more spatio-temporal LST data with linear and non-linear multiple regression model and validate the result for quantify the best regression model for LST prediction.

REFERENCES
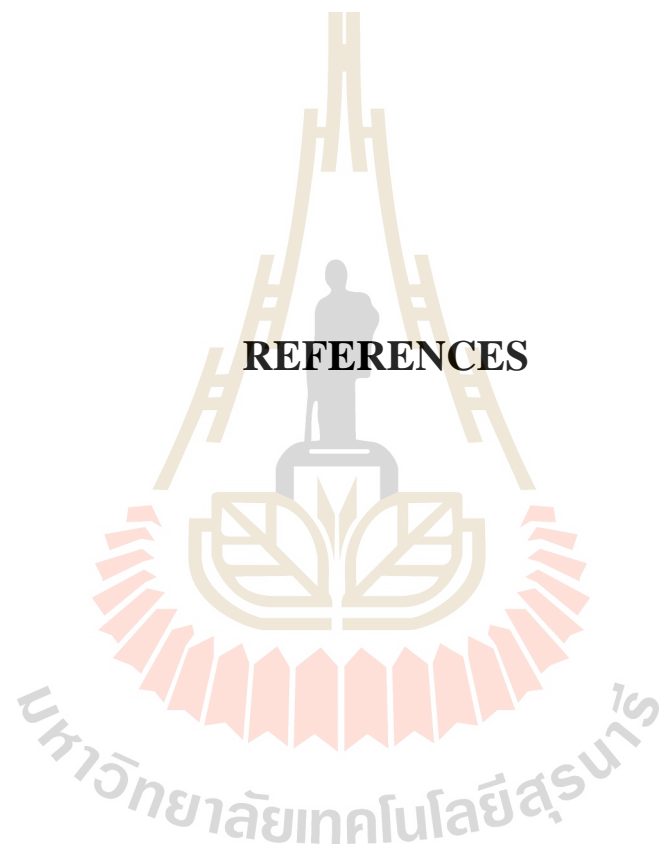
REFERENCES

Aburas, M. M., Abdullah, S. A., Ramli, M. F., and As'shari, Z. H. (2016). Landscape analysis of urban growth patterns in Seremban, Malaysia, using spatio-temporal data. in IOP conference series: **Earth and Environmental Science.** IOP Publishing.

Afrakhteh, R., Asgarian, A., Sakieh, U., and Soffianian, A. (2016). Evaluating the strategy of integrated urban-rural planning system and analyzing its effects on land surface temperature in a rapidly developing region. **Habitat International**. 56:147–156

Afridi, I. (2015). **Khon Kaen – growth and emerging challenges in secondary cities in Thailand.** [On-line]. Available: http://urbanclimateresiliencesea. apps01.yorku.ca/eventactivity/khonkaengrowthandemergingchallengesinsecon darycitiesinthailand/.

Aguilera, F., Valenzuela, L. M., and Botequilha-Leitão, A. (2011). Landscape metrics in the analysis of urban land use patterns: A case study in a Spanish metropolitan area. **Landscape and Urban Planning**. 99: 226–238.

Akin, A., Aliffi, S., and Sunar, F. (2014). Spatio-temporal Urban Change Analysis and the Ecological Threats Concerning The Third Bridge in Istanbul City. Int. Arch. Photogramm. Remote Sens. **The International Archives of the Photogrammetry, Remote Sensing and Spatial Information Sciences Technical Commission VII Symposium**. XL-7: 9–14.

Al-shalabi, M., Billa, L., Pradhan, B., Mansor, S., and Al-Sharif, A. A. A. (2013). Modelling urban growth evolution and landuse changes using GIS based

cellular automata and SLEUTH models the case of Sana'a metropolitan city, Yemen. **Environmental Earth Sciences**. 70: 425–437.

Antrop, M. (2001). The language of landscape ecologists and planners. A comparative content analysis of concepts used in landscape ecology. **Landscape and Urban Planning.** 55: 163–173.

Baker, W. L., and Cai, Y. (1992). The r.le programs formultiscale analysis of landscape structure using the GRASS geographical information system. **Landscape Ecology.** 7: 291–302.

Barnes, K. B., Morgan, J. M., III, Roberge M. C., and Lowe, S. (2001). Sprawl Development: Its Patterns, Consequences, and Measurement. **A white paper, Towson University.** [On-line]. Available: http://chesapeake.towson.edu/landscape/urbansprawl/download/Sprawl_white _paper.pdf.

Batty, M. (2002). Thinking about cities as spatial events. **Environ. Plann.** B 29: 1–2.

Benfield, F. K., Raimi, M., and Chen, D. (1999). Once ThereWere Greenfields: How Urban Sprawl Is Undermining America's Environment. **Economy and Social Fabric.** The Natural Resources Defense Council, Washington, DC.

Berling-Wolf, S., Wu, J. (2004). Modelling urban landscape dynamics: a case study in Phoenix, USA. **Urban Ecosystems.** 7: 215–240.

Bernales, A. M., Antolihao, A., Samonte, C., Campomanes, F., Rojas, R. J., Serna, A. M. d., and Silapan, J. (2016). Modelling the relationship between land surface temperature and landscape patterns of land use land cover classification using multi linear regression models. In **The International Archives of the**

Photogrammetry, Remote Sensing and Spatial Information Sciences, Prague, Czech Republic.

Berry, D., and Plaut, T. (1978). Retaining agricultural activities under urban pressures: a review of land use conflicts and policies**. Policy Sciences.** 9: 153–178.

Bettini, V., Gianoni, P., Di Noto, F., Stevanin, M., and Zannin, D. (2001). Landscape ecologye la teoria della percolazione in ecologia urbana: un'applicazione alla revisions di un PRG: il caso Pozzallo, Ragusa (Landscape ecology and percolation theory in urban ecology: an application in the Masterplan of Pozzallo, Italy). **Arpa Ecosistemi Urbani**. Bologna (in Italian).

Bhatta, B. (2010). Causes and Consequences of Urban Growth and Sprawl. **Analysis of Urban Growth and Sprawl from Remote Sensing Data** (pp. 17-48): Springer-Verlag Berlin Heidelberg.

Bihamta, N., Soffianian, A., Fakheran, S., and Gholamalifard, M. (2014). Using the SLEUTH Urban Growth Model to Simulate Future Urban Expansion of the Isfahan Metropolitan Area. **Journal of the Indian Society of Remote Sensing.**

Bihamta, N., Soffianian, A., Fakheran, S., and Gholamalifard, M. (2015). Using the SLEUTH Urban Growth Model to Simulate Future Urban Expansion of the Isfahan Metropolitan Area. **Journal of the Indian Society of Remote Sensing.** 43(2): 407–414.

Botequilha-Leitão, A., Miller, J., Ahern, J., and Mcgarigal, K. (2006). Measuring Landscapes. **A Planner's Handbook.** Island Press, Washington, DC.

Buiton, P. J. (1994). A vision for equitable land use allocation. **Land Use Policy**. 12(1): 63–68.

Burchell, R. W., Downs, A., McCann, B., and Mukherji, S. (2005). **Sprawl Costs: Economic Impacts of Unchecked Development.** Washington, DC: Island Press.

Burchfield, M., Overman, H., Puga, D., and Turner, M. (2006). Causes of sprawl: a portrait from space. **Quarterly Journal of Economics.** 121(2): 587–633, May 2006.

Burgess, E. W. (2008). The Growth of the City: An Introduction to a Research Project. In J. M. Marzluff, E. Shulenberger, W. Endlicher, M. Alberti, G. Bradley, C. Ryan, U. Simon, and C. ZumBrunnen (eds.). **Urban Ecology: An International Perspective on the Interaction Between Humans and Nature** (pp. 71–78). Boston, MA: Springer US.

Castella, J-C., Kamb, S. P., Quangc, D. D., Verburg, P. H., and Hoanh, C. T. (2007). Combining top-down and bottom-up modeling approaches of land use/cover change to support public policies: Application to sustainable management of natural resources in northern Vietnam. **Land Use Policy.** 24(3): 531–545.

Chander, G., and Markham, B. (2003). Revised Landsat-5 TM radiometric calibration procedures and postcalibration dynamic ranges. **IEEE Transactions on Geoscience and Remote Sensing**. 41 (11): 2674–2677.

Congalton, R. G., and Green, K. (2009). **Assessing the accuracy of remotely sensed data: principles and practices.** Florida, USA: CRC Press.

Connors, J.P., Galletti, C. S., and Chow, W. T. (2013). Landscape configuration and urban heat island effects: assessing the relationship between landscape characteristics and land surface temperature in Phoenix, Arizona. **Landscape Ecology.** 28(2):271–283.

Corry, R. C., and Nassauer, J. (2005). Limitations of using landscape pattern indices to evaluate the ecological consequences of alternative plans and designs. **Landsc. Urban Plann.** 72: 265–280.

Costanza, R., d'Arge, R., Groot, R. d., Farberk, S., Grasso, M., Hannon, B., and Belt, M. v. d. (1997). The value of the world's ecosystem services and natural capital. **Nature**. 387: 253–260.

Costanza, R., Groot, R. d., Sutton, P., Ploeg, S. v. d., Anderson, S. J., Kubiszewski, I Ida, K., Stephen, F., and Turner, R. K. (2014). Changes in the global value of ecosystem services. **Global Environmental Change**. 26: 152–158.

Crawford, T. W. (2007). Where does the coast sprawl the most? Trajectories of residential development and sprawl in coastal North Carolina, 1971–2000. **Landscape and Urban Planning.** 83: 294–307.

Daily, G. C. (ed.). (1997). Nature's Services: **Societal Dependence on Natural Ecosystems.** Washington, DC: Island Press.

Daily, G. C., Polasky, S., Goldstein, J., Kareiva, P. M., Mooney, H. A., Pejchar, L., Ricketts, T. H., Salzman, J., and Shallenberger, R. (2009). Ecosystem services in decision making: time to deliver. **Frontiers in Ecology and the Environment**. 7(1): 21–28

De Souza Soler, L., Verburg, P., and Veldkamp, A. (2007). Statistical analysis and feedback exploration of land use change determinants at local scale in the Brazilian Amazon. **In Geoscience and Remote Sensing Symposium 2007** (pp 3462–3465). IGARSS: IEEE International.

Deng, J. S., Wang, K., Hong, Y., and Qi, J. G. (2009). Spatio-temporal dynamics and evolution of land use change and landscape pattern in response to rapid urbanization. **Landscape and Urban Planning.** 92: 187–198.

Dhabhalabutr, K. (2011). Process and Impact of Urban Driving Force to the Development of Khon Kaen City, Thailand. Paper presented at the **Spaces and Flows: Second International Conference on Urban and ExtraUrban Studies.**, Monash University Prato Centre, Prato, Tuscany, Italy.

DiBari, J. (2007). Evaluation of five landscape-level metrics for measuring the effects of urbanization on landscape structure: the case of Tucson, Arizona, USA. Landsc. **Urban Plann.** 79: 308–313.

Dunn, C. P., Sharpe, D. M., Guntensbergen, G. R., Stearns, F., and Yang, Z. (1991). Methods for analyzing temporal changes in landscape pattern. In: M.G. Turner and R.H. Gardner (eds.). **Quantitative Methods in Landscape Ecology: The Analysis and Interpretation of Landscape Heterogeneity** (pp 173–198). New York: Springer Verlag.

Ecosystem Assessment, M. (2005). Ecosystems and Human Well-being: **A Framework for Assessment.** Washington, DC: Island Press.

Elmqvist, T., Redman, C. L., Barthel, S., and Costanza, R. (2013). Urbanization, Biodiversity and Ecosystem Services: Challenges and Opportunities. In M. F. Thomas Elmqvist, Julie Goodness, Burak Güneralp, Peter J. Marcotullio, Robert I. McDonald, Susan Parnell, Maria Schewenius, Marte Sendstad, Karen C. Seto, Cathy Wilkinson (eds.). **A Global Assessment: A Part of the Cities and Biodiversity Outlook Project.** New York London: Springer Dordrecht Heidelberg.

Elmqvist, T., Setälä, H., Handel, S., Ploeg, S. v. d., Aronson, Blignaut, J., and Groot, R. d. (2015). Benefits of restoring ecosystem services in urban areas. **Current Opinion in Environmental Sustainability.** 14: 101–108.

er.pdf.

Estoque, R. C., and Murayama, Y. (2013). Landscape pattern and ecosystem service value changes: Implications for environmental sustainability planning for the rapidly urbanizing summer capital of the Philippines. **Landscape and Urban Planning.** 116: 60–72.

Ewing, R. (1997). Is Los Angeles-style sprawl desirable?. **Journal of the American Planning Association.** 63(1): 107–126.

Fan. Q., and Ding, S. (2016). Landscape pattern changes at a county scale: A case study in Fengqiu, Henan Province, China from 1990 to 2013. **Catena.** 137: 152–160.

Fang. X., Tang. G., Li. B., and Han. R. (2014). Spatial and Temporal Variations of Ecosystem Service Values in Relation to Land Use Pattern in the Loess Plateau of China at Town Scale. **PLoS One.** 9(10): e110745. Published online 2014 Oct 20. doi: 10.1371/journal.pone.0110745.

Farina, A. (1998). **Principles and Methods in Landscape Ecology**. Chapman & Hall, London.

Farrow, A., and Winograd, A. (2001). Land use modelling at the regional scale: an input to rural sustainability indicators for Central America. **Agriculture, Ecosystems & Environment.** 85(1–3): 249–268.

Fichera, C. R., Modica, G., and Pollino, M. (2017). Land Cover classification and change-detection analysis using multi-temporal remote sensed imagery and

landscape metrics. **European Journal of Remote Sensing.** 45: 1, 1–18, DOI: 10.5721/EuJRS20124501.

Fischel, W. A. (1982). The urbanization of agricultural land: a review of the National Agricultural Lands Study. **Land Economics.** 58(2): 236–259.

Fishera, B., Turnera, K., and Morlingb, P. (2009). Defining and classifying ecosystem services for decision making. **Ecological Economics.** 68: 643–653.

Fitzpatrick-Lins, K. (1981). Comparison of sampling procedures and data analysis for a land-use and land-cover map. **Photogrammetric Engineering and Remote Sensing.** 47(3):343-51.

Forman, R. T. T. (1995). **Land mosaics: the ecology of landscapes and regions.** Cambridge University Press, Cambridge.

Forman, R. T. T., and Godron, M. (1986). **Landscape Ecology.** Wiley, New York.

Freemark, K., Hummon, C., White, D., and Hulse, D. (1996). Modeling risks to biodiversity in past, present and future landscapes. Technical Report No. 268. **Canadian Wildlife Service.** Ottawa, 60 pp.

Frumkin, H. (2002). Urban sprawl and public health. **Public Health Report.** 117: 201–217.

Gabriel, S. A., Fariaa, J. A., and Moglen, G. E. (2006). A multiobjective optimization approach to smart growth in land development. **Socio-Economic Planning Sciences.** 40: 212–248.

Gao-di, X., Chun-xia, L., Yun-fa, L., Du, Z., and Shuang-cheng, L. (2003). Ecological assets valuation of Tibeta Plateau. **Journal of Natural Resources.** 18(2): 189–196.

Gaodi, X., Lin, Z., Chunxi, L., Yu, X., and Wenhua, L. (2010). Applying Value Transfer Method for Eco-Service Valuation in China. **Journal of Resources and Ecology.** 1(1): 51–59.

Githui, F., Mutua, F., and Bauwens, W. (2009). Estimating the impacts of land-cover change on runoff using the soil and water assessment tool (SWAT): case study of Nzoia catchment, Kenya. **Hydrological Sciences.** 54(5): 899–908.

Gómez-Baggethun, E., and Barton, D. N. (2013). Classifying and valuing ecosystem services for urban planning. **Ecological economics.** 86: 235–245.

Grimm, N. B., Grove, J. M., Pickett, S. T. A., and Redman, C. L. (2000). Integrated approaches to long-term studies of urban ecological systems. **BioScience.** 50 7: 571–584.

Groot, R. d., Brander, L., Sander, v. d. P., Costanza, R., Bernard, F., Braat, L., Christie, M., Crossman, N., Ghermandi, A., Hein, L., Hussain, S., Kumar, P., McVittie, A., Portela, R., Rodriguez, L. C., Brink, P. t., and Pieter, v. B. (2012). Global estimates of the value of ecosystems and their services in monetary units. **Ecosystem Services**. 1: 50–61.

Guillevic P. C., Privette J. L., Coudert B., Palecki M. A., Demarty J., and Ottlé C. (2012). Land Surface Temperature product validation using NOAA's surface climate observation networks - Scaling methodology for the Visible Infrared Imager Radiometer Suite (VIIRS). **Remote Sensing of Environment.** 124: 282–298.

Gustafson, E. J. (1998). Quantifying landscape spatial pattern: what is the state of the art? **Ecosystems.** 1: 143–156.

Hardin, P. J.; Jackson, M. W.; and Otterstrom, S. M. (2007). Mapping, Measuring, and Modeling Urban Growth. In Jensen, J.D. Gatrell and D. McLean (eds.). **Geo-Spatial Technologies in Urban Environments.** (2nd ed., pp. 141–176). Berlin/Heidelberg, Germany: Springer.

Harvey, R. O., and Clark, W. A. V. (1965). The nature and economics of urban sprawl. **Land Economics.** 41(1): 1–9.

Hedblom, M., and Soderstrom, B. (2008). Woodlands across Swedish urban gradients: status, structure and management implications. **Landscape and Urban Planning** 84: 62–73.

Hergis, C. D., Bissonette, J. A., and David, J. L. (1998). The behavior of landscape metrics commonly used in the study of habitat fragmentation. **Landscape Ecology.** 13: 167–186.

Herold, M., Couclelis, H., and Keith C. Clarke. (2005). The role of spatial metrics in the analysis and modeling of urban land use change. **Computers, Environment and Urban Systems.** 29: 369–399.

Herold, M., Goldstein, N. C., and Clarke, K. C. (2003). The spatial temporal form of urban growth: measurement, analysis and modeling. **Remote Sensing Environ.** 86: 286–302.

Herold, M., Hempholl, j., and Clarke, K. C. (2007). Remote Sensing and Urban Growth theory. In Q. Weng and D. A. Quattrochi (eds.), **Urban Remote Sensing** (pp. 201–219). Broken Sound Parkway NW: CRC Press Taylor & Francis Group.

Herold, M., Menz, G., and Clarke, K. C. (2001). Remote Sensing and Urban Growth Models – Demands and Perspectives. In **The Symposium on remote sensing of urban areas.** Regensburg, Germany.

Hu, Z-L., Du, P-J., and Guo, D-Z. (2007). Analysis of urban expansion and driving forces in Xuzhou city based on remote sensing. **Journal of China University of Mining and Technology.** 17(2), 267–271

Hualou Long, Y. L., Xuegang Hou, Tingting Li and Yurui Li (2014). Effects of land use transitions due to rapid urbanization on ecosystem services: Implications for urban planning in the new developing area of China. **Habitat International.** 44: 536–544.

Huang, J., Lu, X. X., and Sellers, J. M. (2007). A Global Comparative Analysis of Urban Form: Applying Spatial Metrics and Remote Sensing. **Landscape and Urban Planning.** 82: 184–197.

Iamchuen, N. (2014). **Intergration of geospatial models for an optimal land use allocation using land use and land cover changes and their impacts in upper Lam Phra Phloeng watershed, Nakhon Ratchasima province, Thailand.** Ph.D. Dissertation, Suranaree University of Technology.

Jacquin, A., Misakova, L., and Gay, M. (2008). A hybrid object-based classification approach for mapping urban sprawl in periurban environment. **Landscape and Urban Planning.** 84: 152–165.

Jan Haas, D. F., and Yifang Ban. (2015). Satellite monitoring of urbanization and environmental impacts - A comparison of Stockholm and Shanghai. **International Journal of Applied Earth Observation and Geoinformation**. 38: 138–149.

KHON KAEN (2015). **Provincial statistical report: 2014.** [On-line]. Available: Statistical Forecasting Bureau, National Statistical Office: http://khonkaen.nso.go.th/index.php.

Kikuchi, H., Fukuda, A., and Fukuda, F. (2014). Study on the Impact of CO^2 Emission Depending on Change of the Urban Structure: Case Study of Khon Kaen, Thailand. In **The 32nd International Conference of the System Dynamics Societ.** Delft, Netherlands.

Kikuko Shoyama, and Yoshiki Yamagata. (2014). Predicting land-use change for biodiversity conservation and climate-change mitigation and its effect on ecosystem services in a watershed in Japan. **Ecosystem Services**. 8: 25–34.

Kim, J., and Ellis, C. (2009). Determining the effects of local development regulations on landscape structure: comparison of the woodlands and North Houston, TX. **Landscape and Urban Planning.** 92: 293–303.

Kindu, M., Schneider, T., Teketay, D., and Knoke, T. (2016). Changes of ecosystem service values in response to land use/land cover dynamics in Munessa–Shashemene landscape of the Ethiopian highlands. **Science of the Total Environment.** 547: 137–147.

Kong, F., Yin, H., Nakagoshi, N., and James, P. (2012). Simulating urban growth processes incorporating a potential model with spatial metrics. **Ecological Indicators.** 20, 82–91.

Kreuter, U. P., Harris, H. G., Matlock, M. D., and Lacey, R. E. (2001).Change in ecosystem service values in the San Antonio area, Texas. **Ecological Economics** 39, 333–346.

Kunstler, J. H. (1993). **The Geography of Nowhere.** New York: Touchstone Books.

Lal. K., Kumar. D., and Kumar. (2017). A. Spatio-temporal landscape modeling of urban growth patterns in Dhanbad Urban Agglomeration, India using

geoinformatics techniques. **The Egyptian Journal of Remote Sensing and Space Sciences.** 20: 91–102.

Lassila, K. D. (1999). The new suburbanites: how American plants and animals are threatened by the sprawl. **The Amicus Journal**. 21: 16–22.

Li, F., Ye, P. Y., Song, B.W., Wang, R. S., and Tao, Y. (2014). Assessing the changes in land use and ecosystem services in Changzhou municipality, Peoples' Republic of China, 1991–2006. **Ecological Indicators.** 42: 95–103.

Li, G., Fang, C., and Wang, S. (2016). Exploring spatiotemporal changes in ecosystem-service values and hotspots in China. **Science of the Total Environment**. 545–546: 609–620.

Li, H., and Wu, J. (2004). Use and misuse of landscape indices. **Landsc. Ecol.** 19: 389–399.

Li, H., Li, Z., Li, Z., Yu, J., and Liu, B. (2015). Evaluation of ecosystem services: A case study in the middle reach of the Heihe River Basin, Northwest China. **Physics and Chemistry of the Earth**. 89–90: 40–45.

Li, Z.-L., Tang, B.-H., Wu, H., Ren, H., Yan, G., Wan, Z., and Sobrino, J. A. (2013). Satellite-derived land surface temperature: Current status and perspectives. **Remote Sensing of Environment**. 131: 14–37.

Lin, Y-P., Lin, Y-B., Wang, Y-T., and Hong, N-M. (2008). Monitoring and Predicting Land-use Changes and the Hydrology of the Urbanized Paochiao Watershed in Taiwan Using Remote Sensing Data, Urban Growth Models and a Hydrological Model. **Sensors.** 8(2): 658–680.

Linh, N. H. K., Erasmi, S., and Kappas, M. (2012). Quantifying land use/cover change and landscape fragmentation in Danang city, Vietnam: 1979-2009**.**

International Archives of the Photogrammetry, **Remote Sensing and Spatial Information Sciences**, Volume XXXIX-B8, 2012 XXII ISPRS Congress, 25 August – 01 September 2012, Melbourne, Australia.

Linyu Xu, Z. L., Huimin Song, and Hao Yin. (2013). Land-Use Planning for Urban Sprawl Based on the CLUE-S Model: A Case Study of Guangzhou, China. **Entropy.** 15: 3490–3506.

Liu, T., and Yang, X. (2015). Monitoring land changes in an urban area using satellite imagery, GIS and landscape metrics. **Applied Geography.** 56: 42–54.

Liu, Y. (2009). **Modelling urban development with geographical information systems and cellular automat.** Broken Sound Parkway NW: CRC Press Taylor & Francis Group.

Lo, C. P. (2004). Testing urban theories using remote sensing. **GISci. Remote Sensing** 41(2): 95–115.

Longley, P. A., and Mesev, V. (2002). On the measurement of urban form. **Environment and Planning.** A 32: 473–488

Luck, M., and Wu, J. (2002). A gradient analysis of the landscape pattern of urbanization in the Phoenix metropolitan area of USA. **Landscape Ecology.** 17: 327–339.

Luederitz, C., Brink, E., Gralla, F., Hermelingemeier, V., Meyer, M., Niven, L., and Wehrden, H. v. (2015). A review of urban ecosystem servics: six key challenges for future research. **Ecosystem Servics.** 14: 98–112.

MacDonald, K., and Rudel, T. K. (2005). Sprawl and forest cover: what is the relationship? **Applied Geography.** 25: 67–79.

Macie, E., and Moll, G. (1989). Trees and exurban sprawl. **American Forests**. 61–64.

Mamat. A., Halik. U., and Rouzi. A. (2018).Variations of Ecosystem Service Value in Response to Land-Use Change in the Kashgar Region, Northwest China. **Sustainability.** 10: 200; doi:10.3390/su10010200.

Markandu A., Johannus. J. A., Craig F. Nichol., and Xiaohua. A. W. (2016). Modelling spatial association in pattern based land use simulation models. **Journal of Environmental Management**. 181: 465-476.

Martin Herold, H. C., and Keith C. Clarke. (2005). The role of spatial metrics in the analysis and modeling of urban land use change. Computers, **Environment and Urban Systems**. 29: 369–399.

McArthur, R. H., and Wilson, E. O. (1967). **The Theory of Island Biogeography.** Princeton University Press, Princeton, NJ.

McGarigal, K. (2013). Landscape pattern metrics. Pages 1441-1451 in AH El-Shaarawi and W Piegorsch (eds.), **Encyclopedia of Environmetrics, Second Edition.** Chichester, England: John Wiley & Sons Ltd. [On-line]. Available: http://onlinelibrary.wiley.com/book/10.1002/9780470057339.

McGarigal, K. (2015). **FRAGSTATS: Spatial Pattern Analysis Program for Categorical Maps.** [On-line]. Available: http://www.umass.edu/landeco /fragstats/documents/fragstats_documents.html.

McGarigal, K., and McComb, W. C. (1995). Relationships between landscape structure and breeding birds in the Oregon Coast Range. **Ecological Monographs**. 65: 235–260.

McGarigal, K., Cushman, S. A., Neel, M. C., and Ene, E. (2002). **FRAGSTATS: Spatial Pattern Analysis Program for Categorical Maps.** Computer software

program produced by the authors at the University of Massachusetts, Amherst. [On-line]. Available: http://www.umass.edu/landeco/research/fragstats fragstats.html.

Megahed, Y., Cabral, P., Silva, J., and Caetano, M. (2015). Land Cover Mapping Analysis and Urban Growth Modelling Using Remote Sensing Techniques in Greater Cairo Region—Egypt. **ISPRS International Journal of Geo-Information.** 4: 1750–1769; doi:10.3390/ijgi4031750.

Mitchell, J. G. (2001). Urban sprawl: the American dream? **National Geographic**. 200(1): 48–73.

Nelson, A. C. (1990). Economic critique of prime farmland preservation policies in the United States. **Journal of Rural Studie.** 6(2): 119–142.

New man, P. W. G., and Kenworthy, J. R. (1988). The transport energy trade-off: fuel-efficient traffic versus fuel-efficient cities. **Transportation Research A.** 22A (3): 163–174.

Nikam, B. R., Ibragimov, F., Chouksey, A., Garg, V., and Aggarwal, S. P. (2016). Retrieval of land surface temperature from Landsat 8 TIRS for the command area of Mula irrigation project. **Environ Earth Science**. 75: 1169. doi: 10.1007/s12665-016-5952-3.

Ninh. T. V., and Waisurasingha, C. (2018). Land use/cover change and landscape fragmentation analyses in Khon Kaen city, Northeastern Thailand. **International Journal of GEOMATE**. 15(47):201-8.

O'Connor, K. F., Overmars, E. B., and Ralston, M. M. (1990). **Land Evaluation for Nature Conservation**. Wellington, New Zealand: Caxton Press.

O'Neill, R. V., Krummel, J. R., Gardner, R. H., Sugihara, G., Jackson, B., DeAngelis, D. L., Milne, B. T., Turner, M. G., Zygmunt, B., Christensen, S. W., Dale, V. H., and Graham, R. L. (1988). Indices of landscape pattern. **Landscape Ecology.** 1: 153–162.

Oh, Y-G., Yoo, S-H., Lee, S-H., and Choi, J-Y. (2011). Prediction of paddy field change based on climate change scenarios using the CLUE model. **Paddy Water Environ.** 9(3): 309–323.

Orekan, V. O. A. (2007). **Implementation of the local land-use and land-cover change model CLUE-S for Central Benin by using socio-economic and remote sensing data.** Doctoral dissertation, Universitäts- Bonn.

Padmanaban. R., Bhowmik, A. K., Cabral, P., Zamyatin, A., Almegdadi, O., and Wang, S. (2017). Modelling Urban Sprawl Using Remotely Sensed Data: A Case Study of Chennai City, Tamilnadu. **Entropy.** 19: 163. doi:10.3390/e19040163.

Parker, D. C., Evans, T. P., and Meretsky, V. (2001). Measuring emergent properties of agent-based landuse/landcover models using spatial metrics. In **Seventh annual conference of the international society for computational economics.** [On-line]. Available: http://www.php.indiana.edu/~dawparke/park

Paudel, S., and Yuan. F. (2012). Assessing landscape changes and dynamics using patch analysis and GIS modeling. **International Journal of Applied Earth Observation and Geoinformation.** 16: 66–76.

Pérez-Soba, M., Verburg, P. H., Koomen, E., Hilferink, M. H. A., Benito, P., Lesschen, J. P., Banse, M., Woltjer, G., Eickhout, B., Prins, A-G., and Staritsky, I. (2010). Land use modelling - implementation. Preserving and enhancing the environmental benefits of "land-use services". **Final report to the European**

Commission, DG Environment. Alterra Wageningen UR: Geodan, Object Vision, BIOS, LEI and PBL.

Pham, H. M., Yamaguchi, Y., and Bui, T. Q. (2011). A case study on the relation between city planning and urban growth using remote sensing and spatial metrics. **Landscape and Urban Planning.** 100: 223–230.

Pontius, R. G., and Schneider, L. C. (2001). Land-cover change model validation by an ROC method for the Ipswich watershed, Massachusetts, USA. Agriculture, **Ecosystems and Environment.** 85: 239-248.

Putnam, R. D. (2000). **Bowling Alone:** The Collapse and Revival of American Community. Simon and Schuster (eds.). New York.

Qian, Y., Zhou, W., Yan, J., Li, W., and Han, L. (2015). Comparing machine learning classifiers for object-based land cover classification using very high resolution imagery. **Remote Sensing.** 7(1): 153-68.

Ramachandra, T. V., Aithal, B. H., and Sanna, D. D. (2012). Insights to urban dynamics through landscape spatial pattern analysis. **International Journal of Applied Earth Observation and Geoinformation.** 18: 329–343.

Ritters, K. H., O'Neill, R. V., Hunsaker, C. T., Wickham, J. D., Yankee, D. H., Timmins, S. P., Jones, K. B., and Jackson, B. L. (1995). A factor analysis of landscape pattern and structure metrics. **Landscape Ecology**. 10(1): 23–39.

Savitch, H. V. (2003). How suburban sprawl shapes human well-being. Journal of Urban Health: **Bulletin of the New York Academy of Medicine**. 80(4): 590–607.

Schneider, Seto, K. C., and Webster, D. R. (2005). Urban growth in Chengdu Western China: application of remote sensing to assess planning and policy outcomes. **Environment and Planning B-Planning and Design**. 32(3): 323–345.

Schroeder, T. A., Cohen, W. B., Song, C. H., Canty, M. J., and Yang, Z. Q. (2006). Radiometric correction of multi-temporal Landsat data for characterization of early successional forest patterns in western Oregon**. Remote Sens. Environ.** 103: 16–26.

Seto, K. C., and Fragkias, M. (2005). Quantifying Spatiotemporal Patterns of Urban Land-use Change in Four Cities of China Time Series Landscape Metrics. **Landscape Ecology**. 20(7): 871–888. doi: 10.1007/ s10980-005-5238-8.

Shetty, P. J., Gowda, S., Gururaja, K. V., and Sudhira, H. S. (2012). Effect of Landscape Metrics on Varied Spatial Extents of Bangalore, India. **Asian Journal of Geoinformatics.** 12:1.

Shihong Du, Z. X., Yi-Chen W., and Luo Guo. (2016). Quantifying the multilevel effects of landscape composition and configuration on land surface temperature. **Remote Sensing of Environment.** 178: 84–92.

Shiliang Su, Xiao, X., Jiang, Z., and Zhang, Y. (2012). Characterizing landscape pattern and ecosystem service value changes for urbanization impacts at an eco-regional scale. **Applied Geography**. 34: 295–305.

Snyder, W. C., Wan, Z., Zhang, Y., and Feng, Y. Z. (1998). Classification based emissivity for land surface temperature measurement from space. **International Journal of Remote Sensing**. 19: 2753–2774.

Squires, G. D. (2002). **Urban Sprawl Causes, Consequences and Policy Responses.** Washington, DC: Urban Institute Press.

Steinitz, C., Arias, H., Bassett, S., Flaxman, M., Goode, T., Maddock III, T., Mouat, D., Peiser, R., and Shearer, A. (2003). **Alternative Futures for Changing Landscapes. The Upper San Pedro River Basin in Arizona and Sonora.** Washington, DC: Island Press.

Stoel Jr., T. B. (1999). Reining in urban sprawl. **Environment**. 41(4): 6–33.

Stone Jr., B. (2008). Urban sprawl and air quality in large US cities. **Journal of Environmental Management**. 86: 688–698.

Sturm, R., and Cohen, D. A. (2004). Suburban sprawl and physical and mental health. **Public Health**. 118: 488–496.

Su, S., Li, D., Hu, Y. n., Xiao, R., and Zhang, Y. (2014). Spatially non-stationary response of ecosystem service value changes to urbanization in Shanghai, China**. Ecological Indicators**. 45: 332–339.

Su, S., Xiao, R., Jiang, Z., and Zhang, Y. (2012). Characterizing landscape pattern and ecosystem service value changes for urbanization impacts at an eco-regional scale. **Applied Geography.** 34: 295–305.

Subasinghe, S., Estoque, R. C., and Murayama, Y. (2016) Spatiotemporal Analysis of Urban Growth Using GIS and Remote Sensing: A Case Study of the Colombo Metropolitan Area, Sri Lanka. **International Journal ofGeo-Information.** 5: 197.

Sun, Q., Wu, Z., and Tan, J. (2012). The relationship between LST and land use/land cover in Guangzhou China. **Environmental Earth Sciences**. 65: 1687–1694.

Tan, K. C., Lim, H. S., MatJafri M. Z., and Abdullah, K. (2010). Landsat data to evaluate urban expansion and determine land use/land cover changes in Penang Island, Malaysia. **Environmental Earth Sciences**. 60: 1509–1521.

Taslima, S., Paraparib, D. M., and Shafaghat, A. (2015). Urban Design Guidelines to Mitigate Urban Heat Island (UHI) Effects in Hot- Dry Cities. **Jurnal Teknologi** (Sciences & Engineering). 74: 4: 119–124.

TEEB. (2010). **The Economics of Ecosystems and Biodiversity for Local and Regional Policy Makers**. [On-line]. Available: http://www.teebweb.org/publication/teeb-for-local-and-regional-policy-makers-2/.

Tianhonga, L., Wenkaia, L., and Zhenghanb, Q. (2010). Variations in ecosystem service value in response to land use changes in Shenzhen. **Ecological Economics**. 69: 1427–1435.

Trisurat, Y., Alkemade, R., and Verburg, P. (2010). Projecting land use change and its consequences for biodiversity in Northern Thailand. **Environmental Management.** 45: 626–639.

Turner, B. L., and Meyer, W. B. (1994). Global land use and land cover change: an overview. In: Turne, B.L., Meyer, W. B. (eds.) **Changes in land use and land cover: a global perspective** (pp. 1–11). New York.

Turner, M. G. (1989). Landscape ecology: the effect of pattern on process. **Annual Review of Ecology and Systematics**. 20: 171–197.

Turner, M. G., and Gardner, R. H. (1991). **Quantitative Methods in Landscape Ecology.** New York: Springer-Verlag,

Turner, M. G., Gardner, R. H., and O'Neill, R. V. (2001). **Landscape Ecology. In Theory and Practice: Pattern and Process.** New York: Springer.

Uuemaa, E., Antrop, M., Roosaare, J., Marja, R., and Mander, U. (2009). Landscape metrics and indices: an overview of their use in landscape research. Living Rev.

Living Reviews in landscape research. 3. [On-line]. Available: http://www.livingreviews.org/lrlr-2009-1 (last accessed 5 December 2016).

Van Asselen, S., Verburg, P. H. (2013). Land cover change or land-use intensification: simulating land system change with a global-scale land change model. **Global Change Biology.** 19(12): 3648-67

Veldkamp, A., and Fresco, L. O. (1996a). CLUE: A Conceptual Model to Study the Conversion of Land Use and Its Effects. Ecological Modeling 85(2-3): 253–270. Quoted in Agarwal C., Green G. M., Grove J. M., Evans T. P. and Schweik C. M. (2002). A Review and Assessment of Land-use Change Models. Dynamics of Space, Time, and Human Choice. **Apollo The International Magazine of Art and Antiques.** 1(1): 1–61.

Veldkamp, A., and Fresco, L. O. (1996b). CLUE-CR: An Integrated Multi-scale Model to Simulate Land Use Change Scenarios in Costa Rica. Ecological Modeling. 91(1–3): 231–248. Quoted in Agarwal C., Green G. M., Grove J. M., Evans T. P. and Schweik C. M. (2002). A Review and Assessment of Land-use Change Models. Dynamics of Space, Time, and Human Choice. **Apollo The International Magazine of Art and Antiques.** (1): 1–61.

Verburg, P. H. (2010). **The CLUE model Hands-on exercises**. Amsterdam: Institute for Environmental Studies, University Amsterdam.

Verburg, P. H., and Overmars, K. P. (2009). Combining top-down and bottom-up dynamics in land use modeling: exploring the future of abandoned farmlands in Europe with the Dyna-CLUE model. **Landscape Ecology.** 24(9): 1167–1181.

Verburg, P. H., and Veldkamp, A. (2001). The role of spatially explicit models in land-use change research: A case study for cropping patterns in China. Agriculture. **Ecosystems & Environment.** 85(1-3): 177-190.

Verburg, P. H., De Koning, G. H. J., Kok, K., Veldkamp, A., and Bouma, J. (1999). A spatial explicit allocation procedure for modeling the pattern of land use change based upon actual land use. **Ecological Modeling.** 116(1): 45–61.

Verburg, P. H., De Nijs, T. C. M., Van Eck, J. R., Visser, H., and de Jong, K. (2004b). A method to analyse neighbourhood characteristics of land use patterns. Computers, **Environment and Urban Systems.** 28(6): 667–690.

Verburg, P. H., Soepboer, W., Veldkamp, A., Limpiada, R., Espaldon, V., and Mastura, S. S. (2002). Modeling the spatial dynamics of regional land use: the CLUE-S model. **Environmental Management.** 30(3): 391–405.

Verburg, P. H., Steeg, J. Van de., and Schulp, N. (2005). **Manual for the CLUE-Kenya application.** Wageningen: Department of Environmental Sciences, Wageningen University.

Verburg, P. H., Van Eck, J. R., De Nijs, T. C. M., Dijst, M. J., and Schot, P. (2004c). Determinants of land use change patterns in the Netherlands. **Environment and Planning B Planning and Design.** 31(1): 125–150.

Wan, L., Zhang, Y., Zhang, X., Qi, S., and Na, X. (2015). Comparison of land use/land cover change and landscape patterns in Honghe National Nature Reserve and the surrounding Jiansanjiang Region, China. **Ecological Indicators .**51: 205–214.

Wang, W., Zhu, L., Wang, R., and Shi, Y. (2003). Analysis on the spatial distribution variation characteristic of urban heat environmental quality and its mechanism a case study of Hangzhou city. **Chinese Geographical Science.** 13(1): 39–47.

Weng, Q. (2009). Thermal infrared remote sensing for urban climate and environmental studies: Methods applications and trends. **ISPRS Journal of Photogrammetry and Remote Sensing.** 64(4): 335–344.

Weng, Q., Liu, H., and Lu, D. (2007). Assessing the effects of land use and land cover patterns on thermal conditions using landscape metrics in city of Indianapolis. United States. **Urban Ecosystem**. 10: 203–219.

White, R., Luo, W., and Hatna, E. (2001). Fractral structure in land use pattern of European cities: form and process. **12th European Colloquium on Quantitative and Theoretical Geography.** St-Valery-en-Caux, France.

Wilson, E. H., Hurd, J. D., Civco, D. L., Prisloe, S., and Arnold, C. (2003). Development of a geospatial model to quantify, describe and map urban growth. **Remote Sensing of Environment.** 86(3): 275–285.

With, K. A. (1999). Is landscape connectivity necessary and sufficient for wildlife management? In Rochelle, J. A., Lehmann, L. A. and Wisniewski, J. (eds.). **Forest Fragmentation: Wildlife and Management Implications** (pp. 97–115). Brill.

Wittmer, H., and Gundimeda, H. (2012). The Economics of Ecosystems and Biodiversity in Local and Regional Policy and Management. **Earthscan 2 Park Square.** Milton Park, Abingdon, Oxon OX14 4RN.

Wu, J., Jelinski, E. J., Luck, M., and Tueller, P. T. (2000). Multiscale analysis of landscape heterogeneity: scale variance and pattern metrics. **Geographic Information Sciences.** 6(1): 6–16.

Yanos, P. T. (2007). Beyond "Landscapes of despair": the need for new research on the urban environment sprawl and the community integration of persons with severe mental illness. **Health&Place**. 13: 672–676.

Yu, M. (2013). **To analyze urban sprawl using remote sensing: a case study of London, Ontario, Canada.** Master of Science (Urban Planning), The University of Hong Kong. [On-line]. Available: http://www.hdl.handle.net/ 10722/195105.

Yu, X. J., and Ng, C. N. (2007). Spatial and temporal dynamics of urban along two urban-rural transects: A case study of Gungzhou, China. **Landscape and Urban Planning.** 79(1): 96–109.

Yu, X. Y., and Ng, C. N. (2007). Spatial and temporal dynamics of urban sprawl along two urban–rural transects: A case study of Guangzhou, China. **Landscape and Urban Planning.** 79: 96–109.

Yu, X., Guo, X., and Wu, Z. (2014). Land Surface Temperature Retrieval from Landsat 8 TIRS - Comparison between Radiative Transfer Equation-Based Method, Split Window Algorithm and Single Channel Method. **Remote sensing.** 6: 9829–9852.

Yuan, F., and Bauer, M. E. (2007). Comparison of impervious surface area and normalized difference vegetation index as indicators of surface urban heat island effects in Landsat imagery. **Remote Sensing of Environmen.** 106: 375–386.

Yuan, F., Sawaya, K. E., Loeffelholz, B. C., and Bauer, M. E. (2005). Land cover mapping and change analysis in the Twin Cities Metropolitan Area with Landsat remote sensing. **Remote Sensing of Environment.** 98 (2–3): 317–328.

Zhang, X., Chen, J., Tan, M., and Sun, Y. (2007). Assessing the impact of urban sprawl on soil resources of Nanjing city using satellite images and digital soil databases. **Catena**. 69: 16–30.

Zhang, Y., Balzter, H., Zou, C., Xu, H., and Tang, F. (2015). Characterizing bi-temporal patterns of land surface temperature using landscape metrics based on sub-pixel classifications from Landsat TM/ETM+. **International Journal of Applied Earth Observation and Geoinformation.** 42: 87–96.

Zhang, Y., Inakwu, O. A. O., and Han, C. (2009). Bi-temporal characterization of land surface temperature in relation to impervious surface area, NDVI and NDBI, using a sub-pixel image analysis. **International Journal of Applied Earth Observation and Geoinformation**. 11: 256–264.

Zheng, X-O., Zhao, L., Xiang, W-N., Li, N., Lv, L-N., and Yang, X. (2012). A coupled model for simulating spatio-temporal dynamics of land-use change: A case study in Changqing, Jinan, China. **Landscape and Urban Planning.** 106(1): 51–61.

Zhou, W., Huang, G., and Cadenasso, M. L. (2011). Does spatial configuration matter? Understanding the effects of land cover pattern on land surface temperature in urban landscapes. **Landscape and Urban Planning.** 102(1): 54–63.

CURRICULUM VITAE

Name   Mr. ANAKE SRISUWAN

Date of Birth   December 17, 1982

Place of Birth Surat Thani

Education

- 2002 Bachelor of Science in Rural Technology,

  Thammasat University, Thailand.

- 2006 Master of Science (Geoinformatics): Institute of

  Science, Suranaree University of Technology, Thailand

Publications

Ongsomwang, S., and Srisuwan, S. (2010). Landscape Pattern and Its Changes in Thap Lan National Park Using Geo-Informatics Data. **The 3rd Suranaree University of Technology Graduate Conference (SUTGRAD)**. Suranaree University of Technology.

Ongsomwang, S., and Srisuwan, S. (2010). A Study on Landscape Pattern Changes in Thap lan National Park. **Geoinfotech 2010**. Impact Convention Center, Muang Thong Thani, Nonthaburi, Thailand.

Grants and Fellowships

- Biodiversity Research and Training program (BRT)

- Nakhon Ratchasima Rajabhat University (NRRU)